

INTRADUCTAL DELIVERY OF AN ABLATIVE AGENT AS A LOCAL INTERVENTION FOR  
BREAST CANCER PREVENTION IN RODENT MODELS

By

Erin Zaluzec

A DISSERTATION

Submitted to  
Michigan State University  
in partial fulfillment of the requirements  
for the degree of

Pharmacology and Toxicology – Environmental Toxicology – Doctor of Philosophy

2024

## ABSTRACT

Breast cancer (BC) is the leading cancer diagnosis accounting for 31% of all cancer cases for women in the United States. Equally as impactful, BC is also the second leading cause of cancer deaths among women. Despite the rise of BC diagnoses, the number of preventive interventions to mitigate the prevalence of cases is inadequate. Currently, only three BC prevention options are approved and implemented for women. Prophylactic mastectomy removes the entirety of the breast and reduces breast cancer risk by up to 90%. However, it's a highly invasive procedure that takes many painful weeks to heal and can be emotionally exhausting. Tamoxifen and raloxifene are selective estrogen receptor modulators that have less risk reduction, only 50%. These drugs can increase the risk of stroke, endometrial cancer, and can induce postmenopausal symptoms early. Watchful waiting does not lower BC risk and relies on attentiveness, self-breast exams and annual checkups to detect tumor formation before it becomes cancerous. The harsh realities of the detrimental side effects outweigh the risk reduction benefits and deter most women from opting for these preventions. Consequently, only 'high-risk' women, those with a prevalent family history or BRCA1/2 mutations, even consider the choices. Therefore, it is imperative to investigate modern prevention methods with high-risk reduction while minimalizing side effects associated with current preventions because while treatments can save lives, prevention can save more.

Unlike other organs, the breast, specifically the ductal tree, is accessible externally. The ductal tree is primarily composed of epithelial cells that line the lumen and are responsible for milk production and secretion but are the origin of most breast cancer cases. Intraductal (ID) injections are a unique approach solely for the breast that can directly target epithelial cells of the ductal tree through entry at the nipple. By utilizing ID injections to deliver an ablating agent, epithelial cells can be eradicated before they have a chance to become malignant with minimum invasion to the organ and no systemic processing. Ethanol is an inexpensive, readily available, ablating agent used for treatments such as unresectable liver tumors and breast pseudoaneurysms that can be repurposed for ID ablation as an effective prevention method. Therefore, the objective of this dissertation is to identify the impact of 70% ethanol ID ablation as a novel competitive approach for BC prevention that mitigates the shortcomings of existing preventive

measures.

Herein I demonstrated that ID ablation with 70% ethanol is an effective preventive for BC. A single injection can ablate a majority of epithelial cells within the ductal tree without inducing a cancerous effect. I investigated the minimum volume necessary for effective prevention while maintaining a high ablation rate. The translational ability of ID ablation was demonstrated by successful ablation and increased tumor latency from mouse to rat BC models. I explored the combination of ethanol and ethyl cellulose, a clinically used gelling agent, with the aim to mitigate ethanol dispersion which yielded no reduction in dispersion. The addition of tantalum oxide, a versatile X-ray contrast agent further supports the translational ability of ID ablation into clinics. However, further studies are needed to identify the impact on the local immune response and the exact mechanisms behind wound healing. The work is highly translational with tools readily available for repurposing and can have a direct impact on saving human lives.

Copyright by  
ERIN ZALUZEC  
2024

This dissertation is dedicated to my husband Zak and my three cats Cloe, Echo, and Azula.  
Thank you for your unwavering love and support throughout all these years.

## ACKNOWLEDGEMENTS

To Beth, Katie, Brooke, Alan, Bryan, Jamie, Sam, Adriana, Tam, Shay, Nazanin, Jacob, and Elizabeth, thank you for bringing laughter and happiness into my every day and for keeping me sane. From teatime to team bonding and every lunch in between, these years were hard, but you all made it so much easier. To Omar, Olivia, Lauren, and Brad, I could've have asked for a better cohort. Although Covid made it difficult to see each other, I'm grateful for all the time we had inside and outside of school. To Malique, you were my first friend to make during graduate school. You have inspired me, encouraged me, and supported me in a way I didn't know I needed. I will always cherish the friendship we share. To Jess whom I have always looked up to, thank you for every coffee date and every push to keep me going. It is one thing to go through a Ph.D. program and another to do it with friends. I couldn't have asked for better friends throughout this journey.

To Zak, thank you for being the "Yes you can" to every "I can't do this" and every coffee shop study date. To mom, dad, and Ryan, thank you for inspiring me to pursue my Ph.D. I'm lucky to have my family as my friends. Mom and dad, you really are the cool parents. To the Malott family, I married into the best and most supportive family one could ask for. To my cats, thanks for all the cuddles and apologies that I couldn't meet every treat demand while studying.

To my advisor Dr. Lorenzo Sempere, thank you for your guidance on my academic journey. Lastly, I would like to thank my committee, Dr. Jamie Bernard, Dr. Karen Liby, and Dr. Richard Neubig for their insight into my research and support as a person and scientist throughout these years.

**TABLE OF CONTENTS**

LIST OF ABBREVIATIONS..... viii

CHAPTER 1: SYSTEMIC AND LOCAL STRATEGIES FOR PRIMARY PREVENTION OF BREAST  
CANCER ..... 1  
    REFERENCES .....34

CHAPTER 2: DUCTAL TREE ABLATION BY LOCAL DELIVERY OF ETHANOL PREVENTS  
TUMOR FORMATION IN AN AGGRESSIVE MOUSE MODEL OF BREAST CANCER .....49  
    REFERENCES .....81

CHAPTER 3: TANTALUM OXIDE NANOPARTICLES AS VERSATILE AND HIGH-RESOLUTION  
X-RAY CONTRAST AGENT FOR INTRADUCTAL IMAGE-GUIDED ABLATIVE PROCEDURE IN  
RODENT MODELS OF BREAST CANCER.....85  
    REFERENCES ..... 108

CHAPTER 4: IMAGE-GUIDED LOCAL ABLATION FOR PRIMARY PREVENTION OF BREAST  
CANCER IN RAT MODELS ..... 112  
    REFERENCES ..... 136

CHAPTER 5: GENERAL CONCLUSIONS ..... 139  
    REFERENCES ..... 154

## LIST OF ABBREVIATIONS

BC	Breast Cancer
Brca	Breast Cancer Gene
CDDO-me	2-Cyano-3,12-dioxooleana-1,9-dien-28-oic acid methyl ester
CI	Confidence Interval
CK19	Cytokeratin 19
CNN	Convolutional Neural Network
Cox-2	Cyclooxygenase-2
Cre	Cre-recombinase
DMBA	4,7,12-Dimethylbenz[a]anthracene
DL	Deep Learning
EC	Ethyl Cellulose
EGFR	Epidermal growth factor receptor
ErbB2	Avian erythroblastic leukemia viral oncogene homolog 2
ER	Estrogen Receptor
EtOH	Ethanol
FFPE	Formalin-Fixed paraffin-embedded
FOV	Field of View
GLUT1	Glucose Transporter Protein Type 1
HER2	Human epidermal growth factor receptor 2
Hox1A	Homeobox protein 1A
HRP	Horseradish peroxidase
IACUC	Institutional Animal Care & Use Committee
I-Bet	Inhibitor of Bromodomain and extra-terminal domain
ID	Intraductal
IHC	Immunohistochemistry

Jak3	Janus Kinase 3
μCT	Microcomputed tomography
MIND	Mouse Mammary Intraductal
MMTV	Mouse Mammary Tumor Virus
MNU	N-methyl-N-nitrosourea
MRI	Magnetic Resonance Imaging
NC	Nanocrystal
NP	Nanoparticles
PBS	Phosphate Buffered Saline
Py-MT	Polyoma middle tumor-antigen
RankL	Receptor activator of nuclear factor kappa beta ligand
siRNA	Short interfering RNA
SMA	α-Smooth Muscle Actin
TAM	Tamoxifen
TaO <sub>x</sub>	Tantalum Oxide
TEB	Terminal End Bud
Trp53	Tumor Protein P53
Vim	Vimentin
WAPcre	Whey Acidic Protein Cre-Recombinase

**CHAPTER 1: SYSTEMIC AND LOCAL STRATEGIES FOR PRIMARY PREVENTION OF  
BREAST CANCER**

Published in *Cancers* 2024, 16(2):248 DOI: 10.3390/cancers16020248

Erin K. Zaluzec<sup>1,2</sup>, Lorenzo F. Sempere<sup>1,3</sup>

<sup>1</sup>Precision Health Program, Michigan State University, East Lansing, MI 48824, USA

<sup>2</sup>Department of Pharmacology & Toxicology, College of Veterinary Medicine, Michigan State University, East Lansing, MI 48824, USA

<sup>3</sup>Department of Radiology, College of Human Medicine, Michigan State University, East Lansing, MI 48824, USA

### **Contributions to Science.**

Within this chapter, Dr. Lorenzo Sempere and I were responsible for conception and design of this review. Dr. Sempere and I contributed to drafts and critical revisions for intellectual content with the exception of the risk assessment introductory paragraph, prophylactic vaccine introduction paragraph, and ductal tree ablation paragraph that were led by Dr. Sempere, and hormonal regulation and chemoprevention paragraphs that were led by me. Dr. Sempere and I designed tables and figures, and I generated their final versions.

### **Simple Summary.**

Current interventions for breast–cancer prevention are associated with adverse side effects that frequently deter women from selecting these evidence-based risk-reducing procedures. In addition, modifiable lifestyle changes can improve breast cancer risk but can be challenging in execution. Therefore, women who are considered high risk due to non-modifiable factors, such as *BRCA1/2* mutations or a strong family history of breast cancer, are in need of alternative prevention procedures. Here, we review investigational preclinical and clinical approaches at a systemic and local level that focus on non-modifiable breast cancer risk-reducing interventions.

### **Abstract.**

One in eight women will develop breast cancer in the US. For women with moderate (15–20%) to average (12.5%) risk of breast cancer, there are few options available for risk reduction. For high-risk (>20%) women, such as *BRCA* mutation carriers, primary prevention strategies are limited to evidence-based surgical removal of breasts and/or ovaries and anti-estrogen treatment. Despite their effectiveness in risk reduction, not many high-risk individuals opt for surgical or hormonal interventions due to severe side effects and potentially life-changing outcomes as key deterrents. Thus, better communication about the benefits of existing strategies and the development of new strategies with minimal side effects are needed to offer women adequate risk-reducing interventions. We extensively review and discuss innovative

investigational strategies for primary prevention. Most of these investigational strategies are at the pre-clinical stage, but some are already being evaluated in clinical trials and others are expected to lead to first-in-human clinical trials within 5 years. Likely, these strategies would be initially tested in high-risk individuals but may be applicable to lower-risk women, if shown to decrease risk at a similar rate to existing strategies, but with minimal side effects.

## **Background.**

For women in the US, breast cancer (BC) is the most prevalent cancer and the second-leading cause of cancer-related deaths. Projections for 2023 estimate that 55,720 women will be diagnosed with carcinoma in situ, 297,790 with invasive carcinoma, and 43,170 women will die from BC [1]. With the number of new diagnoses still on the rise, one in eight women will develop BC within their lifetime, but all women are at risk. Therefore, there is a need to develop new strategies for primary prevention with a focus on high-risk (>20%) individuals, but that can also be applied to moderate- (15–20%) and average (12.5%)-risk individuals.

There are well-established risk factors that contribute to the absolute risk of developing BC [2,3]. There are modifiable risk factors such as having a healthy diet, regular exercise, and limiting alcohol consumption [2,4]. Cumulative exposure of breast tissue to estrogen is an important risk factor for BC. This risk can be minimized by various actions such as having their first-born before age 30, limiting the use of hormonal birth control medications, and avoiding hormone replacement therapy. Non-modifiable risk factors that increase cumulative exposure to estrogen include younger age at menarche and older age at natural menopause [2]. There are non-modifiable genetic risk factors that include known mutations in a high-penetrant BC gene such as *BRCA1* and *BRCA2*, cumulative interaction of risk-associated alleles of BC susceptible SNPs, and/or family history with multiple incidences of BC [5]. There are also non-modifiable risk factors related to the personal history of radiation therapy to the chest, and the number of breast biopsies [4].

For women in the US, a 1.67% increased risk over 5 years at any age or 20% increased risk over a 20-year period is considered a high-risk individual [3]. This review is focused on federal agency guidelines and regulatory approvals that pertain specifically to US women. It is worth noting that some of these guidelines are different in other countries. For example, for women in Europe, high risk is defined as a >30% lifetime risk [6]. This difference and other considerations may affect how risk-reducing interventions are applied, perceived, and complied with in different geographical regions and countries. Many non-modifiable factors contribute to this increased risk. *BRCA* mutation carriers are considered high-risk individuals (>50% chance of BC development) and are the most prevalent and counseled group for primary intervention. Women with other genetic predispositions including mutation in *CDHI* (hereditary diffuse gastric cancer syndrome), *PALB2*, *PTEN* (Bannayan–Riley–Ruvalcaba, Cowden, or hamartoma tumor syndromes), *TP53* (Li-Fraumeni syndrome), *STK11* (Peutz–Jeghers syndrome) are also considered high-risk individuals and eligible for bilateral prophylactic mastectomy [7,8].

Guidelines for risk reduction of moderate (15–20%)-risk individuals are not as well-delineated in part due to the difficulty of identifying this subset of individuals and how modifiable risk factors such as diet, alcohol consumption, and BMI can affect and compound absolute risk [4,5]. However, women with genetic predispositions including mutations in *ATM* and *CHK2*, or who carry risk-associated alleles for multiple of the 92 susceptibility genes are generally considered moderate-risk individuals [9]. Genetic counseling based on multi-gene panels captures the most frequent mutations [7,8,10,11]. Recommendation for mammography and other monitoring modalities varies by risk [3,12].

There are several risk assessment models available that calculate an individual's risk based on various risk factors [2,13]. The BCRAAT tool (<https://bcrisktool.cancer.gov/> (accessed on 30 December 2023)) uses the Gail model and is appropriate for women without a genetic predisposition or previous BC [14]. The IBIS tool (<https://ibis.ikonopedia.com/> (accessed on 30 December 2023)) uses the Tyrer–Cuzick model and is appropriate for women with known or suspected genetic predisposition, including mutations in *BRCA1* or *BRCA2*, using extensive personal and family history risk factors [15].

For high-risk women in the US, FDA-approved primary prevention strategies include surgical removal of the breasts and/or ovaries and the use of anti-estrogen therapies. Bilateral prophylactic mastectomy is currently the most effective procedure for preventing BC: it can reduce the incidence of BC by up to 90% in high-risk individuals [16]. Anti-estrogen treatments have been shown to reduce BC risk by up to 50% in high-risk women [16]. Though effective in risk reduction, less than 50% and less than 10% of high-risk individuals opt for surgical or hormonal interventions, respectively, with life-changing consequences and severe side effects as major contributing dissuading factors [16–18]. These prevention interventions are readily available but may be underused due to a lack of clinician or patient information regarding risk level, lack of clinical confidence to discuss appropriate prevention options, personal social dynamics, and fully informed choice, which can result in a low uptake of prevention methods [16]. Bilateral prophylactic mastectomy uptake is well documented in women who are *BRCA* mutation carriers. However, on average, only 20% of women at high risk without the *BRCA* mutations undergo this surgical procedure but have reported ranges from 11–50% [19,20]. Population studies on hormonal interventions have reported low uptake for eligible women (1–5%); however, this falls short when compared to high-risk proactive women interested in using these interventions, which can be as high as 40% [16,21]. A recent study conducted in Europe showed that women who were informed of their risk and provided information on preventive options within 8 weeks of risk identification had a large increase in uptake (77.5%) of hormonal interventions compared to much lower uptake in standard clinical settings (11–20%) [18,22–24]. Therefore, prevention interventions, either currently approved or investigational, should take into consideration education and informed decision-making in addition to clinically established risk reduction and management of adverse side effects.

These primary prevention interventions treat the entire breast as a unit, but neoplasia originates in discrete regions within one or more ductal tree systems [25,26]. A woman's breast contains the stroma and 8–12 ductal trees [27–29]. Surrounding the ductal tree is the stroma, which is composed of adipocytes, immune cells, endothelial cells, fibroblasts, and extracellular matrix (**Figure 1.1A**). The ductal trees are composed of luminal epithelial cells, myoepithelial cells, and mammary epithelial stem cells from which

most BC arises and are not readily accessible without highly invasive surgical procedures. This review focuses on preclinical and clinical approaches that target the premalignant epithelial niche and minimize adverse side effects while maintaining the effectiveness of current surgical and systemic interventions for women with non-modifiable risk.

### **Evidence-based Interventions for Primary Prevention.**

We briefly review the limited number of FDA-approved drugs and interventions for primary prevention of BC. Due to adverse side effects, recommendation for these interventions is generally restricted to high-risk individuals.

### **Surgical Intervention.**

Surgical interventions target areas of the breast that are associated with a higher risk of BC development through the complete removal of the tissue. Due to the invasive nature of these procedures, only high-risk women consider these options. Dual mastectomy directly removes both breasts and in doing so removes the ductal tree, whereas salpingo-oophorectomy removes fallopian tubes and/or ovaries for reduced hormonal contribution in BC development. Here, we discuss the advantages and disadvantages of surgical intervention.

### **Prophylactic Mastectomy.**

This procedure completely removes the breast tissue in both breasts, including the ductal tree and surrounding stroma. Bilateral prophylactic mastectomy is a highly invasive procedure that can be executed as a total mastectomy, skin-sparing mastectomy, or total skin-sparing mastectomy. In removing the entirety of the breast, this risk-reducing surgery removes the epithelial cells, the intended target cells, from which breast carcinomas arise [30,31]. With nipple reconstructive techniques available, total mastectomy is the most commonly selected choice [32]. However, despite risk reduction and available reconstructive surgery, less than 50% of women undergo this preventive procedure (**Figure 1.1B**) due to the pain, cosmetic,

psychological, and social impact [17,33,34]. Pain, local, and systemic inflammation in response to mastectomy varies on the surgical procedure which can include musculoskeletal manipulation and tissue advancement for reconstruction in addition to the excision of the breast tissue. Bilateral prophylactic mastectomy studies focusing on patient-reported outcomes after breast reconstruction have noted higher body pain or breast discomfort and decreased sexual interest, but overall satisfaction with the procedure lowered cancer-related anxiety and increased satisfaction with breast cosmesis [35–40]. However, it is important to note that these reports vary due to factors such as number of patients, the timing of reconstructive surgery, and pre- vs. post-operation comparisons [35]. Nevertheless, the potential positive and negative impacts should be equally addressed with women for them to make fully informed decisions.

### **Salpingo-oophorectomy.**

Surgical removal of the fallopian tubes and ovaries is a commonly recommended BC prevention for premenopausal *BRCA* mutation carriers that had a previously reported risk reduction of up to 50% [41]. These findings have been called into question after considering the salpingo-oophorectomy procedure as a time-varying covariate. Recent studies investigating BC risk reduction in *BRCA* mutation carriers following salpingo-oophorectomy have found minimal to no impact in women when taking into consideration the time-varying covariate [41–43]. Following salpingo-oophorectomy, women may experience symptoms typically associated with menopause due to the reduction of estrogen and progesterone production in the body. However, these symptoms are often reportedly tolerable and do not require further treatment [44]. Hormone replacement therapy for women experiencing severe symptoms is available. *BRCA* mutation carriers taking hormone replacement therapy after undergoing oophorectomy do not have an increased risk of BC if <45 years old but those >45 have an increased risk of triple-negative BC [45]. Other studies have shown that *BRCA* mutation carriers who receive only estrogen after an oophorectomy have no increased risk of BC. However, the risk of only progesterone use has yet to be determined [46,47].

### **Hormonal Modulation.**

Selective estrogen receptor modulators (SERMs), tamoxifen and raloxifene, are commonly used in the treatment of various diseases including BC and osteoporosis and are the only two FDA-approved compounds for primary prevention of BC [5,48]. An estrogen-bound estrogen receptor (ER) forms a complex that hetero- or homo-dimerizes with a second estrogen-bound estrogen receptor. This complex is able to translocate into the nucleus and can act directly and indirectly on genes to promote cell growth, migration, and metastasis while simultaneously preventing functions such as apoptosis and necrosis [49–51]. These SERMs compete with and block the binding of estrogen to the ER within the breast epithelia and antagonize its functions (**Figures 1.1C and 1.2A**); interaction of these SERMs with ERs in other cell types throughout the body can have partial antagonistic or even agonistic effects [52].

### **Tamoxifen.**

Tamoxifen was originally developed in the 1960s as a contraceptive but was ultimately unsuccessful. In the 1990s, it was repurposed as a BC treatment due to its therapeutic benefits in reducing tumor recurrence at the origin site, lowering the incidence of cancer in the contralateral breast, and increasing overall survival. These benefits led to the selection of tamoxifen as a preventive agent for BC [53,54]. By 1992, the National Surgical Adjuvant Breast and Bowel Project had enrolled 13,175 high-risk women in a trial investigating the role of tamoxifen as an oral drug for the prevention of primary formation of BC. By the end of the five-year clinical trial, tamoxifen had reduced the incidence of invasive and non-invasive BC by 49% and 50%, respectively, compared to placebo groups [53]. Women who developed invasive BC had lower occurrence and tumor size in the tamoxifen-treated groups. Despite the reduction of BC incidence, increased hot flashes and vaginal discharge were reported among women in the tamoxifen-treated groups. More alarming was the associated risk of stroke and a 1.5-to-6.9-fold increased risk of developing endometrial cancer due to long-term exposure to tamoxifen [53,55,56]. Additional studies of tamoxifen as a preventive agent reported these adverse effects as major factors contributing to discontinuation of treatment, especially among women taking tamoxifen for primary prevention as opposed to adjuvant therapy for BC [57,58]. However, adverse

effects ceased after treatment, and long-term follow-up studies showed extended tamoxifen protection for BC prevention [59–61].

### **Raloxifene.**

Similar to tamoxifen, raloxifene was originally developed for non-BC disease. Initially under investigation for treatment and prevention of osteoporosis in postmenopausal women, the Multiple Outcomes of Raloxifene Evaluation (MORE) study in 1998 was conducted to investigate bone fractures in 7700 postmenopausal women diagnosed with osteoporosis [62]. Interestingly, during this study, raloxifene was associated with a lower incidence of BC. Raloxifene treatment resulted in a 76% decrease in invasive BC after 3 years of treatment [62]. Like tamoxifen, reports of hot flashes along with leg cramps were higher among women taking raloxifene. Additionally, thromboembolic events were 3.1 times higher with raloxifene but did not increase the risk of endometrial cancer [62,63]. Direct comparison of tamoxifen and raloxifene revealed equal risk reduction of invasive BC, but endometrial cancer in postmenopausal women, thromboembolic events, and stroke occurred in both groups [64]. The raloxifene-treated group had a 30% lower rate of endometrial cancer, had fewer side effects on the uterus, and had a lower incidence of thromboembolic events which was consistent over the 81-month follow-up [64,65].

### **Watchful Waiting.**

Despite the evidence-based effectiveness of these surgical procedures and hormonal interventions, up to 50–70% of women presented with prevention and treatment options choose a watchful waiting strategy with enhanced surveillance [66,67]. These strategies may include annual or more frequent mammography and magnetic resonance imaging, monthly self-examination, and other monitoring protocols. Watchful waiting strategies do not reduce the risk of developing BC (**Figure 1.1A**) and up to 70% of high-risk individuals do not adhere to their enhanced surveillance protocols decreasing the benefit of early detection and intervention [68–70].

### **Investigational Approaches for Primary Prevention.**

There are several investigational approaches that aim to reduce or limit adverse side effects of current interventions and/or develop novel interventions with a high safety profile that may be offered more broadly to women seeking proactive options for primary prevention of BC. These approaches can be divided into systemic and local approaches. Systemic approaches consist of intravenous, intramuscular, or oral delivery of a drug, whereas local approaches consist of intraductal (ID) injection, transdermal application, or subcutaneous implant for drug delivery (**Figures 1.1D,E, 1.2B–D, and 3B–E**). Some of these approaches have already reached the clinical trial stage (**Table 1.1**) as discussed below, whereas many are still at an early stage of development in preclinical animal models (**Tables 1.2 and 1.3**).

Preclinical models of primary prevention and local treatment of BC include genetically engineered mouse models, chemical carcinogen-induced rat models, and orthotopic cell line models. These models present different advantages and limitations. Genetically engineered mouse models (GEMMs) have, in principle, an inexhaustible potential of developing malignancy, whereas chemical carcinogen-induced and orthotopic models have a limited number of neoplastic cells. In some of these models, the line between primary prevention and local treatment is difficult to establish. Different GEMMs have been used to model human BC (**Tables 1.2 and 1.3**). Several studies have used similar *Brca1*-deficient GEMMs as they are more relevant to high-risk *BRCA* mutation carriers. However, other GEMMs, including MMTV-PyMT, MMTV-ErbB2, and C3(1)-TAg, often considered more aggressive models, have also been used in this setting. Chemically induced rat models have been used for almost 40 years to study hormonal control [74] and more recently have been used to investigate local approaches for BC prevention (**Table 1.3**). Common limitations of these rodent models include the relative simplicity of linear architectures of their ductal trees, smaller ductal tree volumes with different surface area to volume ratios, different stromal density compared to human counterparts for translation of local intervention, duration, and frequency of chronic treatment in rodents vs. humans, and establishing effective dose for translation of systemic interventions.

### **Systemic Approaches for Primary Prevention in Preclinical Models and Clinical Trials.**

Systemic interventions require ADME (absorption, distribution, metabolism, and excretion) processing of the drug leading to drug delivery throughout the body. There are many well-characterized drugs with known modes of action and systemic effects on the body. Scientists are now investigating the repurposing of some of these drugs for the primary prevention of BC.

### **Hormonal Therapy with Aromatase Inhibitors.**

Similar to tamoxifen and raloxifene, aromatase inhibitors are already approved for BC treatment. These drugs mimic androstenedione and bind to aromatase enzymes to prevent the conversion of testosterone to estrogens [102]. Type I inhibitors bind irreversibly to aromatase, whereas type II inhibitors have reversible, competitive inhibition [102]. Reduction in contralateral BC and overall survival improvement in the treatment of early-stage BC led researchers to investigate aromatase inhibitors for primary prevention. Currently, a type I inhibitor (exemestane) and two type II inhibitors (letrozole and anastrozole) are in clinical trials as preventive agents for BC. Exemestane clinical trials recruited 4500 high-risk, post-menopausal women for a median 3-year study [103]. Like tamoxifen, exemestane was taken orally and daily. Compared to the placebo, the exemestane group reported a 65% reduction in invasive BC incidence [103]. Hot flashes, fatigue, sweating, and insomnia were reported in both groups and mild bone density loss occurred in the exemestane group [104]. After a 5-year follow-up, no serious adverse effects, such as bone fractures, endometrial cancer, or thrombotic effects had occurred [103]. A phase 2 clinical trial (NCT00579826) with letrozole was recently completed and findings of this study have not yet been published.

The phase 3 clinical trial IBIS II (NCT00078832) with anastrozole involved 3864 post-menopausal women for a 10-year follow-up study [105]. Anastrozole was given orally and daily for 5 years. Compared to the placebo, the anastrozole group reported a 49% reduction in BC significantly within and after the first 5 years of treatment. Additionally, a significant decrease in non-BC was also observed. Arthralgia, joint stiffness, hot flashes, sweating, hypertension, and vulvovaginal dryness had higher reports among

anastrozole groups compared to placebo treatment groups. Additionally, major adverse effects such as fractures, myocardial infarction, deep vein thrombosis, pulmonary embolism, stroke, and transient ischemic attacks were non-significantly different between anastrozole and placebo treatment groups [105]. Recently, anastrozole has received regulatory approval for BC prevention use in the United Kingdom; however, the FDA has yet to approve this or any other IA in a primary prevention setting [3].

### **Chemoprevention.**

Chemoprevention involves a variety of drugs used to prevent or delay the onset of cancer. These drugs are used as an alternative to invasive surgical procedures, such as bilateral prophylactic mastectomy, to lower a person's risk of cancer development. Although chemoprevention drugs may have life-saving benefits, women can be hindered by the associated side effects. Therefore, most women who qualify for BC chemoprevention are high-risk individuals.

### **Retinoids & Rexinoids.**

Retinoids are vitamin A analogs that primarily bind to retinoid acid receptors for growth regulation, differentiation, and apoptosis. However, these drugs have limited use due to their toxicity. Fenretinide is a synthetic derivative of all-trans-retinoic acid that has been shown to accumulate in human breast tissue and prevent BC development in animal models [106–108] and has low toxicity compared to other retinoids. This led to a clinical trial for secondary prevention in pre- and post-menopausal women in 1987. A total of 1750 women participated in this 5-year study with up to a 15-year follow-up. Interestingly, pre-menopausal women had up to a 50% risk reduction of both ipsilateral and contralateral BC which was not seen in women over the age of 55 years. However, no significant difference was seen with distant metastases formation; new, non-breast, primary tumor formations; or overall mortality [58]. A follow-up study on the safety of fenretinide was conducted in 2800 women with stage I or ductal carcinoma in situ given the same dosage for 5 years. Under 20% of women reported diminished dark adaptations or dermatological effects, 13% reported gastrointestinal symptoms, which all decreased over the 5-year period, whereas 11% reported

ocular surface disorders which had a slight increase in occurrence [73]. Liver function and lipid profile were also tested with no significant difference between the treatment and control groups. No significant differences were found between pre- and post-menopausal women for adverse effects [73]. These results led to a clinical trial for high-risk pre-menopausal women but it was terminated due to low patient accrual (NCT01479192).

Retinoid X receptor is another class of retinoid receptors that has different affinities for naturally occurring ligands and can dimerize with a plethora of receptors such as vitamin D, thyroid hormone, and liver X receptors. This vast access to regulator networks makes this an ideal target for cancer prevention and treatment [109]. Currently, bexarotene, otherwise known as LGD1069, is a rexinoid that is selective for the retinoid X receptor. It is the only FDA-approved rexinoid for the treatment of cutaneous T-cell lymphoma. However, preclinical studies of bexarotene for BC prevention have led to active, ongoing clinical trials (NCT03323658, NCT00055991) in patients at high risk for BC development [86,87].

### **Erlotinib.**

Women with *BRCA* mutations do not frequently express hormonal receptors and develop triple-negative BC. However, epidermal growth factor receptor (EGFR) is highly expressed in these triple-negative BCs and is suggested to be associated with *BRCA1* mutations in this cancer subtype [110–112]. Erlotinib is a small molecule inhibitor that blocks the phosphorylation and activation of EGFR and has been tested as a chemopreventive agent in *Brcal*-deficient GEMM [78]. At three months of age, animals were given an oral daily dose of 100 mg/kg of erlotinib, equivalent to ~8 mg/kg in humans, to study tumor-free survival and tolerability of chronic erlotinib treatment. Alopecia was the main side effect observed and was only found in 30% of all animals [78]. Erlotinib treatment significantly delayed or prevented the formation of ER- tumors but had a minimal effect on the formation of ER+ tumors [78]. Implicit from these findings is that a combination treatment with hormone therapy and erlotinib could prevent the formation of both ER-dependent and ER-independent EGFR-dependent tumors. However, the combination treatment may also exacerbate the side effects of either drug.

### **Bromodomain Inhibitors.**

Epigenetics acts on gene regulation that can impact cancer initiation and progression. Unlike genetic modifications, these events are considered reversible making them a desirable drug target. Several drugs have already been developed to modulate DNA methylation or histone modifications. One of the drug targets are chromatin readers such as the bromodomain and extra-terminal (BET) protein family whose conserved bromodomain binds to specific epigenetically modified sites [113]. BET inhibitors such as iBET 762 have recently shown promising efficacy in preclinical models for cancer treatments with clinical trials underway for breast and lung cancer treatments (NCT02964507, NCT01587703). Additional studies focused on iBET's involvement in the tumor microenvironment. A 1-week short-term experiment showed an increase in helper T cells in the spleen of iBET-treated mice, but a 9-week study found a decrease in helper T cell population in the mammary glands of iBET-treated mice [79]. As a chemopreventive agent, oral treatment (60 mg/kg) of iBET significantly delayed mammary gland tumor formation by 3 weeks compared to control treatment in the MMTV-PyMT GEMM [79]. This 60 mg/kg dose was well tolerated with no signs of toxicity in mice [79].

### **Vitamins and Micronutrients.**

Vitamins and micronutrients have been found to impact various pathways in BC development. Among these, vitamin D3, folate, omega-3 polyunsaturated fatty acids, piperine, sulforaphane, indole-3-carbinol, epigallocatechine gallate, and quercetin along with curcumin have extensively been reviewed [114].

### **Curcumin.**

Curcumin is a hydroponic phenol derived from turmeric that has gained attention in the scientific community over the past decade for its effects as an anticancer agent. However, a large dose is required for effectiveness due to its low absorption. In vitro studies on curcumin have shown inhibition of migration, invasion, and angiogenesis, as well as induction of apoptosis and tumor suppressor genes [115]. Xenograft mouse models given oral doses of dendrosomal curcumin support these findings by showing reductions in

tumor size, weight, and incidence compared to controls. Suppression of NF- $\kappa$ B, COX-2, and VEGF in these treated mice further supports curcumin as an anti-metastatic cancer agent [84]. Several clinical trials of curcumin in treatment of BC alone, or in combination with chemotherapy are currently active (NCT03980509, NCT03072992, NCT01740323, NCT01975363).

### **Rank.**

RankL is a protein secreted from osteoblasts which are most commonly known for their role in the formation of osteoclasts and bone remodeling. However, RankL is also expressed in the mammary gland during development and tumor formation [116–118]. Expression of RankL has been documented in BC cell lines and is associated with increased proliferation and poor survival in primary human BC [81]. Therefore, suppression of RankL is a promising new strategy in BC prevention. Xenograft mouse models given a RankL inhibitor, OPG-Fc, had increased tumor latency and reduced hyperplasia compared to the control mice. This was also supported in GEMMs treated with RankL-specific monoclonal antibodies [82].

### **Prophylactic Vaccines.**

In the late 2000s, there was a great interest in developing universal preventive vaccines against BC, in part spurred by the success of preventive vaccines against HPV-associated cervical cancer [119,120]. The Artemis project is the most well-known effort, supported by the National Breast Cancer Coalition and their initiative, to know how to eradicate BC by 2020 [121]. The scientific premise is to mount a specific immune response against mammary epithelial cells that would eliminate any neoplastic BC cells. As this initiative moved forward, the Artemis project Steering Committee in consultation with the FDA and other agencies raised concerns about clinical translation [122]. The main concern was the lack of a known antigen that would be expressed in 100% of the cells of all BC tumors.  $\alpha$ -lactalbumin, mammaglobin-A, HER2, and survivin are among the best candidates, but studies suggest that none of them are represented in more than 80% of tumors [123]. More recently, the focus of the Artemis project has shifted from universal prophylaxis as primary prevention to targeted vaccination of specific subgroups of high-risk individuals for primary

prevention or in specific patient subgroups to prevent metastatic recurrence [123]. Despite these caveats and challenges for a universal vaccine, progress has been made both in preclinical models and clinical trials that suggest the refinement and selection of the target population and combinatorial approach of vaccination, immunotherapy, and/or immune modulation could increase therapeutic efficacy in a preventive setting [119,120,124].

Preclinical models have shown a significant delay in tumor formation in mice vaccinated against  $\alpha$ -lactalbumin [75,77] and HER2 [76,77].  $\alpha$ -lactalbumin is expressed at high levels exclusively during lactation in normal mammary epithelial cells, but  $\alpha$ -lactalbumin expression is upregulated in about 50% of hormone receptor-positive and more than 70% of triple-negative BC tumors [119]. Subcutaneous injection of  $\alpha$ -lactalbumin protein significantly delayed tumor formation in the MMTV-ErbB2 GEMM and elicited anti- $\alpha$ -lactalbumin-specific T cell response. However,  $\alpha$ -lactalbumin vaccination can inhibit tumor growth but cannot delay tumor formation in more aggressive BC models [75,125]. In late 2020, a phase I clinical trial (NCT04674306) was started to investigate the safety of  $\alpha$ -lactalbumin vaccine as adjuvant therapy in triple-negative BC patients at high risk of recurrence. HER2 is overexpressed in 20–30% of invasive BC tumors but expressed at very low levels in normal mammary epithelia. Intramuscular injections of virus-like particles studded with full-length HER2 or oncogenic variant Delta16HER2 extracellular domains in GEMMs significantly delayed or prevented tumor formation along with eliciting a robust anti-HER-2 production immune response [76]. A dendritic cell-mediated vaccine against HER2 also provided a tumor prevention effect in the full-length HER2-driven GEMM [77]. Mammaglobin A is a small glycoprotein that belongs to a family of epithelial secretory proteins. Mammaglobin A expression is upregulated in 40–80% of BCs [126]; unlike  $\alpha$ -lactalbumin and HER2, mammaglobin A is more broadly expressed in normal mammary epithelial cells. Mammaglobin-A is exclusively expressed in BC cells, making it a suitable targeted protein for BC immunotherapy. Intramuscular injections of Mammaglobin A cDNA inhibit the growth of established tumors derived from multiple human BC cell lines in SCID-beige host animals and elicit a strong anti-Mammaglobin A T cell response [127,128]. Using this DNA vaccination approach

(**Figure 1.3A**), anti-mammaglobin-specific T cells are readily detected in treated preclinical models, BC patients in phase 1 clinical trials, and metastatic BC patients in phase 1 clinical trials (NCT00807781) [89,129]. The results of this phase 1 clinical trial demonstrated the safety of this DNA vaccine and suggested a therapeutic effect based on extended progression-free survival of vaccinated participants [129]. These encouraging results have led to the ongoing phase 1b clinical trial (NCT02204098) investigating mammaglobin-A DNA in non-metastatic BC patients undergoing neoadjuvant endocrine therapy or chemotherapy [126]. However, this DNA vaccination approach has not been tested in a primary prevention setting in either preclinical models or in clinical trials.

### **Local Approaches for Primary Prevention in Preclinical Models and Clinical Trials.**

Each of the two mammary glands of a woman contains 8–12 ductal trees with the main duct of each tree opening at the nipple orifice [27,28]. The main function of these ductal tree systems is to produce, express, and deliver milk during lactation. Alveolar cells arranged in lobules at the ends of the ductal tree produce and secrete milk components into ductules that join into larger ducts and eventually the main duct to transport the milk outwardly. Breast carcinoma predominantly arises from the terminal ductal lobular units (TDLUs) [130,131] within a single ductal tree [26]. Remodeling of TDLUs during an individual's childbearing years and aging influences cancer risk. Epidemiological and genetic susceptibility studies suggest that the number and differentiation state of mammary epithelial cells correlated with BC risk; for example, increased lobular involution (fewer TDLU) as a result of the aging process is protective against BC [132–134]. The opening at the nipple into the ductal tree offers a unique opportunity for BC prevention by directly targeting the epithelial cells of the ductal tree. In 2002, Sivaraman et al. introduced the concept of local ablation for primary prevention and local treatment of early BC by intraductal (ID) delivery of a suicidal gene system [97]. Although this study was unsuccessful in reducing tumor incidence, it unveiled a new approach and local strategy for BC prevention. Within the last twenty years, several groups have built on this local treatment concept that focuses on the ductal tree as a functional unit consisting of individual pre-malignant and/or malignant cells for primary prevention of BC (**Table 1.3**). A common theme of many

of these local approaches is the delivery of the active compound at a lower dose that achieves the same efficacy on targeted cells and/or minimizes the undesired side effects of systemic exposure (**Figures 1.1D,E, 1.2B–D, and 1.3B–E**).

### **Gene Therapy.**

Gene therapy utilizes DNA or RNA sequences to modify gene activity or expression. Some gene therapy approaches such as viral delivery of DNA or genetic editing of a patient's genome may offer a more permanent treatment compared to continuous and multi-dose treatment of chemoprevention and endocrine therapies. Here, we discuss the ID delivery of components of different gene therapy platforms.

### **Suicide Gene Therapy.**

An adenoviral vector was used to intraductally deliver a thymidine kinase-based suicidal gene system in an N-methyl-N-nitrosourea (MNU)-induced rat model of BC [97]. The therapeutic intent was to prevent tumor formation by ablating the proliferating cells of the terminal end buds akin to human TDLUs. However, treated rats paradoxically developed tumors earlier than control rats despite the high transduction efficiency, high thymidine kinase expression, and 50–90% epithelial ablation by suicidal gene activation.

### **RNAi-based Gene Silencing.**

ID delivery of lipidoid nanoparticles containing small interfering RNAs (siRNAs) against *Hox1A* in the C3(1)-TAg GEMM resulted in a significant delay in tumor latency [98]. *Hox1A* is a homeodomain transcription factor involved in autocrine growth hormone dysregulation and was identified as an early driver of mammary cell carcinogenesis [98]. Knocking down *Hox1A* mRNA maintained hormone receptor status and reduced the proliferative rate of pre-malignant cells [85]. Remarkably, researchers were able to sustain this knockdown effect by repeatedly cannulating and delivering 20  $\mu$ L of therapeutic siRNAs in nine biweekly procedures without causing any damage or perforation to ductal trees. This study also

demonstrated the efficiency of in vivo transfection of the ductal tree using components of RNAi technology and opened the possibility of introducing components of other gene-silencing or -editing technologies.

### **CRISPR-based Genetic Editing.**

CRISPR/Cas9 is a versatile gene-editing tool to produce loss of function or knockout alleles in in vitro cell line systems and in vivo animal models [135]. CRISPR technology has already reached the clinical trial stage. Although the majority of these trials involved ex vivo editing of hematopoietic stem cells and T cells, in vivo editing of liver cells with a systemic delivery approach and eye cells with a local delivery approach have been successful [135]. ID delivery of the CRISPR system to target mammary epithelial cells has been applied to develop new models of BC and to study cooperative interactions of multiple driver genes [136–140]. ID delivery of CRISPR components (Cas9 mRNA and guide RNA) via lentiviral vector achieved up to 21.5% editing efficacy of the target gene [137]. An alternative approach to minimize the immunogenicity of de novo Cas9 expression is to intraductally deliver the guide RNA in a lentiviral vector in animals endogenously expressing Cas9 [137,140]. Up to 32.6% editing efficacy of the target gene may be achievable using this modified system [140]. Although further development of this technology will be required to identify a safe delivery system with an improved editing efficacy, ID delivery of CRISPR or similar system for editing and/or inactivation of early driver genes of mammary carcinogenesis such as estrogen receptor  $\alpha$  (*ESR1*), *HOXA1*, and/or *EGFR* may offer new opportunities for BC prevention. It is tempting to speculate that such genetic editing approaches to dampen mitogenic activity of ER signaling may provide a local alternative to systemic hormonal control but with minimal adverse effects (**Figure 1.2D**).

### **Local Hormone Therapy.**

Different approaches are being investigated to minimize side effects of systemic hormone therapy. More readily available than the above-mentioned genetic editing approach is the local delivery of a selective

estrogen receptor modulator (SERM) or degrader (SERD). Local delivery methods include topical transdermal gel application, ID injection, and slow-releasing drug implants (**Figure 1.2B** and C).

### **Transdermal Gel for Hormone Therapy.**

Topical application to the skin of the breast area of a gel containing active metabolite 4-hydroxy tamoxifen achieved a high local concentration of this SERM [141,142]. A phase 2 clinical trial (NCT00952731) divided 27 women diagnosed with DCIS into two groups to receive transdermal gel application or tamoxifen orally for six to ten weeks before surgery. Due to the early stage of the disease, the proliferation index Ki-67 was used as the endpoint rather than tumor incidence. Compared to pre-treatment tissue samples, the proliferative index was reduced by 52% in the transdermal gel group and by 61% in the tamoxifen group. At a local level, both groups had the same concentration of this SERM. Systemically, the transdermal gel group had reduced plasma concentrations of the SERM compared to the tamoxifen group. However, side effects such as hot flashes did not significantly differ between the two groups [59]. The timeframe of this study limited the assessment of long-term side effects, but this is currently being evaluated in a phase 2 clinical trial (NCT03063619) whose primary objective is to determine risk reduction in BC by transdermal gel application (**Table 1.1, Figure 1.2B**). An alternative study was conducted using z-form endoxifen, a tamoxifen metabolite with the highest affinity to the ER, to study BC prevention [71]. Groups of 30 women self-applied 10 mg, 20 mg, or a placebo topically to each breast daily for three months and were monitored for breast density changes, systemic side effects, and plasma concentration of endoxifen [71]. Before the end of the three-month period, there was a significant decrease in mammographic density of women applying 20 mg endoxifen which was not seen in the 10 mg treatment group. Dose-dependent plasma concentrations of endoxifen were observed in the treatment groups without systemic side effects [71]. However, severe skin reactions occurred in both treatment groups which caused almost all women (58 out of 60) to prematurely discontinue the gel application and no therapeutic window was identified [58]. Therefore, endoxifen has the potential to reduce BC incidence but requires further studies due to severe skin toxicity.

### **Intraductal Hormone Therapy.**

ID delivery of tamoxifen did not provide a protective effect on an MNU-induced rat model of BC most likely due to the lack of active metabolite production in the liver. However, ID delivery of 4-hydroxytamoxifen provided a protective effect comparable to subcutaneous injection of tamoxifen [91]. Fulvestrant acts as a selective estrogen receptor degrader (SERD). Fulvestrant binds with a higher affinity to the ER than tamoxifen and unlike tamoxifen is a pure antagonist by degrading ER upon binding [143]. ID delivery of fulvestrant in a mammary intraductal (MIND) ER+ MCF7 xenograft model provided superior protection than intramuscular injection, whereas ID delivery of fulvestrant provided a protective effect comparable to intramuscular injection in an MNU-induced rat model [95]. Locally delivered fulvestrant was more effective at inhibiting cell proliferation, angiogenesis, and decreasing ER expression. In both mouse and rat models, the total amount of fulvestrant received per animal was the same by ID delivery (fragmented dosing per ductal tree) and by intramuscular injection [95]. A phase 2 clinical trial (NCT02540330) was initiated to investigate the pharmacokinetics and local and systemic side effects of ID delivery compared to intramuscular injection (**Table 1.1, Figure 1.2C**). However, due to a business decision, the study was terminated after the recruitment of only three participants.

### **Slow-release Implant of Hormone Therapy.**

To expand on the application of fulvestrant as a local long-term prevention treatment, bilateral fulvestrant-loaded silastic tubing was subcutaneously implanted next to the abdominal mammary glands of NSG mice [96]. One week after implantation, the mice were orthotopically injected with MCF7 cells in both fat pads of the abdominal glands [96]. A significant tumor growth reduction was observed in the fulvestrant-loaded silastic tubing group compared to vehicle control treatment [96]. Importantly, the treatment efficacy of fulvestrant-loaded implants was very similar to weekly treatment with subcutaneous injection of fulvestrant. This is an encouraging study to consider for local drug delivery to the mammary gland. However, more investigations are needed to have a more controlled and homogenous release of fulvestrant or other drugs throughout the entire mammary gland since a much more pronounced decrease in the Ki-67 proliferation

marker was measured in tumor areas adjacent to the tubing implant [96].

### **Intraductal Chemotherapy and Targeted Treatments.**

Several research groups have used ID delivery of cytotoxic compounds, targeted agents, and/or targeted particles for both primary prevention of BC (**Table 1.3, Figure 1.3C–E**) and preclinical models for local disease control [144].

### **Infusion of Cytotoxic Agents.**

Cytotoxic compounds such as pegylated liposomal doxorubicin, carboplatin, or paclitaxel when ID delivered in the chemically induced (MNU) rat model significantly reduced tumor incidence [90–92]. Similarly, liposomal doxorubicin showed greater therapeutic efficacy at reducing tumor incidence when ID was delivered rather than systemic administration in the genetic MMTV-ErbB2 mouse model [91]. Several groups have already tested the feasibility of this approach in first-human clinical studies. Stearns et al. 2011 reported an 88% success rate by administering pegylated liposomal doxorubicin into one ductal tree per patient [92]. Love et al. 2013 reported a 96.6% success rate in administering pegylated liposomal doxorubicin into 5-8 ductal trees per patient [145]. These studies provide strong support for the translational feasibility of ID delivery of cytotoxic or other solutions. Unfortunately, local cytotoxic treatment with pegylated liposomal doxorubicin, 5-fluorouracil, and/or cisplatin can induce tumors with long latency in non-transgenic animals [89,94,146]. This result has diminished enthusiasm for such local chemotherapy delivery unless it is needed to minimize systemic exposure [89,146].

### **Infusion of Targeted Agents.**

*Pseudomonas* exotoxin has been engineered to serve as an anti-cancer agent thanks to its effect on protein translation and cell death [147]. However, systemic delivery of this exotoxin has undesired effects that lead to inflammation and vascular leakage. Transferrin receptor is overexpressed in the majority of BC cells, in many cases starting at a preneoplastic stage. To harness the anti-tumoral effect of this exotoxin, but to keep

it contained locally within the ductal tree, Wang et al. 2022 fused a monoclonal antibody targeting the human transferrin receptor to a 40 kDa fragment of this exotoxin [100]. ID delivery of this antibody–toxin conjugate shows therapeutic efficacy in HER2+ MIND models of MCF7 and SUM225 human BC cells that recreate the early stage of DCIS lesions [100]. A similar approach was utilized to deliver an  $\alpha$ -emitter radionuclide, as the killing agent, conjugated to a HER2-targeting antibody (trastuzumab).  $\alpha$ -emitters can cause irreparable double-strand DNA damage that leads to cell death [148]. The radionuclide used in this study was  $^{225}\text{Ac}$  with a half-life of 9.9 days [148]. ID delivery of this antibody– $^{225}\text{Ac}$  conjugate shows therapeutic efficacy in the HER2+ MIND model of SUM225 BC cells [99]. However, this treatment can induce tumor formation in the mammary gland or lung due to sustained radiation exposure [99]. As the field of radionuclides and conjugation chemistry continues to mature [148,149], the use of  $\alpha$ -emitters with shorter half-life (<12 h) such as  $^{211}\text{At}$  and  $^{212}\text{Pb}$  could minimize the undesirable iatrogenic effects of trastuzumab– $^{225}\text{Ac}$ . Although these studies were proof-of-concept for clinical treatment of DCIS due to the requirement of transferrin receptor or HER2 expression, conjugating these cell-killing agents to other antibodies, peptides, or targeting moieties could expand their applications to primary prevention of BC and/or local control of uninvolved ductal trees in DCIS-affected breast. Similarly, antibody–drug conjugates [150] such as trastuzumab deruxtecan for HER2-low BC and sacituzumab govitecan for triple-negative BC could be considered for primary prevention.

### **Ductal Tree Ablation.**

We have been intrigued by the concept of a universal prophylactic intervention for several years. Our approach aims at combining the effectiveness of prophylactic mastectomy, with the universality of an ideal vaccine and delivery method of ID chemotherapy (**Figures 1.1D** and **1.3B**). We are investigating different chemical and thermal ablation approaches to locally kill mammary epithelial cells while causing minimal collateral tissue damage and side effects. We have extensively studied ethanol as a cell-killing solution for chemically ablating the ductal tree [101,151–155]. In clinical settings for ablation or sclerotherapy, tens of

milliliters of 95–100% ethanol (EtOH) can be locally delivered to the target area [156–170]. In some procedures up to 50 mL of EtOH can be administered per session, indicating its low toxicity [156,166]. We have demonstrated in preclinical rodent models the feasibility of ablating the entire ductal tree system before epithelial cells become malignant [101,152,153]. Our study in the C3(1)-TAg GEMM showed that ID injection of 70% EtOH significantly delayed tumor formation and reduced tumor incidence [101]. ID injection of 70% EtOH provides similar or superior tumor risk reduction compared to other prevention interventions in this or similar GEMMs (**Table 1.3**; refs [91,98]). This chemical ablation approach has advantages over other ID approaches for clinical translation. It would be a one-time treatment in contrast to other ID approaches that require repeated administration of active agents which can be a challenge, especially for chemotherapy agents that may compromise ductal tree structure and leak out of intended targeted area in later cycles. Currently, there are no reports linking clinical uses of EtOH to iatrogenic cancer, but this is a concern for other local treatments that cause DNA damage such as radioimmunotherapy and chemotherapy (**Figure 1.3D and E**; refs [94,99,146,171]). The International Agency for Research on Cancer considers EtOH to be carcinogenic to humans [172]; however, this is based on chronic exposure to EtOH as an alcoholic beverage. EtOH is metabolized into acetaldehyde, a toxic chemical that causes DNA damage and DNA-protein cross-linking. This is considered a main contributing mechanism for EtOH-induced cancers but the exact molecular mechanism(s) of EtOH and increased cancer risk is not fully established [172]. No significant DNA damage was seen with acute EtOH exposure in mice [173,174]. Our studies showed no evidence of iatrogenic effects of EtOH injections in non-transgenic mice after 22 months of follow-up [101]. There are also some unique challenges with this chemical ablation approach. Image guidance will be required for precisely infusing each ductal tree with the appropriate volume. We and others have used different contrast agents for in vivo imaging of the ductal tree in rodents [101,151–154,175,176] and rabbits [177] after ID infusion. Controlling the diffusion of EtOH outside the ductal tree will be required to further minimize collateral tissue damage [101]. The use of ethyl cellulose as a gelling agent to limit ethanol diffusion has been reported for clinical treatment of venous malformation and in preclinical models of BC, cervical cancer, and liver cancer [152,159–165,178]. We have shown that ethyl cellulose is

compatible with a 70% EtOH ablative solution and with imaging contrast agents such as tantalum oxide nanoparticles in both mouse and rat models [152,153].

Similar to chemical ablation, thermal ablation aims to target the ductal tree with minimal collateral damage and improved cosmesis. This technique uses physical energy to raise or lower the temperature to internally target local tumors instead of surgical removal [180]. Procedures such as microbubble solutions with high-intensity ultrasound or an iron rod nanoparticle solution coupled with a magnetic field have been previously used in cancer models such as pancreatic xenograft mouse models [181,182]. These thermal ablation techniques, coupled with their imaging abilities, may be applied toward targeting epithelial cells within the ductal tree for BC prevention.

### **Conclusions and Future Directions.**

BC is the leading cause of new cancer cases and is the second leading cause of cancer-related deaths in women. The limited, approved prevention interventions available for high-risk individuals can have severe and long-term side effects that deter many women from making proactive choices. Regrettably, BC prevention is an area of translational research that is currently underfunded by federal agencies [183]. Therefore, emerging, and novel approaches for the primary prevention of BC that provide the same or superior protection while minimizing the side effects of current interventions should be pursued and prioritized. These approaches seek to eradicate BC and align well with NIH's All of US Research Program—a nationwide initiative for precision health interventions that proactively prevent rather than treat disease in high-risk individuals. We provide a comprehensive review of emerging approaches for BC prevention based on non-modifiable risk factors that put women at a higher risk of developing BC. Virtually all of these studies were performed in rodent models of BC, which have some limitations and challenges for direct translation to at-risk individuals. Additional scalability and validation studies in larger animal models will be an important step in bridging the gap between discovery and clinical evaluation. Although currently underutilized, rabbit studies should be considered as an appropriate intermediate model. Evolutionarily, anatomically, and physiologically, rabbit mammary glands are more similar to humans than

those of rodent models or other large animals such as cows and sheep [184,185]. Female rabbits have four pairs of mammary glands each containing four ductal trees [177], which can be cannulated for ID injection [177,186–190] using a procedure very similar to ID administration of contrast agents in clinical ductography [191,192] and chemotherapeutic agents in first-in-human clinical research [92,145]. Alternatively, or complementary to validation studies in larger animals, judicious determination based on the scientific rigor and clinical feasibility of these emerging approaches should be applied to prioritize those interventions more likely to have an impact on primary prevention of BC.

## Figures

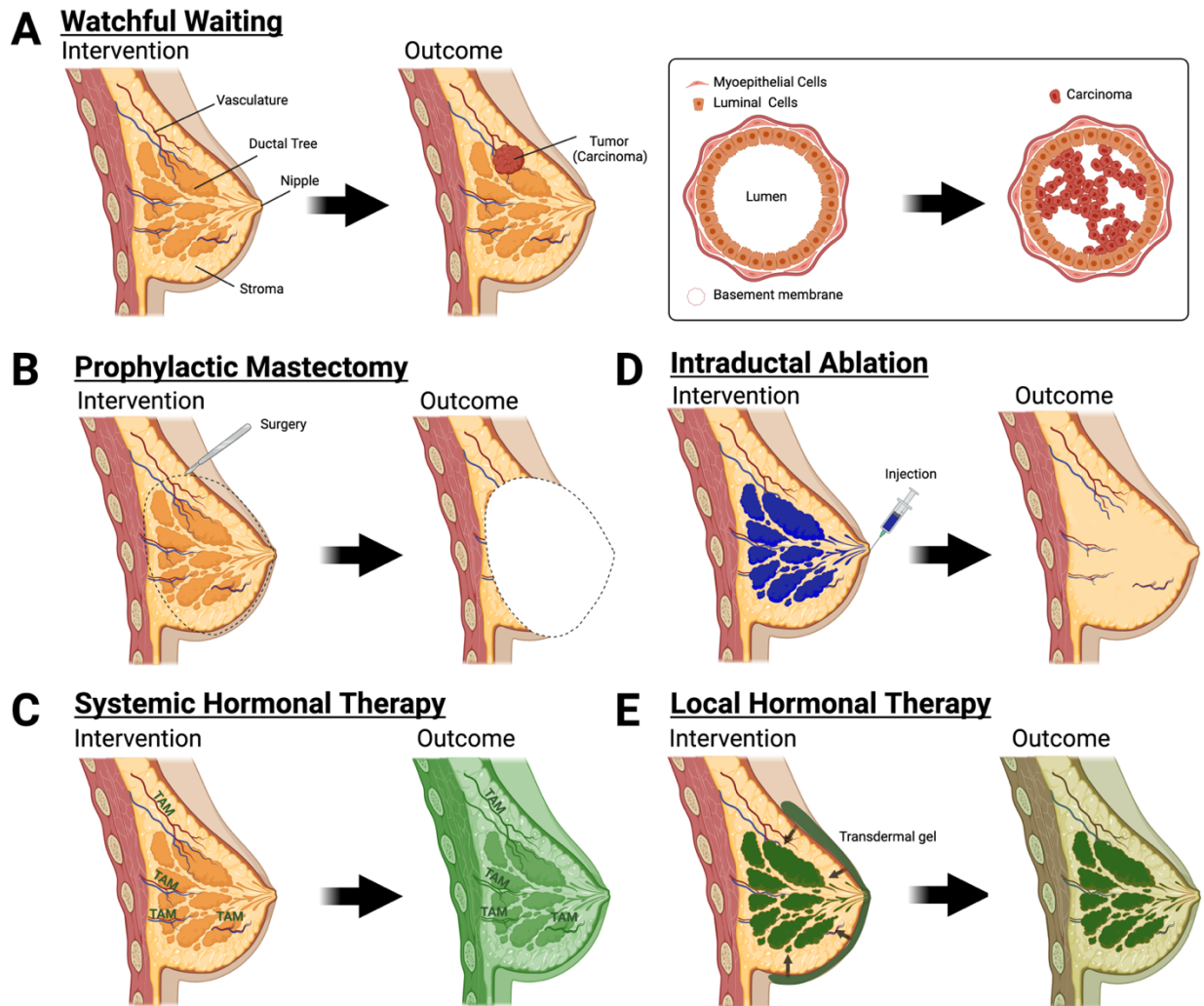


**Figure 1.1. Evidence-based and investigational approaches for primary prevention.** **A)** Watchful waiting with no preventive outcome. **B)** Bilateral prophylactic mastectomy is an effective risk-reducing surgery. **C)** Hormonal therapy such as tamoxifen (TAM) or raloxifene can reduce risk but with high systemic exposure (dark green shading). **D)** and **E)** Intraductal approaches for breast cancer prevention. **(D)** Intraductal injections ablate epithelial cells leaving the breast stroma intact. **(E)** Local hormonal therapy with moderate systemic exposure (light green shading).

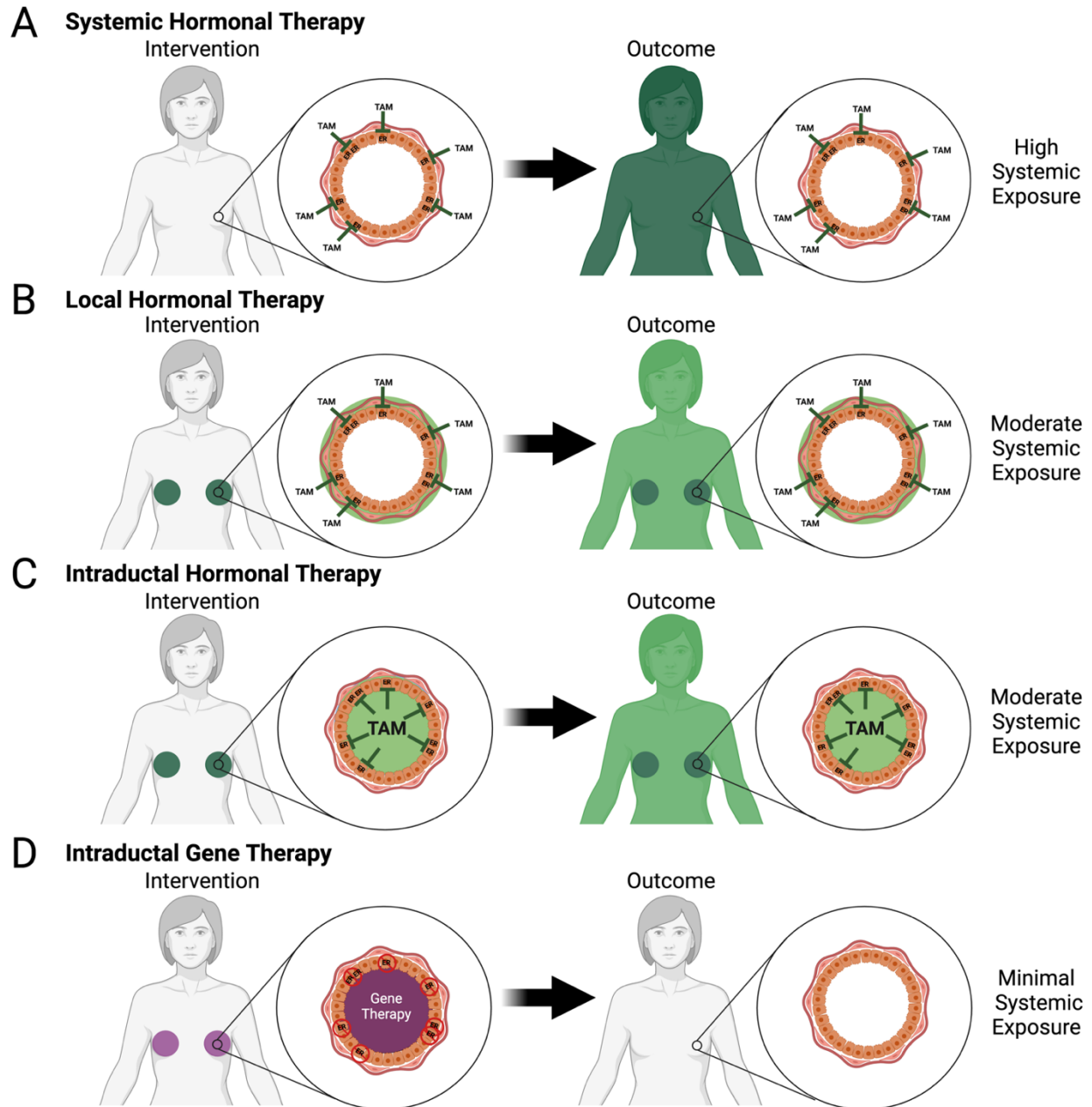


**Figure 1.2. Systemic and local hormone therapy approaches for breast cancer prevention. A)** Systemic hormonal therapy with high systemic exposure (dark green shading). **B)** Local hormonal therapy with concentrated exposure to the ductal tree (dark green shading) and moderate systemic exposure to the body (light green shading). **C and D)** Intraductal delivery directly to the ductal tree by hormonal therapy with moderate systemic exposure (light green shading) or gene therapy with minimal systemic exposure (no shading).

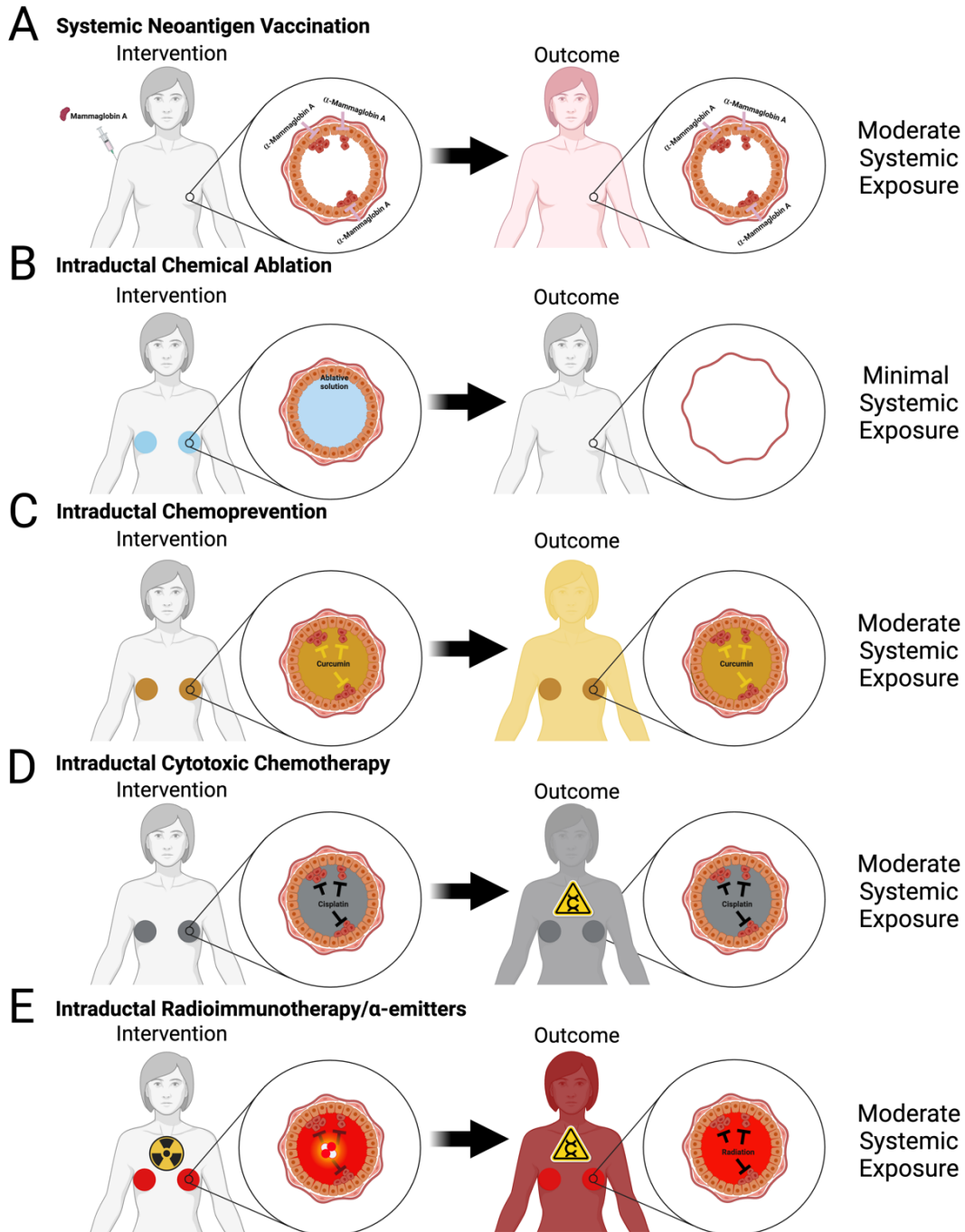


**Figure 1.3. Systemic vaccination and intraductal approaches for breast cancer prevention.** A) Vaccines target cancer cell-expressed proteins and mount an immune response against (pre)malignant epithelial cells. B–E) Intraductal injections provide direct delivery to epithelial cells that may become malignant. This form of delivery can be used with multiple solutions including ablative solutions (ethanol in (B)), chemopreventives (curcumin in (C)), cytotoxic chemotherapeutics (cisplatin in (D)), or radioimmunotherapy/α-emitters in (E). Intraductal chemical ablation and vaccines only require 1–2 injections and have minimal to moderate systemic exposure, unlike cytotoxic chemotherapeutics-radioimmunotherapeutics with potential iatrogenic carcinogenesis.

## Tables

**Table 1.1. New approaches for primary prevention of breast cancer in clinical trials.**

Approach	Intervention	Active Agent	Number of Participants	Results	Reference(s)
Hormonal therapy	Local	Endoxifen gel	90	1.9% Reduction in mammographic density	NCT04616430, Completed [71]
		4-Hydroxytamoxifen transdermal gel	194	52% Decrease in Ki-67 labeling index	NCT03063619, Active [72]
		Fulvestrant	3	N/A	NCT02540330, Terminated
	Systemic	Aromatase inhibitors (Anastrozole)	3864	N/A	NCT00078832, Completed
		Aromatase inhibitors (Letrozole)	55	N/A	NCT00579826 Completed
Chemoprevention		Retinoid (Fenretinide)	20	≤50% Risk reduction	NCT01479192 [58,73] Terminated

**Table 1.2. Systemic approaches for breast cancer prevention in preclinical models.**

Approach	Active Agent	Experimental Model <sup>1</sup>	Level of Evidence <sup>2</sup>	Results	Reference (s)	
Prophylactic Vaccine	α-Lactalbumin	MMTV-HER2 ( <i>n</i> = 6)	A	Increased latency ( <i>p</i> -value = 0.0004)		
		MMTV-PyMT ( <i>n</i> = 8)	D	Reduced tumor burden ( <i>p</i> -value < 0.0006)	[75]	
		4T1 isograft ( <i>n</i> = 8)	D	Reduced tumor burden until day 13 post injection ( <i>p</i> value = 0.0006)		
	HER2	MMTV-HER2 ( <i>n</i> = 10)	A	Increased latency ( <i>p</i> -value < 0.01)	[76]	
	HER2	MMTV-HER2 ( <i>n</i> = 5–8)	A	Increased latency ( <i>p</i> -value < 0.02)	[77]	
Chemo-prevention	Erlotinib	<i>Brcal</i> <sup>fl/fl</sup> ; Trp53 <sup>+/-</sup> ; MMTV-Cre ( <i>n</i> = 13)	A	Increased latency ( <i>p</i> -value = 0.0001)	[78]	
	I-BET 762	MMTV-PyMT ( <i>n</i> = 13)	B	Increased latency ( <i>p</i> -value < 0.05)	[79]	
	CCDO-Me	<i>Brcal</i> <sup>fl/fl</sup> ; Trp53 <sup>+/-</sup> ; MMTV-Cre ( <i>n</i> = 15)	A	Increased latency ( <i>p</i> -value < 0.05)	[80]	
	RankL inhibitor	<i>Brcal</i> <sup>fl/fl</sup> ; Trp53 <sup>+/-</sup> ; MMTV-Cre ( <i>n</i> = 17)	A	Increased latency ( <i>p</i> -value < 0.001)	[81]	
	RankL monoclonal antibody	<i>Brcal</i> <sup>fl/fl</sup> ; MMTV-Cre ( <i>n</i> = 9)	A	Increased latency ( <i>p</i> -value < 0.001)	[82]	
	Cox-2 inhibitor	MMTV-ErbB2 ( <i>n</i> = 24)	A	Reduced tumor incidence ( <i>p</i> -value = 0.003)	[83]	
	Curcumin	4T1 isograft ( <i>n</i> = 9)	C	Reduced tumor burden ( <i>p</i> -value < 0.05)	[84]	
	Bis-phosphonates (zoledronic acid and risdrionate)	MDA-MB-231 xenograft ( <i>n</i> = 12)	D	Reduced tumor burden ( <i>p</i> -value < 0.05)	[85]	
	Rexinoids (Bexarotene)	MMTV-ErbB2 ( <i>n</i> = 20)	A	Increased latency ( <i>p</i> -value < 0.0001)	[86]	
		MMTV-ErbB2 ( <i>n</i> = 19)	A	Increased latency ( <i>p</i> -value < 0.001)	[87]	
	JAK3 and EGFR inhibitor (WHI-P131)	DMBA-induced Balb/c mice ( <i>n</i> = 20)	B	Increased latency ( <i>p</i> -value = 0.0014)	[88]	
	Cytotoxic	Paclitaxel	DMBA-induced Balb/c mice ( <i>n</i> = 20)	B	Increased latency ( <i>p</i> -value = 0.0041)	[88]

Notes: <sup>1</sup> “*n*” denotes the number of animals in investigational treatment group instead of overall number of animals in all groups of the study. <sup>2</sup> A = animals were observed for 6 months to 2 years; B = for 8 weeks to 6 months; C = for 4 to 8 weeks; D = for <4 weeks. Abbreviations: Brca: breast cancer gene, CDDO-me: 2-Cyano-3,12-dioxooleana-1,9(11)-dien-28-oic acid methyl ester, Cox-2: Cyclooxygenase-2, Cre: cre-

**Table 1.2. (cont'd)**

recombinase, DMBA: 4,7,12-Dimethylbenz[a]anthracene, EGFR: epidermal growth factor receptor, Erbb2: avian erythroblastic leukemia viral oncogene homolog 2, HER2: human epidermal growth factor receptor 2, I-Bet: inhibitor of Bromodomain and extra-terminal domain, Jak3: Janus Kinase 3, MMTV: Mouse Mammary Tumor Virus, Py-MT: polyoma middle tumor-antigen, RankL: receptor activator of nuclear factor kappa beta ligand, Trp53: Tumor Protein P53.

**Table 1.3. Intraductal and local approaches for breast cancer prevention in preclinical models.**

Intervention	Active Agent	Experimental Model <sup>1</sup>	Level of Evidence <sup>2</sup>	Results	Reference (s)
Chemo-prevention	Oral-free curcumin	free MNU-induced Sprague Dawley rats ( <i>n</i> = 12)	A	Reduced tumor incidence (HR = 3.95, <i>p</i> -value 0.007)	
	Intraductal curcumin			Reduced tumor incidence (HR = 2.85, [89] <i>p</i> -value 0.020)	
	Nanocurc encapsulated curcumin		A	Reduced tumor incidence (HR = 2.88, <i>p</i> -value 0.028)	
Cytotoxic	Paclitaxel	MNU-induced Sprague-Dawley rats ( <i>n</i> = 15)	A	Reduced tumor burden ( <i>p</i> -value < 0.05)	[90]
	Pegylated Liposomal Doxorubicin	MMTV-ErbB2 ( <i>n</i> = 12)	B	Reduced tumor incidence (HR = 6.40, [91] <i>p</i> -value < 0.0001)	
		MNU-induced Sprague Dawley rats ( <i>n</i> = 15)	B	Reduced tumor incidence ( <i>p</i> -value < [91] 0.001)	
		MNU-induced Sprague Dawley rats ( <i>n</i> = 5)	B	No change compared to control	
	5-fluorouracil	MNU-induced Sprague Dawley rats ( <i>n</i> = 5)	B	Reduced tumor incidence (HR = 3.30, <i>p</i> -value = 0.018)	
	Carboplatin	MNU-induced Sprague Dawley rats ( <i>n</i> = 5)	B	Reduced tumor incidence (HR = 10.4, [92] <i>p</i> -value < 0.0001)	
	Nanoparticle albumin-bound paclitaxel	MNU-induced Sprague Dawley rats ( <i>n</i> = 5)	B	No change compared to control	
	Methotrexate	MNU-induced Sprague Dawley rats ( <i>n</i> = 5)	B	No change compared to control	
	Nanoparticle albumin-bound paclitaxel	MNU-induced Sprague Dawley rats ( <i>n</i> = 6)	B	Reduced tumor burden ( <i>p</i> -value < [93] 0.05)	
Cisplatin	<i>Brcal</i> <sup>fl/fl</sup> Trp53 <sup>L/L</sup> ; WAPcre ( <i>n</i> = 20)	A	Increased latency ( <i>p</i> -value < 0.0001)	[94]	

**Table 1.3. (cont'd)**

Hormonal therapy	4-hydroxytamoxifen (4-OHT)	MNU-induced Sprague Dawley rats ( $n = 20$ )	A	Reduce tumor incidence ( $p$ -value < [91] 0.0001)
	Fulvestrant	MIND MCF-7 xenograft ( $n = 3$ )	B	Reduced tumor burden ( $p$ -value < 0.001)
		MNU-induced Sprague Dawley rats ( $n = 10$ )	B	Increased latency ( $p$ < [95] 0.0001), reduced tumor incidence (HR = 2.08)
	Fulvestrant and silastic tubing	MCF-7 xenograft ( $n = 8$ )	C	Reduced tumor burden ( $p$ -value < [96] 0.05)
Suicidal gene vector	Adenovirus vector with thymidine kinase and gancyclovir	MNU-induced Wistar Furth rats ( $n = 30$ )	A	(paradoxical) Decreased latency and increased tumor incidence [97]
Gene silencing	Liposomal siRNA silencing	Hox1AC3(1)-TAg ( $n = 8$ )	B	Reduced tumor incidence [98]
Radio-immunotherapy	Radio-conjugated trastuzumab	MIND SUM225 xenograft ( $n = 3, 4$ )	C	Dose-dependent reduced tumor burden [99]
Targeted immunotoxin	Anti-transferrin receptor-antibody conjugated pseudomonas exotoxin	MIND MCF7 xenograft ( $n = 20$ )	C	Increased latency and reduced tumor burden [100] ( $p$ -value < 0.001)
Chemical ablation	Ethanol	C3(1)-TAg ( $n = 13$ )	A	Increased latency ( $p$ -value < 0.0001), reduced incidence [101] (HR = 4.76, $p$ -value < 0.0001)

Notes: <sup>1</sup> “ $n$ ” denotes the number of animals in the investigational treatment group instead of the overall number of animals in all groups of the study. <sup>2</sup> A = animals were observed for 6 months to 2 years; B = for 8 weeks to 6 months; C = for 4 to 8 weeks; D = for < 4 weeks. *Abbreviations*: Brca: breast cancer gene, Cre: cre-recombinase, Erbb2: avian erythroblastic leukemia viral oncogene homolog 2, Hox1A: homeobox protein 1A, MIND: Mouse Mammary Intraductal, MMTV: Mouse Mammary Tumor Virus, MNU: *N-methyl-N-nitrosourea*, siRNA: short interfering RNA, Trp53: Tumor Protein P53, WAPcre: Whey Acidic Protein Cre-Recombinase.

## REFERENCES

1. Siegel RL, Miller KD, Wagle NS, Jemal A: Cancer statistics, 2023. *CA Cancer J Clin* 2023, 73(1):17-48.
2. Britt KL, Cuzick J, Phillips KA: Key steps for effective breast cancer prevention. *Nat Rev Cancer* 2020, 20(8):417-436.
3. Michaels E, Worthington RO, Rusiecki J: Breast Cancer: Risk Assessment, Screening, and Primary Prevention. *Med Clin North Am* 2023, 107(2):271-284.
4. Engmann NJ, Golmakani MK, Miglioretti DL, Sprague BL, Kerlikowske K, Breast Cancer Surveillance C: Population-Attributable Risk Proportion of Clinical Risk Factors for Breast Cancer. *JAMA Oncol* 2017, 3(9):1228-1236.
5. Maas P, Barrdahl M, Joshi AD, Auer PL, Gaudet MM, Milne RL, Schumacher FR, Anderson WF, Check D, Chattopadhyay S *et al*: Breast Cancer Risk From Modifiable and Nonmodifiable Risk Factors Among White Women in the United States. *JAMA Oncol* 2016, 2(10):1295-1302.
6. In: *Familial Breast Cancer: Classification and Care of People at Risk of Familial Breast Cancer and Management of Breast Cancer and Related Risks in People with a Family History of Breast Cancer*. edn. Cardiff (UK); 2013.
7. Rosenthal ET, Evans B, Kidd J, Brown K, Goringe H, van Orman M, Manley S: Increased Identification of Candidates for High-Risk Breast Cancer Screening Through Expanded Genetic Testing. *J Am Coll Radiol* 2017, 14(4):561-568.
8. Gallagher S, Hughes E, Wagner S, Tshiaba P, Rosenthal E, Roa BB, Kurian AW, Domchek SM, Garber J, Lancaster J *et al*: Association of a Polygenic Risk Score With Breast Cancer Among Women Carriers of High- and Moderate-Risk Breast Cancer Genes. *JAMA Netw Open* 2020, 3(7):e208501.
9. Hughes E, Tshiaba P, Gallagher S, Wagner S, Judkins T, Roa B, Rosenthal E, Domchek S, Garber J, Lancaster J *et al*: Development and Validation of a Clinical Polygenic Risk Score to Predict Breast Cancer Risk. *JCO Precis Oncol* 2020, 4.
10. Hu C, Hart SN, Gnanaolivu R, Huang H, Lee KY, Na J, Gao C, Lilyquist J, Yadav S, Boddicker NJ *et al*: A Population-Based Study of Genes Previously Implicated in Breast Cancer. *N Engl J Med* 2021, 384(5):440-451.
11. Breast Cancer Association C, Dorling L, Carvalho S, Allen J, Gonzalez-Neira A, Luccarini C, Wahlstrom C, Pooley KA, Parsons MT, Fortuno C *et al*: Breast Cancer Risk Genes - Association Analysis in More than 113,000 Women. *N Engl J Med* 2021, 384(5):428-439.
12. Smith RA, Andrews KS, Brooks D, Fedewa SA, Manassaram-Baptiste D, Saslow D, Wender RC: Cancer screening in the United States, 2019: A review of current American Cancer Society guidelines and current issues in cancer screening. *CA Cancer J Clin* 2019, 69(3):184-210.
13. Evans DG, Howell A: Can the breast screening appointment be used to provide risk assessment and prevention advice? *Breast Cancer Res* 2015, 17(1):84.

14. Gail MH, Anderson WF, Garcia-Closas M, Sherman ME: Absolute risk models for subtypes of breast cancer. *J Natl Cancer Inst* 2007, 99(22):1657-1659.
15. Kurian AW, Hughes E, Simmons T, Bernhisel R, Probst B, Meek S, Caswell-Jin JL, John EM, Lanchbury JS, Slavin TP *et al*: Performance of the IBIS/Tyrer-Cuzick model of breast cancer risk by race and ethnicity in the Women's Health Initiative. *Cancer* 2021, 127(20):3742-3750.
16. Padamsee TJ, Wills CE, Yee LD, Paskett ED: Decision making for breast cancer prevention among women at elevated risk. *Breast Cancer Res* 2017, 19(1):34.
17. Evans DG, Gandhi A, Wisely J, Clancy T, Woodward ER, Harvey J, Highton L, Murphy J, Barr L, Howell SJ *et al*: Uptake of bilateral-risk-reducing-mastectomy: Prospective analysis of 7195 women at high-risk of breast cancer. *Breast* 2021, 60:45-52.
18. Jahan N, Jones C, Rahman RL: Endocrine prevention of breast cancer. *Mol Cell Endocrinol* 2021, 530:111284.
19. Skytte AB, Gerdes AM, Andersen MK, Sunde L, Brondum-Nielsen K, Waldstrom M, Kolvraa S, Cruger D: Risk-reducing mastectomy and salpingo-oophorectomy in unaffected BRCA mutation carriers: uptake and timing. *Clin Genet* 2010, 77(4):342-349.
20. Metcalfe KA, Mian N, Enmore M, Poll A, Llacuachaqui M, Nanda S, Sun P, Hughes KS, Narod SA: Long-term follow-up of Jewish women with a BRCA1 and BRCA2 mutation who underwent population genetic screening. *Breast Cancer Res Treat* 2012, 133(2):735-740.
21. Ralph AF, Ager B, Bell ML, Collins IM, Andrews L, Tucker K, Phillips KA, Butow P: Women's preferences for selective estrogen reuptake modulators: an investigation using protection motivation theory. *Patient Educ Couns* 2014, 96(1):106-112.
22. Gareth Evans D, McWilliams L, Astley S, Brentnall AR, Cuzick J, Dobrashian R, Duffy SW, Gorman LS, Harkness EF, Harrison F *et al*: Quantifying the effects of risk-stratified breast cancer screening when delivered in real time as routine practice versus usual screening: the BC-Predict non-randomised controlled study (NCT04359420). *Br J Cancer* 2023, 128(11):2063-2071.
23. Donnelly LS, Evans DG, Wiseman J, Fox J, Greenhalgh R, Affen J, Juraskova I, Stavrinou P, Dawe S, Cuzick J *et al*: Uptake of tamoxifen in consecutive premenopausal women under surveillance in a high-risk breast cancer clinic. *Br J Cancer* 2014, 110(7):1681-1687.
24. Howell A, Gandhi A, Howell S, Wilson M, Maxwell A, Astley S, Harvie M, Pegington M, Barr L, Baildam A *et al*: Long-Term Evaluation of Women Referred to a Breast Cancer Family History Clinic (Manchester UK 1987-2020). *Cancers (Basel)* 2020, 12(12).
25. Tot T, Gere M, Hofmeyer S, Bauer A, Pellas U: The clinical value of detecting microcalcifications on a mammogram. *Semin Cancer Biol* 2021, 72:165-174.
26. Tan MP, Tot T: The sick lobe hypothesis, field cancerisation and the new era of precision breast surgery. *Gland Surg* 2018, 7(6):611-618.
27. Love SM, Barsky SH: Anatomy of the nipple and breast ducts revisited. *Cancer* 2004, 101(9):1947-1957.

28. King BL, Love SM: The intraductal approach to the breast: raison d'etre. *Breast Cancer Res* 2006, 8(2):206.
29. Cooper SAP B: On the anatomy of the breast, volume I. 1840.
30. Newman LA, Kuerer HM, Hung KK, Vlastos G, Ames FC, Ross MI, Singletary SE: Prophylactic mastectomy. *J Am Coll Surg* 2000, 191(3):322-330.
31. Euhus DM, Diaz J: Breast cancer prevention. *Breast J* 2015, 21(1):76-81.
32. Alaofi RK, Nassif MO, Al-Hajeili MR: Prophylactic mastectomy for the prevention of breast cancer: Review of the literature. *Avicenna J Med* 2018, 8(3):67-77.
33. Tuttle TM, Habermann EB, Grund EH, Morris TJ, Virnig BA: Increasing use of contralateral prophylactic mastectomy for breast cancer patients: a trend toward more aggressive surgical treatment. *J Clin Oncol* 2007, 25(33):5203-5209.
34. Morrow M, Mehrara B: Prophylactic mastectomy and the timing of breast reconstruction. *Br J Surg* 2009, 96(1):1-2.
35. Ticha P, Sukop A: Patient-reported outcomes in bilateral prophylactic mastectomy with breast reconstruction: A narrative review. *Breast* 2023, 73:103602.
36. Gandhi A, Duxbury P, Murphy J, Foden P, Lalloo F, Clancy T, Wisely J, Kirwan CC, Howell A, Evans DG: Patient reported outcome measures in a cohort of patients at high risk of breast cancer treated by bilateral risk reducing mastectomy and breast reconstruction. *J Plast Reconstr Aesthet Surg* 2022, 75(1):69-76.
37. Gahm J, Wickman M, Brandberg Y: Bilateral prophylactic mastectomy in women with inherited risk of breast cancer--prevalence of pain and discomfort, impact on sexuality, quality of life and feelings of regret two years after surgery. *Breast* 2010, 19(6):462-469.
38. Gopie JP, Mureau MA, Seynaeve C, Ter Kuile MM, Menke-Pluymers MB, Timman R, Tibben A: Body image issues after bilateral prophylactic mastectomy with breast reconstruction in healthy women at risk for hereditary breast cancer. *Fam Cancer* 2013, 12(3):479-487.
39. Brandberg Y, Sandelin K, Erikson S, Jurell G, Liljegren A, Lindblom A, Linden A, von Wachenfeldt A, Wickman M, Arver B: Psychological reactions, quality of life, and body image after bilateral prophylactic mastectomy in women at high risk for breast cancer: a prospective 1-year follow-up study. *J Clin Oncol* 2008, 26(24):3943-3949.
40. McCarthy CM, Hamill JB, Kim HM, Qi J, Wilkins E, Pusic AL: Impact of Bilateral Prophylactic Mastectomy and Immediate Reconstruction on Health-Related Quality of Life in Women at High Risk for Breast Carcinoma: Results of the Mastectomy Reconstruction Outcomes Consortium Study. *Ann Surg Oncol* 2017, 24(9):2502-2508.
41. Choi YH, Terry MB, Daly MB, MacInnis RJ, Hopper JL, Colonna S, Buys SS, Andrulis IL, John EM, Kurian AW *et al*: Association of Risk-Reducing Salpingo-Oophorectomy With Breast Cancer Risk in Women With BRCA1 and BRCA2 Pathogenic Variants. *JAMA Oncol* 2021, 7(4):585-592.

42. Mavaddat N, Antoniou AC, Mooij TM, Hoening MJ, Heemskerk-Gerritsen BA, Genepso, Nogues C, Gauthier-Villars M, Caron O, Gesta P *et al*: Correction to: Risk-reducing salpingo-oophorectomy, natural menopause, and breast cancer risk: an international prospective cohort of BRCA1 and BRCA2 mutation carriers. *Breast Cancer Res* 2020, 22(1):25.
43. Mai PL, Miller A, Gail MH, Skates S, Lu K, Sherman ME, Ioffe OB, Rodriguez G, Cohn DE, Boggess J *et al*: Risk-Reducing Salpingo-Oophorectomy and Breast Cancer Risk Reduction in the Gynecologic Oncology Group Protocol-0199 (GOG-0199). *JNCI Cancer Spectr* 2020, 4(1):pkz075.
44. Modaffari P, Ponzone R, Ferrari A, Cipullo I, Liberale V, D'Alonzo M, Maggiorotto F, Biglia N: Concerns and Expectations of Risk-Reducing Surgery in Women with Hereditary Breast and Ovarian Cancer Syndrome. *J Clin Med* 2019, 8(3).
45. Michaelson-Cohen R, Gabizon-Peretz S, Armon S, Srebnik-Moshe N, Mor P, Tomer A, Levy-Lahad E, Paluch-Shimon S: Breast cancer risk and hormone replacement therapy among BRCA carriers after risk-reducing salpingo-oophorectomy. *Eur J Cancer* 2021, 148:95-102.
46. Kotsopoulos J, Gronwald J, Karlan BY, Huzarski T, Tung N, Moller P, Armel S, Lynch HT, Senter L, Eisen A *et al*: Hormone Replacement Therapy After Oophorectomy and Breast Cancer Risk Among BRCA1 Mutation Carriers. *JAMA Oncol* 2018, 4(8):1059-1065.
47. Gordhandas S, Norquist BM, Pennington KP, Yung RL, Laya MB, Swisher EM: Hormone replacement therapy after risk reducing salpingo-oophorectomy in patients with BRCA1 or BRCA2 mutations; a systematic review of risks and benefits. *Gynecol Oncol* 2019, 153(1):192-200.
48. Sauter ER: Breast Cancer Prevention: Current Approaches and Future Directions. *Eur J Breast Health* 2018, 14(2):64-71.
49. Saha Roy S, Vadlamudi RK: Role of estrogen receptor signaling in breast cancer metastasis. *Int J Breast Cancer* 2012, 2012:654698.
50. Patel HK, Bihani T: Selective estrogen receptor modulators (SERMs) and selective estrogen receptor degraders (SERDs) in cancer treatment. *Pharmacol Ther* 2018, 186:1-24.
51. Chimento A, De Luca A, Avena P, De Amicis F, Casaburi I, Sirianni R, Pezzi V: Estrogen Receptors-Mediated Apoptosis in Hormone-Dependent Cancers. *Int J Mol Sci* 2022, 23(3).
52. Sweet Das SK, Yogesh Singh, Pradeep Kumar, Suresh Thareja: elective Estrogen Receptor Modulators (SERMs) for the treatment of ER+ breast cancer: An overview. *Journal of Molecular Structure* 2022, 1270.
53. Fisher B, Costantino JP, Wickerham DL, Cecchini RS, Cronin WM, Robidoux A, Bevers TB, Kavanah MT, Atkins JN, Margolese RG *et al*: Tamoxifen for the prevention of breast cancer: current status of the National Surgical Adjuvant Breast and Bowel Project P-1 study. *J Natl Cancer Inst* 2005, 97(22):1652-1662.
54. Fisher B, Costantino JP, Wickerham DL, Redmond CK, Kavanah M, Cronin WM, Vogel V, Robidoux A, Dimitrov N, Atkins J *et al*: Tamoxifen for prevention of breast cancer: report of the

- National Surgical Adjuvant Breast and Bowel Project P-1 Study. *J Natl Cancer Inst* 1998, 90(18):1371-1388.
55. Cohen I: Endometrial pathologies associated with postmenopausal tamoxifen treatment. *Gynecol Oncol* 2004, 94(2):256-266.
  56. Bergman L, Beelen ML, Gallee MP, Hollema H, Benraadt J, van Leeuwen FE: Risk and prognosis of endometrial cancer after tamoxifen for breast cancer. Comprehensive Cancer Centres' ALERT Group. Assessment of Liver and Endometrial cancer Risk following Tamoxifen. *Lancet* 2000, 356(9233):881-887.
  57. Powles T, Eeles R, Ashley S, Easton D, Chang J, Dowsett M, Tidy A, Viggers J, Davey J: Interim analysis of the incidence of breast cancer in the Royal Marsden Hospital tamoxifen randomised chemoprevention trial. *Lancet* 1998, 352(9122):98-101.
  58. Veronesi U, Mariani L, Decensi A, Formelli F, Camerini T, Miceli R, Di Mauro MG, Costa A, Marubini E, Sporn MB *et al*: Fifteen-year results of a randomized phase III trial of fenretinide to prevent second breast cancer. *Ann Oncol* 2006, 17(7):1065-1071.
  59. Cuzick J, Forbes JF, Sestak I, Cawthorn S, Hamed H, Holli K, Howell A, International Breast Cancer Intervention Study II: Long-term results of tamoxifen prophylaxis for breast cancer--96-month follow-up of the randomized IBIS-I trial. *J Natl Cancer Inst* 2007, 99(4):272-282.
  60. Powles TJ, Ashley S, Tidy A, Smith IE, Dowsett M: Twenty-year follow-up of the Royal Marsden randomized, double-blinded tamoxifen breast cancer prevention trial. *J Natl Cancer Inst* 2007, 99(4):283-290.
  61. Cuzick J, Sestak I, Cawthorn S, Hamed H, Holli K, Howell A, Forbes JF, Investigators I-I: Tamoxifen for prevention of breast cancer: extended long-term follow-up of the IBIS-I breast cancer prevention trial. *Lancet Oncol* 2015, 16(1):67-75.
  62. Cummings SR, Eckert S, Krueger KA, Grady D, Powles TJ, Cauley JA, Norton L, Nickelsen T, Bjarnason NH, Morrow M *et al*: The effect of raloxifene on risk of breast cancer in postmenopausal women: results from the MORE randomized trial. Multiple Outcomes of Raloxifene Evaluation. *JAMA* 1999, 281(23):2189-2197.
  63. Ettinger B, Black DM, Mitlak BH, Knickerbocker RK, Nickelsen T, Genant HK, Christiansen C, Delmas PD, Zanchetta JR, Stakkestad J *et al*: Reduction of vertebral fracture risk in postmenopausal women with osteoporosis treated with raloxifene: results from a 3-year randomized clinical trial. Multiple Outcomes of Raloxifene Evaluation (MORE) Investigators. *JAMA* 1999, 282(7):637-645.
  64. Vogel VG, Costantino JP, Wickerham DL, Cronin WM, Cecchini RS, Atkins JN, Bevers TB, Fehrenbacher L, Pajon ER, Wade JL *et al*: Effects of tamoxifen vs raloxifene on the risk of developing invasive breast cancer and other disease outcomes: the NSABP Study of Tamoxifen and Raloxifene (STAR) P-2 trial. *JAMA* 2006, 295(23):2727-2741.
  65. Vogel VG, Costantino JP, Wickerham DL, Cronin WM, Cecchini RS, Atkins JN, Bevers TB, Fehrenbacher L, Pajon ER, Wade JL, 3rd *et al*: Update of the National Surgical Adjuvant Breast and Bowel Project Study of Tamoxifen and Raloxifene (STAR) P-2 Trial: Preventing breast cancer. *Cancer Prev Res (Phila)* 2010, 3(6):696-706.

66. Quinlan A, O'Brien KK, Galvin R, Hardy C, McDonnell R, Joyce D, McDowell RD, Aherne E, Keogh C, O'Sullivan K *et al*: Quantifying patient preferences for symptomatic breast clinic referral: a decision analysis study. *BMJ Open* 2018, 8(5):e017286.
67. McCaffery K, Nickel B, Moynihan R, Hersch J, Teixeira-Pinto A, Irwig L, Barratt A: How different terminology for ductal carcinoma in situ impacts women's concern and treatment preferences: a randomised comparison within a national community survey. *BMJ Open* 2015, 5(11):e008094.
68. Gomez SL, Tan S, Keegan TH, Clarke CA: Disparities in mammographic screening for Asian women in California: a cross-sectional analysis to identify meaningful groups for targeted intervention. *BMC Cancer* 2007, 7:201.
69. Vadaparampil ST, Miree CA, Wilson C, Jacobsen PB: Psychosocial and behavioral impact of genetic counseling and testing. *Breast Dis* 2006, 27:97-108.
70. Van Bockstal MR, Agahozo MC, Koppert LB, van Deurzen CHM: A retrospective alternative for active surveillance trials for ductal carcinoma in situ of the breast. *Int J Cancer* 2020, 146(5):1189-1197.
71. Bäcklund M, Eriksson M, Gabrielson M, Hammarström M, Quay S, Bergqvist J, Hellgren R, Czene K, Hall P: Topical Endoxifen for Mammographic Density Reduction-A Randomized Controlled Trial. *Oncologist* 2022, 27(7):e597-e600.
72. Lee O, Page K, Ivancic D, Helenowski I, Parini V, Sullivan ME, Margenthaler JA, Chatterton RT, Jovanovic B, Dunn BK *et al*: A randomized phase II presurgical trial of transdermal 4-hydroxytamoxifen gel versus oral tamoxifen in women with ductal carcinoma in situ of the breast. *Clin Cancer Res* 2014, 20(14):3672-3682.
73. Camerini T, Mariani L, De Palo G, Marubini E, Di Mauro MG, Decensi A, Costa A, Veronesi U: Safety of the synthetic retinoid fenretinide: long-term results from a controlled clinical trial for the prevention of contralateral breast cancer. *J Clin Oncol* 2001, 19(6):1664-1670.
74. Russo J: Significance of rat mammary tumors for human risk assessment. *Toxicol Pathol* 2015, 43(2):145-170.
75. Jaini R, Kesaraju P, Johnson JM, Altuntas CZ, Jane-Wit D, Tuohy VK: An autoimmune-mediated strategy for prophylactic breast cancer vaccination. *Nat Med* 2010, 16(7):799-803.
76. Palladini A, Thrane S, Janitzek CM, Pihl J, Clemmensen SB, de Jongh WA, Clausen TM, Nicoletti G, Landuzzi L, Penichet ML *et al*: Virus-like particle display of HER2 induces potent anti-cancer responses. *Oncoimmunology* 2018, 7(3):e1408749.
77. Bryson PD, Han X, Truong N, Wang P: Breast cancer vaccines delivered by dendritic cell-targeted lentivectors induce potent antitumor immune responses and protect mice from mammary tumor growth. *Vaccine* 2017, 35(43):5842-5849.
78. Burga LN, Hu H, Juvekar A, Tung NM, Troyan SL, Hofstatter EW, Wulf GM: Loss of BRCA1 leads to an increase in epidermal growth factor receptor expression in mammary epithelial cells, and epidermal growth factor receptor inhibition prevents estrogen receptor-negative cancers in BRCA1-mutant mice. *Breast Cancer Res* 2011, 13(2):R30.

79. Zhang D, Leal AS, Carapellucci S, Zydeck K, Sporn MB, Liby KT: Chemoprevention of Preclinical Breast and Lung Cancer with the Bromodomain Inhibitor I-BET 762. *Cancer Prev Res (Phila)* 2018, 11(3):143-156.
80. Kim EH, Deng C, Sporn MB, Royce DB, Risingsong R, Williams CR, Liby KT: CDDO-methyl ester delays breast cancer development in BRCA1-mutated mice. *Cancer Prev Res (Phila)* 2012, 5(1):89-97.
81. Infante M, Fabi A, Cognetti F, Gorini S, Caprio M, Fabbri A: RANKL/RANK/OPG system beyond bone remodeling: involvement in breast cancer and clinical perspectives. *J Exp Clin Cancer Res* 2019, 38(1):12.
82. Nolan E, Vaillant F, Branstetter D, Pal B, Giner G, Whitehead L, Lok SW, Mann GB, Rohrbach K, Huang LY *et al*: RANK ligand as a potential target for breast cancer prevention in BRCA1-mutation carriers. *Nat Med* 2016, 22(8):933-939.
83. Howe LR, Subbaramaiah K, Patel J, Masferrer JL, Deora A, Hudis C, Thaler HT, Muller WJ, Du B, Brown AM *et al*: Celecoxib, a selective cyclooxygenase 2 inhibitor, protects against human epidermal growth factor receptor 2 (HER-2)/neu-induced breast cancer. *Cancer Res* 2002, 62(19):5405-5407.
84. Farhangi B, Alizadeh AM, Khodayari H, Khodayari S, Dehghan MJ, Khori V, Heidarzadeh A, Khaniki M, Sadeghizadeh M, Najafi F: Protective effects of dendrosomal curcumin on an animal metastatic breast tumor. *Eur J Pharmacol* 2015, 758:188-196.
85. Stachnik A, Yuen T, Iqbal J, Sgobba M, Gupta Y, Lu P, Colaianni G, Ji Y, Zhu LL, Kim SM *et al*: Repurposing of bisphosphonates for the prevention and therapy of nonsmall cell lung and breast cancer. *Proc Natl Acad Sci U S A* 2014, 111(50):17995-18000.
86. Wu K, Zhang Y, Xu XC, Hill J, Celestino J, Kim HT, Mohsin SK, Hilsenbeck SG, Lamph WW, Bissonette R *et al*: The retinoid X receptor-selective retinoid, LGD1069, prevents the development of estrogen receptor-negative mammary tumors in transgenic mice. *Cancer Res* 2002, 62(22):6376-6380.
87. Li Y, Zhang Y, Hill J, Kim HT, Shen Q, Bissonette RP, Lamph WW, Brown PH: The retinoid, bexarotene, prevents the development of premalignant lesions in MMTV-erbB2 mice. *Br J Cancer* 2008, 98(8):1380-1388.
88. Sahin K, Yabas M, Orhan C, Tuzcu M, Sahin TK, Ozercan IH, Qazi S, Uckun FM: Prevention of DMBA-induced mammary gland tumors in mice by a dual-function inhibitor of JAK3 and EGF receptor tyrosine kinases. *Expert Opin Ther Targets* 2020, 24(4):379-387.
89. Chun YS, Bisht S, Chenna V, Pramanik D, Yoshida T, Hong SM, de Wilde RF, Zhang Z, Huso DL, Zhao M *et al*: Intraductal administration of a polymeric nanoparticle formulation of curcumin (NanoCurc) significantly attenuates incidence of mammary tumors in a rodent chemical carcinogenesis model: Implications for breast cancer chemoprevention in at-risk populations. *Carcinogenesis* 2012, 33(11):2242-2249.
90. Okugawa H, Yamamoto D, Uemura Y, Sakaida N, Tanano A, Tanaka K, Kamiyama Y: Effect of periductal paclitaxel exposure on the development of MNU-induced mammary carcinoma in female S-D rats. *Breast Cancer Res Treat* 2005, 91(1):29-34.

91. Murata S, Kominsky SL, Vali M, Zhang Z, Garrett-Mayer E, Korz D, Huso D, Baker SD, Barber J, Jaffee E *et al*: Ductal access for prevention and therapy of mammary tumors. *Cancer Res* 2006, 66(2):638-645.
92. Stearns V, Mori T, Jacobs LK, Khouri NF, Gabrielson E, Yoshida T, Kominsky SL, Huso DL, Jeter S, Powers P *et al*: Preclinical and clinical evaluation of intraductally administered agents in early breast cancer. *Sci Transl Med* 2011, 3(106):106ra108.
93. Gao D, Liu J, Yuan J, Wu J, Kuang X, Kong D, Zheng W, Wang G, Sukumar S, Tu Y *et al*: Intraductal administration of N-methyl-N-nitrosourea as a novel rodent mammary tumor model. *Ann Transl Med* 2021, 9(7):576.
94. de Groot JS, van Diest PJ, van Amersfoort M, Vlug EJ, Pan X, Ter Hoeve ND, Rosing H, Beijnen JH, Youssef SA, de Bruin A *et al*: Intraductal cisplatin treatment in a BRCA-associated breast cancer mouse model attenuates tumor development but leads to systemic tumors in aged female mice. *Oncotarget* 2017, 8(37):60750-60763.
95. Wang G, Chen C, Pai P, Korangath P, Sun S, Merino VF, Yuan J, Li S, Nie G, Stearns V *et al*: Intraductal fulvestrant for therapy of ER $\alpha$ -positive ductal carcinoma in situ of the breast: a preclinical study. *Carcinogenesis* 2019, 40(7):903-913.
96. Park J, Thomas S, Zhong AY, Wolfe AR, Krings G, Terranova-Barberio M, Pawlowska N, Benet LZ, Munster PN: Local delivery of hormonal therapy with silastic tubing for prevention and treatment of breast cancer. *Sci Rep* 2018, 8(1):92.
97. Sivaraman L, Gay J, Hilsenbeck SG, Shine HD, Conneely OM, Medina D, O'Malley BW: Effect of selective ablation of proliferating mammary epithelial cells on MNU induced rat mammary tumorigenesis. *Breast Cancer Res Treat* 2002, 73(1):75-83.
98. Brock A, Krause S, Li H, Kowalski M, Goldberg MS, Collins JJ, Ingber DE: Silencing HoxA1 by intraductal injection of siRNA lipidoid nanoparticles prevents mammary tumor progression in mice. *Sci Transl Med* 2014, 6(217):217ra212.
99. Yoshida T, Jin K, Song H, Park S, Huso DL, Zhang Z, Liangfeng H, Zhu C, Bruchertseifer F, Morgenstern A *et al*: Effective treatment of ductal carcinoma in situ with a HER-2- targeted alpha-particle emitting radionuclide in a preclinical model of human breast cancer. *Oncotarget* 2016, 7(22):33306-33315.
100. Wang G, Kumar A, Ding W, Korangath P, Bera T, Wei J, Pai P, Gabrielson K, Pastan I, Sukumar S: Intraductal administration of transferrin receptor-targeted immunotoxin clears ductal carcinoma in situ in mouse models of breast cancer-a preclinical study. *Proc Natl Acad Sci U S A* 2022, 119(24):e2200200119.
101. Kenyon E, Westerhuis JJ, Volk M, Hix J, Chakravarty S, Claucherty E, Zaluzec E, Ramsey L, Madaj Z, Hostetter G *et al*: Ductal tree ablation by local delivery of ethanol prevents tumor formation in an aggressive mouse model of breast cancer. *Breast Cancer Res* 2019, 21(1):129.
102. Miller WR: Aromatase inhibitors: mechanism of action and role in the treatment of breast cancer. *Semin Oncol* 2003, 30(4 Suppl 14):3-11.

103. Maunsell E, Goss PE, Chlebowski RT, Ingle JN, Alés-Martínez JE, Sarto GE, Fabian CJ, Pujol P, Ruiz A, Cooke AL *et al*: Quality of life in MAP.3 (Mammary Prevention 3): a randomized, placebo-controlled trial evaluating exemestane for prevention of breast cancer. *J Clin Oncol* 2014, 32(14):1427-1436.
104. Goss PE, Ingle JN, Alés-Martínez JE, Cheung AM, Chlebowski RT, Wactawski-Wende J, McTiernan A, Robbins J, Johnson KC, Martin LW *et al*: Exemestane for breast-cancer prevention in postmenopausal women. *N Engl J Med* 2011, 364(25):2381-2391.
105. Cuzick J, Sestak I, Forbes JF, Dowsett M, Cawthorn S, Mansel RE, Loibl S, Bonanni B, Evans DG, Howell A *et al*: Use of anastrozole for breast cancer prevention (IBIS-II): long-term results of a randomised controlled trial. *Lancet* 2020, 395(10218):117-122.
106. Formelli F, Clerici M, Campa T, Di Mauro MG, Magni A, Mascotti G, Moglia D, De Palo G, Costa A, Veronesi U: Five-year administration of fenretinide: pharmacokinetics and effects on plasma retinol concentrations. *J Clin Oncol* 1993, 11(10):2036-2042.
107. Mehta RG, Moon RC, Hawthorne M, Formelli F, Costa A: Distribution of fenretinide in the mammary gland of breast cancer patients. *Eur J Cancer* 1991, 27(2):138-141.
108. Moon RC, Thompson HJ, Becci PJ, Grubbs CJ, Gander RJ, Newton DL, Smith JM, Phillips SL, Henderson WR, Mullen LT *et al*: N-(4-Hydroxyphenyl)retinamide, a new retinoid for prevention of breast cancer in the rat. *Cancer Res* 1979, 39(4):1339-1346.
109. Howe LR: Retinoids and breast cancer prevention. *Clin Cancer Res* 2007, 13(20):5983-5987.
110. Sukumar J, Gast K, Quiroga D, Lustberg M, Williams N: Triple-negative breast cancer: promising prognostic biomarkers currently in development. *Expert Rev Anticancer Ther* 2021, 21(2):135-148.
111. Toyama T, Yamashita H, Kondo N, Okuda K, Takahashi S, Sasaki H, Sugiura H, Iwase H, Fujii Y: Frequently increased epidermal growth factor receptor (EGFR) copy numbers and decreased BRCA1 mRNA expression in Japanese triple-negative breast cancers. *BMC Cancer* 2008, 8:309.
112. Arnes JB, Begin LR, Stefansson I, Brunet JS, Nielsen TO, Foulkes WD, Akslen LA: Expression of epidermal growth factor receptor in relation to BRCA1 status, basal-like markers and prognosis in breast cancer. *J Clin Pathol* 2009, 62(2):139-146.
113. Sarnik J, Poplawski T, Tokarz P: BET Proteins as Attractive Targets for Cancer Therapeutics. *Int J Mol Sci* 2021, 22(20).
114. Mokbel K, Mokbel K: Chemoprevention of Breast Cancer With Vitamins and Micronutrients: A Concise Review. *In Vivo* 2019, 33(4):983-997.
115. Wang Y, Yu J, Cui R, Lin J, Ding X: Curcumin in Treating Breast Cancer: A Review. *J Lab Autom* 2016, 21(6):723-731.
116. Boyce BF, Xing L: Biology of RANK, RANKL, and osteoprotegerin. *Arthritis Res Ther* 2007, 9 Suppl 1:S1.

117. Kim NS, Kim HJ, Koo BK, Kwon MC, Kim YW, Cho Y, Yokota Y, Penninger JM, Kong YY: Receptor activator of NF-kappaB ligand regulates the proliferation of mammary epithelial cells via Id2. *Mol Cell Biol* 2006, 26(3):1002-1013.
118. Gonzalez-Suarez E, Jacob AP, Jones J, Miller R, Roudier-Meyer MP, Erwert R, Pinkas J, Branstetter D, Dougall WC: RANK ligand mediates progestin-induced mammary epithelial proliferation and carcinogenesis. *Nature* 2010, 468(7320):103-107.
119. Tuohy VK, Johnson JM, Mazumder S: Primary immunoprevention of adult onset cancers by vaccinating against retired tissue-specific self-proteins. *Semin Immunol* 2020, 47:101392.
120. Crews DW, Dombroski JA, King MR: Prophylactic Cancer Vaccines Engineered to Elicit Specific Adaptive Immune Response. *Front Oncol* 2021, 11:626463.
121. <https://www.stopbreastcancer.org/wp-content/uploads/2011/12/artemis-project-plan-saic-1.pdf>
122. <https://www.stopbreastcancer.org/wp-content/uploads/2020/04/2015-artemis-preventive.pdf>
123. [https://www.stopbreastcancer.org/wp-content/uploads/2021/01/2020\\_ArtemisReport-Final-PDF-for-Website-1.pdf](https://www.stopbreastcancer.org/wp-content/uploads/2021/01/2020_ArtemisReport-Final-PDF-for-Website-1.pdf) 82.
124. Nicolas-Morales ML, Luisa-Sanjuan A, Gutierrez-Torres M, Vences-Velazquez A, Ortuno-Pineda C, Espinoza-Rojo M, Navarro-Tito N, Cortes-Sarabia K: Peptide-Based Vaccines in Clinical Phases and New Potential Therapeutic Targets as a New Approach for Breast Cancer: A Review. *Vaccines (Basel)* 2022, 10(8).
125. Jaini R, Rayman P, Cohen PA, Finke JH, Tuohy VK: Combination of sunitinib with anti-tumor vaccination inhibits T cell priming and requires careful scheduling to achieve productive immunotherapy. *Int J Cancer* 2014, 134(7):1695-1705.
126. Kim SW, Goedegebuure P, Gillanders WE: Mammaglobin-A is a target for breast cancer vaccination. *Oncoimmunology* 2016, 5(2):e1069940.
127. Bharat A, Benshoff N, Fleming TP, Dietz JR, Gillanders WE, Mohanakumar T: Characterization of the role of CD8+T cells in breast cancer immunity following mammaglobin-A DNA vaccination using HLA-class-I tetramers. *Breast Cancer Res Treat* 2008, 110(3):453-463.
128. Narayanan K, Jaramillo A, Benshoff ND, Campbell LG, Fleming TP, Dietz JR, Mohanakumar T: Response of established human breast tumors to vaccination with mammaglobin-A cDNA. *J Natl Cancer Inst* 2004, 96(18):1388-1396.
129. Tiriveedhi V, Tucker N, Herndon J, Li L, Sturmoski M, Ellis M, Ma C, Naughton M, Lockhart AC, Gao F *et al*: Safety and preliminary evidence of biologic efficacy of a mammaglobin-a DNA vaccine in patients with stable metastatic breast cancer. *Clin Cancer Res* 2014, 20(23):5964-5975.
130. Visvader JE: Keeping abreast of the mammary epithelial hierarchy and breast tumorigenesis. *Genes Dev* 2009, 23(22):2563-2577.
131. Paine IS, Lewis MT: The Terminal End Bud: the Little Engine that Could. *J Mammary Gland Biol Neoplasia* 2017, 22(2):93-108.

132. Henson DE, Tarone RE, Nsouli H: Lobular involution: the physiological prevention of breast cancer. *J Natl Cancer Inst* 2006, 98(22):1589-1590.
133. Radisky DC, Visscher DW, Frank RD, Vierkant RA, Winham S, Stallings-Mann M, Hoskin TL, Nassar A, Vachon CM, Denison LA *et al*: Natural history of age-related lobular involution and impact on breast cancer risk. *Breast Cancer Res Treat* 2016, 155(3):423-430.
134. Ghosh K, Vachon CM, Pankratz VS, Vierkant RA, Anderson SS, Brandt KR, Visscher DW, Reynolds C, Frost MH, Hartmann LC: Independent association of lobular involution and mammographic breast density with breast cancer risk. *J Natl Cancer Inst* 2010, 102(22):1716-1723.
135. Rasul MF, Hussen BM, Salihi A, Ismael BS, Jalal PJ, Zanichelli A, Jamali E, Baniahmad A, Ghafouri-Fard S, Basiri A *et al*: Strategies to overcome the main challenges of the use of CRISPR/Cas9 as a replacement for cancer therapy. *Mol Cancer* 2022, 21(1):64.
136. Chen Y, Zhang Y: Application of the CRISPR/Cas9 System to Drug Resistance in Breast Cancer. *Adv Sci (Weinh)* 2018, 5(6):1700964.
137. Annunziato S, Kas SM, Nethe M, Yücel H, Del Bravo J, Pritchard C, Bin Ali R, van Gerwen B, Siteur B, Drenth AP *et al*: Modeling invasive lobular breast carcinoma by CRISPR/Cas9-mediated somatic genome editing of the mammary gland. *Genes Dev* 2016, 30(12):1470-1480.
138. Annunziato S, de Ruiter JR, Henneman L, Brambillasca CS, Lutz C, Vaillant F, Ferrante F, Drenth AP, van der Burg E, Siteur B *et al*: Comparative oncogenomics identifies combinations of driver genes and drug targets in BRCA1-mutated breast cancer. *Nat Commun* 2019, 10(1):397.
139. Annunziato S, Lutz C, Henneman L, Bhin J, Wong K, Siteur B, van Gerwen B, de Korte-Grimmerink R, Zafra MP, Schatoff EM *et al*: In situ CRISPR-Cas9 base editing for the development of genetically engineered mouse models of breast cancer. *EMBO J* 2020, 39(5):e102169.
140. Heitink L, Whittle JR, Vaillant F, Capaldo BD, Dekkers JF, Dawson CA, Milevskiy MJG, Surgenor E, Tsai M, Chen HR *et al*: In vivo genome-editing screen identifies tumor suppressor genes that cooperate with Trp53 loss during mammary tumorigenesis. *Mol Oncol* 2022, 16(5):1119-1131.
141. Pujol H, Girault J, Rouanet P, Fournier S, Grenier J, Simony J, Fourtillan JB, Pujol JL: Phase I study of percutaneous 4-hydroxy-tamoxifen with analyses of 4-hydroxy-tamoxifen concentrations in breast cancer and normal breast tissue. *Cancer Chemother Pharmacol* 1995, 36(6):493-498.
142. Rouanet P, Linares-Cruz G, Dravet F, Pujol S, Gourgou S, Simony-Lafontaine J, Grenier J, Kramar A, Girault J, Le Nestour E *et al*: Neoadjuvant percutaneous 4-hydroxytamoxifen decreases breast tumoral cell proliferation: a prospective controlled randomized study comparing three doses of 4-hydroxytamoxifen gel to oral tamoxifen. *J Clin Oncol* 2005, 23(13):2980-2987.
143. Osborne CK, Wakeling A, Nicholson RI: Fulvestrant: an oestrogen receptor antagonist with a novel mechanism of action. *Br J Cancer* 2004, 90 Suppl 1:S2-6.

144. Sapienza Passos J, Dartora V, Cassone Salata G, Draszesski Malago I, Lopes LB: Contributions of nanotechnology to the intraductal drug delivery for local treatment and prevention of breast cancer. *Int J Pharm* 2023, 635:122681.
145. Love SM, Zhang W, Gordon EJ, Rao J, Yang H, Li J, Zhang B, Wang X, Chen G, Zhang B: A feasibility study of the intraductal administration of chemotherapy. *Cancer Prev Res (Phila)* 2013, 6(1):51-58.
146. Teo WW, Sukumar S: Combining the strength of genomics, nanoparticle technology, and direct intraductal delivery for breast cancer treatment. *Breast Cancer Res* 2014, 16(2):306.
147. Havaei SM, Aucoin MG, Jahanian-Najafabadi A: Pseudomonas Exotoxin-Based Immunotoxins: Over Three Decades of Efforts on Targeting Cancer Cells With the Toxin. *Front Oncol* 2021, 11:781800.
148. Poty S, Francesconi LC, McDevitt MR, Morris MJ, Lewis JS: alpha-Emitters for Radiotherapy: From Basic Radiochemistry to Clinical Studies-Part 1. *J Nucl Med* 2018, 59(6):878-884.
149. Xie L, Zhang L, Hu K, Hanyu M, Zhang Y, Fujinaga M, Minegishi K, Ohkubo T, Nagatsu K, Jiang C *et al*: A (211)At-labelled mGluR1 inhibitor induces cancer senescence to elicit long-lasting anti-tumor efficacy. *Cell Rep Med* 2023, 4(4):100960.
150. Mark C, Lee JS, Cui X, Yuan Y: Antibody-Drug Conjugates in Breast Cancer: Current Status and Future Directions. *Int J Mol Sci* 2023, 24(18).
151. Chakravarty S, Hix JML, Wiewiora KA, Volk MC, Kenyon E, Shuboni-Mulligan DD, Blanco-Fernandez B, Kiupel M, Thomas J, Sempere LF *et al*: Tantalum oxide nanoparticles as versatile contrast agents for X-ray computed tomography. *Nanoscale* 2020, 12(14):7720-7734.
152. Kenyon E, Zaluzec E, Powell K, Volk M, Chakravarty S, Hix J, Kiupel M, Shapiro EM, Sempere LF: X-Ray Visualization of Intraductal Ethanol-Based Ablative Treatment for Prevention of Breast Cancer in Rat Models. *J Vis Exp* 2022(190).
153. Kenyon E, Zaluzec EK, Powell K, Volk M, Chakravarty S, Hix J, Arora R, Westerhuis JJ, Kiupel M, Shapiro EM *et al*: Intraductal Delivery and X-ray Visualization of Ethanol-Based Ablative Solution for Prevention and Local Treatment of Breast Cancer in Mouse Models. *J Vis Exp* 2022(182).
154. Robertson N, Sempere L, Kenyon E, Mallet C, Smith K, Hix J, Halim A, Fan J, Moore A: Omniparticle Contrast Agent for Multimodal Imaging: Synthesis and Characterization in an Animal Model. *Mol Imaging Biol* 2023, 25(2):401-412.
155. Metcalfe KA, Birenbaum-Carmeli D, Lubinski J, Gronwald J, Lynch H, Moller P, Ghadirian P, Foulkes WD, Klijn J, Friedman E *et al*: International variation in rates of uptake of preventive options in BRCA1 and BRCA2 mutation carriers. *Int J Cancer* 2008, 122(9):2017-2022.
156. Kuang M, Lu MD, Xie XY, Xu HX, Xu ZF, Liu GJ, Yin XY, Huang JF, Lencioni R: Ethanol ablation of hepatocellular carcinoma Up to 5.0 cm by using a multipronged injection needle with high-dose strategy. *Radiology* 2009, 253(2):552-561.

157. Ansari D, Andersson R: Radiofrequency ablation or percutaneous ethanol injection for the treatment of liver tumors. *World J Gastroenterol* 2012, 18(10):1003-1008.
158. Zhang WY, Li ZS, Jin ZD: Endoscopic ultrasound-guided ethanol ablation therapy for tumors. *World J Gastroenterol* 2013, 19(22):3397-3403.
159. Mueller JL, Morhard R, DeSoto M, Chelales E, Yang J, Nief C, Crouch B, Everitt J, Previs R, Katz D *et al*: Optimizing ethyl cellulose-ethanol delivery towards enabling ablation of cervical dysplasia. *Sci Rep* 2021, 11(1):16869.
160. Nief C, Morhard R, Chelales E, Adrianzen Alvarez D, Bourla Bs I, Lam CT, Sag AA, Crouch BT, Mueller JL, Katz D *et al*: Polymer-assisted intratumoral delivery of ethanol: Preclinical investigation of safety and efficacy in a murine breast cancer model. *PLoS One* 2021, 16(1):e0234535.
161. Chelales E, Morhard R, Nief C, Crouch B, Everitt JI, Sag AA, Ramanujam N: Radiologic-pathologic analysis of increased ethanol localization and ablative extent achieved by ethyl cellulose. *Sci Rep* 2021, 11(1):20700.
162. Morhard R, Nief C, Barrero Castedo C, Hu F, Madonna M, Mueller JL, Dewhirst MW, Katz DF, Ramanujam N: Development of enhanced ethanol ablation as an alternative to surgery in treatment of superficial solid tumors. *Sci Rep* 2017, 7(1):8750.
163. Morhard R, Mueller JL, Tang Q, Nief C, Chelales E, Lam CT, Alvarez DA, Rubinstein M, Katz DF, Ramanujam N: Understanding Factors Governing Distribution Volume of Ethyl Cellulose-Ethanol to Optimize Ablative Therapy in the Liver. *IEEE Trans Biomed Eng* 2020, 67(8):2337-2348.
164. Sannier K, Dompmartin A, Theron J, Labbe D, Barrellier MT, Leroyer R, Toure P, Leroy D: A new sclerosing agent in the treatment of venous malformations. Study on 23 cases. *Interv Neuroradiol* 2004, 10(2):113-127.
165. Dompmartin A, Blaizot X, Theron J, Hammer F, Chene Y, Labbe D, Barrellier MT, Gaillard C, Leroyer R, Chedru V *et al*: Radio-opaque ethylcellulose-ethanol is a safe and efficient sclerosing agent for venous malformations. *Eur Radiol* 2011, 21(12):2647-2656.
166. Zhang J, Li HB, Zhou SY, Chen KS, Niu CQ, Tan XY, Jiang YZ, Lin QQ: Comparison between absolute ethanol and bleomycin for the treatment of venous malformation in children. *Exp Ther Med* 2013, 6(2):305-309.
167. Wohlgenuth WA, Muller-Wille R, Teusch V, Hammer S, Wildgruber M, Uller W: Ethanolgel sclerotherapy of venous malformations improves health-related quality-of-life in adults and children - results of a prospective study. *Eur Radiol* 2017, 27(6):2482-2488.
168. Steiner F, FitzJohn T, Tan ST: Ethanol sclerotherapy for venous malformation. *ANZ J Surg* 2016, 86(10):790-795.
169. Chin M, Chen CL, Chang K, Lee J, Samarasena J: Ethanol Ablation of a Peripheral Nerve Sheath Tumor Presenting as a Small Bowel Obstruction. *ACG Case Rep J* 2015, 3(1):31-32.

170. Gueng MK, Chou YH, Tiu CM, Chiou SY, Cheng YF: Pseudoaneurysm of the Breast Treated with Percutaneous Ethanol Injection. *J Med Ultrasound* 2014, 22(2):114-116.
171. Chun YS, Yoshida T, Mori T, Huso DL, Zhang Z, Stearns V, Perkins B, Jones RJ, Sukumar S: Intraductally administered pegylated liposomal doxorubicin reduces mammary stem cell function in the mammary gland but in the long term, induces malignant tumors. *Breast Cancer Res Treat* 2012, 135(1):201-208.
172. <https://monographs.iarc.fr/wp-content/uploads/2018/06/mono100E-11.pdf>
173. Garaycoechea JI, Crossan GP, Langevin F, Mulderrig L, Louzada S, Yang F, Guilbaud G, Park N, Roerink S, Nik-Zainal S *et al*: Alcohol and endogenous aldehydes damage chromosomes and mutate stem cells. *Nature* 2018, 553(7687):171-177.
174. Patel S, Sparman NZR, Arneson D, Alvarsson A, Santos LC, Duesman SJ, Centonze A, Hathaway E, Ahn IS, Diamante G *et al*: Mammary duct luminal epithelium controls adipocyte thermogenic programme. *Nature* 2023, 620(7972):192-199.
175. Markiewicz E, Fan X, Mustafi D, Zamora M, Conzen SD, Karczmar GS: MRI ductography of contrast agent distribution and leakage in normal mouse mammary ducts and ducts with in situ cancer. *Magn Reson Imaging* 2017, 40:48-52.
176. Markiewicz E, Fan X, Mustafi D, Zamora M, Roman BB, Jansen SA, Macleod K, Conzen SD, Karczmar GS: High resolution 3D MRI of mouse mammary glands with intra-ductal injection of contrast media. *Magn Reson Imaging* 2015, 33(1):161-165.
177. Clark A, Bird NK, Brock A: Intraductal Delivery to the Rabbit Mammary Gland. *J Vis Exp* 2017(121).
178. Lai YE, Morhard R, Ramanujam N, Nolan MW: Minimally invasive ethyl cellulose ethanol ablation in domesticated cats with naturally occurring head and neck cancers: Six cats. *Vet Comp Oncol* 2021, 19(3):492-500.
179. Tamoxifen for early breast cancer: an overview of the randomised trials. Early Breast Cancer Trialists' Collaborative Group. *Lancet* 1998, 351(9114):1451-1467.
180. Zhao Z, Wu F: Minimally-invasive thermal ablation of early-stage breast cancer: a systemic review. *Eur J Surg Oncol* 2010, 36(12):1149-1155.
181. Yu MH, Lee JY, Kim HR, Kim BR, Park EJ, Kim HS, Han JK, Choi BI: Therapeutic Effects of Microbubbles Added to Combined High-Intensity Focused Ultrasound and Chemotherapy in a Pancreatic Cancer Xenograft Model. *Korean J Radiol* 2016, 17(5):779-788.
182. Ashikbayeva Z, Tosi D, Balmasov D, Schena E, Saccomandi P, Inglezakis V: Application of Nanoparticles and Nanomaterials in Thermal Ablation Therapy of Cancer. *Nanomaterials (Basel)* 2019, 9(9).
183. Wild CP: The global cancer burden: necessity is the mother of prevention. *Nat Rev Cancer* 2019, 19(3):123-124.

184. Hughes K: Comparative mammary gland postnatal development and tumourigenesis in the sheep, cow, cat and rabbit: Exploring the menagerie. *Semin Cell Dev Biol* 2021, 114:186-195.
185. Schoniger S, Degner S, Jasani B, Schoon HA: A Review on Mammary Tumors in Rabbits: Translation of Pathology into Medical Care. *Animals (Basel)* 2019, 9(10).
186. Bourne RA, Bryant JA, Falconer IR: Stimulation of DNA synthesis by prolactin in rabbit mammary tissue. *J Cell Sci* 1974, 14(1):105-111.
187. Falconer IR: The distribution of <sup>131</sup>I- or <sup>125</sup>I-labelled prolactin in rabbit mammary tissue after intravenous or intraductal injection. *J Endocrinol* 1972, 53(3):58-59.
188. Fiddler TJ, Birkinshaw M, Falconer IR: Effects of intraductal prolactin on some aspects of the ultrastructure and biochemistry of mammary tissue in the pseudopregnant rabbit. *J Endocrinol* 1971, 49(3):459-469.
189. Fiddler TJ, Falconer IR: The effect of intraductal prolactin on protein and nucleic acid biosynthesis in the rabbit mammary gland. *Biochem J* 1969, 115(5):58P-59P.
190. Chadwick A: Detection and Assay of Prolactin by the Local Lactogenic Response in the Rabbit. *J Endocrinol* 1963, 27:253-263.
191. Slawson SH, Johnson BA: Ductography: how to and what if? *Radiographics* 2001, 21(1):133-150.
192. Sheiman LS, Levesque PH: The In's and Out's of Ductography: A Comprehensive Review. *Curr Probl Diagn Radiol* 2016, 45(1):61-70.

**CHAPTER 2: DUCTAL TREE ABLATION BY LOCAL DELIVERY OF ETHANOL PREVENTS  
TUMOR FORMATION IN AN AGGRESSIVE MOUSE MODEL OF BREAST CANCER**

Published in Breast Cancer Research, 2019, 21:129, DOI: 10.1186/s13058-019-1217-x

Elizabeth Kenyon<sup>1</sup>, Jennifer Westerhuis<sup>2</sup>, Maximilian Volk<sup>1</sup>, Jeremy Hix<sup>3</sup>, Shatadru Chakravarty<sup>3</sup>, Ethan Claucherty<sup>1</sup>, Erin Zaluzec<sup>1</sup>, Lisa Ramsey<sup>2</sup>, Zach Madaj<sup>2</sup>, Galen Hostetter<sup>2</sup>, Bryn Eagleson<sup>2</sup>, Erik Shapiro<sup>3</sup>,  
Anna Moore<sup>1</sup>, Lorenzo F. Sempere<sup>1</sup>

<sup>1</sup> Precision Health Program, Michigan State University, East Lansing, Michigan, 48824

<sup>2</sup> Van Andel Research Institute, Grand Rapids, Michigan, 49503

<sup>3</sup> Department of Radiology, College of Human Medicine, Michigan State University, East Lansing,  
Michigan, 48824

## **Contributions to Science.**

Within the chapter, my primary responsibility was analysis of data. I was an instrumental part of ethanol ablation quantitation of the H&E stained mammary glands. I performed annotations of live and dead epithelial cells which contributed to the epithelial graphic representations. I selected and formatted representative ductal tree and whole gland images for figure generation.

## **Abstract.**

**Background:** Prophylactic mastectomy is the most effective intervention to prevent breast cancer. However, this major surgery has life-changing consequences at the physical, emotional, psychological, and social levels. Therefore, only high-risk individuals consider this aggressive procedure, which completely removes the mammary epithelial cells from which breast cancer arises along with surrounding tissue. Here, we seek to develop a minimally invasive procedure as an alternative to prophylactic mastectomy by intraductal (ID) delivery of a cell-killing solution that locally ablates the mammary epithelial cells before they become malignant.

**Methods:** After ID injection of a 70% ethanol-containing solution in FVB/NJ female animals, *ex vivo* dual stained whole-mount tissue analysis and *in vivo* X-ray microcomputed tomography imaging were used to visualize ductal tree filling, and histological and multiplex immunohistochemical assays were used to characterize ablative effects and quantitate the number of intact epithelial cells and stroma. After ID injection of 70% ethanol or other solutions in cancer-prone FVB-Tg-C3(1)-TAg female animals, mammary glands were palpated weekly to establish tumor latency and examined after necropsy to record tumor incidence. Statistical difference in median tumor latency and tumor incidence between experimental groups was analyzed by log-rank test and logistic mixed-effects model, respectively.

**Results:** We report that ID injection of a 70% ethanol effectively ablates the mammary epithelia with limited collateral damage to surrounding stroma and vasculature in the murine ductal tree. ID injection of

70% ethanol into the mammary glands of C3(1)-TAg multifocal breast cancer model significantly delayed tumor formation (median latency of 150 days in untreated control group [n = 25] vs. 217 days in ethanol-treated group [n = 13], p-value <0.0001) and reduced tumor incidence (34% of glands with tumors [85 of 250] in untreated control group vs 7.3% of glands with tumor [7 of 95] in ethanol-treated group, Risk Ratio = 4.76 [CI 95% : 1.89 to 11.97, p-value < 0.0001]).

**Conclusions:** This preclinical study demonstrates the feasibility of local ductal tree ablation as a novel strategy for primary prevention of breast cancer. Given the existing clinical uses of ethanol, ethanol-based ablation protocols could be readily implemented in first-in-human clinical trials for high-risk individuals.

### **Background.**

An average-risk woman has a 12.5% lifelong risk of developing breast cancer [1]. For high-risk women, primary prevention strategies include surgical removal of the breasts and/or ovaries, and the use of anti-estrogen medications. Despite the evidence-based effectiveness of these interventions, fewer than 30% of high-risk individuals, such as *BRCA* mutation carriers, opt for bilateral prophylactic mastectomy and fewer than 15% opt for anti-estrogen therapy as their first choice of preventive treatment [2]. The reasons for this choice are highly personal and vary among individuals and communities, but life-changing consequences and severe side effects are contributing factors [2]. For moderate- and, especially, low-risk women there are even fewer options available to reduce their risk. Therefore, there is a need to develop new strategies for primary prevention with a focus on high-risk individuals, but strategies that can also benefit moderate- and low-risk individuals.

We seek to develop a minimally invasive procedure as an alternative to prophylactic mastectomy by intraductally delivering a cell-killing solution that locally ablates the mammary epithelial cells before they can become malignant. Our approach is informed by a growing body of literature on the use of intraductal (ID) delivery in the clinic for disease detection such as ductography, and in preclinical and clinical research studies [3-17]. ID delivery of cytotoxic compounds, selective estrogen receptor

modulators, targeted agents, and/or radioactive particles can prevent tumor formation or provide local disease control in preclinical models [4, 9-17]. The ID delivery of cytotoxic compounds (e.g., fluorouracil, pegylated liposomal doxorubicin, carboplatin) significantly reduced tumor incidence in an *N*-methyl-*N*-nitrosourea–induced rat model [4, 10, 12]. Similarly, ID delivery of pegylated liposomal doxorubicin into the mammary glands of the MMTV-Neu mouse model [10] or cisplatin to the WAP-Cre;Brca1<sup>fl/fl</sup>;p53<sup>fl/fl</sup> mouse model [9] significantly reduced tumor incidence. Intraductal delivery of lipidoid nanoparticles containing siRNAs against Hox1A into the mammary glands of 12-week-old C3(1)-TAg transgenic mice resulted in a significant decrease in the number of tumors relative to the control group after nine weekly treatments, but tumors eventually developed in most treated glands [16]. Independent clinical studies reported a >88% success rate in ID administration of pegylated liposomal doxorubicin or carboplatin in up to 8 ductal trees per patient [4, 5]. However, there are limitations with these ID approaches for primary prevention in humans: i) local cytotoxic therapy (e.g., doxorubicin, fluorouracil, and cisplatin) can induce tumors in treated animals [9, 14, 18], a result that has diminished the enthusiasm for its clinical application; ii) local hormonal or siRNA-based therapy would require frequent and repeated intraductal injections [10, 16, 17], which makes it impractical for general clinical application.

Our approach circumvents these limitations by ablating in a single injection per ductal tree all its mammary epithelial cells rather than the targeted killing of existing, highly proliferative, pre-malignant and/or malignant cells. In this preclinical study, we investigated a chemical ablation approach with ethanol (EtOH) as the cell-killing compound. EtOH is a readily available, stable, inexpensive, and safe compound that has long been used in the clinic. Percutaneous injection of EtOH as an ablative agent is used for treatment of unresectable liver tumors, renal and adrenal neoplasms, pancreatic cystic tumors, and breast pseudoaneurysms [19-22]; and for celiac plexus neurolysis to reduce pain [23]. Intravascular injection of EtOH as a sclerosing agent is used for treatment of venous malformations, and of spider veins and varicose veins [24-28]. Here, we demonstrate that the entire ductal tree of a mouse can be filled with a solution containing up to 70% EtOH and that such a filled ductal tree can be imaged *in vivo* by X-ray microcomputed tomography (microCT). Our results indicate that a 70% EtOH solution is more effective than lower

concentrations at locally ablating mammary epithelial cells while causing limited collateral damage to adjacent stroma. Our prevention study using the aggressive and multifocal C3(1)-TAg mouse model of breast cancer shows that ID treatment with EtOH significantly delays tumor formation and significantly decreases tumor incidence. This preclinical study provides support for investigating local ablation as a new strategy for primary prevention of breast cancer.

## **Materials and Methods.**

**Intraductal Injection Procedure:** FVB/NJ (n = 3-5 per time point and per solution; jax.org stock 001800) or FVB-Tg-C3(1)-TAg (n = 6-13 per solution; jax.org stock 013591) females, 9-12 weeks old, were administered 5 mg/Kg of carprofen in drinking water (0.067 mg/mL of carprofen in 5% sucrose-supplemented sterile water). Then isoflurane-anesthetized mice were injected intraductally as described [29] with either PBS or EtOH (30% to 70%) that included up to 1% of blue dye (Evans Blue injected at 0.2-0.5% [w/v]) and up to 29% of CT contrast agent (Isovue-300 injected at 87 mg Iodine/mL, Bracco Diagnostics; or tantalum oxide (TaO<sub>x</sub>) nanocrystals (NCs) injected at 60 mM of tantalum). Detailed preparation and characterization of TaO<sub>x</sub> NCs used in this study are provided in supplemental materials. Mice were injected up to 30 µL of a solution into cervical (#1,#6) or inguinal (#5, #10) glands, and up to 50 µL into thoracic (#2, #3, #7,#8) or abdominal (#4, #9). All experiments were conducted under protocols approved by Institutional Animal Care and Use Committee at Van Andel Research Institute and/or Michigan State University.

**MicroCT Imaging and Analysis:** Animals were serially imaged using a PerkinElmer Quantum GX microCT scanner at different times after ID injection with a solution containing Isovue-300 or Tantalum oxide nanocrystals as contrast agent. The following image acquisition scan parameters were standardized and used at each scan interval time point: 90kVp/88uA; Field of View (FOV), 36 mm; number of slices, 512; slice thickness, 72 µm; voxel resolution, 72 µm<sup>3</sup>. Standard (2 min) acquisition time was used for

animals used in longitudinal studies to minimize radiation exposure, and or high-resolution (4 to 14 min) acquisition time was used for short-term follow up (less than 7 days) or terminal procedure. microCT image rendering, segmentation, and analysis of whole body or individual gland were performed using Caliper AnalyzeDirect©, v12.0 (Biomedical Imaging Resource, Mayo Clinic, Rochester, MN).

**Whole Mount Dual Staining and Imaging:** Immediately after ID injection with a solution containing Evans Blue 0.2-0.5% (w/v), animals were euthanized and whole mammary glands were dissected, mounted on glass slides, and processed for carmine staining as described [30] with the following modifications. After Carnoy's fixation, glands were dehydrated in EtOH series from 70% to 100% and incubated overnight in xylene. Cleared glands were transferred to 70% EtOH, submerged in glycerol, and scanned at 1200 dpi on an Epson Perfection V39 Photo Scanner to acquire Evans blue staining. Then, glands were rehydrated and stained with carmine alum without further modifications. Finally, glands were scanned as above to acquire carmine alum staining.

**Histological and Immunohistochemical Analyses:** Animals were euthanized at different times after ID injections. Mammary glands were dissected and fixed in formalin for 6-8 hrs before processing and embedding in paraffin as previously described [31]. Four micron sections of formalin-fixed paraffin-embedded (FFPE) tissue samples were stained with H&E and were scanned on an Aperio Versa 8 Brightfield&Fluorescence imaging system (Leica Biosystems, Buffalo Grove, IL). ImageScope tools were used for annotation and quantitative analysis. Fluorescence-based IHC multiplex assays were conducted on a Leica Bond Rx automated staining station as we described [31, 32]. These assays use covalently linked deposition of horseradish peroxidase (HRP)-reactive tyramides conjugated with fluorescent dyes (i.e., fluorescein, rhodamine, Dylight 680). The appropriate combination of primary (anti-cytokeratin 19 rat antibody at 0.576 µg/mL, Developmental Studies Hybridoma Bank, Troma-III; anti- $\alpha$ -smooth muscle actin rabbit antibody at 0.4 µg/mL, Abcam, ab5694; anti-vimentin chicken antibody at a 1:250 dilution, Lifespan Biosciences, Lot # 125753, LS-B291-100) and HRP-conjugated

secondary antibodies (anti-rat goat/HRP at 2  $\mu\text{g}/\text{mL}$ , Abcam, ab7097; anti-rabbit goat/HRP at 1  $\mu\text{g}/\text{mL}$ , Biorad, 170-6515; and anti-chicken goat/HRP at 0.8  $\mu\text{g}/\text{mL}$ , Santa Cruz Biotechnology, sc-2901) enabled sequential detection of multiple markers on the same tissue section, with a hydrogen peroxide blocking step in between stains to inactivate HRP from the prior round. Tissue sections were counterstained with DAPI and mounted with Prolong Gold (Invitrogen, p36930). Multi-channel images of each tissue sample were acquired and analyzed using Aperio Versa system with customized narrow-width band excitation and emission filter cubes (Chroma Technology Corp, Bellows Falls, VT)

**Statistical Analysis:** Unpaired Welch's t-tests were used to assess statistical significance of difference between different experimental groups of continuous values obtained from tissue analyses. Kaplan-Meier curves for tumor-free survival (the time between birth and initial time of tumor detection by palpation or time of death) were constructed separately for non-injected vs injected glands of the same animal (experimental class) and for overall survival (the time between birth and time of death from any cause) for animals in each experimental group. For tumor-free survival data, time of death was used to censor injected glands with no evidence of tumor by palpation. Log-rank test (Mantel-Cox) was used to compare Kaplan-Meier curves between specific experimental classes or groups. GraphPad Prism 8 was used to perform these statistical analyses. Analyses of relative risk of tumor formation were divided into three parts comparing tumor incidence at necropsy of: non-injected vs. untreated glands or injected vs. untreated glands between different experimental groups, and non-injected vs. injected glands within the same experimental group. Retrospective contingency tables of tumor incidence were constructed to determine relative risk of tumor formation between two different experimental classes and were analyzed using logistic mixed-effects models via the R v3.5.1 (<https://cran.r-project.org/>) package 'lme4' [33] with random intercepts for each animal to account for multiplicity of tumor formation within the same animal. Tukey adjusted linear contrasts were used to test specific two-sided hypotheses of interest. We set a p-value of 0.01 as the threshold to report statistical significance.

## Results.

**Feasibility of Filling the Entire Ductal Tree with a 70% Ethanol Solution:** Each of the 10 mammary glands of a mouse contains a single ductal tree that opens at the nipple orifice. The ductal tree elongates during pubertal development (4 to 7 weeks of age) and reaches the edge of the fat pad by 9 weeks of age. After that, growth and expansion of the ductal tree is tightly linked to the growth rate of the fat pad and of the mouse in general [34]. Terminal end buds (TEBs) are the highly proliferative structures at the tips of the elongating ductal tree that direct ductal branching. TEBs become less proliferative after puberty, and in 9-week-old young adults they regress and become anatomically indistinguishable from terminal ducts or alveolar buds [35]. In humans, terminal ductal lobular units serve a similar function as TEBs (and later alveolar buds) and are the sites from which breast cancer predominantly arises [35, 36]. These similarities make the mouse an appropriate model to test this ID injection approach for breast cancer prevention.

We modified and implemented an ID injection procedure [29] to accommodate for the delivery of EtOH into the ductal tree(s) of female mice. This procedure places a 34-gauge needle inside the nipple opening of an isoflurane-anesthetized animal to inject the test solution. Some key improvements of our procedure include the use of gastight syringes for volatile liquids and extended anti-inflammatory treatment with 5 mg/Kg of carprofen in 5% sucrose drinking water [37] from 2 d before to 7 d after ID injection in order to reduce inflammation and fibrosis associated with wound healing and tissue repair [38, 39].

Clinical uses of EtOH as an ablative or sclerosing agent consist of local delivery of tens of milliliters of 95% to 100% EtOH. In some cases, repeated administration is required due to rapid dehydration caused by EtOH. We observed this effect in initial attempts to intraductally deliver 95% to 100% EtOH: the ductal tree was occluded, preventing filling of the entire tree. To circumvent this problem, we decreased the EtOH concentration and established the feasibility of injecting a solution of up to 70% EtOH (**Figure 2.1**). To demonstrate that 70% EtOH can fill the entire ductal tree, abdominal mammary glands were injected with PBS or 70% EtOH solution containing Evans blue dye, promptly dissected and processed for whole-mount dual staining with Evans blue and carmine alum. Overlap of Evans blue and carmine alum indicated that

both PBS and 70% EtOH solution reached the terminal ends and entirely filled the murine ductal tree (**Figure 2.1**).

**In vivo Monitoring of Ductal Tree Filling:** To monitor filling of the ductal trees, we performed serial microCT imaging on animals injected PBS or 70% EtOH solution containing iodine-based contrast agent Isovue-300 in up to three abdominal and/or thoracic mammary glands (see **Supplementary Figure 2.6**). Isovue-300 is used in clinical ductography [3]. In the initial image, contrast signal and rendered volumes of PBS-injected or 70% EtOH-injected were comparable; it was apparent that contrast agent-containing solution reached the ends of the ductal trees as signal was detected between the distal end of the mammary gland fat pad and the external side of the peritoneal cavity (see **Supplementary Figure 2.6**). There was a relatively faster loss of contrast signal in PBS-injected glands at 30 min and at later time points after ID injection compared to EtOH-injected glands (see **Supplementary Figure 2.6**). We surmise that this signal retention is due to the fixative effect of EtOH. However, this imaging approach does not provide sufficient resolution to identify individual ducts or branches of the ductal tree network or to quantitatively determine the volume of a filled ductal tree. To overcome these limitations, we used tantalum oxide ( $\text{TaO}_x$ ) nanocrystals (NC) as much larger contrast agent (see **Supplementary Figures 2.7** and **2.8**) with the expectation that it would have a much lower rate of outward diffusion. We performed serial microCT imaging on animals injected PBS or 70% EtOH solution containing  $\text{TaO}_x$  NCs in up to three abdominal and/or thoracic mammary glands (**Figure 2.1**). The entire ductal tree network was visualized in great detail after initial ID injection and architectural changes could be monitored for more than 24 hrs thanks to local retention of  $\text{TaO}_x$  NCs in both PBS and EtOH solutions (**Figure 2.1**).  $\text{TaO}_x$  NCs can be detected and provide a similar image reconstruction of the murine ductal tree using a standard clinical 2D/3D digital mammography system (data not show). This *in vivo* imaging approach can be used to infer, but cannot directly assess at single-cell resolution, ablative effects of EtOH and stromal fibrosis.

**70% Ethanol Ablates Epithelial Cells with Limited Tissue Damage:** To obtain microscopic evidence of the extent of epithelial cell ablation and collateral tissue damage, PBS- or 70% EtOH-injected mammary glands of non-transgenic mice were dissected 1 or 3 d after the ID procedure. Contralateral non-injected mammary glands of PBS- or 70% EtOH-injected animals were also dissected as controls. Analysis of H&E-stained mammary glands revealed local killing of epithelial cells. At 1 d after the ID procedure, the number of epithelial structures in 70% EtOH-injected glands was significantly reduced, or when present, cells had hypochromatic cytoplasm and were devoid of nuclei (**Figure 2.2**), whereas most adipocytes and blood vessels were intact. At 3 d after the ID procedure, inflammatory and fibrotic cells were observed around some of the ablated ducts and alveolar buds (**Figure 2.2**), suggesting the start of wound healing and tissue repair. Histology of contralateral non-injected and PBS-injected mammary glands was comparable to PBS-injected glands (**Figure 2.2**).

To complement and expand on these histological analyses, we conducted multiplex immunohistochemical analysis with cell type-specific markers to determine residual epithelial cell content and extent of peri-ductal tissue damage. Cytokeratin 19 signal was detected in “ghost” anucleate luminal epithelial cells and served as a landmark to identify and follow the clearance of ablated epithelial structures from 1d to 7 d after injection (**Figure 2.2**). To a lesser extent, there was  $\alpha$ -smooth muscle actin (SMA) signal in anucleate myoepithelial cells in some ablated ducts at 3 d after injection, but no SMA signal was detectable at later time points (**Figure 2.2**). These staining patterns indicate that EtOH penetrates sufficiently from the lumen through the luminal cells to reach the myoepithelial cells. SMA signal was strong in intact, nucleated smooth muscle cells of blood vessels at all time points examined (**Figure 2.2**). Similarly, vimentin staining highlighted the mostly intact adipocyte network (**Figure 2.2**). These staining patterns indicate that the ablative effects of EtOH are mostly confined to the injected ductal tree(s).

**70% Ethanol Provides More Effective Killing of Epithelial Cells Than Lower Concentrations:** To determine whether lower concentrations of EtOH could be as effective as 70%, mammary glands were injected with different EtOH concentration (30% to 70%) and dissected 3 d after the ID procedure. The

number of intact epithelial cells was significantly lower in 70% EtOH-injected glands compared to lower concentrations (30% vs. 70% EtOH,  $p < 0.001$ ; 50% vs. 70% EtOH,  $p = 0.014$ ) based on the interpretation of the H&E-stained tissue sections (**Figure 2.3**). While there was not a statistically significant difference between 60% EtOH- and 70% EtOH-injected mammary glands, the estimated lower average of residual epithelial cells in this limited sample size suggested that 70% EtOH could be more effective. To evaluate collateral tissue damage and long-term effects of the ablative solution, abdominal mammary glands were injected with up to 50  $\mu$ L of 50% EtOH or 70% EtOH. Collateral tissue damage was more contained and the time to complete wound healing resolution was shortened in 50% EtOH-injected glands (**Figure 2.3**). However, maximal epithelial ablation was only consistently achieved with 70% EtOH.

### **Intraductal Injection of 70% Ethanol Prevents Tumor Formation in the C3(1)-TAg Breast Cancer**

**Model:** To determine whether 70% EtOH was effective at preventing tumor formation, up to 8 mammary glands were injected per cancer-prone C3(1)-TAg female mouse with different solutions. The C3(1)-TAg is an aggressive and multifocal model of breast cancer, in which expression of the SV40 T antigen in mammary epithelial cells is driven by the rat prostatic steroid binding protein C3(1) promoter [40]. Animals received the ID injections between 9-12 weeks of age when there were still no hyperplastic or *in situ* carcinoma lesions [16, 40]. The following experimental and control groups were used in this prevention study. There were three experimental groups that received ID injections of different EtOH concentrations and/or different formulations. One group received injections of 50% EtOH in PBS and iodine-containing contrast agent. This group served mainly to determine if partial ablation would still provide protection or would accelerate tumor formation due to epithelial cell regeneration in an inflammatory milieu. The other two experimental groups received ID injections of 70% EtOH either in deionized distilled water or in a solution of PBS and iodine-containing contrast agent to compare if diluent affected ablative properties. Control groups included a group that received no treatment, a non-injected control group that received anti-inflammatory treatment but no ID injections, and a PBS-injected

group that received injections in some mammary glands. These control groups served to separate the effects of anti-inflammatory treatment and the ID procedure.

The two primary endpoints for this study were tumor latency and tumor incidence. A secondary endpoint was overall survival, which was reached in all cases by tumor burden and not by cancer-related death. Animals were palpated weekly from 14 weeks of age until they met euthanasia criteria. First instance of tumor formation and number of tumors at necropsy were recorded separately for non-injected and injected mammary glands per mouse, where appropriate (**Figure 2.4**). ID injections of EtOH significantly delayed tumor formation in EtOH-injected mammary glands in all experimental groups (50% or 70% in PBS/Contrast, 70% in water) compared to the untreated group (**Figure 2.4** and **Table 2.1**). ID injection of EtOH also delayed tumor formation in non-injected mammary glands in all experimental groups, though only reached statistical significance in the 70% EtOH-in-water group (**Table 2.1**). We noted but did not investigate further whether this is an abscopal effect of injected glands systemically affecting the non-injected glands or simply a reduction in the number of mammary glands susceptible to develop tumors. In either case, the preventive effect of EtOH injection was significantly higher in injected glands than in non-injected glands in both 70% EtOH-injected experimental groups based on delayed tumor latency (**Table 2.1**). Overall survival of 70% EtOH-injected animals in both experimental groups was significantly longer compared to the untreated control group (**Figure 2.4** and **Table 2.2**). Similarly, there was a significant reduction in the risk of tumor formation in 70% EtOH-injected glands compared to the untreated control group or non-injected glands within the 70% EtOH-injected experimental groups (**Table 2.3**). Intriguingly, both the injected and non-injected mammary glands in PBS-injected control group had a higher tumor incidence than the untreated and non-injected control groups, suggesting that non-ablative ID injection may create a pro-tumorigenic environment that negates protection of anti-inflammatory treatment (**Table 2.3**). Together, these results indicate that 70% EtOH in either of the tested formulations is effective, and more so than 50% EtOH, at preventing tumor formation in the C3(1)-TAg breast cancer model.

**No Iatrogenic Cancer or Other Long-Term Adverse Effects After ID Injection of Ethanol:** To evaluate longitudinally any potential side effects or complications of this ID ablation procedure such as infection, open wounds, or chronic inflammation, non-transgenic animals were injected in up to 6 mammary glands with up to 50  $\mu\text{L}$  of 70% EtOH. Animals were monitored daily until the designated time point for mammary gland tissue collection. No signs of infection or open wounds nor any changes in grooming, locomotive or social behavior that would indicate pain or discomfort were noted. Touch test with von Frey filaments before or after ID injection did not detect any withdrawal response in either non-injected or injected glands at target forces that elicit a response in the rear paw (data not shown). Ten animals were followed for more than 14 months after 70% EtOH injection in multiple mammary glands. Three of these animals were selected for tissue collection at 18 months after ID injection in order to perform tissue analyses (**Figure 2.5**). The other seven animals died of natural causes with no signs of breast cancer or other diseases with a median overall survival of  $> 630$  days (**Figure 2.5**).

### **Discussion.**

We investigated and recorded short-term and long-term effects of ID 70% EtOH injections on breast biology and mouse physiology and evaluated whether any of these effects and/or experimental requirements of EtOH-based ablative procedure pose an obvious impediment for human translation. The short-term effects of ID EtOH injection were relatively mild when precautions were taken. The two short-term side effects of EtOH injection were ethylic intoxication and skin laceration. Mice injected with 150  $\mu\text{L}$  of 70% EtOH (3 mammary glands) exhibited signs of alcohol intoxication (about 0.4 g/dL of EtOH content in blood) which was minimized by intraperitoneal injection of 5% sucrose in PBS before and after the ID procedure; animals fully recovered within 4 h after the ID procedure. For injection of more than 3 glands per mouse, sequential procedure were performed to allow enough recovery time. The risk of alcohol intoxication in women will be much lower; injection of ductal trees in both breasts, assuming 24 main ducts [41, 42] and 2 mL per duct [3, 8], with 70% EtOH will result in less than 0.1 g/dL of EtOH content in blood, which approximates to drinking three glasses of wine (15 oz), and may cause mild impairment. The total

volume of 50 mL of 70% EtOH and total EtOH quantity (27.61 g) is comparable to the up to 50 mL of 95-100% EtOH (up to 39.45 g) reported in percutaneous EtOH injection procedures for treatment of liver tumors [20] and venous malformations [28]. Skin lacerations were observed in some mice due to small leakage of EtOH from the injected duct or from the needle while exiting the nipple. These were topical lacerations due to direct skin contact and not from internal tissue damage. The risk of these lacerations will be much lower by taping the nipple after ductal injection as it is routine practice for ductography [3, 8]. We did not observe any long-term effects of EtOH injection; specifically, none of the mice had open wounds or infection in injected glands nor did they exhibit any overt signs of pain, distress or discomfort. Histologically, glands injected with 50  $\mu$ L of 70% EtOH started to heal by 14 d after the injection. We observed that by 1 month there was limited scarring and subsiding inflammation (**Figure 2.3**). Long-term follow-up of glands showed no signs of scarring or inflammation at 18 months after EtOH injection (**Figure 2.5**). Nonetheless, improvement in the EtOH formulation such as addition of ethyl cellulose as gelling agent to limit the outward diffusion of EtOH should be considered to further minimize the collateral tissue damage. Use of ethyl cellulose for this purpose is routine in some sclerosing protocols for treatment of venous malformation [26, 27] and has also been reported to improve ablative efficacy in percutaneous EtOH injection in pre-clinical model of liver cancer [43].

The safety bar for new preventive agents and approaches is very high. Thus, safety is our primary concern when considering translation of this ID procedure. While the International Agency for Research on Cancer considers EtOH in alcoholic beverages to be carcinogenic to humans (<https://monographs.iarc.fr/wp-content/uploads/2018/06/mono100E-11.pdf>), this conclusion is based on chronic exposure to EtOH. The exact molecular mechanism(s) of how EtOH increases cancer risk have not been completely established; EtOH metabolization into acetaldehyde, a toxic chemical that can cause DNA damage and DNA-protein crosslinking, is considered a main contributing mechanism for EtOH-induced cancer (<https://monographs.iarc.fr/wp-content/uploads/2018/06/mono100E-11.pdf>). Nonetheless, we are not aware of any reports of iatrogenic cancer linked to clinical uses of EtOH. Acute exposure to EtOH in mice does not cause significant DNA damage [44]. In addition, we have no evidence from our study that

EtOH injection promotes or enhances tumor initiation in cancer-prone C3(1)-TAg animals followed up until they met euthanasia criteria (**Figure 2.4**) nor in non-transgenic animals followed up more than 15 months after ID EtOH injection (**Figure 2.5**). Note that breast tumors were observed in non-transgenic mice within a year of exposure to ID chemotherapy or immunoradiotherapy [9, 13, 14, 18].

We need to mention several limitations of our study. While we attempted to inject as many mammary glands as technically possible, most mice were injected in fewer than 6 glands. Thoracic and abdominal glands were more often injected than cervical or inguinal glands (see **Supplementary Table 2.6**). Other studies showed the feasibility of injecting all 10 glands [10, 16], but in our hands cervical glands are not often suitable for injection. There is no need to inject all glands to assess whether EtOH can prevent breast cancer in injected glands with statistical methods that we and other groups used [4, 9, 10]. However, glands that were more accessible for injection may not develop tumors at the same rate as the non-injected glands (see **Supplementary Figure 2.6**; see also reference [45]). We addressed in part this potential bias with a control group of animals injected with PBS in a similar number of glands and locations (see **Supplementary Figure 2.6**). In these animals, tumors arose with similar latency and tumor incidence in injected and non-injected glands. Tumor latency in 70% EtOH-injected glands was significantly delayed and tumor incidence significantly reduced compared to PBS-injected glands. Intriguingly, tumor incidence was significantly increased in PBS-injected animals, but not tumor latency, compared to untreated control animals (**Table 2.1**). Thus, we used the untreated control group as baseline reference for statistical analysis rather than the PBS-injected group. Typically, the tumor burden in non-injected glands was the reason for euthanasia in EtOH-injected animals, which limited the follow up time in EtOH-injected glands that might have eventually developed breast tumors. Future prevention studies in other mouse models such as genetically engineered MMTV-Neu [10] and WAP-Cre;Brca1<sup>fl/fl</sup>;p53<sup>fl/fl</sup> [9] with longer latency and/or lower multiplicity and/or inducible models by ID injection of Cre recombinase [46] would be useful to provide an extended follow up period and determine the general application of the EtOH ablation procedure to tumor formation driven by different molecular alterations and cell of origin. There are technical challenges in consistently and reproducibly achieving ablation of all mammary epithelial cells of an injected

ductal tree. The ductal tree is not completely hollow; it may contain proteinaceous secretions and cellular debris that could affect accessibility and diffusion and/or dilute the EtOH concentration. Architectural changes during the estrous cycle may also affect filling of the ductal tree. These changes are more prominent during alveolar growth in diestrus and subsequent alveolar collapse in proestrus [47]. Thus, injection of the same EtOH volume in ductal tree of different mammary glands of the same mouse or in different mice may have not caused the same rate of ablation providing at least partial explanation as to why tumors still developed in EtOH-injected mammary glands. We observed a varying degree of residual epithelial cell structures in some of the injected glands in non-transgenic animals (**Figure 2.3, Figure 2.5**). By design, we injected up to 50  $\mu$ L of ablative solution, it is likely that some ductal trees were not fully filled and a larger volume could have effectively ablated more or all of the cells. Due to the size and fragility of the mouse nipple, cannulation to deliver a contrast solution to determine the exact volume requirements before filling with the EtOH solution would be extremely challenging. However, these volume measurements and architectural difference per individual ductal tree could be obtained in women by combining a standard ductography procedure with a preparatory solution for flushing each ductal tree as is often done for ductal lavage collection.

We wish to acknowledge that previous preventive studies directly investigated the idea of epithelial cell ablation as treatment or observed epithelial cell ablation as an indirect consequence of treatment. In a chemically induced rat model, ID injection of a suicidal gene adenoviral vector with the intent of ablating proliferating cells of the TEB to prevent tumor formation, paradoxically promoted tumor initiation and increased tumor incidence [11]. Despite the high efficiency transduction, high expression of thymidine kinase, and 50-90% ablation rate upon suicidal gene activation by ganciclovir administration, intraductally treated rats developed tumors at shorter latency than control rats exposed to *N*-methyl-*N*-nitrosourea [11]. In genetically engineered mouse models, ID treatment with doxorubicin or cisplatin caused partial destruction of the ductal tree and cell ablation [4, 9], but these treatments were not more effective than those that did not cause cell ablation [4].

Given the existing clinical uses of EtOH and relatively straightforward ID injection procedure,

EtOH-based ablation protocols could be readily implemented in clinical trials for primary prevention of breast cancer. We envision that this ablative procedure would most closely approximate the cosmetic treatment of venous malformations. Our preclinical procedure is in line with clinical sclerosing therapy for venous malformation in which patients receive treatment under systemic anesthesia followed by 2 days of anti-inflammatory medications such as NSAIDs that may be extended for a few more days to reduce local inflammation and any possible pain [26]. Typically, the sclerosing therapy reduces chronic pain associated with swollen and deformed vasculature in most patients; this intervention can cause short-term pain in a few patients that is easily managed with medication. In contrast, the physiological response to mastectomy includes local and systemic inflammation, and the scale of these responses and the pain management plan depend on the surgical procedure, including musculoskeletal manipulation and tissue advancement for reconstruction. Typical peri-operative pain management includes a combination of analgesics with regional anesthesia, narcotics, benzodiazepines, and anti-inflammatory medications such as NSAIDs over a course of 2-6 weeks. Regrettably, at least 25% of patients suffer from chronic pain or post-mastectomy chronic pain syndrome [48, 49].

We foresee challenges for clinical implementation that will need to be addressed. i) The EtOH concentration may need to be adjusted for application in humans due to anatomical differences from rodents, such as the size and complexity of their ductal trees; progressive scalability studies in rats [10, 17] or rabbits [50], and larger animal models, such as pigs, will be required before translation to humans. ii) if the total amount of EtOH is much larger than 50 mL due individual ducts accommodating more than estimated 2 mL as reported for intraductal delivery of chemotherapeutic agents [4, 5], sequential treatment of each breast in separate visits and/or intravenous administration of thiamine and sugar solution may be required to minimize effects of EtOH intoxication iii) The typical human breast is composed of 8-12 ductal trees [41, 42]; successful cannulation and injection in each main duct will be needed to preventively treat the whole breast. iv) Evidence that the entire tree was filled will be required. EtOH could be injected with a radiocontrast agent to visualize ductal tree filling (as shown in **Figure 2.1** for mice) using existing ductography methods [3, 8] or could be intrinsically labeled for visualization using other imaging modalities

such as EtOH-<sup>17</sup>O for magnetic resonance imaging [51]. In some cases, hyperplastic or proliferative regeneration may occlude a duct, preventing filling of the entire ductal tree. It may be possible to dilate or clear passage of such a duct by flushing with a preparatory solution. v) Pathological evidence that all epithelial cells were ablated may be required. This would be feasible in first-in-human trials in women undergoing elective prophylactic mastectomy, from whom tissue samples of the entire breast will be accessible. We would follow a similar experimental design as described for ID administration of chemotherapeutic agents [4, 5]. Going forward, cell ablation would need to be assessed using *in vivo* imaging and/or limited tissue sampling by core needle biopsy, since pathological assessment of whole-breast tissue would defeat the purpose of this local, minimally invasive procedure. vi) The amount of pain, scarring, and other complications associated with this procedure will need to be determined and compared to those of a mastectomy. This procedure will need to have a good safety profile if it were to replace mastectomy in a preventive setting. As with mastectomy, this procedure will eliminate the ability of a woman to lactate or breastfeed.

## **Conclusions.**

This preclinical study provides support for further investigating local ablation as a new strategy for primary prevention of breast cancer in high-risk individuals. This study could also stimulate the evaluation of other chemical and/or thermal ablation strategies. This ID procedure could lead to a breakthrough in breast cancer prevention by providing a universal prophylactic intervention, one not only for high-risk individuals but potentially for those with moderate or low risk; by improving the individual's quality of cancer-free life; and by decreasing the personal and societal costs of breast cancer.

## Figures

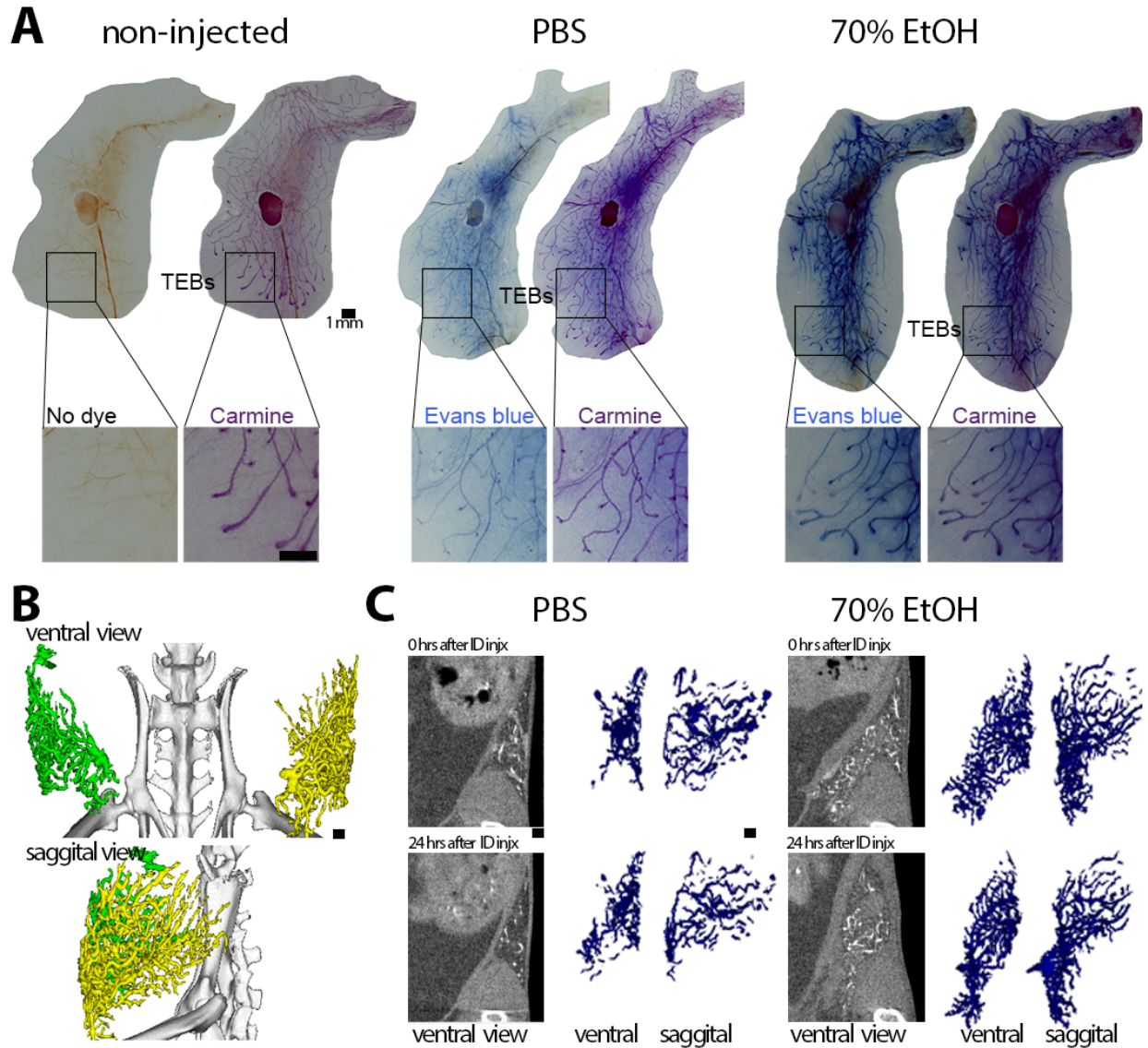


**Figure 2.1. Feasibility of ductal tree filling and *in vivo* imaging of mammary glands with a 70% ethanol-containing solution.** **A)** Dual stain on whole-mount preparation of abdominal glands injected with Evans blue-containing solution of PBS or 70% EtOH. Evans blue serves to track injected solution within the lumen of the ductal tree, and carmine alum stains epithelial cells of the ductal tree. **B)** Tantalum-based contrast agent-containing solution in PBS was sequentially injected within 15 min in left abdominal (#4 and right abdominal gland (#9); 14-min high-resolution microCT scan was acquired 24 hrs after ID injection and processed for 3D image reconstruction. **C)** Longitudinal 2-min standard microCT scans were acquired from independent animals whose abdominal glands were injected with tantalum-based contrast agent-containing solution of PBS or 70% EtOH. Different angle views and time points of the same representative glands are shown. Voxels with signal intensities from -500 to 500 Hounsfield units in original CT slices were selected for volume rendition of diffused contrast agent. Scale bars indicate 1 mm in image panels at different magnification.

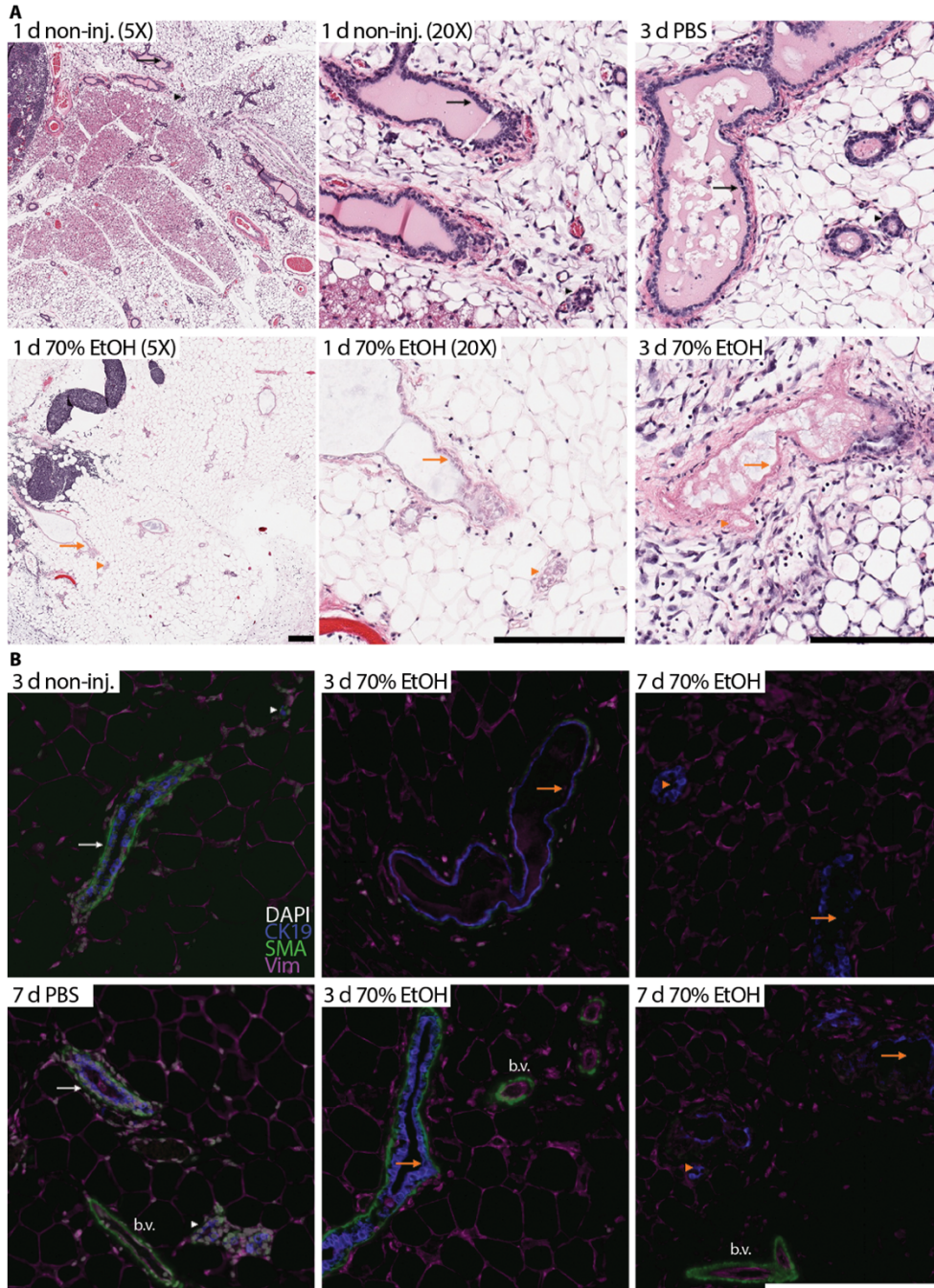


**Figure 2.2. Tissue analyses of mammary glands within 7 days after ID injection of 70% ethanol. A)** Representative H&E staining of contralateral non-injected or 70% EtOH-injected glands 1 d after ID procedure (same tissues are shown at two different magnifications), and of PBS- or 70% EtOH-injected glands 3 d after ID procedure. **B)** Representative multiplex staining of contralateral non-injected, PBS- or 70% EtOH-injected glands 3d and 7d after ID injection. After sequential detection of cytokeratin 19 (CK19),  $\alpha$ -smooth muscle actin (SMA) and vimentin (Vim), tissue were counterstained with DAPI. Live duct (black arrow in **A** and white arrow in **B**) and ductule (black arrowhead in **A** and white arrow in **B**) or ablated duct (orange arrow) and ductule (orange arrowhead) are indicated. b.v. denotes blood vessel with SMA-stained smooth muscle cells. Scale bars indicate 200  $\mu$ m in image panels at different magnification.

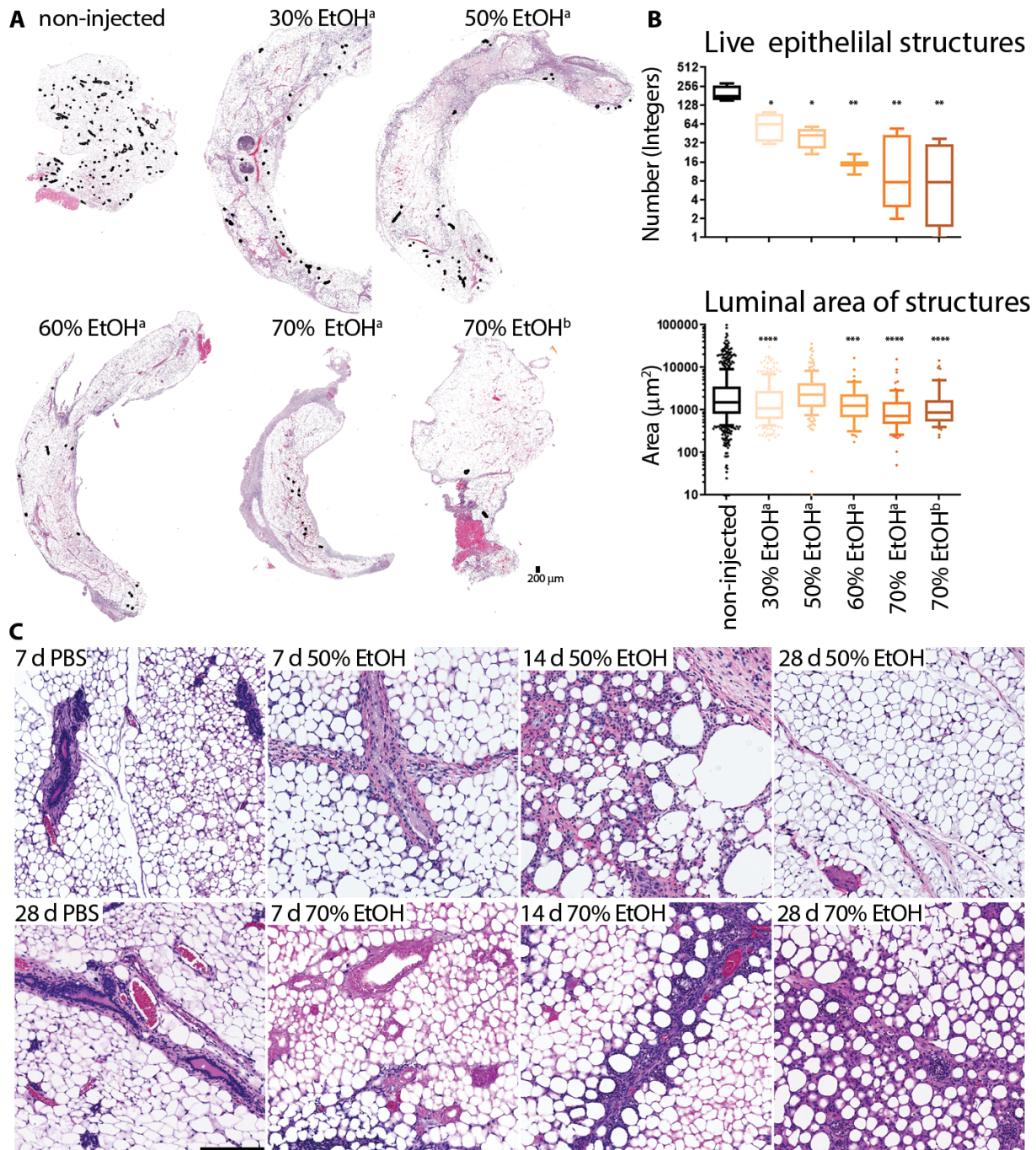


**Figure 2.3. Effects of different ethanol volumes and concentration on epithelial ablation and collateral tissue damage.** **A)** H&E staining of representative non-injected and EtOH-injected whole mammary glands 3 d after the ID procedure. Intact, live epithelial structures are outlined in black. **B)** Box-whisker plot (90/10 percentiles) of number (in integers) of live epithelial structures or luminal areas (in  $\mu\text{m}^2$ ) of these structures 3 d after the injection based on whole-breast tissue cross-sectional analysis of H&E stain slides; at least four glands were quantitated per group. An epithelial structure is defined as a lobular or ductal structure with more than two adjacent live epithelial cells. Asterisks indicate p-value of unpaired Welch's t-test of each EtOH-injected group compared to non-injected control animals (\* = 0.01, \*\* < 0.01, \*\*\* < 0.001, \*\*\*\* < 0.0001). **C)** H&E staining of representative tissue field of 50% or 70% EtOH-injected glands at different times after ID injection.

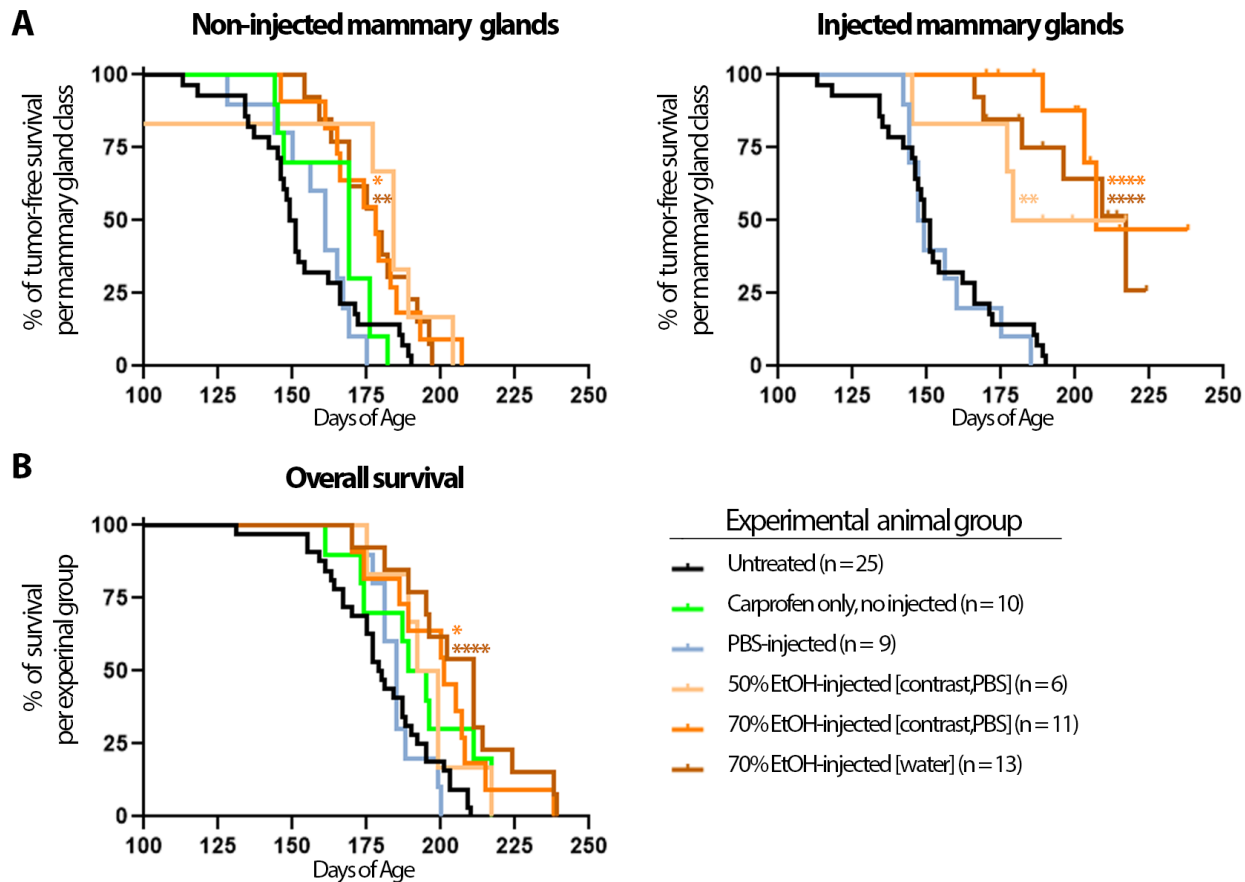


**Figure 2.4. Kaplan-Meier curves of tumor-free and overall survival.** **A)** Kaplan-Meier curves for tumor-free survival were plotted separately for non-injected and injected glands from the same animal, where appropriate. **B)** Kaplan-Meier curves for overall survival were plotted for all experimental groups. Legend indicates which plotted curve corresponds to each experimental group and number of animals per group (**A** and **B**). Colored asterisks indicate p-value of log-rank test of matched experimental class or group compared to non-injected control animals (\*\* < 0.01, \*\*\*\* < 0.0001); see **Tables 1** and **2** for more details.

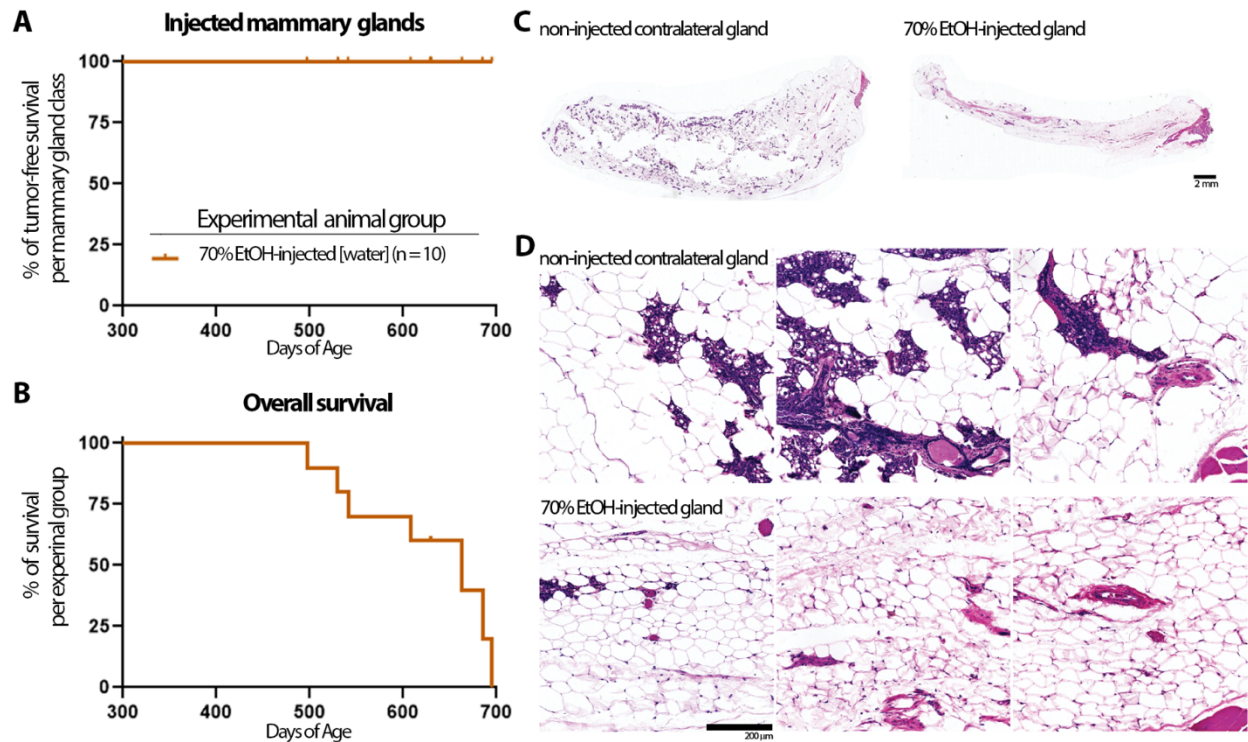


**Figure 2.5. No iatrogenic breast cancer in aged mice after ID EtOH injection.** **A** and **B**) Kaplan-Meier curve for tumor-free survival (**A**) and for overall survival (**B**) were plotted for non-transgenic FVB animals injected with 70% EtOH in multiple glands. All animals died of natural causes, with the exception of three animals that were euthanized at designated time point for tissue analyses and censored at this time (630 days of age) for tumor-free and overall survival curves. **C** and **D**) Representative H&E staining of contralateral non-injected or 70% EtOH-injected glands 18 months after ID procedure. Whole gland tissue is shown in **C** and representative field along each gland are shown at high power magnification in **D**. **D**) Some residual epithelial structures can be observed only in the upper left quadrant of the left image of the EtOH-injected gland. Size of the scale bar is 2 mm for images in **C** and 200  $\mu\text{m}$  for images in **D**.

## Tables

**Table 2.1. Intraductal injection of ethanol delays onset of tumor formation.**

Animal groups	Animal s (n)	Non-injected vs non-injected glands			Non-injected vs. injected glands		
		Latency (days)	Glands (n)	p- value	Latency (days)	Glands (n)	p- value
Untreated vs. not injected	25 vs. 10	150 vs. 169	250 vs. 100	0.427 9	n/a	n/a	n/a
Untreated vs. PBS- injected	25 vs. 10	150 vs. 161	250 vs. 43	0.911 0	150 vs. 148	250 vs. 57	0.657 0
Untreated vs. 50% EtOH-injected <sup>a</sup>	25 vs. 6	150 vs. 184	250 vs. 36	0.036 6	150 vs. 198	250 vs. 24	0.004 9
Untreated vs. 70% EtOH-injected <sup>a</sup>	25 vs. 11	150 vs. 178	250 vs. 58	0.015 1	150 vs. 207	250 vs. 52	<0.0 001
Untreated vs. 70% EtOH-injected <sup>b</sup>	25 vs. 13	150 vs. 176.5	250 vs. 35	0.005 9	150 vs. 217	250 vs. 95	<0.0 001
Within PBS-injected	10	n/a	n/a	n/a	161 vs. 148	43 vs. 57	0.727 4
Within 50% EtOH- injected <sup>a</sup>	6	n/a	n/a	n/a	184 vs. 198	36 vs. 24	0.298 7
Within 70% EtOH- injected <sup>a</sup>	11	n/a	n/a	n/a	178 vs. 207	58 vs. 52	0.000 2
Within 70% EtOH- injected <sup>b</sup>	13	n/a	n/a	n/a	176.5 vs. 217	35 vs. 95	0.000 6

Median latency in days of age is provided for indicated animal treatment group or mammary gland treatment class. P-values were calculated by the log-rank test (Mantel-Cox) comparing tumor-free survival between indicated treatment groups or classes (reference vs. test). <sup>a</sup>EtOH was diluted in sterile PBS with iodine-containing contrast agent. <sup>b</sup>EtOH was diluted in sterile water.

**Table 2.2. Intraductal injection of ethanol increases overall survival.**

Group comparison	Animals (n)	Overall Survival (days)	p-value
Untreated vs. not injected	25 vs. 10	179.5 vs 192	0.0394
Untreated vs. PBS-injected	25 vs. 10	179.5 vs. 185	0.9655
Untreated vs. 50% EtOH-injected <sup>a</sup>	25 vs. 6	179.5 vs. 195.5	0.1199
Untreated vs. 70% EtOH-injected <sup>a</sup>	25 vs. 11	179.5 vs. 201	0.0184
Untreated vs. 70% EtOH-injected <sup>B</sup>	25 vs. 13	179.5 vs. 211	<0.0001
50% EtOH-injected <sup>a</sup> vs. 70% EtOH- injected <sup>a</sup>	6 vs. 11	195.5 vs. 201	0.5495
50% EtOH-injected <sup>a</sup> vs. 70% EtOH- injected <sup>b</sup>	6 vs. 13	195.5 vs. 211	0.1801
70% EtOH-injected <sup>a</sup> vs. 70% EtOH- injected <sup>b</sup>	11 vs. 13	201 vs. 211	0.2789

Median overall survival in days of age is provided for indicated animal treatment groups. P-values were calculated by the log-rank test (Mantel-Cox) comparing overall survival between indicated treatment groups (reference vs. test). <sup>a</sup>EtOH was diluted in sterile PBS with iodine-containing contrast agent. <sup>b</sup>EtOH was diluted in sterile water.

**Table 2.3. Intraductal injection of ethanol reduces risk of developing cancer in C3(1)-TAg mouse model (Tumor incidence at necropsy).**

Animal groups	Non-injected vs non-injected glands			Non-injected vs. injected glands		
	Tumor incidence (% <i>, n</i> )	RR (95% CI)	p-value	Tumor incidence (% <i>, n</i> )	RR (95% CI)	p-value
Untreated vs. not injected	34% (85/250) vs. 28% (28/100)	1.21 (0.76 – 1.93)	0.6848	n/a	n/a	n/a
Untreated vs. PBS-injected	34% (85/250) vs. 58% (25/43)	0.58 (0.39 – 0.86)	0.0147	34% (85/250) vs. 52% (30/57)	0.64 (0.44 – 0.94)	0.0347
Untreated vs. 50% EtOH-injected <sup>a</sup>	34% (85/250) vs. 36% (13/36)	0.94 (0.51 – 1.72)	0.9924	34% (85/250) vs. 16% (4/24)	2.12 (0.67 – 6.70)	0.2328
Untreated vs. 70% EtOH-injected <sup>a</sup>	34% (85/250) vs. 51% (30/58)	0.65 (0.44 – 0.97)	0.0555	34% (85/250) vs. 9.6% (5/52)	3.53 (1.21 – 10.29)	0.0048
Untreated vs. 70% EtOH-injected <sup>b</sup>	34% (85/250) vs. 57% (20/35)	0.61 (0.39 – 0.94)	0.0599	34% (85/250) vs. 7.3% (7/95)	4.76 (1.89 – 11.97)	<0.0001
Within PBS-injected	n/a	n/a	n/a	58% (25/43) vs. 52% (30/57)	1.10 (0.77 – 1.57)	0.6765
Within 50% EtOH-injected <sup>a</sup>	n/a	n/a	n/a	36% (13/36) vs. 16% (4/24)	2.25 (0.83 – 6.13)	0.0579
Within 70% EtOH-injected <sup>a</sup>	n/a	n/a	n/a	51% (30/58) vs. 9.6% (5/52)	5.37 (2.24 – 12.86)	<0.0001
Within 70% EtOH-injected <sup>b</sup>	n/a	n/a	n/a	57% (20/35) vs. 7.3% (7/95)	7.77 (3.58 – 16.85)	<0.0001

Tumor incidence indicates the number of glands with tumors at necropsy in each gland class (i.e., untreated, non-injection, or injected). Relative Risk (RR) indicates the likelihood of having a tumor in one class of mammary glands vs. another within a treatment group (same animals) or among treatment groups (independent animals) with 95% confidence interval (CI). RR >1 indicates a lower risk of tumor formation for that particular group or intervention compared to reference group (reference vs. test). Logistic mixed-effects models with random intercepts for each animal and Tukey adjusted linear contrasts were used for this per-gland analysis to account for multiplicity of tumor formation in the same animal. <sup>a</sup>EtOH was diluted in sterile PBS with iodine-containing contrast agent. <sup>b</sup>EtOH was diluted in sterile water.

## Supplemental Figures

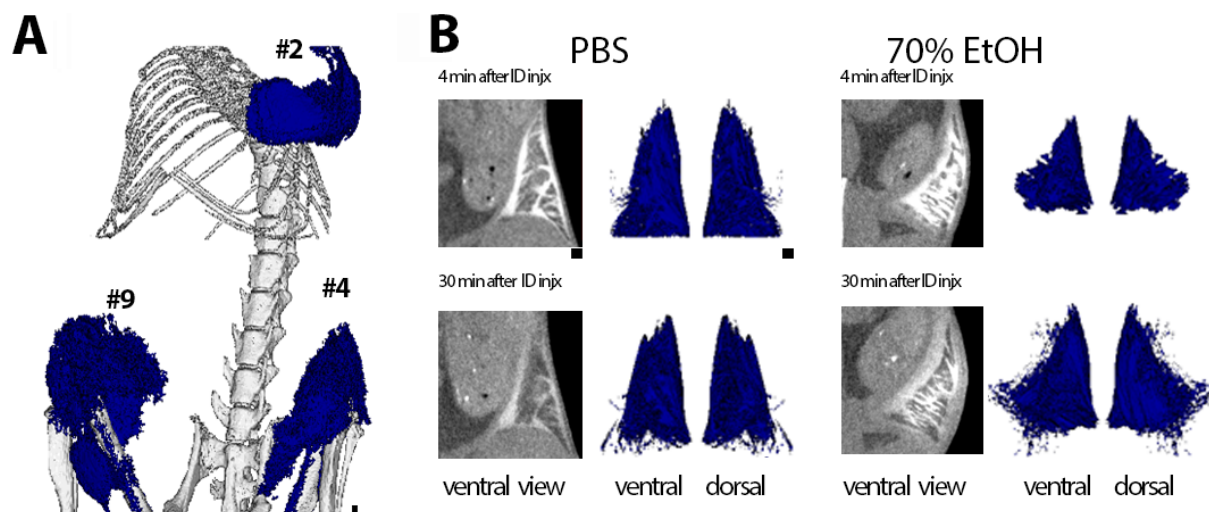


**Figure 2.6. *In vivo* imaging of mammary glands with Iovue-300 in 70% ethanol-containing solution.** A) Iodine-based contrast agent-containing solution of 70% EtOH was sequentially injected within 15 min in left abdominal (#4), left thoracic (#2), and right abdominal gland (#9); full-body microCT scan was acquired immediately after the last ID injection. B) Sequential 4 min. high-resolution microCT scans were acquired from independent animals whose abdominal glands were injected with iodine-based contrast agent-containing solution of PBS or 70% EtOH. Different angle views and time points of the same representative glands are shown. Voxels with signal intensities from -500 to 500 Hounsfield units in original CT slices were selected for volume rendition of diffused contrast agent. Scale bars indicate 1 mm in image panels at different magnification.

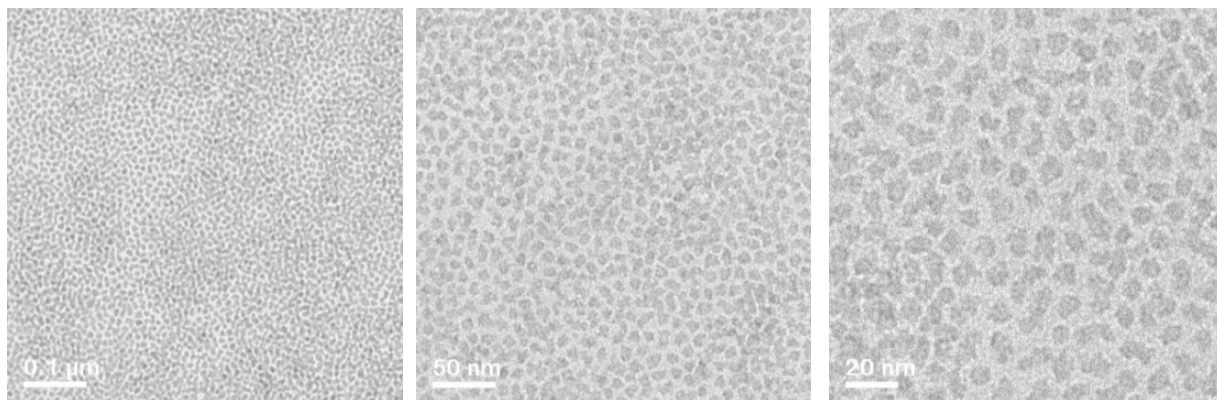


**Figure 2.7. Characterization of tantalum oxide (TaO<sub>x</sub>) nanocrystals (NCs) by transmission electron microscopy (TEM).** TEM images show excellent homogeneity in size and morphology of TaO<sub>x</sub> NCs. TEM images were acquired on a 2200FS JEOL electron microscope. These TaO<sub>x</sub> NCs were prepared as follows: In a 250 mL, one neck round bottom flask, fitted with a septa, IGEPAL®-CO-520 (average  $M_n$  441, ALDRICH, 23.0 g), Cyclohexane ( $\geq 99\%$ , A.C.S. spectrophotometric grade, SIGMA-ALDRICH, 200 mL) and Ethanol (200 Proof, Anhydrous, KOPTEC USP, 2.5 mL), were added and the contents were stirred to obtain a clear solution. To this stirring mixture, a solution of Sodium Hydroxide (100 mM, 2.5 mL) was added and the micro-emulsion was sonicated in a water bath to ensure homogeneity. Next, Tantalum (V) ethoxide, (Ta<sub>2</sub>O<sub>5</sub>, 99.98% trace metal basis, ALDRICH, 0.5 mL) was added in one portion and the contents were stirred at ambient temperature for 20 minutes. To the micro-emulsion mixture containing uncoated TaO<sub>x</sub> NCs, 2-[Methoxy (polyethyleneoxy)-9-12-propyl]trimethoxysilane (PEG-Silane, tech-90, MW 591-723, GELEST INC., 3.0 mL), quickly followed by (3-Aminopropyl)trimethoxysilane (APTMS, 97%, ALDRICH, 0.028 mL) were added. The resulting milky white suspension solution was stirred at room temperature for 16 h. After 16 h, the reaction mixture was diluted to three times volume using a 1:1 mixture of Ethyl Ether (Anhydrous, Certified ACS, Fisher Scientific, 110 mL) and Hexane (meets ACS specifications, VWR Chemicals, 110 mL) and the NCs were isolated via centrifugation (15,000 rpm, 10 minutes, 10 °C) as white oily residue. This residue was suspended in ethyl ether and washed using a similar centrifugation procedure twice. The supernatants were discarded and the residue pellet so obtained was suspended in 100 mL Ethanol and Methoxy-poly(ethylene-glycol)-succinimidyl glutarate (m-PEG-SG-2000, Average MW 2000, LAYSAN BIO INC., 50 mg) was added to it. The contents so obtained were stirred at room temperature in the dark for 12 h. Then, the solvent was removed on a rotary evaporator to reduce the volume to about 5 mL. This final residual solution was dissolved in water (10 mL) and transferred to Dialysis Membrane bags (SPECTRA/POR® 6 Dialysis Membrane, Standard RC Tubing, MWCO: 1 kD), clipped at both ends and dialyzed against water with regular change of external media after 2, 4, 16, 4, 4 and 16 h. After extensive dialysis, the contents in the dialysis bags were lyophilized to obtain the TaO<sub>x</sub> NCs as a white fluffy powder. Product Yield: 940 mg. Ta% = 30% (calculated from ICP-OES).

## Results

	Size (d.nm):	% Number	Width (d.nm...)
<b>Z-Average (d.nm):</b> 43.05	<b>Peak 1:</b> 9.036	100.0	2.616
<b>Pdl:</b> 0.458	<b>Peak 2:</b> 0.000	0.0	0.000
<b>Intercept:</b> 0.758	<b>Peak 3:</b> 0.000	0.0	0.000

**Result quality :** **Good**

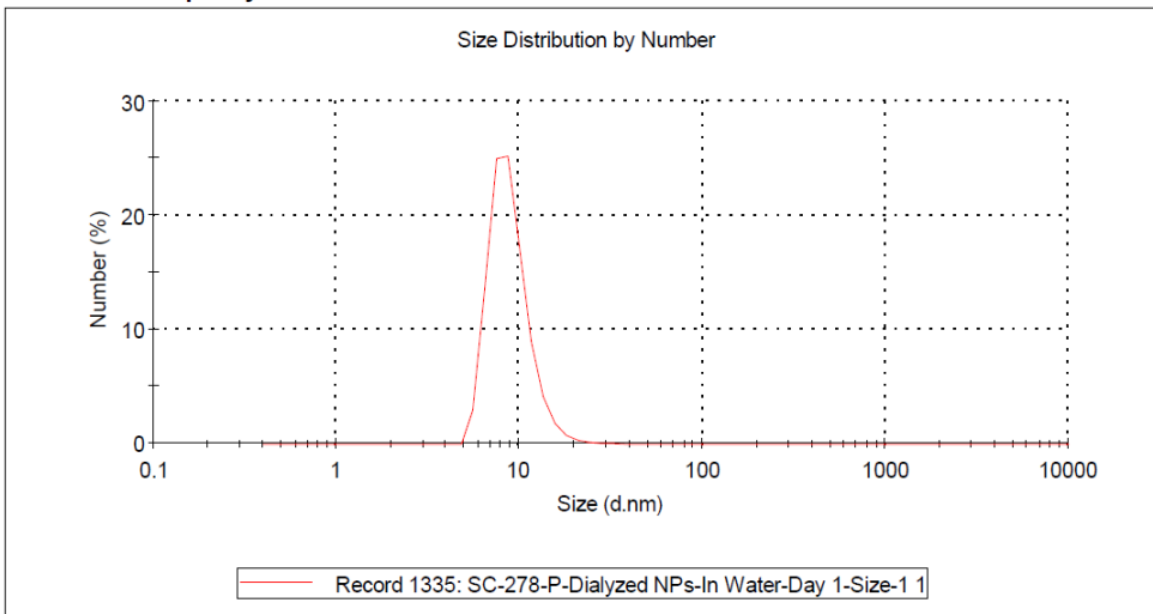


**Figure 2.8. Characterization of TaO<sub>x</sub> nanocrystals by Dynamic Light Scattering (DLS).** DLS plot shows a narrow range of particle size distribution. TaO<sub>x</sub> were analyzed in hydrophilic conditions by dissolving TaO<sub>x</sub> nanocrystals at 1 mg/mL in water. DLS plot was acquired on a Zetasizer instrument (Malvern, USA).

**Supplemental Tables**

**Table 2.4. Tumor formation in non-injected and injected mammary glands assessed at necropsy.**

ID	experimental group	Tumor in non-injected gland										Tumor in injected gland									
		1	2	3	4	5	6	7	8	9	10	1	2	3	4	5	6	7	8	9	10
90	untreated	N	N	N	N	N	Y	N	N	N	N										
101	untreated	Y	Y	N	N	N	Y	N	Y	Y	Y										
106	untreated	Y	Y	N	N	N	N	N	Y	N	Y										
108	untreated	Y	Y	N	Y	Y	Y	N	N	N	N										
109	untreated	Y	N	Y	N	N	N	N	N	N	N										
112	untreated	Y	N	N	N	N	Y	N	Y	N	N										
115	untreated	N	Y	N	Y	N	N	N	N	N	Y										
121	untreated	N	Y	Y	N	N	Y	N	N	Y	N										
124	untreated	Y	Y	Y	N	N	Y	N	N	N	N										
137	untreated	Y	N	Y	N	N	N	Y	Y	Y	N										
155	untreated	Y	N	N	Y	N	Y	N	N	N	N										
156	untreated	Y	Y	N	N	N	Y	N	N	N	N										
158	untreated	N	Y	N	Y	Y	Y	N	N	Y	Y										
161	untreated	N	N	N	N	N	Y	N	N	N	N										
167	untreated	N	N	Y	Y	Y	Y	N	N	N	N										
170	untreated	N	N	N	Y	Y	N	N	N	N	Y										
175	untreated	Y	N	N	N	N	Y	Y	N	N	N										
192	untreated	Y	N	N	N	N	Y	N	Y	Y	N										
196	untreated	N	N	Y	N	N	N	N	N	Y	N										
202	untreated	Y	N	N	Y	N	Y	N	Y	Y	N										
203	untreated	Y	N	N	N	N	Y	N	N	N	Y										
208	untreated	N	N	N	N	N	N	Y	Y	N	N										
213	untreated	N	Y	Y	N	N	Y	N	N	N	Y										
218	untreated	Y	N	N	Y	N	Y	N	N	N	Y										
219	untreated	N	N	N	N	N	Y	N	N	N	N										

**Table 2.4. (cont'd)**

311	carprofen only	N	Y	N	N	Y	N	Y	N	N	Y										
312	carprofen only	Y	N	N	N	N	N	Y	N	N	N										
314	carprofen only	N	N	N	N	N	N	Y	Y	N	N										
315	carprofen only	Y	N	N	N	N	Y	N	N	Y	Y										
318	carprofen only	N	N	N	Y	N	Y	N	N	N	N										
319	carprofen only	Y	N	N	N	N	Y	N	N	N	Y										
322	carprofen only	Y	N	N	N	N	Y	N	N	N	Y										
323	carprofen only	Y	Y	N	N	N	N	Y	N	Y	N										
325	carprofen only	Y	N	N	N	N	Y	N	N	N	N										
327	carprofen only	Y	N	N	N	N	N	Y	N	N	N										
207	PBS	Y					Y			Y			Y	N	Y	N		Y	N	N	
209	PBS					N	N				N	Y	Y	N	N			N	N	N	
215	PBS		Y		Y	N					N	Y			N		Y	Y	N	N	
216	PBS	Y					Y				N		Y	N	Y	N		Y	Y	N	
220	PBS			Y		Y	N	N			N	Y	Y		Y				N	N	
222	PBS			Y			N		N		N	Y	N		N	N		N		N	
231	PBS	Y		N			N	Y		Y			Y		Y	N			Y	Y	
241	PBS	Y		Y			Y	Y		Y			Y		Y	Y			N	Y	
242	PBS	Y		Y	Y		Y			Y			Y		Y			Y		Y	N
243	PBS	Y		N		N	Y			N	N		Y		N			N	Y		

280	50% EtOH[Contrast/ PBS]	N	Y	Y							N							N	N	Y	N	N	
285	50% EtOH[Contrast/ PBS]	Y	N	Y	N	Y	N	Y	N													N	N
286	50% EtOH[Contrast/ PBS]	Y	N	N			Y				N	N						N	N		N	N	
287	50% EtOH[Contrast/ PBS]	Y	N	N			N	N			N							N		N	N	Y	
288	50% EtOH[Contrast/ PBS]	Y	N				Y	Y								N	N			Y	N	Y	N
290	50% EtOH[Contrast/ PBS]	N	N			N	Y	N	N							N						N	N

**Table 2.4. (cont'd)**

297	70% EtOH[Contrast/ PBS]	Y	Y		Y		N				N			N		N		Y	Y	N				
304	70% EtOH[Contrast/ PBS]	N	N	N			N	N		Y						N				N		N		
305	70% EtOH[Contrast/ PBS]	Y					Y	N		Y				N	N	N				N		N		
308	70% EtOH[Contrast/ PBS]	Y	N	N			N	Y			N	N				N				N		N		
309	70% EtOH[Contrast/ PBS]	N	Y					N		Y	N					N	N	N		N			N	
316	70% EtOH[Contrast/ PBS]		Y				N	Y	N			N	N			N	N					N	N	
317	70% EtOH[Contrast/ PBS]	Y				N	Y	Y		Y				Y	Y	N	N					N		N
324	70% EtOH[Contrast/ PBS]	Y				Y	N	Y				N			N	Y						N	N	N
338	70% EtOH[Contrast/ PBS]			Y				Y				N	Y	N	N	N						N	N	N
341	70% EtOH[Contrast/ PBS]	Y						N		Y		N			N	N	N	N				N		N
342	70% EtOH[Contrast/ PBS]	Y		Y			N	Y		Y		Y		Y		N						N		N

**Table 2.4. (cont'd)**

188	70% EtOH[H2O]	Y	N	N						N	N				N	N	N	N	N			
190	70% EtOH[H2O]	Y					N	N	N				N	N	N	N					N	N
193	70% EtOH[H2O]					N	Y	Y	N				N	N	N	N					N	N
200	70% EtOH[H2O]	N	Y	N			N	N	N						N	N					N	N
291	70% EtOH[H2O]		Y										N		N	N	Y	N	N	N	N	N
292	70% EtOH[H2O]	Y						Y	N	Y				N	N	N	N	N				N
294	70% EtOH[H2O]			Y									N	N		N	N	N	N	N	N	N
296	70% EtOH[H2O]							Y					N	N	N	N	N	N			N	N
299	70% EtOH[H2O]		Y										N		N	N	N	Y	N	N	N	N
300	70% EtOH[H2O]	Y			Y		Y							N	N		Y		N	N	N	N
301	70% EtOH[H2O]		Y						Y				N		N	N	N	Y	Y		N	N
307	70% EtOH[H2O]				Y								Y	N	N		N	N	N	N	N	N
310	70% EtOH[H2O]					Y		Y					N	N	N	N		Y			N	N

Presence of a tumor at necropsy is indicated with a “Y” for yes and absence with a “N” for no.

Fields are left blank for mammary glands that were not part of that experimental group or class. Mammary gland location code: 1 = left cervical; 2 = left upper thoracic; 3 = left lower thoracic; 4 = left abdominal; 5 = left inguinal; 6 = right cervical; 7 = right upper thoracic; 8 = right lower thoracic; 9 = right abdominal; 10 = right inguinal.

## REFERENCES

1. Siegel RL, Miller KD, Jemal A: Cancer statistics, 2019. *CA Cancer J Clin* 2019, 69(1):7-34.
2. Padamsee TJ, Wills CE, Yee LD, Paskett ED: Decision making for breast cancer prevention among women at elevated risk. *Breast Cancer Res* 2017, 19(1):34.
3. Slawson SH, Johnson BA: Ductography: how to and what if? *Radiographics* 2001, 21(1):133-150.
4. Stearns V, Mori T, Jacobs LK, Khouri NF, Gabrielson E, Yoshida T, Kominsky SL, Huso DL, Jeter S, Powers P *et al*: Preclinical and clinical evaluation of intraductally administered agents in early breast cancer. *Sci Transl Med* 2011, 3(106):106ra108.
5. Love SM, Zhang W, Gordon EJ, Rao J, Yang H, Li J, Zhang B, Wang X, Chen G, Zhang B: A feasibility study of the intraductal administration of chemotherapy. *Cancer Prev Res (Phila)* 2013, 6(1):51-58.
6. Gomberawalla A, Love S: The 8th international symposium on the breast: Using next-generation science to understand the normal breast and the development of breast cancer- conference report. *Breast Cancer Res Treat* 2015, 154(3):617-621.
7. Jacobs L, Sukumar S, Stearns V: Intraductal therapy for the prevention of breast cancer. *Curr Opin Investig Drugs* 2010, 11(6):646-652.
8. Sheiman LS, Levesque PH: The In's and Out's of Ductography: A Comprehensive Review. *Curr Probl Diagn Radiol* 2016, 45(1):61-70.
9. de Groot JS, van Diest PJ, van Amersfoort M, Vlug EJ, Pan X, Ter Hoeve ND, Rosing H, Beijnen JH, Youssef SA, de Bruin A *et al*: Intraductal cisplatin treatment in a BRCA-associated breast cancer mouse model attenuates tumor development but leads to systemic tumors in aged female mice. *Oncotarget* 2017, 8(37):60750-60763.
10. Murata S, Kominsky SL, Vali M, Zhang Z, Garrett-Mayer E, Korz D, Huso D, Baker SD, Barber J, Jaffee E *et al*: Ductal access for prevention and therapy of mammary tumors. *Cancer Res* 2006, 66(2):638-645.
11. Sivaraman L, Gay J, Hilsenbeck SG, Shine HD, Conneely OM, Medina D, O'Malley BW: Effect of selective ablation of proliferating mammary epithelial cells on MNU induced rat mammary tumorigenesis. *Breast Cancer Res Treat* 2002, 73(1):75-83.
12. Okugawa H, Yamamoto D, Uemura Y, Sakaida N, Tanano A, Tanaka K, Kamiyama Y: Effect of periductal paclitaxel exposure on the development of MNU-induced mammary carcinoma in female S-D rats. *Breast Cancer Res Treat* 2005, 91(1):29-34.
13. Yoshida T, Jin K, Song H, Park S, Huso DL, Zhang Z, Liangfeng H, Zhu C, Bruchertseifer F, Morgenstern A *et al*: Effective treatment of ductal carcinoma in situ with a HER-2- targeted alpha-particle emitting radionuclide in a preclinical model of human breast cancer. *Oncotarget* 2016, 7(22):33306-33315.

14. Chun YS, Yoshida T, Mori T, Huso DL, Zhang Z, Stearns V, Perkins B, Jones RJ, Sukumar S: Intraductally administered pegylated liposomal doxorubicin reduces mammary stem cell function in the mammary gland but in the long term, induces malignant tumors. *Breast Cancer Res Treat* 2012, 135(1):201-208.
15. Chun YS, Bisht S, Chenna V, Pramanik D, Yoshida T, Hong SM, de Wilde RF, Zhang Z, Huso DL, Zhao M *et al*: Intraductal administration of a polymeric nanoparticle formulation of curcumin (NanoCurc) significantly attenuates incidence of mammary tumors in a rodent chemical carcinogenesis model: Implications for breast cancer chemoprevention in at-risk populations. *Carcinogenesis* 2012, 33(11):2242-2249.
16. Brock A, Krause S, Li H, Kowalski M, Goldberg MS, Collins JJ, Ingber DE: Silencing HoxA1 by intraductal injection of siRNA lipidoid nanoparticles prevents mammary tumor progression in mice. *Sci Transl Med* 2014, 6(217):217ra212.
17. Wang G, Chen C, Pai P, Korangath P, Sun S, Merino VF, Yuan J, Li S, Nie G, Stearns V *et al*: Intraductal fulvestrant for Therapy of ERalpha-positive Ductal Carcinoma in Situ (DCIS) of the breast- a Preclinical Study. *Carcinogenesis* 2019.
18. Teo WW, Sukumar S: Combining the strength of genomics, nanoparticle technology, and direct intraductal delivery for breast cancer treatment. *Breast Cancer Res* 2014, 16(2):306.
19. Gueng M-K, Chou Y-H, Tiu C-M, Chiou S-Y, Cheng Y-F: Pseudoaneurysm of the Breast Treated with Percutaneous Ethanol Injection. *Journal of Medical Ultrasound*, 22(2):114-116.
20. Kuang M, Lu MD, Xie XY, Xu HX, Xu ZF, Liu GJ, Yin XY, Huang JF, Lencioni R: Ethanol ablation of hepatocellular carcinoma Up to 5.0 cm by using a multipronged injection needle with high-dose strategy. *Radiology* 2009, 253(2):552-561.
21. Ansari D, Andersson R: Radiofrequency ablation or percutaneous ethanol injection for the treatment of liver tumors. *World J Gastroenterol* 2012, 18(10):1003-1008.
22. Zhang WY, Li ZS, Jin ZD: Endoscopic ultrasound-guided ethanol ablation therapy for tumors. *World J Gastroenterol* 2013, 19(22):3397-3403.
23. Chin M, Chen CL, Chang K, Lee J, Samarasena J: Ethanol Ablation of a Peripheral Nerve Sheath Tumor Presenting as a Small Bowel Obstruction. *ACG Case Rep J* 2015, 3(1):31-32.
24. Wohlgemuth WA, Muller-Wille R, Teusch V, Hammer S, Wildgruber M, Uller W: Ethanolgel sclerotherapy of venous malformations improves health-related quality-of-life in adults and children - results of a prospective study. *Eur Radiol* 2017, 27(6):2482-2488.
25. Steiner F, FitzJohn T, Tan ST: Ethanol sclerotherapy for venous malformation. *ANZ J Surg* 2016, 86(10):790-795.
26. Sannier K, Dompmartin A, Theron J, Labbe D, Barrellier MT, Leroyer R, Toure P, Leroy D: A new sclerosing agent in the treatment of venous malformations. Study on 23 cases. *Interv Neuroradiol* 2004, 10(2):113-127.

27. Domp Martin A, Blaizot X, Theron J, Hammer F, Chene Y, Labbe D, Barrellier MT, Gaillard C, Leroyer R, Chedru V *et al*: Radio-opaque ethylcellulose-ethanol is a safe and efficient sclerosing agent for venous malformations. *Eur Radiol* 2011, 21(12):2647-2656.
28. Zhang J, Li HB, Zhou SY, Chen KS, Niu CQ, Tan XY, Jiang YZ, Lin QQ: Comparison between absolute ethanol and bleomycin for the treatment of venous malformation in children. *Exp Ther Med* 2013, 6(2):305-309.
29. Krause S, Brock A, Ingber DE: Intraductal injection for localized drug delivery to the mouse mammary gland. *J Vis Exp* 2013, 80 (issue)(80).
30. Plante I, Stewart MK, Laird DW: Evaluation of mammary gland development and function in mouse models. *J Vis Exp* 2011(53).
31. Sempere LF: Fully automated fluorescence-based four-color multiplex assay for co-detection of microRNA and protein biomarkers in clinical tissue specimens. *Methods Mol Biol* 2014, 1211:151-170.
32. Lines JL, Pantazi E, Mak J, Sempere LF, Wang L, O'Connell S, Ceeraz S, Suriawinata AA, Yan S, Ernstoff MS *et al*: VISTA is an immune checkpoint molecule for human T cells. *Cancer Res* 2014, 74(7):1924-1932.
33. Bates D, Mächler M, Bolker B, Walker S: Fitting Linear Mixed-Effects Models Using lme4. *2015* 2015, 67(1):48.
34. Hinck L, Silberstein GB: Key stages in mammary gland development: the mammary end bud as a motile organ. *Breast Cancer Res* 2005, 7(6):245-251.
35. Paine IS, Lewis MT: The Terminal End Bud: the Little Engine that Could. *J Mammary Gland Biol Neoplasia* 2017, 22(2):93-108.
36. Visvader JE: Keeping abreast of the mammary epithelial hierarchy and breast tumorigenesis. *Genes Dev* 2009, 23(22):2563-2577.
37. Ingrao JC, Johnson R, Tor E, Gu Y, Litman M, Turner PV: Aqueous stability and oral pharmacokinetics of meloxicam and carprofen in male C57BL/6 mice. *J Am Assoc Lab Anim Sci* 2013, 52(5):553-559.
38. Sonnemann KJ, Bement WM: Wound repair: toward understanding and integration of single-cell and multicellular wound responses. *Annu Rev Cell Dev Biol* 2011, 27:237-263.
39. Brancato SK, Albina JE: Wound Macrophages as Key Regulators of Repair: Origin, Phenotype, and Function. *Am J Pathol* 2011, 178(1):19-25.
40. Green JE, Shibata MA, Yoshidome K, Liu ML, Jorcyk C, Anver MR, Wigginton J, Wiltrout R, Shibata E, Kaczmarczyk S *et al*: The C3(1)/SV40 T-antigen transgenic mouse model of mammary cancer: ductal epithelial cell targeting with multistage progression to carcinoma. *Oncogene* 2000, 19(8):1020-1027.
41. King BL, Love SM: The intraductal approach to the breast: raison d'etre. *Breast Cancer Res* 2006, 8(2):206.

42. Love SM, Barsky SH: Anatomy of the nipple and breast ducts revisited. *Cancer* 2004, 101(9):1947-1957.
43. Morhard R, Nief C, Barrero Castedo C, Hu F, Madonna M, Mueller JL, Dewhirst MW, Katz DF, Ramanujam N: Development of enhanced ethanol ablation as an alternative to surgery in treatment of superficial solid tumors. *Sci Rep* 2017, 7(1):8750.
44. Garaycochea JI, Crossan GP, Langevin F, Mulderrig L, Louzada S, Yang F, Guilbaud G, Park N, Roerink S, Nik-Zainal S *et al*: Alcohol and endogenous aldehydes damage chromosomes and mutate stem cells. *Nature* 2018, 553(7687):171-177.
45. Green JE, Shibata MA, Shibata E, Moon RC, Anver MR, Kelloff G, Lubet R: 2-difluoromethylornithine and dehydroepiandrosterone inhibit mammary tumor progression but not mammary or prostate tumor initiation in C3(1)/SV40 T/t-antigen transgenic mice. *Cancer Res* 2001, 61(20):7449-7455.
46. Rutkowski MR, Allegranza MJ, Svoronos N, Tesone AJ, Stephen TL, Perales-Puchalt A, Nguyen J, Zhang PJ, Fiering SN, Tchou J *et al*: Initiation of metastatic breast carcinoma by targeting of the ductal epithelium with adenovirus-cre: a novel transgenic mouse model of breast cancer. *J Vis Exp* 2014(85).
47. Chua AC, Hodson LJ, Moldenhauer LM, Robertson SA, Ingman WV: Dual roles for macrophages in ovarian cycle-associated development and remodelling of the mammary gland epithelium. *Development* 2010, 137(24):4229-4238.
48. Vilholm OJ, Cold S, Rasmussen L, Sindrup SH: The postmastectomy pain syndrome: an epidemiological study on the prevalence of chronic pain after surgery for breast cancer. *Br J Cancer* 2008, 99(4):604-610.
49. Waltho D, Rockwell G: Post-breast surgery pain syndrome: establishing a consensus for the definition of post-mastectomy pain syndrome to provide a standardized clinical and research approach - a review of the literature and discussion. *Can J Surg* 2016, 59(5):342-350.
50. Clark A, Bird NK, Brock A: Intraductal Delivery to the Rabbit Mammary Gland. *J Vis Exp* 2017(121).
51. Borowiak R, Groebner J, Haas M, Hennig J, Bock M: Direct cerebral and cardiac 17O-MRI at 3 Tesla: initial results at natural abundance. *MAGMA* 2014, 27(1):95-99.

**CHAPTER 3: TANTALUM OXIDE NANOPARTICLES AS VERSATILE AND HIGH-RESOLUTION X-RAY CONTRAST AGENT FOR INTRADUCTAL IMAGE-GUIDED ABLATIVE PROCEDURE IN RODENT MODELS OF BREAST CANCER**

Published in *npj Imaging*, 2024, DOI: 10.1038/s44303-024-00007-5

Erin K. Zaluzec\*<sup>1,2</sup>, Elizabeth Kenyon\*<sup>1</sup>, Maximilian Volk<sup>1</sup>, Hasaan Hayat<sup>1</sup>, Katherine Powell<sup>1</sup>, Alexander Loomis<sup>1</sup>, Shatadru Chakravarty<sup>3</sup>, Jeremy Hix<sup>3</sup>, Josh Schipper<sup>4</sup>, Chi Chang<sup>5</sup>, Matti Kiupel<sup>6</sup>, Ping Wang<sup>1,3</sup>, Erik M. Shapiro<sup>3</sup>, Lorenzo F. Sempere<sup>1,3</sup>

\*These authors contributed equally.

<sup>1</sup> Precision Health Program, Michigan State University, East Lansing, Michigan, 48824

<sup>2</sup> Department of Pharmacology & Toxicology, College of Veterinary Medicine, Michigan State University, East Lansing, 48824

<sup>3</sup> Department of Radiology, College of Human Medicine, Michigan State University, East Lansing, Michigan, 48824

<sup>4</sup> Van Andel Research Institute, Grand Rapids, Michigan, 49503

<sup>5</sup> Epidemiology and Biostatistics, College of Human Medicine, Michigan State University, East Lansing, Michigan, 48824

<sup>6</sup> Veterinary Diagnostic Laboratory, College of Veterinary Medicine, Lansing, Michigan, 48910

## **Contributions to Science.**

I helped in the acquisition of animal imaging and collection along with Ms. Kenyon. I performed data analysis of mammary gland ablation, local and systemic toxicity for graphical representation. I took representative H&E photos of mammary glands and major organs for the generation of figures and drafted the initial results and discussion portions of this chapter.

## **Abstract.**

There are limited options for primary prevention of breast cancer (BC). Experimental procedures to locally prevent BC have shown therapeutic efficacy in animal models. To determine the suitability of FDA-approved iodine-containing and various metal-containing (bismuth, gold, iodine, or tantalum) preclinical nanoparticle-based contrast agents for image-guided intraductal (ID) ablative treatment of BC in rodent models, we performed a prospective longitudinal study to determine the imaging performance, local retention and systemic clearance, safety profile, and compatibility with ablative solution of each contrast agent. At least six abdominal mammary glands (>3 female FVB/JN mice and/or Sprague-Dawley rats, 10-11 weeks of age) were intraductally injected with commercially available contrast agents (Omnipaque<sup>®</sup> 300, Fenestra<sup>®</sup> VC, MVivo<sup>™</sup> Au, MVivo<sup>™</sup> BIS) or in-house synthesized tantalum oxide (TaO<sub>x</sub>) nanoparticles. Contrast agents were administered at stock concentration or diluted in 70% ethanol (EtOH) and up to 3% ethyl cellulose (EC) as gelling agent to assess their compatibility with our image-guided ablative procedure. Mammary glands were serially imaged by microCT for up to 60 d after ID delivery. Imaging data were analyzed by radiologists and deep learning to measure in vivo signal disappearance of contrast agents. Mammary glands and major organs were ultimately collected for histopathological examination. TaO<sub>x</sub>-containing solutions provided best imaging performance for nitid visualization of ductal tree immediately after infusion, low outward diffusion (< 1 d) and high homogeneity. Of all nanoparticles, TaO<sub>x</sub> had the highest local clearance rate (46% signal decay as stock and 36% as ablative solution 3 d after ID injection) and exhibited low toxicity. TaO<sub>x</sub>-containing ablative solution with 1% EC caused same percentage of epithelial cell death (88.62% ± 7.70% vs 76.38% ± 9.99%, p-value = 0.089) with similar minimal collateral

damage ( $21.56 \pm 5.28\%$  vs  $21.50\% \pm 7.14\%$ ,  $p\text{-value} = 0.98$ ) in mouse and rat mammary glands, respectively. In conclusion, TaO<sub>x</sub>-nanoparticles are a suitable and versatile contrast agent for intraductal imaging and image-guided ablative procedures in rodent models of BC with translational potential to humans.

## **Background.**

Breast cancer (BC) has the highest cancer diagnosis rate among women within the United States and is the second leading cause of cancer-related deaths [1]. Although there are many FDA approved treatments for BC patients, the estimated death rate among women has remained stagnant for the past 22 years [1]. Currently, only two FDA-approved options aid in BC prevention: prophylactic mastectomy and hormone therapy [2]. The severe side effects deter many of the eligible women from choosing these interventions [3]. Therefore, there is a need to develop new strategies of prevention for high-risk individuals that will also benefit women at moderate or low risk for BC.

Intraductal injection (ID) can be used clinically for ductography imaging to establish differential diagnosis of nipple discharge with minimal discomfort [4, 5]. ID injection is a novel strategy for BC prevention and local treatment [6, 7] that has shown promise in preclinical animal models [8-22]. We have repurposed the procedure of ID injections for BC prevention by infusing a cell-killing solution in rodent models [8-12], thereby locally targeting epithelial cells from which BC (carcinoma) arises. We previously demonstrated the feasibility of ID delivery with 70% ethanol (EtOH) as an inexpensive, readily available, cell-killing chemical solution in rodent models [8-12]. Our previous study showed therapeutic efficacy of single ID injection of 70% EtOH for preventing BC formation in the aggressive C3(1)-TAg mouse model [8]. As EtOH is already used clinically as an ablative agent for local cancer treatments, these findings position ID injections of 70% EtOH as a promising procedure [10, 11] to investigate in future first-in-human trials for BC prevention of at-risk individual.

Fluoroscopy and computerized tomography (CT) are clinical imaging modalities that could be used to monitor this ablative procedure for intended application of BC risk reduction in future clinical trials.

These techniques are enhanced by contrast agents that attenuate X-rays giving rise to an imaging signal [23]. We seek to introduce a radiopaque contrast agent into our ablative solution for real-time visualization (e.g., fluoroscopy) and image guidance of complete filling of the ductal tree in animal models. MicroCT is a rapid, high-resolution imaging modality that can visualize full anatomy of the breast in animal models in 3D [24]. Several metallic nanoparticle based X-ray contrast agents have been formulated with small nanoparticle size and high radiopacity (reviewed in ref [25]). We recently developed tantalum oxide ( $\text{TaO}_x$ ) nanoparticles as a novel X-ray contrast agent for CT [9].  $\text{TaO}_x$  nanoparticles have higher radiopacity than iodine at clinical X-ray energies and low toxicity with slower outward diffusion from the ductal tree of rodent models [8-11] than FDA-approved iodine-based contrast agents (e.g., Isovue-300) used in clinical ductography. Here, we systematically and comprehensively compared the diagnostic and therapeutic potential of several commercially available (iodine-, gold-, and bismuth-containing) X-ray contrast agents against  $\text{TaO}_x$  nanoparticles when infused intraductally with the 70% EtOH ablative solution. We set the following criteria to objectively identify suitable contrast agent for image guidance of this investigational ablative procedure: 1) minimal diffusion within 8 hrs of infusion to have a nitid visualization and assess complete filling of the ductal tree immediately after injection; 2) high local clearance by 3 days, so that contrast agent does not interfere with future imaging sessions (CT and/or MRI) assessing anatomical changes of treated mammary gland; 3) low local and systemic toxicity; and 4) compatibility with ablative agent (70% EtOH) to maximize epithelial cell killing.

## **Materials and Methods.**

**Contrast Agent Preparation:** All X-ray contrast agents were used as commercially supplied.

Hydrophilic  $\text{TaO}_x$  nanoparticles were synthesized as described [9]. For all contrast reagents except  $\text{TaO}_x$  nanoparticles (NPs), injection solution was either “stock” as supplied by the manufacturer with no dilution, or three parts stock solution with 7 parts 200 proof EtOH to yield 70% EtOH in the solution: Omnipaque<sup>®</sup> 300 (GE Healthcare, #00407141363, 300 mg I/mL), Fenestra<sup>®</sup> VC (MedLumine, VC-131, <200 nm particles pegylated emulsion, 50 mg I/mL), MVivo<sup>™</sup> Au (MedLumine, Au-315,  $15 \pm 2$  nm

particles, 200 mg Au/mL), MVivo™ BIS (MedLumine, BIS-11, 250 nm nanoparticles, 150 Bi mg/mL). TaO<sub>x</sub> (11.1 ± 1 nm particles) was supplied in lyophilized form as described [9], which allowed for the 70% EtOH solution to contain half the concentration of the “stock” solution rather than 30% as with manufactured contrast agents (specifically 36 mg Ta/mL in “stock” versus 18 mg Ta/mL in 70% EtOH). Ethyl cellulose (Acros Organics, 9004-57-3) was added up to 3 % (w/v) to 70% EtOH solution containing 18 mg Ta/mL of TaO<sub>x</sub>.

**MicroCT Image Acquisition and Analysis:** All experiments were conducted under protocols approved by Institutional Animal Care and Use Committee at Michigan State University. 10-week-old female FVB/JN mice (n = 3-5/solution; [jax.org](http://jax.org) stock 001800) and 11-week-old female Sprague Dawley rats (n = 3-4/solution; [envigo.com](http://envigo.com) order code 002) were prepared and ID injected as described [10, 11]. Serial images of infused ductal trees were acquired at different time points post-injection using a PerkinElmer Quantum GX microCT scanner; for short-term study: 0, 30 min, 1, 2, 4 and 8 hours (**Figures 3.1 and S3.8**) and for long-term study: 0, 1, 3, 7, 14, 30 and 60 days (**Figures 3.3, 3.4 and S3.9**). The following image acquisition scan parameters were standardized and used at each scan interval time point in mice: 90 kVp/88 μA; field of view (FOV), 36 mm; number of slices, 512; slice thickness, 72 μm; voxel resolution, 72 μm<sup>3</sup>; and in rats: 90 kVp/88 μA; FOV, 72 mm; number of slices, 512; slice thickness, 72 μm; voxel resolution, 144 μm<sup>3</sup>. Radiation exposure was minimized in these serial imaging studies by acquisition of standard (2 min) scans. Caliper AnalyzeDirect©, v12.0 (Biomedical Imaging Resource, Mayo Clinic, Rochester, MN) was used for microCT image rendering, segmentation, and analysis of individual glands or tissue phantoms (0.2 mL PCR tubes with contrast solutions) as described [10, 11].

**MicroCT Deep Learning Analysis:** A deep learning algorithm consisting of a Convolutional Neural Network (CNN) with UNET architecture was used for automated segmentation and analysis of the microCT images. Two clinical radiologists (A.L, P.W.) and an imaging specialist (H.H.) generated full volume segmentation masks for 12 image volumes consisting of 256 slices each via the ITK-snap

software. The model consisted of feature extraction, flattening and regression layers, taking the preprocessed image as input. The model was trained using individual 2D slices and corresponding radiologist generated masks from each image volume, which rendered a total dataset size of 3,072 slices used for initial training of the algorithm. Preprocessed image slices of dimensions  $[x, y] = [256, 512]$  were input into the algorithm for training with a batch size = 32, epoch = 100 iterations and a learning rate  $\alpha = 10^{-4}$  using the Adam optimizer. Loss per iteration was calculated using standard gradient descent loss algorithm [26]. A 5-fold cross-validation method was used for training such that 80% of the data was used as a training set and 20% of the data was used for internal validation of algorithm performance. The resulting image segmentations were then used for ROI analysis of mammary gland contrast content using average HU values rendered from each gland bilaterally. For adequate transformation of pixel values to standard Hounsfield units (HU), the inference script used SimpleITK for rendering of the original image and resulting segmentation output from the algorithm after thresholding the original image.

**Histological Analysis:** Animals were euthanized immediately after last scan in serial microCT imaging (for short term study 8 hours after and for long term study 60 days after injections). Dissected mammary glands were processed and embedded in paraffin after 24 h fixation in formalin as described [27]. Formalin-fixed paraffin-embedded (FFPE) tissue samples (4  $\mu\text{m}$ ) were scanned on an Aperio Versa 8 Brightfield & Fluorescence imaging system (Leica Biosystems, Buffalo Grove, IL) following H&E staining. Annotation and quantitative analysis were performed using ImageScope tools as described [8].

**Statistical Analysis:** Unpaired Welch's t-tests were used to assess statistical significance of difference of continuous values obtained from imaging and tissue analyses between experimental groups and a reference control group. GraphPad Prism 9 was used to perform these statistical analyses. We set a p-value of 0.01 as the threshold to report statistical significance.

## Results.

### **TaO<sub>x</sub> Enables Better Imaging of Rodent Ductal Tree Architecture as Compared to FDA Approved**

**Omnipaque:** We conducted a short-term serial imaging study to characterize retention of Omnipaque and TaO<sub>x</sub> within the ductal tree. We injected 40μL of Omnipaque or TaO<sub>x</sub> in PBS (300 mg I/mL and 18 mg Ta/mL, respectively) or 70% EtOH (90 mg I/mL and 18 mg Ta/mL respectively) in the abdominal mammary glands of FVB mice. Animals were imaged by microCT immediately and at 0.5, 1, 2, 4 and 8 hours post injections (**Figure 3.1A**). Stock Omnipaque was detected at all time points, but rapidly diffused outside the ductal tree, flooding the mammary fat pad and reaching the fascia (**Figures 3.1A and B, S3.8**). After local clearance, residual Omnipaque was retained within the ductal tree enabling nitid visualization of its overall structure from 1 hr to 8 hrs after injections. Omnipaque diluted in 70% EtOH had minimal retention in the ductal tree and was undetectable 1hr after injections (**Figures 3.1B, S3.8**). However, TaO<sub>x</sub> remained within the ductal tree with little clearance and had extended ductal tree branching within the 8-hour time frame in both stock PBS solution and 70% EtOH (**Figures 3.1A and B, S3.8**). Most importantly, TaO<sub>x</sub> enables nitid visualization of the ductal tree immediately after infusion with 70% EtOH ablative solution, which is a required feature for intended image guidance application to assess complete filling of the ductal tree. Together, these demonstrate TaO<sub>x</sub> has superior local retention and imaging capabilities as compared to Omnipaque.

### **In vitro and in vivo Comparison of TaO<sub>x</sub> with Commercially Available CT Contrast Agents:**

To ensure that all contrast agents could be visualized by microCT imaging at the injectable range, stock solutions of each agent were serially diluted in PBS or 70% EtOH (**Figure 3.2**). Omnipaque and Mvivo Au dilutions had the highest signal intensity, though all contrast agents produce adequate signal. EtOH did not interfere with signal detection or homogeneity of any of the contrast agent, except for MVivo BIS (**Figure 3.2B and C**). Qualitatively, MVivo BIS signal was heterogenous in tissue phantom.

Quantitatively, linear fitting of MVivo signal was poor in PBS ( $R^2 = 0.59$  compared to other contrast agents  $R^2 > 0.96$ ) and in 70% EtOH ( $R^2 = 0.68$  compared to other contrast agents  $R^2 > 0.91$ ). Commercial

contrast agents were provided at stock concentration ready to inject intravenously in animals. Therefore, the addition of EtOH resulted in lowered concentration of each contrast agents to 30% of maximal concentration, except for TaO<sub>x</sub> nanoparticles that can be reconstituted to up to 60 mg Ta/mL in either PBS or 70% EtOH (**Figure S3.9**). As expected, stronger signal can be observed in infused ductal tree with stock solution rather than EtOH. The decrease of signal intensity of all contrast agents is proportional and consistent with observations in tissue phantoms, except for MVivo BIS (**Figure 3.2B and C**). As observed in tissue phantoms, MVivo BIS signal was inconsistent and heterogeneous within the ductal tree. Moreover, viscous, aggregation prone MVivo BIS solutions diffculted a steady continuous infusion of cannulated nipples.

From the short-term serial imaging study (**Figure 3.1**), we determined that the time point immediately after injection was crucial for the ability of a contrast agent to serve in image guidance application of this ablative procedure. To assess imaging performance of all contrast agents for initial visualization of the ductal tree, we generated 3D reconstructions of the infused ductal trees from segmented images of the mammary gland structures (fat pad/fascia boundary) (**Figure 3.2A**). Omnipaque and Mvivo Au solutions rapidly diffused outside the ductal tree and flooded mammary gland stroma as inferred by the oversaturation and lack of defined ductal tree structure (**Figures 3.3, 3.4, S3.9**). Leaked contrast agent can be easily appreciated as it markedly outlines the mammary gland fascia boundary on single slice microCT images (**Figure 3.2B**) and a solid wall on 3D reconstructions (**Figures 3.3, 3.4**). Fenestra VC and TaO<sub>x</sub> solutions were predominantly retained within the filled ductal tree enabling informative visualization of the overall ductal tree structure (**Figures 3.2C, 3.3, 3.4, S3.9**). Compared to TaO<sub>x</sub>, the ductal tree in Fenestra VC-infused animals was equivocal and not as defined, especially in stock solution, due to local leakage outside the tree and heterogenous distribution of the solution (e.g., air bubbles) (**Figures 3.2C, 3.3, 3.4, S3.9**).

**Local Retention and Long-Term Imaging of Contrast Agents:** To study the long-term effects of local retention and systemic clearance of each contrast agent, we conducted a 60-day serial imaging study.

Mice were ID infused with 40 $\mu$ L of stock solutions or contrast agent in 70% EtOH into the abdominal mammary glands. Animals were imaged by microCT at days 1, 3, 7, 14, 30 and 60 after injections (**Figures 3.3, 3.4, S3.9**). We generated 3D reconstructions of the lower body to determine how contrast agents distributed systemically. We did not detect signal for any contrast agents in major organs (kidney, lung, liver, spleen) (**Figure S3.9**). Mvivo Au solutions accumulated subcutaneously (**Figure S3.9**). Subcutaneous accumulation was occasionally observed in animals infused with TaO<sub>x</sub> (1 out of 15 animals) or Fenestra VC (1 out of 7) stock solutions (**Figure S3.9**). We generated 3D reconstructions of the infused ductal trees from segmented images of the mammary gland structure (fat pad/fascia boundary). As expected after day 1, Omnipaque-infused animals had little signal retention in the mammary gland compared to the other contrast agents (**Figures 3.3, 3.4**). Mvivo Au, TaO<sub>x</sub>, and Fenestra VC remained within the ductal tree for 60 days to varying degrees (**Figures 3.3, 3.4**), except for Mvivo Au in 70% EtOH which was undetectable after 7 days (**Figure 3.4**). Fenestra VC in 70% EtOH appeared to aggregate during the active process of wound healing, hampering local clearance (**Figure 3.3**). Further study will be needed to understand if this aggregation is a macrophage-mediate process, or another foreign object clearance mechanism is at work. The faster clearance and low immunogenicity of TaO<sub>x</sub> is a desirable feature to minimize long-term toxicity and facilitate follow-up procedures.

**AI-assisted Quantitative Metrics of Contrast Agent Signal Decay:** To obtain systematic and quantitative metrics of signal decay over time, we developed a Deep Learning (DL)-based AI algorithm for automated segmentation of mammary gland and extraction of HU values from region of interest (**Figure 3.5A**). We applied this DL algorithm for image analysis of data files obtained from short-term study (**Figure 3.1**) and long-term study (**Figures 3.3, 3.4**). Omnipaque signal was less than 15% of maximum signal in either stock or 70% EtOH after 1 hour of injection (**Figure 3.5B**) and signal was less than 5% after 1 day and undetectable after 3 days (**Figure 3.5C**). TaO<sub>x</sub> signal remained above 60% of maximum both in stock and 70% EtOH solution after 8 hrs of injections (**Figure 3.5B**). After 1 day of injections, TaO<sub>x</sub> signal was less than 40% of maximum and exhibited more rapid local clearance than the

other nanoparticle-based contrast agents, except for MVivo Au in 70% EtOH (**Figure 3.5C**). TaO<sub>x</sub> signal was less than 20% of maximum by 60 days after injections. Comparatively, Mvivo Bis signal declined more slowly during the first 30 days after injections, but precipitously declined to less than 10% by 60 days (**Figure 3.5C**). Unlike other contrast agents, Fenestra VC signal in 70% EtOH declined much slower than in stock solution and almost 50% of signal remained 60 days after injections (**Figure 3.5C**).

#### **Ductal Ablation, Systemic Accumulation, and Toxicity of TaO<sub>x</sub> and Other Contrast Agents: To**

ensure the safety of the contrast agents for application in the ablative procedure, we next looked at local and systemic toxicity of each contrast agent alone or in combination with 70% EtOH. Tissues from mammary glands and major organs (heart, lung, spleen, liver, and kidney) were collected immediately after last imaging session 60 days after injections. For all contrast agents, we observed healthy, nucleated epithelial cells with intact surrounding adipose tissue in H&E stained mammary glands (**Figure 3.6A**). A mild foreign body reaction with periductal fibrosis was observed in MVivo Au- and TaO<sub>x</sub>-infused ductal trees; a stronger foreign body reaction with periductal fibrosis and inflammation as well as intraductal histocyte accumulation was observed in MVivo BIS-infused ones (**Figure 3.6A**). Contrast agents had no or minimal interference with ablative effects of 70% EtOH and wound healing response. A similar amount of tissue damage was observed in all tested contrast agent conditions in 70% EtOH (**Figures 3.6A and C**). Interestingly, pockets of intact epithelial cells were observed in Omnipaque- and Fenestra VC-infused ductal tree, suggesting an incomplete epithelia ablation perhaps due to uneven and heterogenous distribution throughout the lumen of all branches (**Figure 3.6A**). Accumulation of nanoparticle aggregates was only visible in MVivo Au-infused ductal trees (**Figure 3.6A and D**); these aggregates were also observed in distant organs, especially in the spleen and liver (**Figure 3.6B and D**). However, no overt toxicity was observed in major organs whether there were visible nanoparticle aggregates (MVivo Au) or not; there were no atypical tissue presentations in the form of dysplasia, infarction, hemorrhage, fibrotic or immune reaction (**Figure 3.6B**).

### **Compatibility with Ethyl Cellulose and Scalability of TaO<sub>x</sub>-Based Ductal Tree Visualization in**

**Rats:** Together, the above results support the superiority of TaO<sub>x</sub> as contrast agent for this ablative procedure. TaO<sub>x</sub> was retained in the ductal tree and did not cause toxic effects locally or systemically. TaO<sub>x</sub> did not interfere with EtOH ablative effect nor were TaO<sub>x</sub> imaging properties impacted by EtOH. Therefore, our expansion studies exclusively focused on the ability of TaO<sub>x</sub> to be formulated in solution with ethyl cellulose (EC) as gelling agent and the ability of this refined solution and ablative procedure to be scaled up to a rat model. EC is used clinically in 95-100% EtOH solution for ablative treatment of tumors and sclerosing treatment of venous malformations [28-35]. We first assessed the ability of EC to slow down EtOH diffusion using tissue phantoms. EC at 5% w/v concentration is not soluble in less than 70% EtOH because of the increased water content (**Figure 3.7A**). Compared to other tested solutions, 70% EtOH with 5% EC had the lowest rate of diffusion (**Figure 3.7A**). To determine the ability of EC to limit EtOH diffusion throughout the mammary gland *in vivo*, the ductal trees of both mice and rats were infused with a 70% EtOH solution containing TaO<sub>x</sub> (18 mg Ta/mL) and/or EC (1% w/v). ID injections were successfully translated into the rat model and X-ray imaging capabilities of TaO<sub>x</sub> were maintained for visualization of infused rat ductal trees (**Figure 3.7B and C**). Macroscopically, EC-containing solutions provide same infusion properties and ductal tree visualization as undoped solutions (**Figure 3.7C**). Microscopically, EC-containing solutions provide same or higher epithelial cell ablation rate and significantly lower collateral tissue damage both in mouse and rat mammary gland tissues examined 3 days after ID injections (**Figure 3.7D and E**). Together, these results indicate that introducing 1% EC to ablative and imaging solution of 70% EtOH and TaO<sub>x</sub> (18 mg Ta/mL) further improves local targeting epithelial cells with less collateral tissue damage.

### **Discussion.**

We evaluated the short-term and long-term performance of contrast agents in visualizing the infused ductal trees in rodent models and any impact on ablation rate, breast physiology, and scalability to larger animal models and eventually humans. From a clinical standpoint, fluoroscopy or similar real-time imaging

modality will be needed to guide the ductal tree infusion in future first-in-human clinical trials to evaluate this ablative procedure. Given the desired properties of an ideal contrast agent (visualization of fully filled ductal tree, high local clearance, low toxicity, and compatibility with 70% EtOH) for this therapeutic purpose, we identified TaO<sub>x</sub> as the most suitable contrast agent. Rapid outward diffusion, especially in 70% EtOH, of FDA-approved Omnipaque (**Figures 3.1-3.4, S3.8 and S3.9**) and gold nanoparticle-containing MVivo Au (**Figures 3.2-3.4, S3.9**) renders them unsuitable for the intended image guidance application of assessing fully filled ductal tree(s). Omnipaque presumably escapes the ductal tree system after extensive epithelial cell ablation and loss of architectural integrity with hyperintensity in the bladder from 0.5 hr to 2 hr indicating rapid systemic clearance (**Figure S3.8**), but additional experiments are needed to test this directly. An unexpected concern of MVivo Au was the discoloration of mice. Immediately after injections, all mice turned a grey color which did not resolve throughout the study. Although there was no observed discomfort or overt toxicity, the systemic spread to internal organs (**Figure 3.6**) and subcutaneous accumulation (**Figure S3.9**) is a cause for concern for continued use. Other contrast agents (Fenestra VC and MVivo BIS) and TaO<sub>x</sub> exhibited a much higher local retention (**Figure 3.5B**) and enabled initial visualization of infused ductal trees (**Figures 3.2-3.4, S3.9**). However, MVivo BIS produced imaging artifacts that compromised unequivocal and nitid visualization of the true ductal tree architecture (**Figures 3.2-3.4, S3.9**). Fenestra VC enabled similar short-term visualization of the ductal tree as TaO<sub>x</sub>, with some imaging artifacts due to heterogenous dispersion and diffusion through the lumen and leakage outside the ductal tree (**Figures 3.2-3.4, S3.9**). Higher local retention and limited clearance of Fenestra VC, especially in 70% EtOH, is a problematic feature of this contrast agent (**Figures 3.4, S3.9**). In exploratory experiments, animals infused with Fenestra VC or MVivo BIS in more than two mammary glands died shortly after injections. The total amount of contrast injected was above vendor's recommended bolus dose for intravenous administration. This suggests that the maximal tolerated dose of these contrast agents as formulated would be a limiting factor for intended application in ID imaging procedures in women. In contrast, animals infused with TaO<sub>x</sub> in six or more mammary glands tolerated this procedure well [10, 11].

A main goal of this study was the serial imaging of different contrast agents. This required several

sessions with X-ray radiation. While the cumulative X-ray dose delivered was less than 500 mGy [36], radiation may have contributed to foreign object recognition and clearance by the host immune system and overall wound healing process. Short-term effects of radiation (< 7 days after injections) did not appear to interfere with EtOH-induced epithelial ablation with different contrast agents compared to EtOH treatment alone in our previous study [8]. Long-term effects of radiation and/or contrast agent additions appeared to delay wound healing process compared to EtOH treatment alone [8]. We used commercially available contrast agents at stock concentrations recommended by the vendor for intravenous injections. We acknowledge that refinement of the concentration or formulation of these nanoparticle-based contrast agents may make them more suitable for the intended intraductal applications, especially since many of these agents are for preclinical research purposes only. However, under same conditions, off-the-shelf TaO<sub>x</sub> nanoparticles outperformed all these contrast agents. This highlights the versatility of our in-housed synthesized TaO<sub>x</sub> construct that can be reconstituted at a wide range of concentrations in hydrophilic, polar, and hydrophobic solutions (**Figure S3.9**, [9]).

We also broadened the versatility of TaO<sub>x</sub> as imaging agent by scaling up ID procedure and in vivo X-ray visualization of the infused ductal tree in rat models (**Figure 3.7B** and **C**). We introduced ethyl cellulose (EC) as gelling agent to limit collateral tissue damage caused by diffusion of EtOH. EC is safe for human consumption and is clinically used with EtOH for treatment of tumors and venous malformation [28 – 35]. The addition of 1% EC had no impact on ablative rate and aided in reducing EtOH dispersion outside of the ductal tree (**Figure 3.7D** and **E**). However, some animals experienced limb stiffness with the addition of EC. Tissue analyses show wound healing process resolves about one month after ablative procedure (**Figure 3.7A**). However, further investigation will be needed to determine the specific immunological and fibroblastic responses to tissue damage that may be caused and compounded by the combination of 70% EtOH, TaO<sub>x</sub> and/or EC, and if higher % of EC may be beneficial to faster resolution of wound healing. Current protocols for BC diagnosis utilize X-ray or MR imaging for confirmation of masses within the breast and lack of clearance of a contrast agent might interfere or create imaging artifacts. While TaO<sub>x</sub> signal is less than 36% of maximal signal 3 d after injection, there is still about 10% of maximal

signal detected after 60 d (**Figure 3.5B**). Therefore, it will be important to refine TaO<sub>x</sub> formulation to maximize clearance after 3 d and/or determine what amount of residual contrast agent may have a potential impact on follow-up imaging session for anatomical assessment and/or tumor surveillance. While these rodent models are well-established for assessing therapeutic efficacy (tumor latency, tumor incidence, and overall survival), both mice and rats have a single-ductal tree per mammary gland with a relatively simple and linear structure [37, 38]. Rabbits are a larger animal model closer to humans evolutionarily, physiologically, and anatomically with multiple ducts per mammary gland [39-46]. Therefore, utilizing rabbit models and fluoroscopy to guide infusion of cannulated nipples in future studies should improve the success rate of the procedure, address challenges of simultaneous infusion of multi-ductal tree system and impact on cosmesis and collateral tissue damage, and further assess the scalability towards application in humans. In conclusion, this study sets the stage for clinically enabling toxicity and efficacy studies in a large animal model such as rabbit and ultimately first-in-human evaluation of this image-guided ablative procedure for BC risk reduction.

## Figures

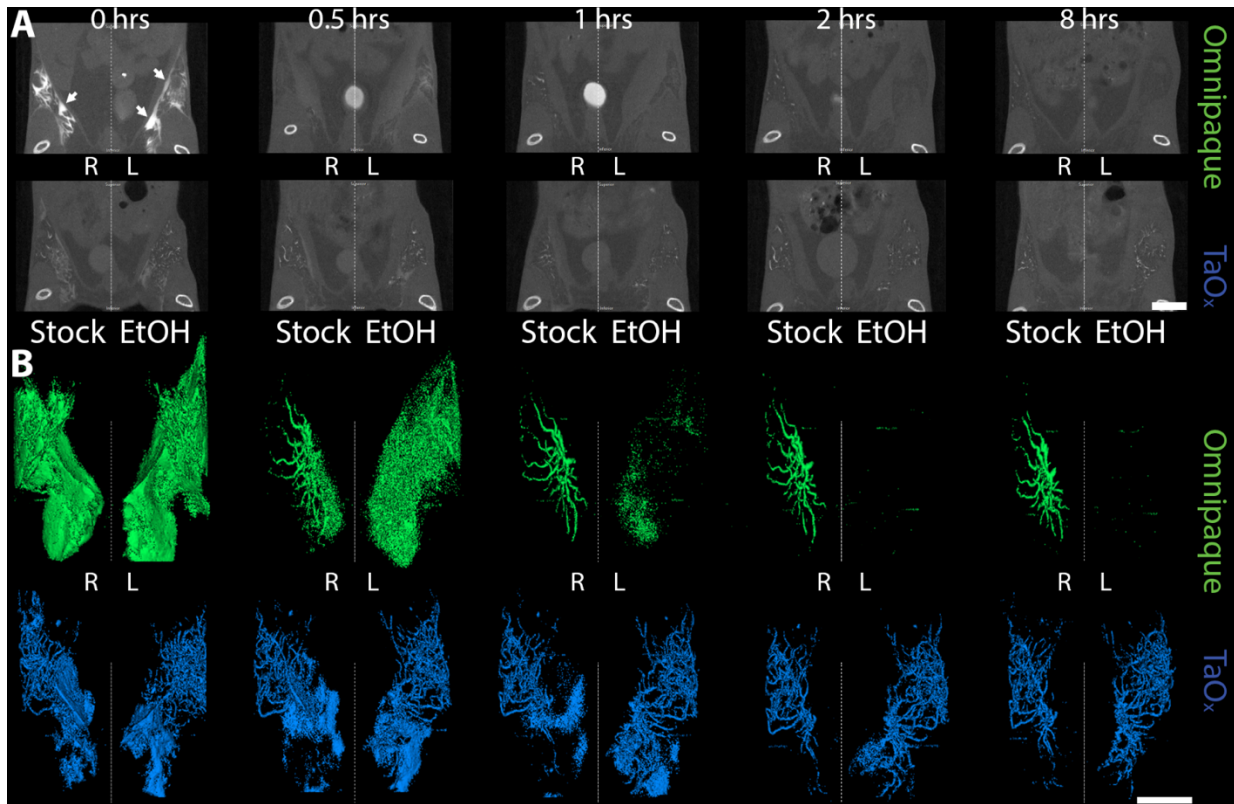


**Figure 3.1. Short-term serial microCT imaging of the murine ductal tree with different contrast agents.** Abdominal mammary glands were injected with 40  $\mu$ l of indicated contrast agent as stock solution (300 mg I/mL Omnipaque or 18 mg Ta/mL in PBS) or in 70% ethanol (EtOH, 90 mg I/mL Omnipaque or 18 mg Ta/mL). **A)** Representative microCT slice of the lower body of the same animals is shown at different imaging time points from immediately after last ID injection (0 hrs) to 8 hrs. Scale bar is 10 mm. **B)** 3D reconstruction of manually segmented region of interest (i.e., ipsi- and contralateral abdominal mammary glands). 3D reconstruction was thresholded to include only voxels with a HU value of  $> 300$ . Arrows indicate areas in which leaked contrast agent accumulates on the fascia boundary. Scale bar is 1 mm.

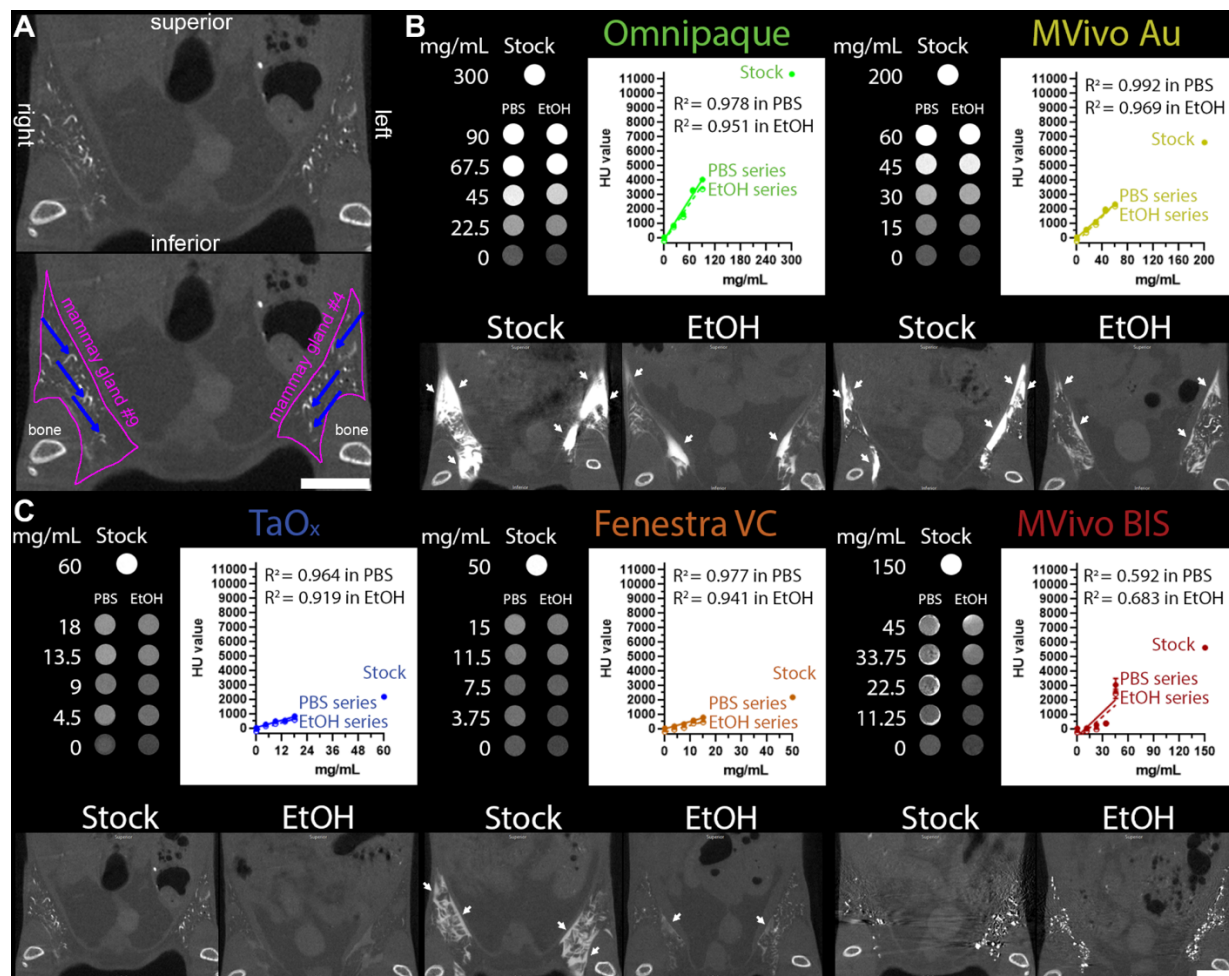


**Figure 3.2. Contrast agent characteristics and signal attenuation profile in different solutions. A)** Annotated views of microCT image of TaO<sub>x</sub>-infused mammary glands (36 mg Ta/mL stock, also shown at lower magnification in C); pink line outlines abdominal mammary glands and blue arrows pinpoint fill branches of the ductal tree. **B** and **C)** Tissue phantoms and mice were scanned with the same microCT imaging parameters. Top panels (tissue phantoms), each contrast agent was diluted from stock reagent (maximal concentration) in PBS or 70% ethanol (EtOH) at indicated concentrations (mg of metal/mL). Linear fitting of signal attenuation as function of the concentration of the metal in each solution. Bottom panels, representative single-slice microCT images of the lower body of animals captured immediately after last ID injection of each indicated solution: Omnipaque (300 mg I/mL stock, 90 mg I/mL in EtOH), MVivo Au (200 mg Au/mL stock, 60 mg Au/mL in EtOH), TaO<sub>x</sub> (36 mg Ta/mL stock, 10.8 mg Ta/mL in EtOH), Fenestra VC (50 mg I/mL stock, 15 mg I/mL in EtOH), MVivo BIS (150 mg Bis/mL stock, 45 mg Bis/mL in EtOH). Arrows indicate areas in which leaked contrast agent accumulates on the fascia boundary. Scale bar is 10 mm in images at different magnification.

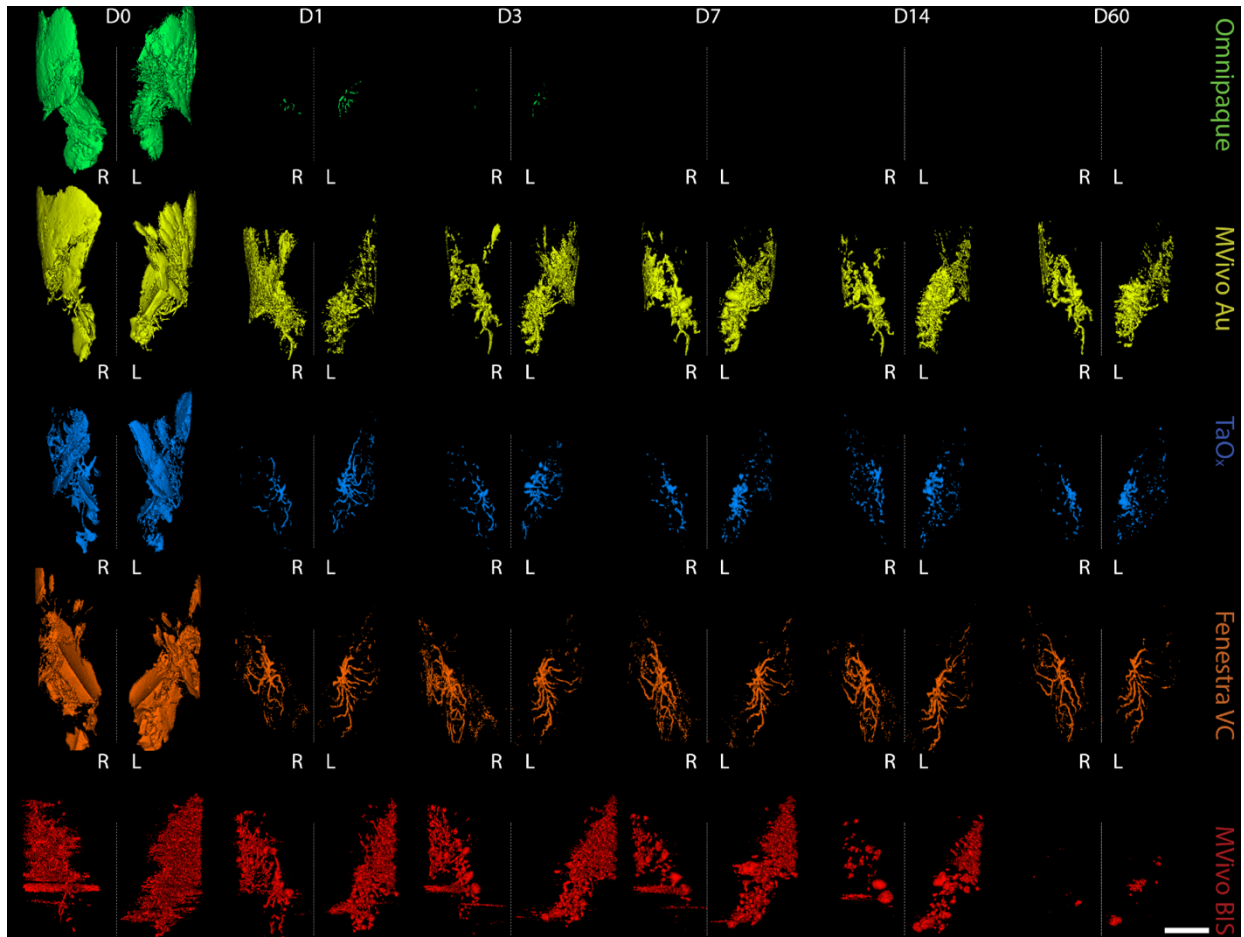


**Figure 3.3. Long-term serial microCT imaging of the murine ductal tree with different contrast agents in stock solution.** Abdominal mammary glands were injected with 40  $\mu$ l contrast agent as stock solution as indicated: Omnipaque (300 mg I/mL), MVivo Au (200 mg Au/mL), TaOx (36 mg Ta/mL), Fenestra VC (50 mg I/mL), MVivo BIS (150 mg Bis/mL). 3D reconstruction of manually segmented regions of interest (i.e., ipsi- and contralateral abdominal mammary glands) of the same animals is shown at different imaging time points from immediately after (D0) last ID injection to 60 days (D60). 3D reconstruction was thresholded to include only voxels with a HU value of  $> 300$ . Scale bar is 1 mm.

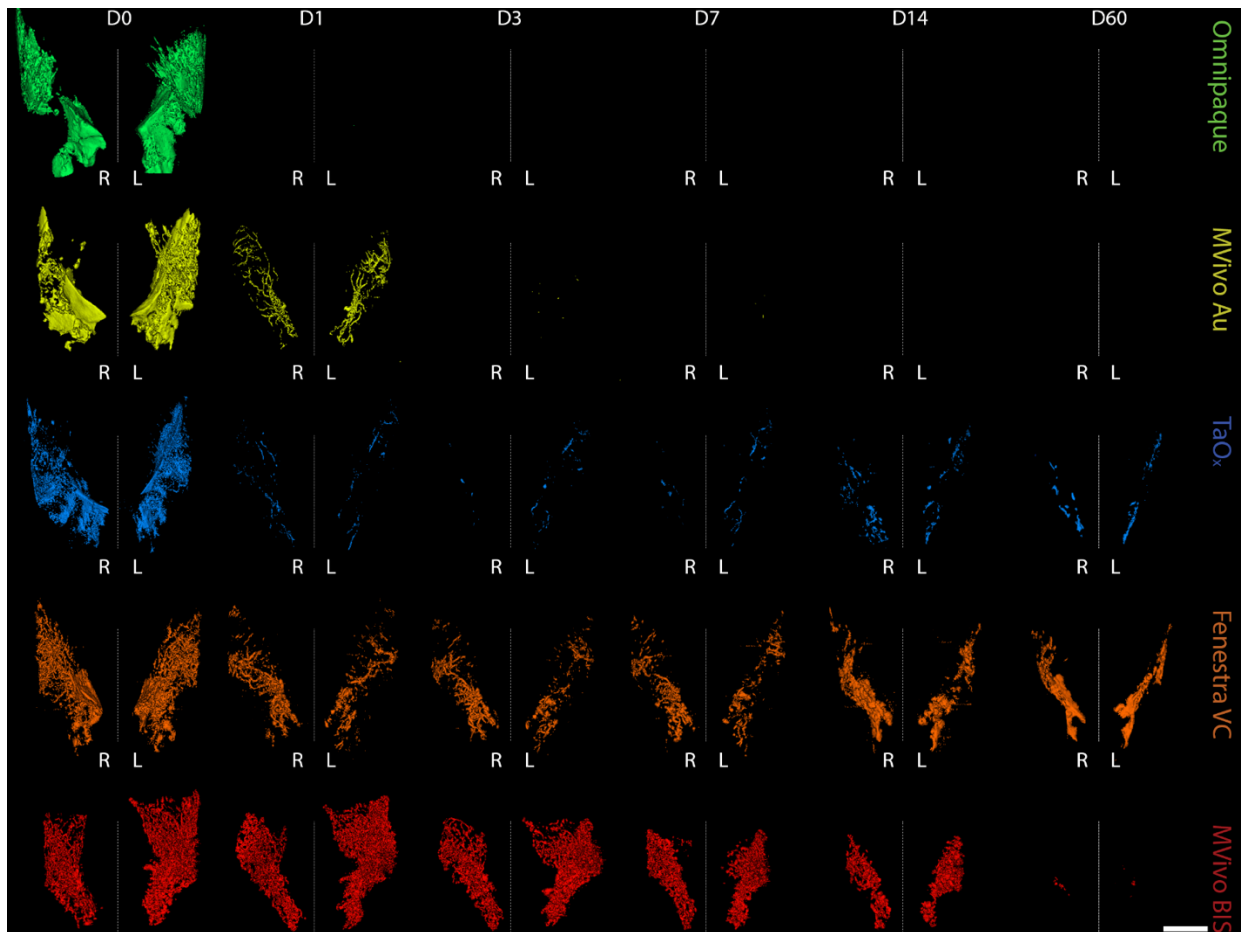


**Figure 3.4. Long-term serial microCT imaging of the murine ductal tree with different contrast agents in 70% ethanol.** Abdominal mammary glands were injected with 40  $\mu$ l of indicated contrast agent in 70% ethanol: Omnipaque (90 mg I/mL), MVivo Au (60 mg Au/mL), TaO<sub>x</sub> (10.8 mg Ta/mL), Fenestra VC (15 mg I/mL), MVivo BIS (45 mg Bis/mL). 3D reconstruction of manually segmented regions of interest (i.e., ipsi- and contralateral abdominal mammary glands) of the same animals is shown at different imaging time points from immediately after (D0) last ID injection to 60 days (D60). 3D reconstruction was thresholded to include only voxels with a HU value of > 300. Scale bar is 1 mm.

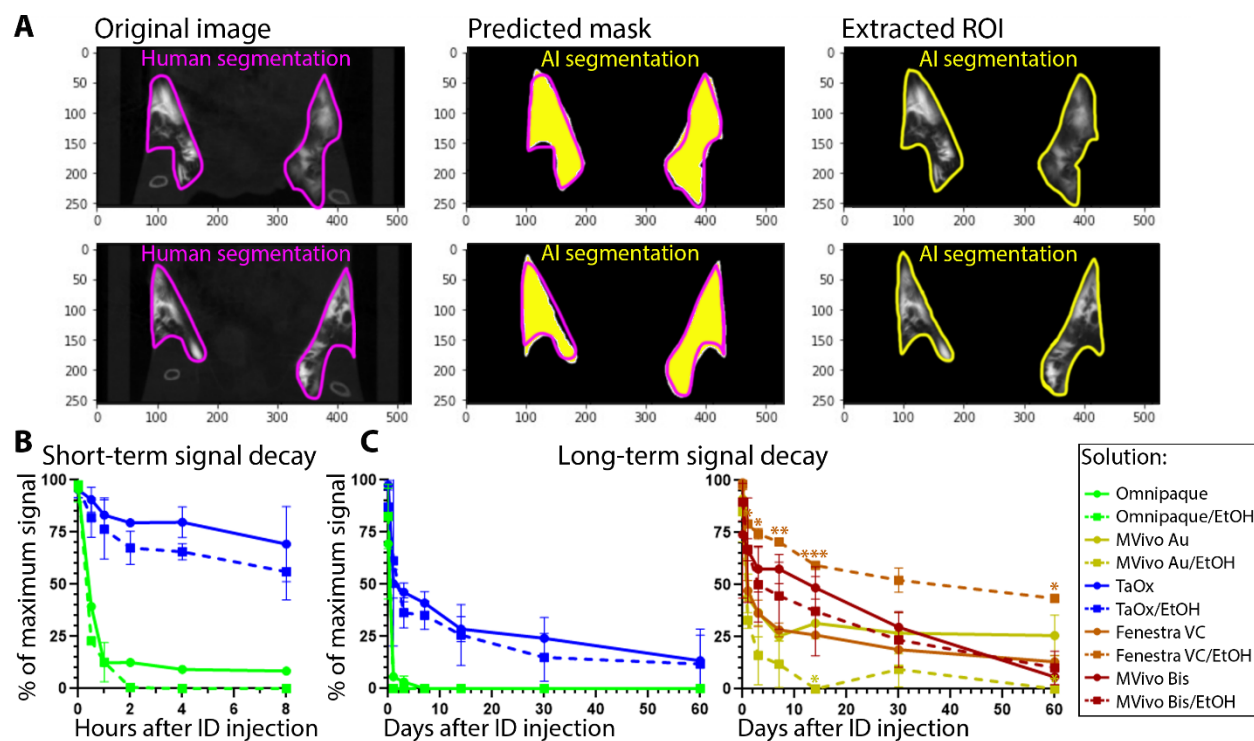


**Figure 3.5. AI assisted quantitation of signal decay and local clearance of each contrast agent.** **A)** A deep learning algorithm was used to train gland segmentation using mask parameters defined by radiologists; Original, representative microCT image slices of contrast agent–injected mammary glands, radiologist-labeled segmentation masks per slice, AI prediction of segmentation masks per slice, automated AI segmentation result for image slice. **B)** AI-assisted quantification of signal decay in short-term serial imaging characterization of indicated solutions (as shown in **Fig. 3.1**). **C)** AI-assisted quantification of signal decay in long-term serial imaging characterization of indicated solutions (as shown in **Figs. 3.3** and **3.4**). Asterisks indicate p-value of unpaired Welch’s t-test of stock compared to 70% EtOH solution of each contrast agent per time point (\* < 0.01, \*\* <0.001, \*\*\* <0.0001).

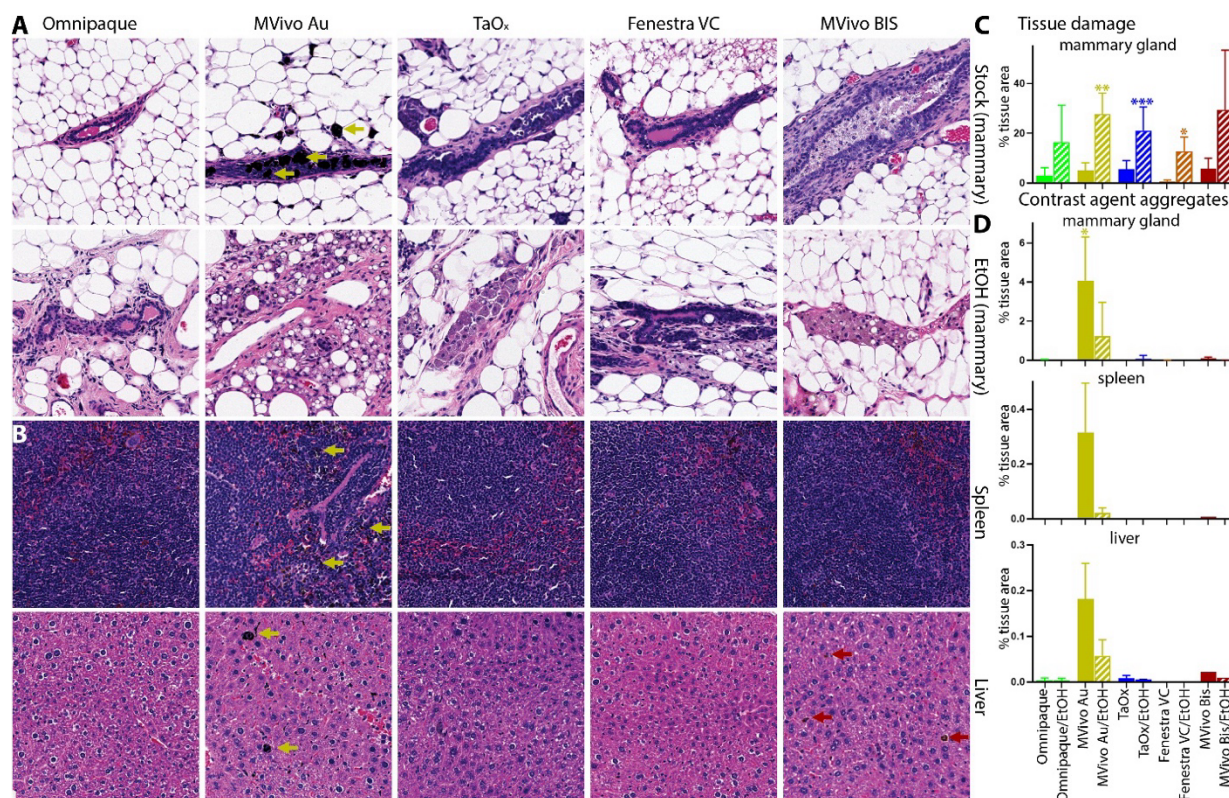


**Figure 3.6. Local and systemic clearance of contrast agents in different solutions.** **A** and **B**) Representative H&E staining of the mammary gland, spleen, and liver 60 days after ID injection of indicated contrast agent as stock solution (**A, B**): Omnipaque (300 mg I/mL), MVivo Au (200 mg Au/mL), TaOx (36 mg Ta/mL), Fenestra VC (50 mg I/mL), MVivo BIS (150 mg Bis/mL), or in 70% ethanol (EtOH) (**A**): Omnipaque (90 mg I/mL), MVivo Au (60 mg Au/mL), TaOx (10.8 mg Ta/mL), Fenestra VC (15 mg I/mL), MVivo BIS (45 mg Bis/mL). Arrows point to nanoparticle aggregates. **C**) Morphology-driven quantitation of tissue damage, which includes fibrosis, inflammation and scarring resulting from ablative effects of 70% EtOH as well as immune cell-mediated foreign object reaction to clear nanoparticle-based contrast agents. **D**) Quantitation of visually apparent aggregates of nanoparticle-based contrast agents in indicated tissues. Asterisks indicate p-value of unpaired Welch's t-test of each solution compared to Omnipaque stock (\* < 0.01, \*\* < 0.001, \*\*\* < 0.0001).

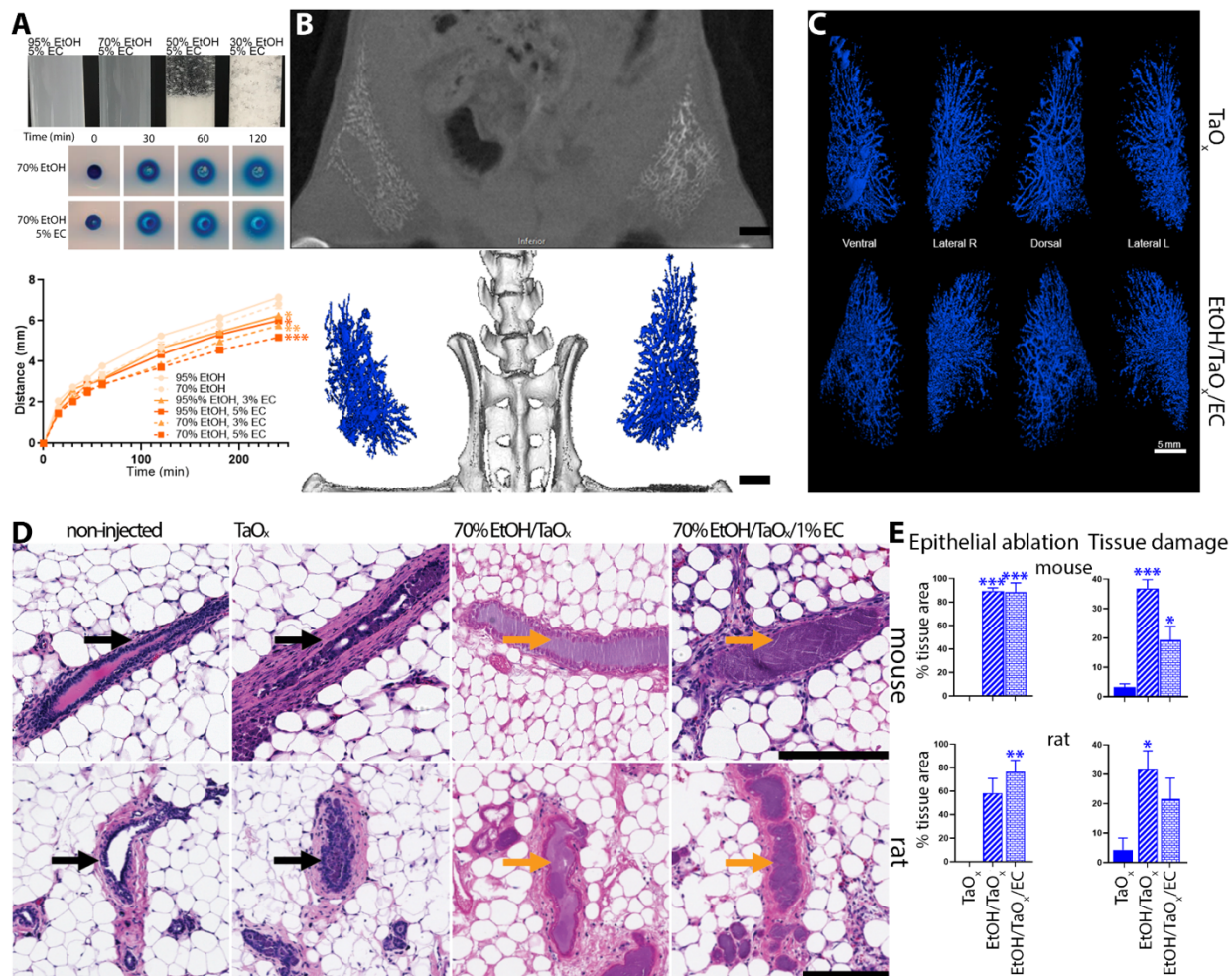


**Figure 3.7. Compatibility and Scalability of TaO<sub>x</sub>-containing solutions.** **A**) Indicated blue dye-containing solutions were dispensed into 1% agarose-casted 5-mm circular cylindrical channels (tissue phantoms). The distance the blue dye front traveled from the edge of each channel ( $x$ ) was plotted over time ( $t$ ). All solutions fit ( $R^2 > 0.99$ ) Fick's equation  $x = (4Dt)^{1/2}$ , where  $D$  is the diffusion constant. Asterisks indicate p-value of unpaired Welch's t-test of each solution compared to 95% EtOH (\* < 0.01, \*\* < 0.001, \*\*\* < 0.0001) **B** and **C**) Ductal trees of abdominal mammary glands were infused with 250  $\mu$ l of indicated TaO<sub>x</sub>-containing solutions (18 mg Ta/mL). **B**) Representative microCT slice of the lower body of an animal is shown immediately after last ID injection. Scale bar is 10 mm. **C**) 3D reconstruction of manually segmented mammary gland per condition is shown at different views. 3D reconstruction was thresholded to include only voxels with a HU value of > 300. Scale bar is 5 mm. **D**) Representative H&E staining of mouse and rat mammary gland 3 days after ID injections of indicated TaO<sub>x</sub>-containing solutions (18 mg Ta/mL). Intact (black arrow) and ablated ducts (orange arrow) are indicated. Scale bar is 200  $\mu$ m in images at different magnification. **E**) Morphology-driven quantitation of epithelial ablation (anucleate cells, cytoplasmic hypochromia) and tissue damage, which includes fibrosis, inflammation and scarring resulting from ablative effects of 70% EtOH as well as immune cell-mediated foreign object reaction to clear nanoparticle-based contrast agents. Asterisks indicate p-value of unpaired Welch's t-test of each solution compared to TaO<sub>x</sub> solution.

## Supplemental Figures

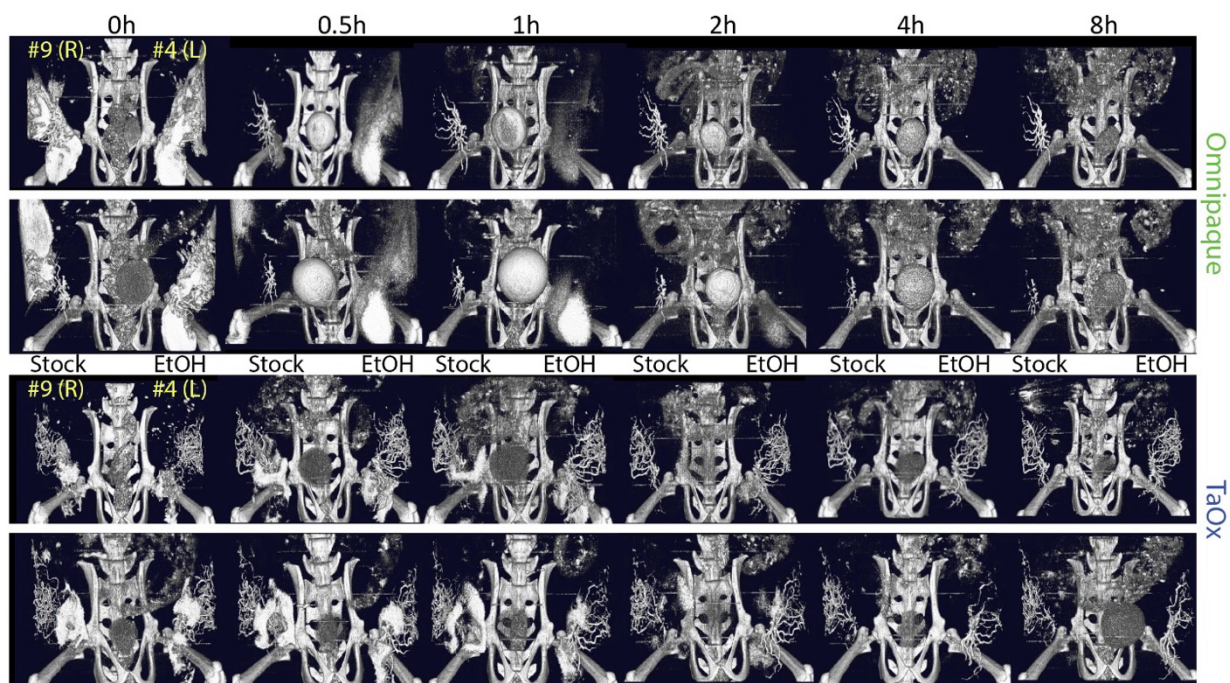


**Figure 3.8. Short-term serial microCT imaging of the murine ductal tree with different contrast agents in different solutions.** Abdominal mammary glands were injected with 40  $\mu$ l of indicated contrast agent as stock solution (300 mg I/mL Omnipaque or 18 mg Ta/mL in PBS) or in 70% ethanol (EtOH, 90 mg I/mL Omnipaque or 18 mg Ta/mL). 3D reconstructions of lower body with PerkinElmer Quantum GX microCT software package include infused ductal trees (i.e., ipsi- and contralateral abdominal mammary glands), skeleton (i.e., lower spine, hip, and femurs), and internal organs (e.g., bladder, hyperchromatic bladder is indicative of Omnipaque's systemic clearance). 3D reconstruction from the same animals are shown at different imaging time points from immediately after to 8 hrs after infusions.

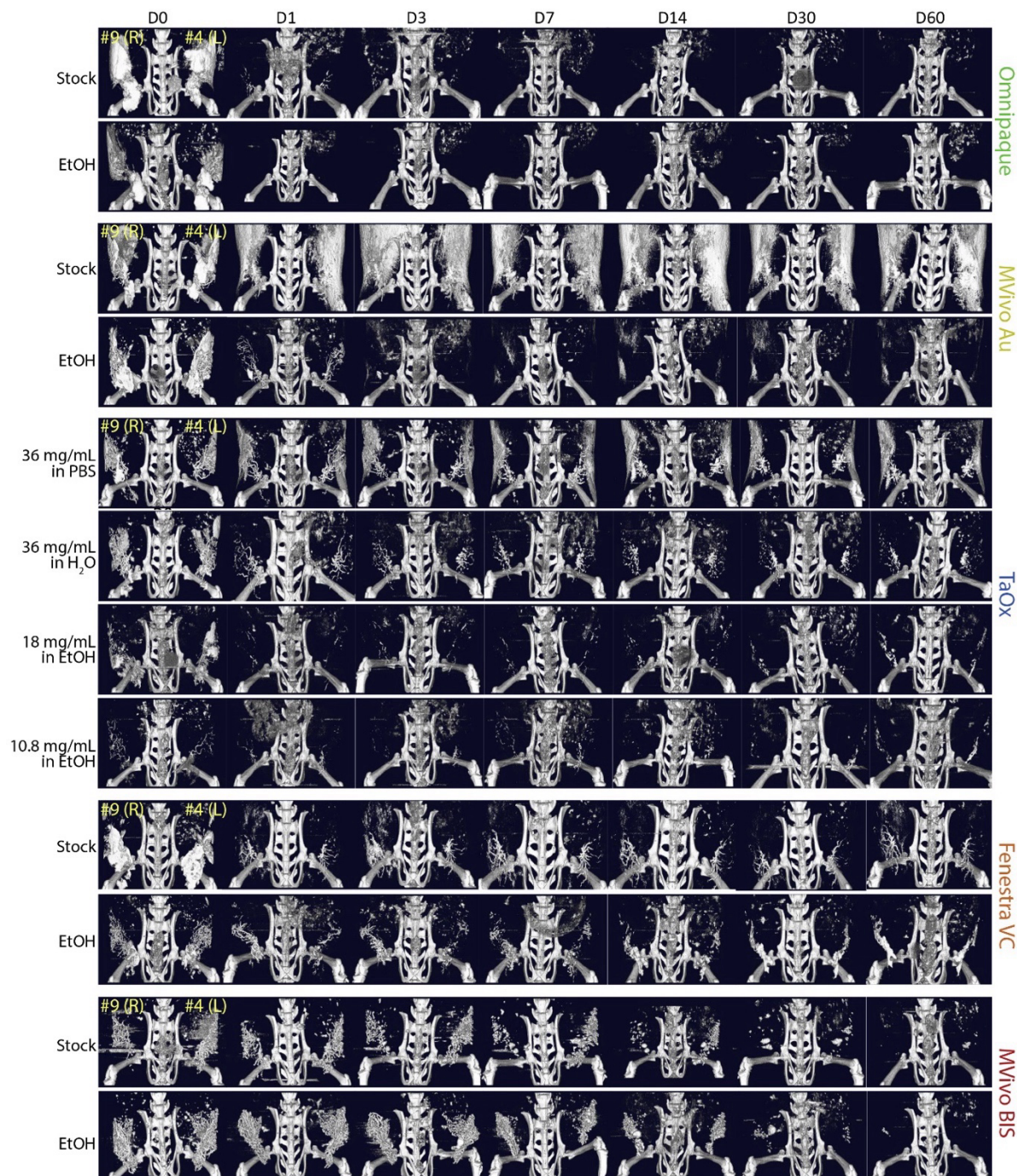


**Figure 3.9. Long-term serial microCT imaging of the murine ductal tree with different contrast agents in different solutions.** Abdominal mammary glands were injected with 40  $\mu$ l of indicated contrast agent as stock solution: Omnipaque (300 mg I/mL), MVivo Au (200 mg Au/mL), TaO<sub>x</sub> (36 mg Ta/mL), Fenestra VC (50 mg I/mL), MVivo BIS (150 mg Bis/mL); or in 70% EtOH: Omnipaque (90 mg I/mL), MVivo Au (60 mg Au/mL), TaO<sub>x</sub> (10.8 mg Ta/mL), Fenestra VC (15 mg I/mL), MVivo BIS (45 mg Bis/mL). 3D reconstructions of lower body with PerkinElmer Quantum GX microCT software package include infused ductal trees (i.e., ipsi- and contralateral abdominal mammary glands), skeleton (i.e., lower spine, hip, and femurs), and internal organs (i.e., skin, hyperchromatic subcutaneous layer is indicative of MVivo Au's regional accumulation). 3D reconstructions from the same animals are shown at different imaging time points from immediately after (D0) to 60 days (D60) after infusions.

## REFERENCES

- 1 Siegel, R. L., Miller, K. D., Wagle, N. S. & Jemal, A. Cancer statistics, 2023. *CA Cancer J Clin* **73**, 17-48, doi:10.3322/caac.21763 (2023).
- 2 Britt, K. L., Cuzick, J. & Phillips, K. A. Key steps for effective breast cancer prevention. *Nat Rev Cancer* **20**, 417-436, doi:10.1038/s41568-020-0266-x (2020).
- 3 Padamsee, T. J., Wills, C. E., Yee, L. D. & Paskett, E. D. Decision making for breast cancer prevention among women at elevated risk. *Breast Cancer Res* **19**, 34, doi:10.1186/s13058-017-0826-5 (2017).
- 4 Slawson, S. H. & Johnson, B. A. Ductography: how to and what if? *Radiographics* **21**, 133-150, doi:10.1148/radiographics.21.1.g01ja15133 (2001).
- 5 Sheiman, L. S. & Levesque, P. H. The In's and Out's of Ductography: A Comprehensive Review. *Curr Probl Diagn Radiol* **45**, 61-70, doi:10.1067/j.cpradiol.2015.05.007 (2016).
- 6 Sapienza Passos, J., Dartora, V., Cassone Salata, G., Draszesski Malago, I. & Lopes, L. B. Contributions of nanotechnology to the intraductal drug delivery for local treatment and prevention of breast cancer. *Int J Pharm* **635**, 122681, doi:10.1016/j.ijpharm.2023.122681 (2023).
- 7 Zaluzec, E. K. & Sempere, L. F. Systemic and Local Strategies for Primary Prevention of Breast Cancer. *Cancers* **16**, 248, doi.org/10.3390/cancers16020248 (2024).
- 8 Kenyon, E. *et al.* Ductal tree ablation by local delivery of ethanol prevents tumor formation in an aggressive mouse model of breast cancer. *Breast Cancer Res* **21**, 129, doi:10.1186/s13058-019-1217-x (2019).
- 9 Chakravarty, S. *et al.* Tantalum oxide nanoparticles as versatile contrast agents for X-ray computed tomography. *Nanoscale* **12**, 7720-7734, doi:10.1039/d0nr01234c (2020).
- 10 Kenyon, E. *et al.* X-Ray Visualization of Intraductal Ethanol-Based Ablative Treatment for Prevention of Breast Cancer in Rat Models. *J Vis Exp*, doi:10.3791/64042 (2022).
- 11 Kenyon, E. *et al.* Intraductal Delivery and X-ray Visualization of Ethanol-Based Ablative Solution for Prevention and Local Treatment of Breast Cancer in Mouse Models. *J Vis Exp*, doi:10.3791/63457 (2022).
- 12 Robertson, N. *et al.* Omniparticle Contrast Agent for Multimodal Imaging: Synthesis and Characterization in an Animal Model. *Mol Imaging Biol* **25**, 401-412, doi:10.1007/s11307-022-01770-w (2023).
- 13 Wang, G. *et al.* Intraductal fulvestrant for Therapy of ERalpha-positive Ductal Carcinoma in Situ (DCIS) of the breast- a Preclinical Study. *Carcinogenesis*, doi:10.1093/carcin/bgz084 (2019).
- 14 Brock, A. *et al.* Silencing HoxA1 by intraductal injection of siRNA lipidoid nanoparticles prevents mammary tumor progression in mice. *Sci Transl Med* **6**, 217ra212, doi:10.1126/scitranslmed.3007048 (2014).

- 15 Chun, Y. S. *et al.* Intraductally administered pegylated liposomal doxorubicin reduces mammary stem cell function in the mammary gland but in the long term, induces malignant tumors. *Breast Cancer Res Treat* **135**, 201-208, doi:10.1007/s10549-012-2138-x (2012).
- 16 Chun, Y. S. *et al.* Intraductal administration of a polymeric nanoparticle formulation of curcumin (NanoCurc) significantly attenuates incidence of mammary tumors in a rodent chemical carcinogenesis model: Implications for breast cancer chemoprevention in at-risk populations. *Carcinogenesis* **33**, 2242-2249, doi:10.1093/carcin/bgs248 (2012).
- 17 Murata, S. *et al.* Ductal access for prevention and therapy of mammary tumors. *Cancer Res* **66**, 638-645, doi:10.1158/0008-5472.CAN-05-4329 (2006).
- 18 Okugawa, H. *et al.* Effect of periductal paclitaxel exposure on the development of MNU-induced mammary carcinoma in female S-D rats. *Breast Cancer Res Treat* **91**, 29-34, doi:10.1007/s10549-004-6455-6 (2005).
- 19 Sivaraman, L. *et al.* Effect of selective ablation of proliferating mammary epithelial cells on MNU induced rat mammary tumorigenesis. *Breast Cancer Res Treat* **73**, 75-83 (2002).
- 20 Stearns, V. *et al.* Preclinical and clinical evaluation of intraductally administered agents in early breast cancer. *Sci Transl Med* **3**, 106ra108, doi:10.1126/scitranslmed.3002368 (2011).
- 21 Yoshida, T. *et al.* Effective treatment of ductal carcinoma in situ with a HER-2- targeted alpha-particle emitting radionuclide in a preclinical model of human breast cancer. *Oncotarget* **7**, 33306-33315, doi:10.18632/oncotarget.8949 (2016).
- 22 de Groot, J. S. *et al.* Intraductal cisplatin treatment in a BRCA-associated breast cancer mouse model attenuates tumor development but leads to systemic tumors in aged female mice. *Oncotarget* **8**, 60750-60763, doi:10.18632/oncotarget.18490 (2017).
- 23 Kim, B. Y., Rutka, J. T. & Chan, W. C. Nanomedicine. *N Engl J Med* **363**, 2434-2443, doi:10.1056/NEJMra0912273 (2010).
- 24 DiCorpo, D. *et al.* The role of Micro-CT in imaging breast cancer specimens. *Breast Cancer Res Treat* **180**, 343-357, doi:10.1007/s10549-020-05547-z (2020).
- 25 Hsu, J. C. *et al.* Nanoparticle contrast agents for X-ray imaging applications. *Wiley Interdiscip Rev Nanomed Nanobiotechnol* **12**, e1642, doi:10.1002/wnan.1642 (2020).
- 26 Zhao, H. *et al.* Molecular imaging and deep learning analysis of uMUC1 expression in response to chemotherapy in an orthotopic model of ovarian cancer. *Sci Rep* **10**, 14942, doi:10.1038/s41598-020-71890-2 (2020).
- 27 Sempere, L. F., Zaluzec, E., Kenyon, E., Kiupel, M. & Moore, A. Automated Five-Color Multiplex Co-detection of MicroRNA and Protein Expression in Fixed Tissue Specimens. *Methods Mol Biol* **2148**, 257-276, doi:10.1007/978-1-0716-0623-0\_17 (2020).
- 28 Lai, Y. E., Morhard, R., Ramanujam, N. & Nolan, M. W. Minimally invasive ethyl cellulose ethanol ablation in domesticated cats with naturally occurring head and neck cancers: Six cats. *Vet Comp Oncol* **19**, 492-500, doi:10.1111/vco.12687 (2021).

- 29 Mueller, J. L. *et al.* Optimizing ethyl cellulose-ethanol delivery towards enabling ablation of cervical dysplasia. *Sci Rep* **11**, 16869, doi:10.1038/s41598-021-96223-9 (2021).
- 30 Nief, C. *et al.* Polymer-assisted intratumoral delivery of ethanol: Preclinical investigation of safety and efficacy in a murine breast cancer model. *PLoS One* **16**, e0234535, doi:10.1371/journal.pone.0234535 (2021).
- 31 Chelales, E. *et al.* Radiologic-pathologic analysis of increased ethanol localization and ablative extent achieved by ethyl cellulose. *Sci Rep* **11**, 20700, doi:10.1038/s41598-021-99985-4 (2021).
- 32 Morhard, R. *et al.* Understanding Factors Governing Distribution Volume of Ethyl Cellulose-Ethanol to Optimize Ablative Therapy in the Liver. *IEEE Trans Biomed Eng* **67**, 2337-2348, doi:10.1109/TBME.2019.2960049 (2020).
- 33 Morhard, R. *et al.* Development of enhanced ethanol ablation as an alternative to surgery in treatment of superficial solid tumors. *Sci Rep* **7**, 8750, doi:10.1038/s41598-017-09371-2 (2017).
- 34 Sannier, K. *et al.* A new sclerosing agent in the treatment of venous malformations. Study on 23 cases. *Interv Neuroradiol* **10**, 113-127, doi:10.1177/159101990401000203 (2004).
- 35 Domp Martin, A. *et al.* Radio-opaque ethylcellulose-ethanol is a safe and efficient sclerosing agent for venous malformations. *Eur Radiol* **21**, 2647-2656, doi:10.1007/s00330-011-2213-4 (2011).
- 36 Fujimichi, Y., Sasaki, M., Yoshida, K. & Iwasaki, T. Effects of irradiation on cumulative mortality in mice: shifting toward a younger age of death. *J Radiat Res* **64**, 412-419, doi:10.1093/jrr/rad006 (2023).
- 37 Russo, I. H. & Russo, J. Developmental stage of the rat mammary gland as determinant of its susceptibility to 7,12-dimethylbenz[a]anthracene. *J Natl Cancer Inst* **61**, 1439-1449 (1978).
- 38 Paine, I. S. & Lewis, M. T. The Terminal End Bud: the Little Engine that Could. *J Mammary Gland Biol Neoplasia* **22**, 93-108, doi:10.1007/s10911-017-9372-0 (2017).
- 39 Hughes, K. Comparative mammary gland postnatal development and tumorigenesis in the sheep, cow, cat and rabbit: Exploring the menagerie. *Semin Cell Dev Biol*, doi:10.1016/j.semcdb.2020.09.010 (2020).
- 40 Schöniger, S., Degner, S., Jasani, B. & Schoon, H.-A. A Review on Mammary Tumors in Rabbits: Translation of Pathology into Medical Care. *Animals* **9**, 762 (2019).
- 41 Falconer, I. R. The distribution of <sup>131</sup>I- or <sup>125</sup>I-labelled prolactin in rabbit mammary tissue after intravenous or intraductal injection. *J Endocrinol* **53**, 58-59 (1972).
- 42 Fiddler, T. J., Birkinshaw, M. & Falconer, I. R. Effects of intraductal prolactin on some aspects of the ultrastructure and biochemistry of mammary tissue in the pseudopregnant rabbit. *J Endocrinol* **49**, 459-469, doi:10.1677/joe.0.0490459 (1971).
- 43 Fiddler, T. J. & Falconer, I. R. The effect of intraductal prolactin on protein and nucleic acid biosynthesis in the rabbit mammary gland. *Biochem J* **115**, 58P-59P, doi:10.1042/bj1150058p (1969).

- 44 Bourne, R. A., Bryant, J. A. & Falconer, I. R. Stimulation of DNA synthesis by prolactin in rabbit mammary tissue. *J Cell Sci* **14**, 105-111 (1974).
- 45 Chadwick, A. Detection and Assay of Prolactin by the Local Lactogenic Response in the Rabbit. *J Endocrinol* **27**, 253-263, doi:10.1677/joe.0.0270253 (1963).
- 46 Clark, A., Bird, N. K. & Brock, A. Intraductal Delivery to the Rabbit Mammary Gland. *J Vis Exp*, doi:10.3791/55209 (2017).

**CHAPTER 4: IMAGE-GUIDED LOCAL ABLATION FOR PRIMARY PREVENTION OF  
BREAST CANCER IN RAT MODELS**

## **Contributions to Science.**

Dr. Lorenzo Sempere and I were responsible for concept and experimental design. I worked with Dr. Mohamed Ashry and Ms. Elizabeth Phelps in data collection and analyses within this chapter. I drafted the paper and performed critical revision for intellectual content with Dr. Sempere. Dr. Sempere and I designed the figures and I executed majority of figures and performed all statistical analysis with guidance from Dr. Chi Chang.

## **Abstract.**

**Background:** Bilateral prophylactic mastectomy is the most effective risk-reducing intervention for primary prevention of breast cancer but has undesired side effects. Local ablation is currently being investigated in preclinical models as an alternative intervention to bilateral prophylactic mastectomy with reduced side effects. Here, we seek to identify the scalability and efficacy of a local ablation approach based on intraductal infusion of a refined 70% ethanol solution in chemically induced rat models of breast cancer.

**Methods:** After intraductal delivery of 70% ethanol (ablative agent), 100mM tantalum oxide (imaging agent), and/or ethyl cellulose (gelling agent) solution, in vivo micro-computed tomography was performed for visual confirmation of ductal tree filling in N-methyl-N-Nitrosourea-induced rat model of breast. Mammary glands were palpated weekly, and tumors were recorded to establish tumor latency. Upon necropsy, mammary glands and/or tumors were collected for tissue correlative analyses. Statistical difference in median tumor latency and tumor incidence between experimental groups was analyzed by log-rank test and logistic mixed-effects model, respectively. Multiplex immunohistochemistry and histological analyses were performed to determine ablative effects of 70% ethanol treatment and to molecularly characterize tumors that formed in each experimental group.

**Results:** In an efficacy study, we report that intraductal 70% ethanol treatment significantly delayed tumor formation at an individual gland level with a risk reduction of 53.89% (HR=2.17, 95% CI: 1.24, 17.44, p-value 0.04), and in whole animals treated with ethanol (n=24) with a median latency of 273 days (p-value 0.001) compared to 135 days in untreated controls (n=6). In a safety study, partial volume of ethanol treatment did not increase tumor incidence compared to untreated controls (15% of ethanol treated glands with tumors (10/65) vs. 24% of untreated glands with tumors (17/72), p-value 0.3265), which ruled out iatrogenic effect of this ablative treatment. Tumors that formed in fully infused ethanol-treated mammary glands did not significantly differ from tumors in untreated mammary glands based on positivity of estrogen receptor, proliferative index, and other molecular markers. This refined ablative solution does not interfere with long-term MR imaging for anatomical assessment of mammary gland and follow-up breast cancer surveillance.

**Conclusions:** Intraductal delivery of 70% ethanol solution is scalable into larger rodent models, can be visually assessed with the addition tantalum oxide nanoparticle without interfering with current imaging modalities for breast cancer screening and surveillance. This study supports the efficacy of single-injection treatment for local ablation of epithelial cells and translatability for continued investigation in breast cancer prevention in large animal models and first-in-human clinical evaluation.

## **Background.**

Breast cancer (BC) is the leading causes of cancer diagnosis and second leading causes of cancer deaths for women in the United States [1]. In 2024, an estimated 310,720 women will be diagnosed with breast cancer which accounts for everyone 1 in 8 women being diagnosed within her lifetime. Despite this high prevalence, women at average or moderate risk for BC have limited options for risk reduction. For high-risk individuals two FDA prevention options are available: Bilateral prophylactic mastectomy and systemic hormonal therapy. Bilateral prophylactic mastectomy completely removes ductal tree epithelial cells, where most breast carcinomas arise, and reduces breast cancer risk by up to 90% but is an invasive

procedure with a painful, extended recovery period [2, 3]. Systemic hormonal therapies, tamoxifen and raloxifene, reduced BC risk by up to 50% but increases an individual's risk of uterine cancer and stroke and induces early menopausal symptoms [4]. However, the undesirable effects from these existing preventive methods deter most women at high risk of BC from selecting either option [2, 3]. Instead, many opt for watchful waiting, a preventive method with no risk reduction [2]. Therefore, there is a need for new innovative breast cancer preventions with equal risk reduction to current approved interventions, but with lowered adverse effects.

Intraductal (ID) delivery of an imaging solution is a clinically used diagnostic procedure known as ductography [3]. BC prevention studies in preclinical models have repurposes this procedure for ID delivery of therapeutic solutions [3, 5]. We and others have used this local intervention approach to intraductally delivery different cell-killing solutions directly to the target ductal tree epithelial cells [3, 5]. ID delivery circumvents the adverse effects associated with systemic treatments, making it a novel local strategy for primary prevention of BC [5]. We previously demonstrated ID treatment with 70% ethanol as an epithelial cell-killing solution to be effective at preventing tumors in the C(3)1-TAg breast cancer mouse model [6]. Ethanol (EtOH) is an inexpensive and safe chemical already used clinically as an ablative agent for cancer treatments such as liver and cystic pancreatic tumors, and breast aneurisms [7-9]. For real-time visualization of the ductal tree after ID infusion, we introduced tantalum oxide (TaO<sub>x</sub>) nanoparticles as a novel X-ray contrast agent for microCT analysis [6, 10-12]. TaO<sub>x</sub> has a high attenuation of X-rays and local retention for high performance visualization of ductal tree filling [6, 10-13].

In this study, we seek to assess the scalability and efficacy of ID delivery with our refined cell-ablative solution in a large rodent model for breast cancer prevention. Using a rat model necessitates larger infusion volumes to fill the ductal tree in the context of denser stroma. The rat model provides a larger ductal tree system with a denser stroma [14]. The N-methyl-N-nitrosourea (MNU)-induced rat model is a well-established model used in previous prevention studies, primarily focusing of hormonal treatment and disruptors [14]. Previous studies with ID treatment of cytotoxic compounds and hormone

therapy in MNU-induced rat model have reported reduced tumor burden [3, 15-18]. However local and systemic toxicity, iatrogenic effects, and/or frequent or repeated ID treatment by infusion present challenges for translation to humans [3]. Here, we demonstrate the effectiveness of our refined solution containing 70% ethanol, 1% ethyl cellulose and tantalum oxide as a single ID infusion cell-killing solution as a local intervention for translation toward human breast cancer prevention.

### **Methods and Materials.**

**N-methyl-N-Nitrosourea (MNU) Rat Model:** Female Sprague Dawley (SD) rats (jax.org, stock 001800) were bred in-house and maintained in Allentown Cages with a light/dark cycle of 12h:12h. Water and food were given ad libitum. MNU (Astatech Inc., Cat#29290, Pennsylvania USA) was prepared immediately prior to and administered by a single intraperitoneal injection on the 7 weeks of age. Rats were injected with 50mg/kg or 75mg/kg body weight dose of MNU dissolved in 0.9% filtered acidified saline solution [19]. At 9 weeks of age, all rats were intraductally infused with designated solutions and were palpated weekly beginning two weeks post ID infusion until Institutional Animal Care & Use Committee (IACUC) euthanasia criteria was met.

**Intraductal Injection Procedure:** 9-week-old female SD rats were administered carprofen in MediGel Sucralose gel cups (1mg/cup; ClearH<sub>2</sub>O) and prepared for ID infusion by depilatory fur removal near the intended mammary glands as described [11]. ID infusion on rats were performed under isoflurane anesthesia. Rats were injected into individual mammary glands (n=1-7 per time point and per solution) with up to 300µL of 70% ethanol, 100mM Tantalum Oxide (TaO<sub>x</sub>) in PBS and/or 1-3% of ethyl cellulose (EC). TaO<sub>x</sub> nanoparticles were supplied in crystalline form as described [10]. Ethyl cellulose (Acros Organics, 9004-57-3) was added up to 3 % (w/v) to 70% EtOH solution containing 36 mg Ta/mL of TaO<sub>x</sub>. For tumor prevention studies, MNU-induced rats were palpated weekly beginning two weeks post ID infusion until IACUC criteria for euthanasia were met (tumor volume >2cm<sup>3</sup> or multiple tumors >4cm). All experiments were conducted under protocols approved by Institutional Animal Care and Use

Committee at Michigan State University.

**MicroCT Image Acquisition and Analysis:** Microcomputer tomography (microCT) images were acquired using a PerkinElmer Quantum GX microCT scanner as described [11]. Briefly, serial images of the rat lower body were acquired at 0, 15, 30, and 60 days (**Figure 4.5**). The following image acquisition scan parameters were standardized and used : 90 kVp/88  $\mu$ A; field of view (FOV), 72 mm; number of slices, 512; slice thickness, 72  $\mu$ m; voxel resolution, 144  $\mu$ m<sup>3</sup>. Radiation exposure was minimized in this longitudinal study by short acquisition time of high resolution (4 min) scans. Caliper AnalyzeDirect©, v12.0 (Biomedical Imaging Resource, Mayo Clinic, Rochester, MN) was used for microCT image rendering, segmentation, and analysis of individual glands as described [11, 12]. 3D renditions were created using Analyze 14.0 software as described [13]. Briefly, intensity threshold was set to minimum and maximum of 300 and 3000 Hounsfield unit (HU), to visualize TaO<sub>x</sub> solutions. Images were spline traced in increments of 3. To remove rat skeleton from 3D renditions, areas of the bone were highlighted and extracted (signal range -770 to 1730 HU).

**MR Image Acquisition and Analysis:** MR images were acquired on Bruker 7T preclinical MRI with an 86mm volume transmit/receive coil, using a T2\_Turbo\_RARE sequence with parameters: TR/TE 3200/46 ms, 10 averages, 300x300um in plane resolution, 30 coronal slices with 0.5 mm intra-slice gap, fat suppression, rare factor 8. Image acquisition time was 14 minutes. The rats were anesthetized with 2% isoflurane in oxygen, and breathing (30-50 bpm) and temperature (35-37°C) were monitored. Free, open-sourced medical imaging Horos Software ([www.horosproject.org](http://www.horosproject.org); Horos Project) for MacOS was used to analyze MRI images imported as DICOM files. Horos software allows for slice-by-slice manual analysis of contoured injected areas of the mammary gland.

**Histological and Immunohistochemical Analyses:** Animals were euthanized at different time points for short-term studies or when they met euthanasia. Dissected mammary gland and tumor tissues were cut,

processed, and embedded in paraffin after formalin fixation. Four-micron thick sections of formalin-fixed paraffin-embedded (FFPE) tissue samples were used for H&E staining and/or multiplex immunohistochemical assays and scanned using Aperio Versa 8 Brightfield&Fluorescence imaging system (Leica Biosystems, Buffalo Grove, IL) as described [6, 20]. Briefly, the Leica Bond Rx automated staining station was used for fluorescence based IHC multiplex assays. Tissue slides were sequentially incubated with appropriate combination of primary antibodies for 30 min at room temperature: anti- $\alpha$ -smooth muscle actin (SMA) rabbit antibody at a 1:500 dilution (Abcam, ab5694), anti-estrogen receptor alpha (ER) mouse antibody at a 1:50 dilution (Thermo Fisher Scientific, MA5-13304), glut1 (E4S6I) rabbit antibody at a 1:250 dilution (Cell Signaling, mAb #73015), anti-Ki-67 rabbit antibody at a 1:200 (Abcam, ab16667), anti-CD68 rabbit at a 1:150 dilution (Abcam, ab283654), anti-sodium potassium ATPase rabbit antibody at a 1:100 dilution (Abcam, ab76020); anti-vimentin chicken antibody at a 1:300 dilution (LSBio, LS-B291). Then, tissue slides were incubated with appropriate horseradish peroxidase (HRP)-conjugated secondary antibodies at 1:500 dilution: anti-rat goat antibody (Abcam, ab7097); anti-rabbit goat antibody (Biorad, 170-6515); or anti-chicken goat antibody (Santa Cruz Biotechnology, sc-2901). Tyramide signal amplification was used to detect expression of each marker with one of the following tyramine-conjugated fluorochromes: fluorescein isothiocyanate (Thermo Fisher Scientific, F143), rhodamine (Thermo Fisher Scientific, 46406), Dylight 594 (Thermo Fisher Scientific, 46608) or Dylight650 (Thermo Fisher Scientific, 62266). Tissue sections were counterstained with DAPI and mounted with Prolong Gold (Invitrogen, p36930).

**Statistical Analysis:** All statistical analysis for tissue analysis comparing multiple different experimental groups (treatment groups n=3, n=4, or n=5) of continuous values was conducted with non-parametric Kruskal-Wallis analysis with post-hoc Dunn's test on Graphpad Prism 8 after all assumptions were confirmed. Kaplan-Meier curves were generated on Graphpad Prism 8 to compare proportional hazard assumptions. When these assumptions were met, Log-rank (Mantel-cox) analysis was conducted in Graphpad Prism 8. However, in the cases of partial and off-target experimental groups for survival

analysis where the proportional hazard assumption was violated, we employed the Tarone-ware test in R studio for a more robust analysis. Kaplan-Meier curves were separately constructed for tumor latency (the time between tumor induction by MNU administration and initial time of tumor detection by palpation or time of death) for whole animal analysis and individual gland analysis. In the latter case, mixed effect cox model analysis was carried out in R studio to account for the clustered structure (multiple treatments in mammary glands of the same animal), non-proportional hazards, and allows for inclusion of random effects which captures the heterogeneity among clusters. The proportional hazards, independence of clusters, distribution of random effects, homogeneity of random effects within clusters, misspecifications, validity of random effects structure, a goodness of fit assumptions for the mixed effect cox model were all assess in R studio (**Figures S4.6 and S4.7**). For tumor-free survival data, time of death was used to censor injected glands with no evidence of tumors by palpation or at necropsy. Tumor incidence and analysis of relative risk were divided into two parts comparing tumor incidence at necropsy of untreated controls vs non-injected glands between different experimental groups or non-injected glands vs injected glands within the same experimental group. Confidence intervals for relative risk were calculated as described [21, 22]. We consider findings to be statistically significant if  $p\text{-value} < 0.05$ .

## **Results.**

**Scalability of the 70% ethanol ablative procedure combined with ethyl cellulose in rats:** Similar to mice, rats have one ductal tree structure for each mammary gland but require larger volume to encompass all epithelial cells within the ductal tree (up to 300 $\mu$ L per gland) and have more fibrous connective tissue, more similar to humans, surrounding the ductal tree [13, 23]. Ethyl cellulose (EC) is a gelatinous substance clinically used as an aid in ethanol treatment of varicose veins due to its ability to retain ethanol [24]. It is being investigated *in vivo* for its potential ethanol retention in cervical dysplasia and in breast cancer mouse models treatments [25, 26]. However, intraductal ablation utilizing EC and scalability of this technique into rats is relatively unexplored. We previously showed that 1% EC provided some retention of 70% ethanol in mice and rats, limiting collateral tissue damage [6, 13]. Here, we conducted a

more comprehensive short-term study characterizing the ablative effect and collateral tissue damage of 70% ethanol with ethyl cellulose at higher percentages (1% to 3%) to further limit ethanol diffusion in rats.

We intraductally infused up to four out of twelve rat mammary glands with 300 $\mu$ L of PBS, 70% ethanol, or 70% ethanol in combination with 1%, 2%, or 3% EC (w/v). H&E analysis of stained mammary glands revealed similar local ablation rates of epithelial cells alone or in combination with all EC percentages and epithelial cells were devoid of nuclei (**Figure 4.1A**). When compared to PBS controls (n=2), both ethanol alone (n=5) and ethanol with 2% EC (n=3) solutions exhibited the higher ablation rates, reaching 96.2% and 88.5% respectively (**Figure 4.1C**). Ethanol combined with 1% EC (n=3) and 3% EC (n=2) showed a slight reduction in ablation rates, measured at 87.4% and 86.1% respectively, although no data was statistically significant likely due to the small sample sizes. Nevertheless, the incorporation of EC with ethanol remains effective in achieving substantial ablation of epithelial cells. To further expand on this analysis, multiplex immunohistochemistry analysis of cell type-specific markers was conducted. Ethanol ablation with all EC percentages was identified by the lack of  $\alpha$ -smooth muscle actin (SMA) in myoepithelial cells and lack of membrane integrity by ATPase (**Figure 4.1B**). The presence of macrophage marker, CD68, and adipocyte network, as indicated by vimentin staining and lack of SMA staining, highlighted mostly intact immune and adipocyte networks respectively (**Figure 4.1B**). Ethanol alone resulted in the highest collateral tissue damage at 63.1% compared to PBS controls. However, when combined with 1%, 2%, and 3% ethyl cellulose, ethanol showed modest improvements in collateral tissue damage (46.7%, 58.6%, and 45.7% respectively, **Figure 4.1D**). This suggests that incorporation of EC may help to reduce collateral tissue damage caused by ethanol alone but requires more investigation with a larger sample size due to the lack of statistical significance. Due to mobility issues with higher EC percentages, 1% EC was incorporated into our refined 70% ethanol ablative solution.

### **Effectiveness of intraductal 70% ethanol treatment at tumor prevention in MNU rat breast cancer**

**model:** The MNU-induced rat model is a well characterized model for studying breast cancer prevention and is mainly used to test prevention of hormonal therapy as formed tumors are driven by the estrogen receptor [14]. To determine therapeutic effectiveness of local ablation, rats received intraductal treatment of refined 70% ethanol ablative solution two weeks after tumor induction with 50 mg/kg of MNU (**Figure 4.2A**). Rats were palpated weekly to determine tumor formation and sacrificed once euthanasia criteria were met. The two primary endpoints for this study were tumor latency and tumor incidence. Mammary glands treated by ID 70% ethanol ablation (n=72) had a significantly lower risk reduction of 53.89% compared to untreated controls (n=73) demonstrating the effectiveness of this prevention treatment (HR=2.17, 95% CI: 1.24, 17.44, p-value 0.04) while account for multiple treatments in individual animals (**Figure 4.2B**). The variability of survival times (362 days) of 70% ethanol treated glands was attributed to differences among animals (variance of random effects = 0.0004), suggesting unmeasured animal-level characteristics may influence survival time. When considering animals as a whole, untreated control animals (n=6) had a median tumor survival of 135 days whereas animals with ID ablation of refined 70% ethanol (n=24) significantly reduced tumor formation with an improved median survival of 273 days as indicated by the log-rank test (**Figure 4.2C**, p-value 0.001). To reflect a more aggressive BC model, a second experiment in an independent cohort of rats using a higher dose of 75m/kg of MNU was conducted. In this cohort, when comparing individual mammary glands by mixed effect cox model analysis, glands intraductally ablated with 70% ethanol (n=81) had a risk reduction of 78.45% compared to untreated controls (n=60) continuously demonstrated the effectiveness of this ablative prevention method (HR=4.64, 95% CI: 1.24, 17.44, p-value 0.02) when controlling for multiple treatment groups in an individual animal (**Figure 4.2D**). The overall survival of glands treated with 70% ethanol (563 days) was also influenced by differences among animals (variance of random effects =1.22) indicating potential unmeasured-level characteristics affect survival times. The rats as a whole treated with 70% ethanol (n=27) had increase tumor latency of 206 days compared to untreated controls (n=5, 62 days) using log-rank analysis (**Figure 4.2E**, p-value <0.0001). We compared tumor incidence of untreated and treated

animals. Within treated animals, ablated glands were compared to non-ablated glands. No significant changes in tumor incidence were observed with either concentration of MNU (**Table 4.1** and **Table 4.2**). Together, these data suggest that ID treatment with the ethanol ablative solution improves tumor-free survival and risk reduction indicating its potential as an effective option for breast cancer prevention.

**Partial ductal tree ablation and off-target stromal ablation do not increase tumor formation:** The primary goal of the refined ethanol treatment is successful infusion and ablation of the entire ductal tree. Nevertheless, it is crucial to consider the impact that an unsuccessful ID procedure may have on the risk of promoting breast cancer. Partial infusion may leave portions of the ductal tree unablated, with remaining epithelial cells having the potential to become malignant (**Figure 4.3A**). An additional risk of off-target stromal ablation may occur if the needle punctures through the ductal tree and may induce inflammatory responses that help fuel epithelial cell transformation (**Figure 4.3A**). To understand the impact of these unsuccessful procedures, we intraductally infused refined 70% ethanol into rat mammary gland with half volume (50 $\mu$ L for cervical and posterior glands, 150 $\mu$ L for remaining glands) for partial ablation or maximum volume (100 $\mu$ L for cervical and posterior glands, 300 $\mu$ L for remaining glands) for maximal ablation of the ductal tree. Glands that were injected directly into the fat pad of the mammary gland were considered off-target stromal ablations. Up to four mammary glands were infused in each rat at indicated volumes and collected at 72 hours for histological analysis. As expected, fully infused mammary glands had the most epithelial cell ablation compared to partially infused or off-target stromal ablation (**Figure 4.3B**). We then quantified the ablation areas of each treatment type. Among the different infusion volumes, full infusion (n=4) showed the highest ablation rate at 78.8% (p-value, 0.01), while partial infusion volumes (n=4) exhibited a lower percentage of epithelial ablation, measured at 54.1%. In comparison to PBS controls (n=4), with a higher trend of ablation in full volume infusions (**Figure 4.3C**). Off-target treatment (n=4) resulted in an ablation rate of 6.7%, although this was not statistically significant when compared to other treatment groups. These findings underline the importance to using full infusion volumes to achieve the highest ablation rate for maximum epithelial cell death.

We further investigated any long-term iatrogenic effects of partial or incomplete ablation in the MNU rat model. Rats received 50mg/kg of MNU and were either intraductally infused with partial volumes, injected directly into the fat pad of the mammary gland to mimic off-target stromal ablation or were left untreated. Lower volumes were used for off-target stromal ablation reflecting the practice to halt such infusions when translated to humans. As anticipated, untreated controls had the worst survival of 135 days. Notably, partial ablation showed improved survival with a median survival of 309 days (p-value 0.0003) and exhibited a hazard ratio of 6.44 (95% CI: 0.73 to 3.00) indicating a lower likelihood of tumor formation compared to untreated control rats as determined by the Tarone-ware analysis (**Figure 4.3D**). Similarly, off-target stromal ablation had an increased median survival of 280 days (p-value <0.0001) and hazard ratio of HR 7.95 (95% CI: 1.02 to 3.13) compared to untreated controls (**Figure 4.3E**). Though not statistically significant, tumor incidence of partially ablated glands (15% of glands with tumors [10/65]) was lower than untreated controls (24% of glands with tumors, [17/72]) and off-target ablation (23% of glands with tumors, [25/107]). These findings suggest that unintended partial or off-target stromal ablation from unsuccessful procedures are not harmful and do not elevate the risk of developing breast cancer.

**Ethanol treated tumor formation follows disease progression of untreated tumors:** We have previously shown that intraductal ethanol treatment does not cause long-term iatrogenic effects in mouse models. However, alcohol consumption is a contributing factor for increase in breast cancer risk [6, 27]. Ethanol is metabolized into acetaldehyde, a toxic metabolite, that can cause DNA damage and is considered a main mechanism for ethanol-induced carcinogenesis. Therefore, we analyzed tumors from ethanol treated mammary glands to determine if there were any histological or molecular changes, suggestive of an increased in DNA damage and mutational load. We did not detect any difference in tumor aggressiveness, there was not an increase in tumors at more advanced histological stages in ethanol treated glands compared to untreated controls (**Table 4.3**). Immunohistochemistry was conducted on tumors formed in untreated controls, partially infused, and fully infused glands and quantitated. We

observed a higher percentage of ER+ cells (29.3%) in tumors formed from fully infused ethanol treated glands (n=3) compared to 8.8% in partially infused treated glands (n=4) and 19.3% in untreated controls (n=3), although this difference was not statistically different (**Figure 4.4A, B**). The presence of a continuous and organized SMA+ cell layers was confirmatory of adenomas and non-invasive carcinomas in tumors that formed in ethanol treated glands (**Figure 4.4A, B**). Fully infused tumors (n=3) exhibited the highest SMA expression at 18.2% compared to 5.6% in partially infused ethanol treated glands (n=4, p-value 0.03) but not when compared to untreated controls (5.2%, n=3). The Ki-67 marker indicated a similar proliferation demand of tumors from untreated (8.7%, n=3), partially infused (1.0%, n=3), and fully infused ethanol treated glands (8.7%, n=3) whereas Glut1 showed a high metabolic demand in fully infused ethanol treated glands (1.2%, n=3) compared to partially infused (0.3%, n=3, p-value 0.03) and a similar expression as untreated tumors (0.5%, n=3) (**Figure 4.4A, B**). Quantitated IHC analysis revealed higher expression of CD68 in tumors from partially infused glands (2.9%, n=3), compared to untreated controls (0.3%, n=3, p-value 0.02) and similar expression from fully infused glands (1.5%, n=3) suggestive of an abscopal effect (**Figure 4.4B**). However, it is important to note that the low sample sizes and small percentages may contribute to these extreme variations, highlighting the need for further investigation with a larger sample size.

**No interference of ablative solution with MRI breast cancer surveillance:** We previously demonstrated tantalum oxide (TaO<sub>x</sub>) as a suitable and versatile contrast agent capable of providing short term nitid visualization and assessment of complete ductal tree infusion without interfering with ablation effects of 70% ethanol via microCT imaging [13]. Introduction of MR imaging for breast cancer surveillance has improved 10-year survival, increased detection of early disease stages, and is being incorporated into annual screenings for high-risk women [28-31]. We performed long-term MR imaging on animals intraductally infused with TaO<sub>x</sub> to investigate any interference with breast cancer surveillance tools. MR imaging was conducted after intraductal ablation with our refined 70% ethanol solution containing 100mM TaO<sub>x</sub>, 100mM TaO<sub>x</sub> in PBS, or was non-injected. microCT scans on day 0 confirmed

successful infusion of solution into the ductal tree of the mammary gland. The imaging modality of our refined ablation solution was governed by the TaO<sub>x</sub>. Subsequent microCT scans on days 15, 30, and 60 post-infusion demonstrated the identification of TaO<sub>x</sub> in our refined 70% ethanol solution as observed through microCT and 3D renditions at all three time points (**Figure 4.5A, B, D, E**). Non-injected glands were absent in microCT and MR imaging analysis (**Figure 4.5D-F**). We have previously shown local TaO<sub>x</sub> signal decay by 60 days [13]. MR imaging detected all TaO<sub>x</sub> containing solutions at day 15 which dissipated by day 30 (**Figure 4.5C, F**). This indicates that intraductal infusion of TaO<sub>x</sub> within our refined 70% ethanol ablative solution can be conducted without interfering with MR imaging diagnostics from detecting potential future tumor formations within the breast.

### **Discussion.**

We have presented strong evidence that intraductal delivery of an ablation solution is a scalable technique from mice to rats for breast cancer prevention translation [6]. Using the established MNU-induced rat model of breast cancer, we have shown the effectiveness and safety of incorporating an imaging agent (TaO<sub>x</sub>), and gelling agent (EC) in our single infusion ablation solution (70% ethanol) for enhanced ID delivery and ablation of epithelial cells in the ductal tree. The lack of iatrogenic effects from unsuccessful ID procedures underlines the low toxicity and safety profile of this approach for potential translation in first in human clinical trials.

The primary objective of this study is the effectiveness of epithelial ablation in larger rodent models of breast cancer prevention. We selected the MNU rat model for our larger rodent studies as it is a well characterized model for studying breast cancer prevention due to the time frame between carcinogen exposure and tumor formation [14]. ID ablation with refined 70% ethanol resulted in a 72.0% tumor-free survival demonstrating the effectiveness a single ID infusion ablation solution for breast cancer prevention (**Figure 4.2**). In comparison, similar prevention studies with ID delivery of an active tamoxifen metabolite, 4-hydroxy tamoxifen, and cytotoxic agent, pegylated liposomal doxorubicin, observed tumor free survival of 99.5% and 98.3% respectively compared to the 100% tumor-free survival

with subcutaneous tamoxifen demonstrating the effectiveness of local intraductal treatment to current approved prevention strategies [18]. Another study investigating ID delivery of fulvestrant observed a 72.5% tumor-free survival and was as effective as the standard intramuscular delivery [15]. While these studies required weekly ID infusions for higher tumor-free survival, our single ID infusion ablation achieved comparable effectiveness without follow-up infusions. Additionally, we observed rats until IACUC tumor criteria for euthanasia were met, approximately 9 months post MNU administration (**Figure 4.2**), whereas these studies ended 5-8 months after MNU administration. The increased time window of our studies allowed for multiple tumors to form in a single rat which may have lowered tumor-free survival and tumor incidence of ethanol ablation (**Table 4.1 and 4.2**). To further determine the effectiveness of our ablative procedure, systematic comparative studies against established prevention treatments are warranted.

We further enhanced our single administration ID ablation prevention procedure with the imaging agent TaO<sub>x</sub> for real-time confirmation of successful ID infusion. This enhancement, which did not interfere with current MR imaging breast cancer surveillance tools, further demonstrates the translatability of our refined ablative procedure for first in human clinical trials (**Figure 4.5**). To our knowledge, this is the first prevention study using image guidance to determine success of ID infusion throughout the ductal tree.

While successful ID infusion is facilitated by TaO<sub>x</sub>, it is important to note that TaO<sub>x</sub> is not physically conjugated to 70% ethanol. Consequently, microCT image guidance selectively detects TaO<sub>x</sub> but no other component of our ablation solution within the ductal tree. Although complete ablation of the entire ductal tree using 70% ethanol cannot be directly verified *in vivo*, ID infusion of our ablative solution through the ductal tree has been shown (**Figure 4.3**) [6, 13].

A limitation to using X-ray imaging agent TaO<sub>x</sub> is the interference with mammography, a current breast cancer diagnostics tool, as microCT and mammography both utilize X-rays for imaging [32, 33]. We have previously observed signal decay, but not complete clearance of tantalum oxide from the ductal tree via microCT and have yet to determine the mechanism of action for clearance (**Figure 4.5** and ref

[13]). Therefore, understanding the complete clearance of tantalum oxide from the ductal tree remains an important consideration for successful translation of our findings into human clinical trials.

A secondary objective of this study was to assess low toxicity and safety profile of this ID procedure for translation to human clinical trials. We tested experimental the negative consequences and potential iatrogenic effects of partial epithelial cell ablation and off -target stromal ablation. Similar to human terminal ducts, the rat terminal ends buds located at the ends of the ductal tree are highly proliferative and are the sites from which breast cancer predominately arises [34-36]. Partial ductal tree infusion had reduced epithelial ablation (**Figure 4.3**) indicative of incomplete ablation of the terminal end buds, raising concerns about regeneration of the ductal tree and/or potential increase in malignancy of residual epithelial cells. We did not observe a lower tumor latency in glands infused with partial volume compared to untreated controls. This indicates the safety of this procedure in the event of unsuccessful infusions which was further confirmed by minimum changes in disease progression in untreated and ethanol infused tumors (**Figure 4.3 and 4.4**). The diminished number of of SMA+ and ER+ cells, and higher number CD68+ immune cells in tumors from partially ablated glands raises the possibility that these representative tumors may have exhibited more invasive characteristics. The potential for a more comprehensive understanding of these characterizes could be enhanced by increasing the sample size for further analysis. Nonetheless, a previous investigation into the adipocyte thermogenic programming utilizing intraductal ethanol ablation observed minimal changes in gene regulation [37]. It is important to note that the genes investigated by Patel et al. are an incomplete representation of all genes in adipocytes. To enhance the depth of our studies, future research should employ RNA sequencing to explore DNA mutations in the microenvironment and epithelial cells of tumors and mammary glands ablated by intraductally delivered ethanol.

The introduction of ethanol into the adipocyte network from off-target stromal ablation introduces the potential for unknown DNA damage thereby elevating the risk of tumor formation. While off-target stromal ablation resulted in minimal epithelial ablation, the observed increase in tumor latency suggests the presence of an abscopal effect, although this phenomenon was not investigated further (**Figure 4.3**).

Future studies conducting ID infusion in all glands within animals may help to avoid this potential confounding effect.

Though rat models play a crucial role in studying tumor latency and survival in breast cancer prevention studies, the use of a stereoscope for successful cannulation of the nipple and ID delivery throughout the ductal tree is required thereby increasing the rate of unsuccessful ID infusions. In contrast, rabbits are a larger animal model that does not require a stereoscope to perform ID infusions and has multiple ducts per mammary gland reflecting an anatomy more similar to the multi-ductal human breast [38-40]. Therefore, utilization of rabbit models for investigating ID infusion with our refined ablation solution may enhance the success rate of this intraductal ablative prevention and minimize the occurrence of unsuccessful infusions while simultaneously addressing concerns for translation to first-in human clinical trials.

### **Conclusion.**

This preclinical study demonstrates the effectiveness of refined 70% ethanol intraductal ablation as a local, minimally invasive ablation solution. A single administration of this solution demonstrates significant effectiveness without compromising tumor surveillance modalities offering promising support for further investigation as a valid strategy for breast cancer prevention for first in human clinical trials. This study could also stimulate the evaluation of genetic changes within the breast after chemical and/or other ablation strategies to further understand the normal function of the mammary gland after ID ablation. The innovation introduced by this ID procedure holds the potential to modernize current breast cancer preventions by delivering long-term effects with short term infusions at minimal costs. This approach is beneficial for high-risk women while holding promise for application in moderate to low-risk women, contributing to an overall improvement in an individual's quality of life.

## Figures

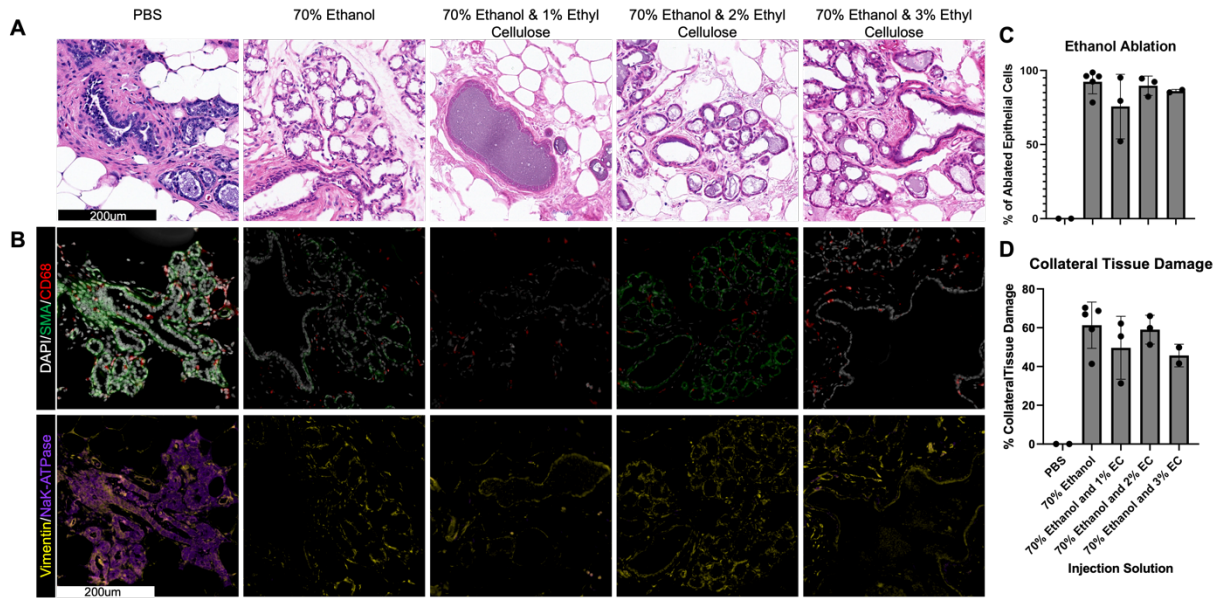


**Figure 4.1. Intraductal infusion of 70% Ethanol with Ethyl Cellulose.** **A)** H&E Staining of representative PBS, 70% ethanol, and 70% Ethanol with ethyl cellulose (EC) percentages 72 hours after ID infusions. **B)** Representative multiplex staining of PBS, 70% ethanol, and 70% ethanol with ethyl cellulose percentages 72 hours after ID infusions. After sequential detection of  $\alpha$ -smooth muscle actin (SMA), macrophages (CD68) tissue was counterstained with DAPI. **C and D)** Quantitative representation of ablative epithelial cells (**C**) and collateral tissue damage (**D**) after ID infusion of PBS (n=2), 70% ethanol (n=5), 70% ethanol with 1% EC (n=3), 2% EC (n=3) or 3% EC (n=2).. Scale bars indicate 200  $\mu$ m.

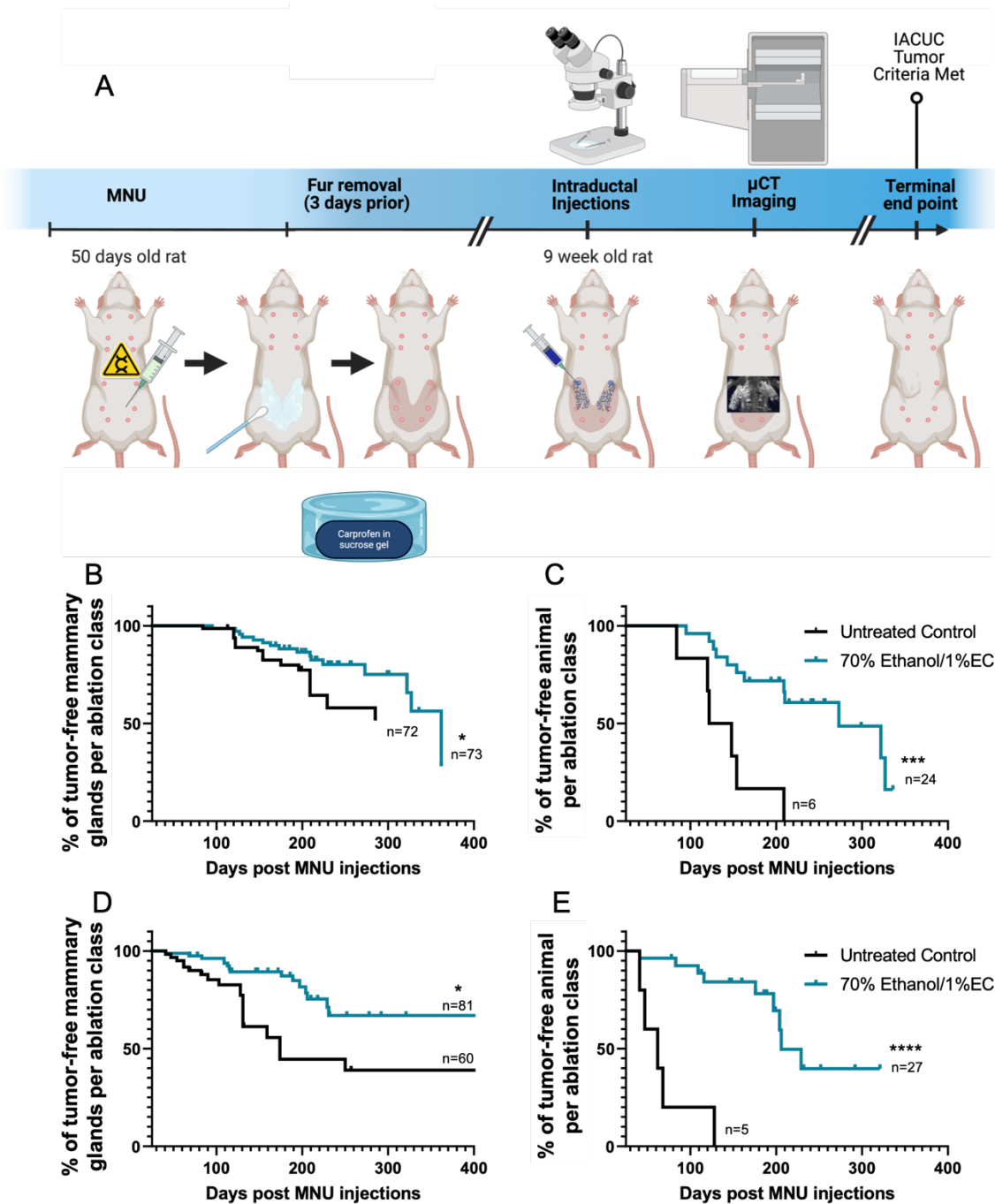


**Figure 4.2. Refined 70% Ethanol Intraductal Ablation Delays Tumor Formation in an MNU Rat Model of Breast Cancer.** **A)** Experimental design for intraductal ablation of refined 70% ethanol after induction of MNU carcinogen. **B and C)** Tumor latency of refined 70% ethanol ID ablation in 50mg/kg MNU induced rats by gland (**B**, p-value  $* < 0.05$ , HR 2.17) and by animal (**C**, p-value  $*** < 0.001$ ). **D and E)** Tumor latency of refined 70% ethanol ID ablation in 75mg/kg MNU induced rats by gland (**D**, p-value  $* < 0.05$ , HR 4.64) and by animal (**E**, p-value  $**** < 0.0001$ ).

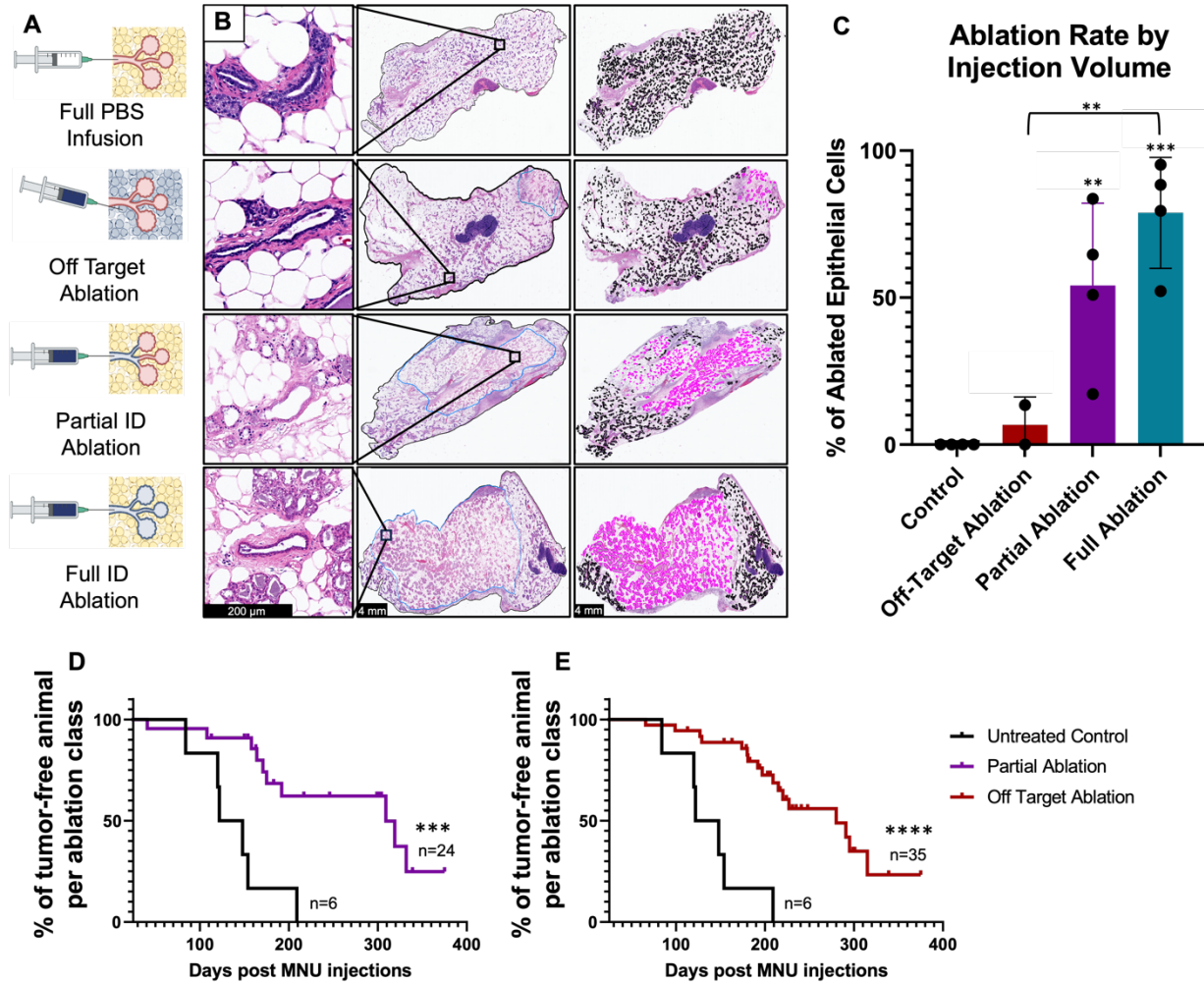
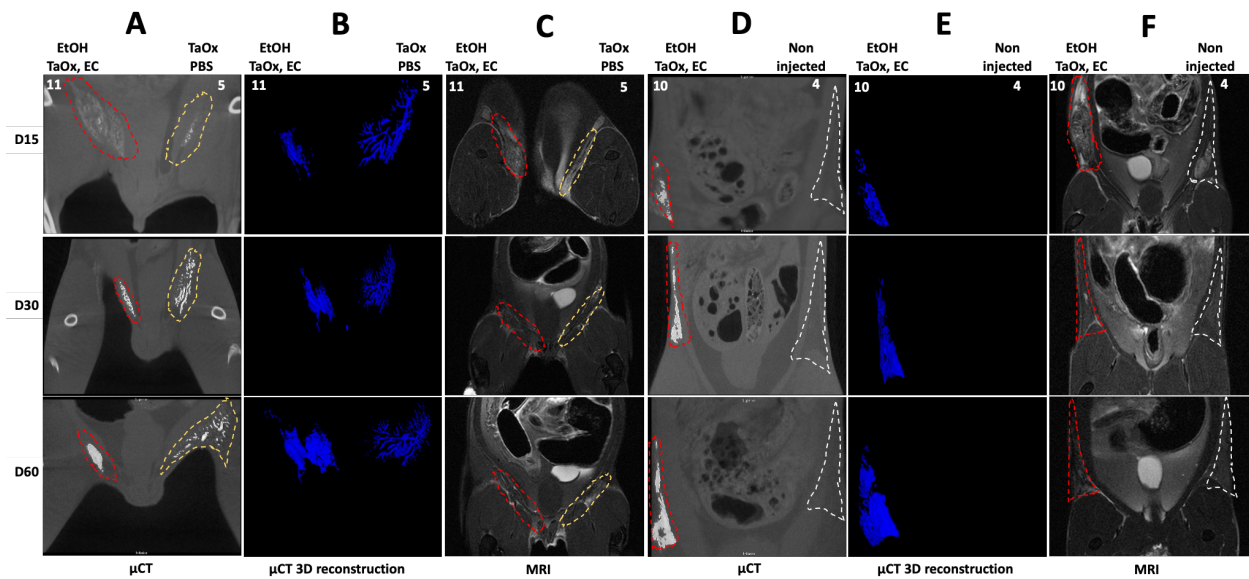
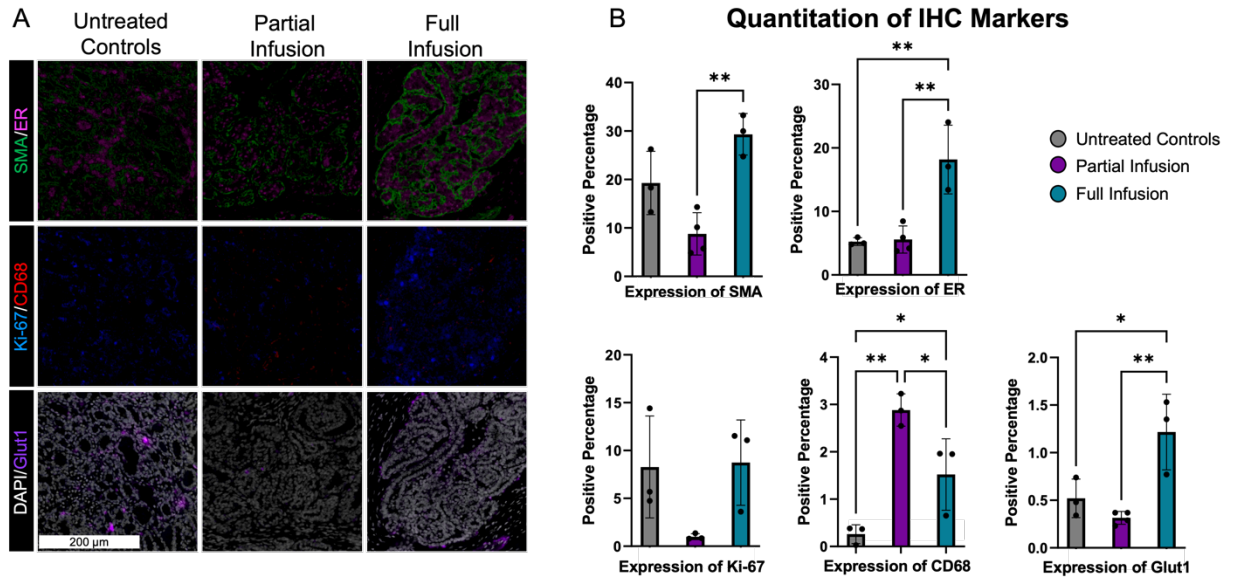


**Figure 4.3. Ablation Rates of Full and Partial Infused Volumes with 70% Ethanol.** **A)** Graphical representation of intraductal ablation potential outcomes. **B)** H&E representation of intraductally ablated ducts (left), whole glands (middle) and quantitated glands (right). **C)** Quantitative representation of ablation rates with ID PBS infusion (n=4), off-target ablation (n=2), ID partial infusion (n=4) and ID full infusion (n=4, p-value  $** < 0.01$  compared to control). **D)** Tumor latency of untreated controls and partial ductal tree ablation. Median survival 135 days and 309 days respectively (p-value  $*** < 0.001$ , HR 6.44). **E)** Tumor latency of untreated controls and off-target stromal ablation. Median survival 135 days and 280 days respectively (p-value  $**** < 0.0001$ , HR 7.95).



## Tables

**Table 4.1. Tumor incidence of 50mg/kg MNU rodent group.**

Tumor Incidence Table 50mg/kg						
	Untreated vs Non-Injected Glands			Non-Injected Glands vs Injected Glands		
Animal Groups	Tumor incidence (% <i>,n</i> )	RR (95% CI)	P-value	Tumor incidence (% <i>,n</i> )	RR (95% CI)	P value
Untreated vs. Refined Ethanol-Ablation	24% (17/72) vs. 24% (47/168)	1.14 (0.70 – 1.88)	0.5944	24% (17/72) vs. 18% (16/73)	0.94 (0.51 – 1.74)	0.8471
Within Ethanol-Ablation	N/A	N/A	N/A	24% (47/168) vs. 18% (16/73)	1.22 (0.73 – 2.03)	0.4529

**Table 4.2. Tumor incidence of 75mg/kg MNU rodent group.**

Tumor Incidence Table 75mg/kg						
	Untreated vs Non-Injected Glands			Non-Injected Glands vs Injected Glands		
Animal Groups	Tumor incidence (% <i>,n</i> )	RR (95% CI)	P-value	Tumor incidence (% <i>,n</i> )	RR (95% CI)	P value
Untreated vs. Refined Ethanol-Ablation	37% (22/60) vs. 29% (47/162)	0.84 (0.54 – 1.30)	0.4287	37% (22/60) vs. 20% (16/81)	0.61 (0.35 – 0.93)	0.0961
Within Ethanol-Ablation	N/A	N/A	N/A	29% (47/162) vs. 20% (16/81)	0.73 (0.44 – 1.23)	0.2370

**Table 4.3. Disease progression of tumors.**

	Untreated Controls	Ethanol Infused Tumors
Adenoma & DCIS Only	28.57% (4/14)	36.67% (11/30)
DCIS & Invasive Mixture	28.57% (4/14)	3.33% (1/30)
Invasive Only	35.71% (5/14)	16.67% (5/30)

## Supplemental Figures

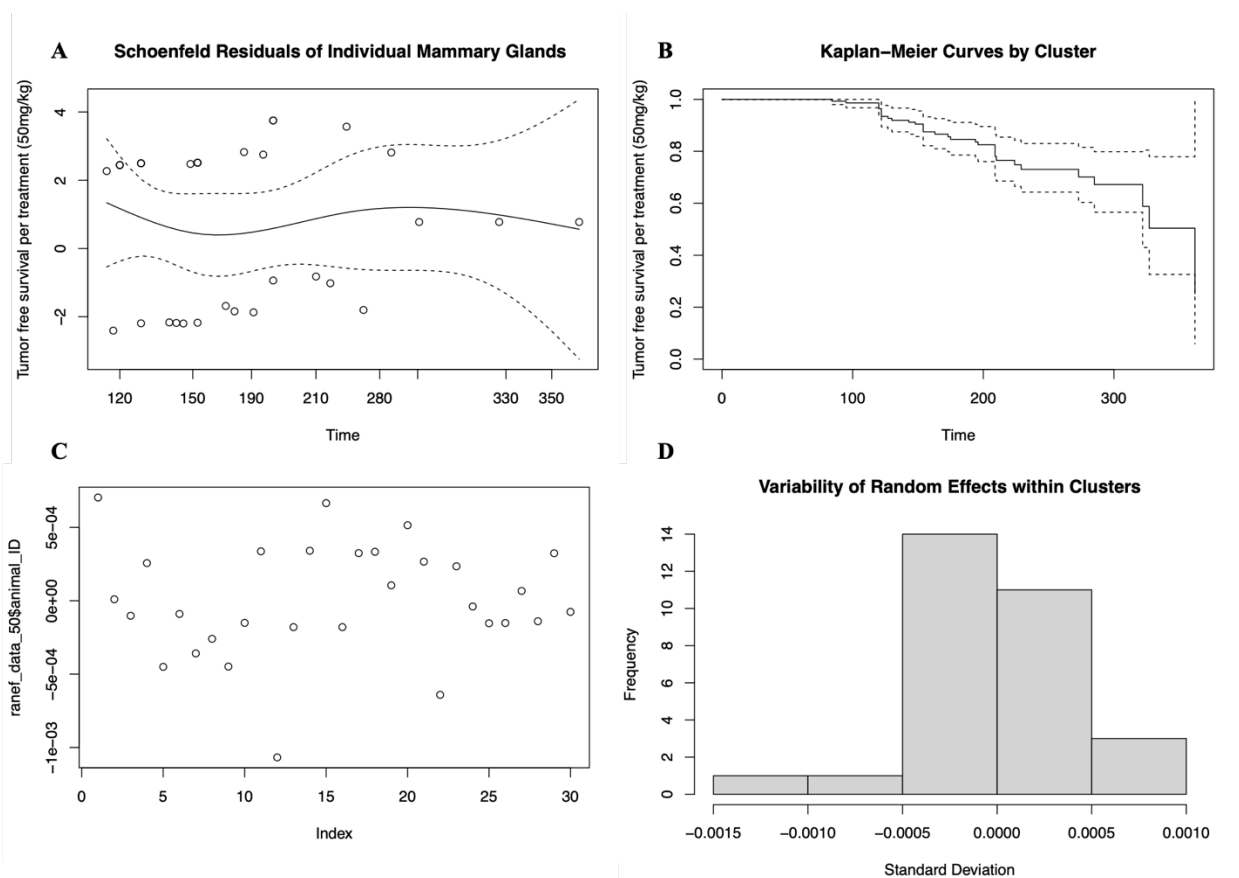


**Figure 4.6. Visual representations of mixed effect cox model assumptions of individual mammary glands in 50mg/kg MNU induced rats. A) Schoenfeld residual analysis to determine proportional hazard assumption. B) Kaplan-Meier Curves for analysis of independence of clusters assumption. C) Visual inspection of the distribution of random effects assumption. D) Visual inspection of the homogeneity of random effects assumption.**

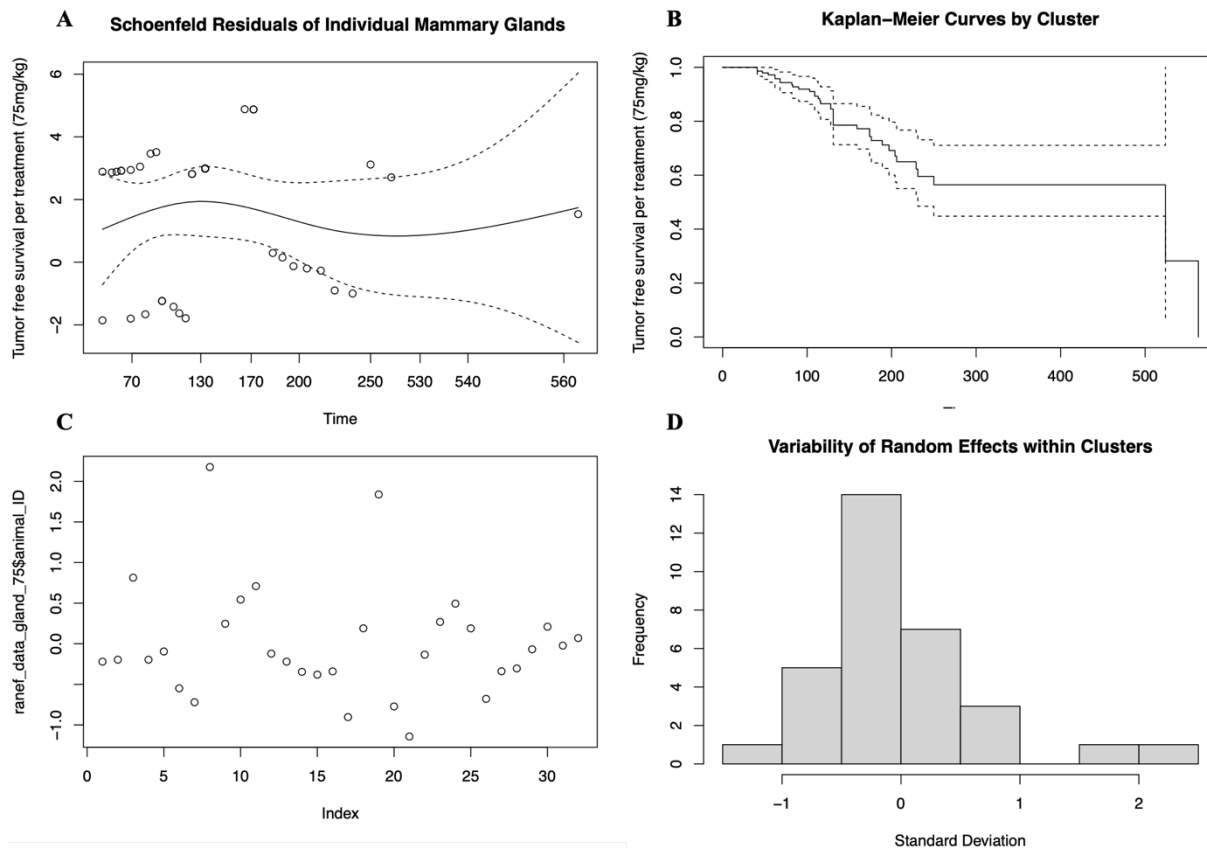


**Figure 4.7. Visual representations of mixed effect cox model assumptions of individual mammary glands in 75mg/kg MNU induced rats. A)** Schoenfeld residual analysis to determine proportional hazard assumption. **B)** Kaplan-Meier Curves for analysis of independence of clusters assumption. **C)** Visual inspection of the distribution of random effects assumption. **D)** Visual inspection of the homogeneity of random effects assumption.

## REFERENCES

1. Siegel RL, Giaquinto AN, Jemal A: Cancer statistics, 2024. *CA Cancer J Clin* 2024, 74(1):12-49.
2. Padamsee TJ, Wills CE, Yee LD, Paskett ED: Decision making for breast cancer prevention among women at elevated risk. *Breast Cancer Res* 2017, 19(1):34.
3. Zaluzec EK, Sempere LF: Systemic and Local Strategies for Primary Prevention of Breast Cancer. *Cancers* 2024, 16(2):248.
4. Fisher B, Costantino JP, Wickerham DL, Cecchini RS, Cronin WM, Robidoux A, Bevers TB, Kavanah MT, Atkins JN, Margolese RG *et al*: Tamoxifen for the prevention of breast cancer: current status of the National Surgical Adjuvant Breast and Bowel Project P-1 study. *J Natl Cancer Inst* 2005, 97(22):1652-1662.
5. Sapienza Passos J, Dartora V, Cassone Salata G, Draszesski Malago I, Lopes LB: Contributions of nanotechnology to the intraductal drug delivery for local treatment and prevention of breast cancer. *Int J Pharm* 2023, 635:122681.
6. Kenyon E, Westerhuis JJ, Volk M, Hix J, Chakravarty S, Claucherty E, Zaluzec E, Ramsey L, Madaj Z, Hostetter G *et al*: Ductal tree ablation by local delivery of ethanol prevents tumor formation in an aggressive mouse model of breast cancer. *Breast Cancer Res* 2019, 21(1):129.
7. Kuang M, Lu MD, Xie XY, Xu HX, Xu ZF, Liu GJ, Yin XY, Huang JF, Lencioni R: Ethanol ablation of hepatocellular carcinoma Up to 5.0 cm by using a multipronged injection needle with high-dose strategy. *Radiology* 2009, 253(2):552-561.
8. Ansari D, Andersson R: Radiofrequency ablation or percutaneous ethanol injection for the treatment of liver tumors. *World J Gastroenterol* 2012, 18(10):1003-1008.
9. Zhang WY, Li ZS, Jin ZD: Endoscopic ultrasound-guided ethanol ablation therapy for tumors. *World J Gastroenterol* 2013, 19(22):3397-3403.
10. Chakravarty S, Hix JML, Wiewiora KA, Volk MC, Kenyon E, Shuboni-Mulligan DD, Blanco-Fernandez B, Kiupel M, Thomas J, Sempere LF *et al*: Tantalum oxide nanoparticles as versatile contrast agents for X-ray computed tomography. *Nanoscale* 2020, 12(14):7720-7734.
11. Kenyon E, Zaluzec E, Powell K, Volk M, Chakravarty S, Hix J, Kiupel M, Shapiro EM, Sempere LF: X-Ray Visualization of Intraductal Ethanol-Based Ablative Treatment for Prevention of Breast Cancer in Rat Models. *J Vis Exp* 2022(190).
12. Kenyon E, Zaluzec EK, Powell K, Volk M, Chakravarty S, Hix J, Arora R, Westerhuis JJ, Kiupel M, Shapiro EM *et al*: Intraductal Delivery and X-ray Visualization of Ethanol-Based Ablative Solution for Prevention and Local Treatment of Breast Cancer in Mouse Models. *J Vis Exp* 2022(182).
13. Zaluzec EK, Kenyon E, Volk M, Hayat H, Powell K, Loomis A, Chakravarty S, Hix JML, Schipper J, Chang C *et al*: Tantalum oxide nanoparticles as versatile and high-resolution X-ray contrast agent for intraductal image-guided ablative procedure in rodent models of breast cancer. *npj Imaging* 2024, 2(1):3.

14. Alvarado A, Lopes AC, Faustino-Rocha AI, Cabrita AMS, Ferreira R, Oliveira PA, Colaço B: Prognostic factors in MNU and DMBA-induced mammary tumors in female rats. *Pathol Res Pract* 2017, 213(5):441-446.
15. Wang G, Chen C, Pai P, Korangath P, Sun S, Merino VF, Yuan J, Li S, Nie G, Stearns V *et al*: Intraductal fulvestrant for therapy of ER $\alpha$ -positive ductal carcinoma in situ of the breast: a preclinical study. *Carcinogenesis* 2019, 40(7):903-913.
16. Wang G, Kumar A, Ding W, Korangath P, Bera T, Wei J, Pai P, Gabrielson K, Pastan I, Sukumar S: Intraductal administration of transferrin receptor-targeted immunotoxin clears ductal carcinoma in situ in mouse models of breast cancer-a preclinical study. *Proc Natl Acad Sci U S A* 2022, 119(24):e2200200119.
17. Love SM, Zhang W, Gordon EJ, Rao J, Yang H, Li J, Zhang B, Wang X, Chen G, Zhang B: A feasibility study of the intraductal administration of chemotherapy. *Cancer Prev Res (Phila)* 2013, 6(1):51-58.
18. Murata S, Kominsky SL, Vali M, Zhang Z, Garrett-Mayer E, Korz D, Huso D, Baker SD, Barber J, Jaffee E *et al*: Ductal access for prevention and therapy of mammary tumors. *Cancer Res* 2006, 66(2):638-645.
19. Thompson HJ, Adlakha H: Dose-responsive induction of mammary gland carcinomas by the intraperitoneal injection of 1-methyl-1-nitrosourea. *Cancer Res* 1991, 51(13):3411-3415.
20. Sempere LF, Zaluzec E, Kenyon E, Kiupel M, Moore A: Automated Five-Color Multiplex Co-detection of MicroRNA and Protein Expression in Fixed Tissue Specimens. *Methods Mol Biol* 2020, 2148:257-276.
21. Altman DG: Confidence intervals for the number needed to treat. *BMJ* 1998, 317(7168):1309-1312.
22. Altman DG: Practical Statistics for Medical Research. New York: Chapman and Hall/CRC; 1991.
23. Robert D. Cardiff SJ, Piper M. Treuting, James J. Goings, Barry Gusterson, Henry J. Thompson: Mammary Gland. In: *Comparative Anatomy and Histology (Second Edition)*. edn. Edited by Piper M. Treuting SMD, Kathleen S. Montine. Academic Press: Academic Press; 2018: 487 - 509.
24. Devesh Kapoor RM, Kanika Verma, Swapnil Sharma, Piyush Ghode, Rakesh K. Tekade,: Coating technologies in pharmaceutical product development. In: *Drug Delivery Systems, Advances in Pharmaceutical Product Development and Research*. edn. Edited by Tekade RK. Academic Press; 2019: 665-719.
25. Mueller JL, Morhard R, DeSoto M, Chelales E, Yang J, Nief C, Crouch B, Everitt J, Previs R, Katz D *et al*: Optimizing ethyl cellulose-ethanol delivery towards enabling ablation of cervical dysplasia. *Sci Rep* 2021, 11(1):16869.
26. Nief CA, Swartz AM, Chelales E, Sheu LY, Crouch BT, Ramanujam N, Nair SK: Ethanol Ablation Therapy Drives Immune-Mediated Antitumor Effects in Murine Breast Cancer Models. *Cancers (Basel)* 2022, 14(19).

27. Seitz HK, Stickel F: Acetaldehyde as an underestimated risk factor for cancer development: role of genetics in ethanol metabolism. *Genes Nutr* 2010, 5(2):121-128.
28. Kuhl C, Weigel S, Schrading S, Arand B, Bieling H, König R, Tombach B, Leutner C, Rieber-Brambs A, Nordhoff D *et al*: Prospective multicenter cohort study to refine management recommendations for women at elevated familial risk of breast cancer: the EVA trial. *J Clin Oncol* 2010, 28(9):1450-1457.
29. Gao Y, Reig B, Heacock L, Bennett DL, Heller SL, Moy L: Magnetic Resonance Imaging in Screening of Breast Cancer. *Radiol Clin North Am* 2021, 59(1):85-98.
30. Evans DG, Kesavan N, Lim Y, Gadde S, Hurley E, Massat NJ, Maxwell AJ, Ingham S, Eeles R, Leach MO *et al*: MRI breast screening in high-risk women: cancer detection and survival analysis. *Breast Cancer Res Treat* 2014, 145(3):663-672.
31. Radhakrishna S, Agarwal S, Parikh PM, Kaur K, Panwar S, Sharma S, Dey A, Saxena KK, Chandra M, Sud S: Role of magnetic resonance imaging in breast cancer management. *South Asian J Cancer* 2018, 7(2):69-71.
32. Boone JM, Nelson TR, Lindfors KK, Seibert JA: Dedicated breast CT: radiation dose and image quality evaluation. *Radiology* 2001, 221(3):657-667.
33. Sarno A, Mettivier G, Russo P: Dedicated breast computed tomography: Basic aspects. *Med Phys* 2015, 42(6):2786-2804.
34. Paine IS, Lewis MT: The Terminal End Bud: the Little Engine that Could. *J Mammary Gland Biol Neoplasia* 2017, 22(2):93-108.
35. Visvader JE: Keeping abreast of the mammary epithelial hierarchy and breast tumorigenesis. *Genes Dev* 2009, 23(22):2563-2577.
36. Russo J, Russo IH: Experimentally induced mammary tumors in rats. *Breast Cancer Res Treat* 1996, 39(1):7-20.
37. Patel S, Sparman NZR, Arneson D, Alvarsson A, Santos LC, Duesman SJ, Centonze A, Hathaway E, Ahn IS, Diamante G *et al*: Mammary duct luminal epithelium controls adipocyte thermogenic programme. *Nature* 2023, 620(7972):192-199.
38. Hughes K: Comparative mammary gland postnatal development and tumorigenesis in the sheep, cow, cat and rabbit: Exploring the menagerie. *Semin Cell Dev Biol* 2021, 114:186-195.
39. Schoniger S, Degner S, Jasani B, Schoon HA: A Review on Mammary Tumors in Rabbits: Translation of Pathology into Medical Care. *Animals (Basel)* 2019, 9(10).
40. Clark A, Bird NK, Brock A: Intraductal Delivery to the Rabbit Mammary Gland. *J Vis Exp* 2017(121).

## **CHAPTER 5: GENERAL CONCLUSIONS**

This dissertation addresses four major factors utilizing intraductal ablation as an innovative new approach towards breast cancer prevention: 1) the feasibility of intraductal delivery *in vivo*, 2) the efficacy of 70% ethanol as an ablative solution for intraductal delivery in rodent models of breast cancer, 3) addressing known challenges of clinical ethanol ablation delivery, and 4) addressing adverse events of the intraductal ablative procedure.

Current breast cancer prevention options are considerably lacking for women at high-risk of developing breast cancer. Therefore, it is crucial to develop new prevention approaches that have equal risk reduction to current prevention methods with minimal adverse events. As discussed in chapter 1, there are many preclinical and clinical investigations into new prevention approaches for breast cancer; however, the low number of approved prevention methods remains unchanged. In chapter 2, I evaluated the ability of intraductal (ID) infusions to directly target the epithelial cells, the cell from which most breast cancer arises, within the ductal tree. Using Evans blue and whole-mount staining, I was able to show that intraductal delivery is a feasible procedure that can fill the entire ductal tree, targeting all epithelial cells with limited physical damage to the mammary gland or rodent. To ablate all epithelial cells prior to any potential cancer formation, ethanol was introduced as a cell-killing ablative solution in chapters 2, 3 and 4. Not only is there precedence for clinical uses of ethanol in ablative procedures, but it is also cost-effective, which makes this an accessible solution for all individuals regardless of their financial status [1-4]. Current clinical applications utilize a dose of 95% ethanol (EtOH); however, this concentration was found to cause ductal occlusion and rapid dehydration of the mammary gland when intraductally delivered. Therefore, the concentration of ethanol was lowered to 70% which maintains ablation effectiveness while avoiding these complications. By combining intraductal delivery with an ablative 70% ethanol solution, I was able to show that a single infusion of ethanol is capable of ablating nearly all epithelial cells within the ductal tree. This results in a local, simple, and direct ablation approach for breast cancer prevention. Furthermore, I was able to show the scalability of intraductal delivery by successfully ablating epithelial cells of the larger rat mammary gland with increased infusion volumes and maintained the ethanol ablation effectiveness demonstrating the ability of translation into

future human clinical trials.

To determine the efficacy of this local ablative technique, I utilized two different rodent models of breast cancer: C3(1)-TAg mouse model and the chemically induced MNU rat model. The C3(1)-TAg mouse model is an aggressive multifocal model of breast cancer that does not rely on pregnancy or hormones for tumor induction [5]. Additionally, the time to development in this model allows for ID ablation to be performed after mammary glands are fully developed but prior to tumor formation. This allows for the study of ID ablation as an innovative approach for a preventive setting. Other models are also available for studying intraductal infusion of 70% ethanol such as MMTV-*Brca1*, MMTV-*erbB2*, or MMTV-PyMT but requires consideration of tumor latency and penetrance for use as a prevention model [6, 7]. To rigorously study the scalability of ID ablation in a breast cancer prevention model, the chemically induced MNU rat model was selected. This rat model closely follows human breast progression from normal tissue to invasive carcinoma and, unlike other commonly used rat models, does not require metabolic activation such as 7,12-Dimethylbenzanthracene [8]. MNU is a DNA alkylating agent that induces tumor formation eight to ten weeks after injections providing a specific time window during which ID ablation can be utilized in a preventive manner [8]. By intraductally infusing 70% ethanol into the ductal tree prior to tumor formation in these models, I was able to show lower tumor incidence in intraductally ablated glands compared to non-ablated controls in mice. These infusions were well tolerated in all rodents with minor external damage and mild intoxication mitigated through intraperitoneal injections of 5% sucrose solutions.

While ethanol is currently utilized in clinical settings, the effectiveness of its ablative properties is hindered by two limitations, leakage outside of the targeted area, and lack of imaging capabilities without additional imaging solutions. I sought to address ethanol diffusion outside of the ductal tree by introducing ethyl cellulose; a gelling agent already used clinically for reduced diffusion of 95% ethanol outside of the desired target area [9-12]. A combination of 70% ethanol with 1% ethyl cellulose reduced collateral tissue damage within the ductal tree of mice, but this did not translate into the larger rat mammary gland. Many possible factors may have contributed to this outcome including structural

differences within rodents such as increased connective tissue surrounding the ductal tree in rats compared to mice, small sample sizes, or technical aspects of intraductal infusions such as needle insertion depth or infusion rate. To address the difficulties with imaging ethanol within the ductal tree, I investigated contrast agents for sharp visualization with *in vivo* imaging modalities. Initial ID infusion of FDA-approved contrast agent isovue-300 demonstrated low resolution and ductal tree retention. Therefore, I explored other contrast agents that have been well characterized *in vivo*. Tantalum oxide was selected as the contrast agent for intraductal infusion due to its local but moderate retention in the ductal tree and high imaging modality without impacting the ablation of the ethanol solution [13, 14].

As with any pharmacological application, undesired adverse effects are a primary obstacle and limiting factor for most women considering the current breast cancer prevention options. In chapters 2 and 4, I address the adverse effects of this ID ablative solution. Physical side effects were minimal. Neither mice nor rats displayed open wounds or showed overt signs of pain or discomfort as measured by touch test with von Frey filaments prior to and following ID ablation and maintained normal grooming and social behaviors throughout the study. Any minor skin lacerations due to ethanol leakage were resolved using topical, triple-antibiotic ointment. Delayed removal of the needle from the nipple after cannulation was found to minimize skin irritation. Some animals showed signs of reduced limb movement with the addition of ethyl cellulose. However, these animals received greater than 1% ethyl cellulose which also reduced the effect of ethanol ablation and therefore were not used for ablative purposes. Immune cells were observed around ablated ducts beginning three days after the intraductal procedure suggesting the initiation of wound healing and tissue repair which was resolved after one month.

Additionally, long term intraductal ablation with 70% ethanol in multiple glands of non-transgenic mice did not form any tumors. The animals died of natural causes thus demonstrating that intraductal ablation with 70% ethanol do not have iatrogenic effects or other diseases. Similarly, partial ablation, and off-target stromal ablation, did not increase breast cancer risk as observed with higher tumor latency compared to controls in MNU rat models of breast cancer.

## **Future Directions.**

**Epithelial Cell Regeneration within the Mammary Gland:** Preventive bilateral prophylactic mastectomies for high risk women is recommended 25 to 30 years or age or older [15]. Intraductal ablation with 70% ethanol is an alternative investigative technique to bilateral prophylactic mastectomies and would be targeted towards women within the same age range. The median age for women entering menopause is 51 years of age [16-19]. Therefore, in the target population, hormone-induced changes in the ductal tree still occur due to menstruation and pregnancy. Within the estrous cycle, epithelial cell proliferation occurs during the luteal phase stage of the estrous cycle in mice and women [20-23]. During initial stages of pregnancy increased levels of estrogen and progesterone influence the proliferation and hypertrophy of mammary gland epithelial cells in preparation for milk secretion that occurs during late stages of pregnancy, and postpartum [24-26]. More specifically, cells within the terminal duct lobular units differentiate into milk producing, secretory alveolar epithelial cells. The regenerative capability of the ductal tree suggests the existence of stem cells within the ductal tree population. Indeed, restoration of the ductal tree was demonstrated in mice by introduction of stem cells implanted into a mammary fat pad cleared of all epithelial cells [27, 28] which maintained self-renewal capacity by serial transplantation into cleared mammary glands of the progeny [29]. It was also observed that resident mammary stem cells were influenced by hormone signaling [22].

The technical challenge of intraductal ablation may result in a minimal number of epithelial cells located near the ends of the ductal tree to remain intact and which may proliferate during pregnancy, reducing the effectiveness of epithelial ablation for breast cancer prevention. Although there has not been any identified influence of the estrous cycle in this ablation study, the distinct markers identifying the phenotype of epithelial cells remaining after ID ablation is unknown. Therefore, further research is needed for understanding the implications of ductal tree restoration via proliferation during estrous cycle and pregnancy after epithelial cell ablation by 70% ethanol intraductal delivery.

**Resident immune response to 70% ethanol infusions:** Resident immune cells within the mammary gland are largely composed of macrophages and lymphocytes [30, 31]. These cells are predominately localized to the ductal tree but can be dispersed throughout the mammary gland and play an important role in normal breast maintenance and wound healing [32, 33]. Upon initial injury, pro-inflammatory macrophage response includes secretion of cytokines, such as transforming growth factor  $\beta$  (TGF $\beta$ ), tumor necrosis factor  $\alpha$  (TNF $\alpha$ ), and interleukin (IL-1), to regulate and recruit other immune cells in addition to clearing dead cells and foreign debris [34]. Effector memory T cells born from cytotoxic T cells are the dominant lymphocyte found in the breast and have increased infiltration in the presence of abnormalities such as benign breast disease [30, 35]. Intraductal delivery of 70% ethanol causes ablation to the ductal tree but also disperses into the stroma and likely ablates other cells including the intraepithelial immune cells. However, infiltration of immune cells and wound healing is still mounted after intraductal ablation. Therefore, upon exposure to ethanol, dead and dying epithelial cells likely release damage associated molecular patterns and macrophages near the ductal tree may release chemokines and cytokines upon ablation. These signals may recruit functional T cells, unaffected by ethanol ablation, from areas outside of the ductal tree to initiate wound healing. Initiation of inflammation, cytokine release and response, and recruitment of immune cells upon tissue damage by intraductal 70% ethanol ablation has yet to be thoroughly investigated. Therefore, more studies looking into the reaction of resident immune cells upon intraductal ethanol ablation and tissue repair is needed.

**Cosmesis:** Prophylactic mastectomy is the gold standard in breast cancer prevention for high-risk women. Despite the 90% risk reduction, removal of breasts can impact women intensely, physically, and mentally, resulting in conditions including anxiety, depression, and reduced body positivity [36-38]. Autologous tissue and/or implant reconstructive surgery options are available to women to ameliorate the physiological impact of breast removal and can be conducted simultaneously or delayed after mastectomy. These surgeries displace tissue taken from elsewhere in the body or insert permanent implants for improved cosmetic breast appearance [39, 40]. Both methods require follow-up surgical

procedures.

No external physical changes of the mammary gland have been observed in the intraductally ablated rodents. However, histological analysis of excised mammary glands from long-term studies revealed reduced tissue mass [41]. This may be more pronounced in human breasts, impacting the physical appearance and quality of life of the individual. While this outcome is not expected, tissue reconstructive surgery may be offered to improve the physical and emotion wellbeing of the individual after wound healing has resolved [14, 41]. An unexpected difficulty of tissue reconstruction surgery to these individuals may be the addition of ethyl cellulose in the ablative solution. Though rare, 1% ethyl cellulose was palpable in some mouse mammary glands throughout the duration of the long-term studies but was not palpable with ID ablation in rats. The palpation of ethyl cellulose in mice is likely due to the small mammary gland size and may be negligible upon translation to human breasts. Nevertheless, the gel-like formation of ethyl cellulose sustained within the breast may interfere with tissue reconstructive surgery and should be explored further upon translation to human clinical trials.

**Altered Ethanol Metabolism:** Alcohol ingestion is considered a risk factor for breast cancer, but the mechanism of action is not fully understood. Acetaldehyde is a toxic metabolite of ethanol with mutagenic and carcinogenic effects in rodent but is further metabolized into non-toxic acetate by aldehyde dehydrogenase (ALDH), an enzyme found throughout the body for continued elimination from the body [42-46]. An *in vitro* study showed long-term exposure to low concentration of ethanol and acetaldehyde induced epithelial to mesenchymal transition in normal immortalized human breast epithelial cells [47]. However, the concentrations were continuously maintained and do not accurately recapitulate alcohol consumption or a single intraductal delivery or administration. Acute exposure to ethanol or acetaldehyde has no significant DNA damage in mice and intraductal infusion of ethanol have minimally observed changes on the surrounding adipocytes [48, 49].

An observed effect of 70% ethanol intraductal administration in rodents is alcohol intoxication (0.4g/dL) which is mitigated through 5% sucrose intraperitoneal injections [41]. In high-risk women, ID

infusions would result in mild impairment; approximately 0.1g/dL of EtOH in the blood, or the equivalent of three glasses of wine [41]. In humans, there are known aldehyde dehydrogenase mutations that affect alcohol metabolism such as ALDH2\*2 that reduces the enzymatic activity to clear acetaldehyde. This single nucleotide polymorphism affects approximately 8% of the world's population, is associated with increased risks of head and neck, esophageal, and colorectal cancer and induces aversion reactions with alcohol consumption [43, 50, 51]. Additionally, a second population that may be negatively affected by intraductal delivery of ethanol are individuals taking disulfiram. This FDA approved drug can irreversibly inhibit aldehyde dehydrogenase for treatment of alcohol use disorder, to induce aversion reactions such as flushing, headaches and nausea as a deterrent for alcohol consumption [52]. Therefore, while ID infusions of 70% ethanol may reduce breast cancer risk, it is important to study the susceptibility of these distinct individuals for increased exposure to acetaldehyde within the breast, increased risk of other cancers, and unanticipated systemic aversion reactions which may deter these women from taking this preventive breast cancer approach.

**Translation into Multi-ductal Models:** A major anatomical limitation with intraductal ablation procedure in rodents is the presence of a single ductal tree per mammary gland whereas the human breast is more complex with 8-12 ducts per breast [53, 54]. Larger animals, such as cats, dogs, pigs, and non-human primates have multiple ducts per teat [55, 56]. Rabbits are the most appropriate next step for assessing scalability as they provide a larger animal model with four ducts per mammary gland and can determine the safety profile of ethanol administration and epithelial cell ablation as intended in a therapeutic setting in women [55]. Although no rabbit breast cancer models have been established, previous studies have identified rabbit ductal orifices and demonstrated successful intraductal infusions into rabbit ductal trees [57-62]. Therefore, using rabbit models to address the challenges of intraductal delivery and *in vivo* imaging of a multi-ductal tree system that could not be anticipated in rodent models will further advance the scalability of this breast cancer prevention technique.

A primary objective of intraductal ethanol infusion in rabbits for an investigative device

exemption study is the safety and toxicity profile for eventual first in human clinical trials. Animals first should be assessed for successful cannulation and delivery of ethanol into all four ductal trees per mammary gland (16 ducts total) [57]. For short term effects, animals intraductally infused with PBS or ethanol should be collected from 3 days up to 60 days post ethanol infusion. Mammary glands should be assessed for epithelial ablation through histological and immunohistochemistry analyses. Blood and major organs should be collected for toxicity and potential tissue lesions or abnormalities. In pet rabbits, mammary tumors may form after three years of age [63, 64]. As such, long term studies should be conducted in which rabbits are intraductally infused with ethanol in up to half of their mammary glands (two out of four mammary glands) and followed for three years to detect any iatrogenic cancer or long-term adverse effects. Rodent models indicated no iatrogenic effects of intraductal ethanol infusion (Chapter 4, [41]) and therefore is not expected to induce breast cancer tumor formation in rabbits.

**Path to Translation:** No animal model can fully recapitulate the effects of intraductal ablation with 70% ethanol into a women's breast but fortunately, tools are readily available for the translation of intraductal ablation into multi-ductal breasts of women. Ductography is a diagnostic imaging procedure used to identify internal concerns of breast ducts resulting from abnormal or unusual nipple discharge. Coupled with mammography to identify the specific duct, ductography is then used to isolate and infuse the duct of concern via cannulation of the nipple [65]. This was demonstrated in initial human clinical studies investigating the feasibility of intraductal delivery in multiple ducts for treatment of breast cancer in an outpatient setting [65, 67]. Therefore, with ductography as an available tool, intraductal delivery is a procedure well-equipped to efficiently transition to first in human clinical trials for breast cancer prevention using this single infusion of a refined ethanol ablative solution.

The FDA guidelines requires the classification of a product as a drug or device for an investigational new drug or investigational device exemption application for clinical trials respectively. Ethanol is a versatile substance with both chemical and physical properties and requires careful consideration when categorizing as a drug or device. The FDA definition of a drug includes the article for

use in prevention of a disease and affects the structure or any function of the body [68]. Whereas a device is similarly defined as a drug but does not achieve its primary intended purpose through chemical action within the body and does not depend on the metabolism of the product by the body [68]. Although ethanol as a sclerosing and ablative agent dehydrates the cells, a chemical action which could place ethanol into the category of a drug, the term must be considered in the context of the device as a whole [68-70]. Due to the use of clinical ductography tools for specific targeted ethanol delivery into the ductal tree, the primary purpose of ethanol cannot be achieved without the use of this medical device and must be included to perform successful ethanol ablation. Thus, the intraductal ablative procedure would categorize our refined ethanol ablative solution as a device for application in clinical trials.

Future first in human phase I clinical trials for intraductal ethanol ablation would initially be conducted in women electing to undergo prophylactic mastectomy to study the logistics and adverse events associated with intraductal ethanol delivery and ablation. Briefly, initial studies assessing ductal tree filling and epithelial cell ablation using a single infusion of PBS or refined ethanol would be conducted in women at the time of bilateral prophylactic mastectomy. Subsequently, this study would be followed by infusion into multiple ductal trees per breast to evaluate simultaneous ablation in multiple ducts. This is reflective of similar experimental designs from clinical reports of ID delivery utilizing chemotherapeutic agents [66, 67]. Immediate observations for adverse events should include successful cannulation of multiple ducts, breast fullness, breast and/or nipple pain/discomfort and physical appearance to the breast such as redness, swelling, or eventual scarring after ethanol infusion. Mild skin lacerations, resolved with triple antibiotic ointment, were observed in rodents after receiving intraductal delivery of ethanol (Chapter 4, [41]), therefore monitoring for this adverse effect should be done in human trials immediately and within 48 hours after ethanol infusion. To understand the systemic distribution of ethanol, plasma should be collected every hour for the first four hours, the observed recovery time within rodents, and 24 hours after infusion for complete alcohol clearance. If substantial alcohol intoxication in humans occur, intravenous administration of thiamine and glucose solution could be used to further minimize alcohol intoxication. Another effect in rodents was the immune response

observed approximately three days after ethanol infusion which was resolved after approximately one month [41]. Following this timeline, prophylactic mastectomy would be performed three days to one month post PBS or ethanol infusion to observe wound healing response and its resolution. Subsequent follow-up appointments would be scheduled weekly, starting one week post bilateral mastectomy to compare the wound healing response between mastectomy and ethanol infusions. During these appointments, surveys should be conducted assessing the timeline for cessation of adverse effects such as pain in comparison to those experienced with bilateral mastectomy alone. Additionally, a follow up study should be conducted in which intraductally infused women who do not undergo mastectomy are monitored for any adverse effects within a year, such as increased risk of ethanol-related cancers or disease [43]. However, no long-term impacts are anticipated due to the lack of iatrogenic effects observed in rodents (Chapter 4, [41]). Success of the phase I clinical trial of ID ethanol ablation would be determined by ethanol ablation, ethanol distribution, wound healing response, and patient satisfaction. Briefly, ethanol ablation should achieve a high epithelial ablation rate, approximately 80% similar to that seen in our rodent studies that is equally distributed among the multiple ductal trees in the breast. Wound healing response should be lower than that of bilateral mastectomy alone with reduced adverse events such as pain, discomfort as indicated by patient surveys.

Upon the success of phase I clinical trials, phase II clinical trials would be conducted to evaluate the prevention effectiveness of this intraductal ablative procedure in women at high-risk of breast cancer. 100-300 Women willing to undergo intraductal ethanol ablation as an alternative to bilateral prophylactic mastectomy would be selected for this study. This study design includes women undergoing successful ethanol infusion in all ductal trees, confirmed through CT imaging of TaO<sub>x</sub> within the ethanol solution. Adverse events should be recorded immediately after these procedures and one to two months post procedure, after wound healing is resolved, to analyze any reduction of adverse effects from intraductal ethanol infusion in comparison to the highly invasive systemic mastectomy. Over the course of their lifetime, women would be monitored for breast cancer diagnosis in comparison to historical data of high-risk women who opted for bilateral prophylactic mastectomy to measure effectiveness of intraductal

ethanol ablation. If breast cancer is diagnosed, age, tumor size, and disease progression at time of diagnosis should be recorded and compared the historical data of women who elected to undergo prophylactic mastectomy. Additionally, this may be compared against women who opted for watchful waiting to investigate if intraductal ethanol treatment delayed cancer diagnosis and/or disease progression. We aim for this intraductal ablative procedure to be rigorous and competitive to that of bilateral prophylactic mastectomy. Therefore, this procedure would be considered beneficial if 90% of women experience a risk reducing effect similar to that seen with bilateral prophylactic mastectomy. Additionally for women diagnosed with breast cancer after ID infusions, lower tumor incidence and tumor grade, better treatment prognosis and tumor characteristic such as hormone positive breast cancers compared to triple negative breast cancer, smaller tumor size at time of diagnosis, and increased age at diagnosis would indicate the success of this ablative procedure for phase II clinical trials.

### **Limitations.**

**Technological Variables of Intraductal Infusions:** Ethanol leakage is a major limitation with intraductal infusions: backflow leakage outside the nipple causes minor skin damage and diffusion outside the ductal tree causes internal damage to surrounding adipocytes (Chapter 4, [14, 41]). We introduced ethyl cellulose as a gelling agent to mitigate internal diffusion which has yet to be fully resolved (Chapter 4, [41]) and may be a result of the technical challenge of intraductal infusions. Needle depth and insertion rate, infusion rate, and volume may all contribute to the success of 70% ethanol intraductal ablation with ethyl cellulose. A previously conducted study using ethanol and ethyl cellulose has shown that 2mm/s and 10mm/s needle infusion rates minimized injection dimpling and subsequent tissue damage [11]. Infusion rates varied by ethyl cellulose percentage, but lower rates had overall reduced tissue damage [11, 71]. However, these infusions were conducted in swine models for cervical dysplasia and liver cancer and focused on ablation around the infusion site. Solution volumes for intraductal ablation was previously established for mice and rats and calculated for humans but other technical aspects of intraductal ablation have yet to be investigated [72, 73]. In this study, needles are

inserted such that the bevel of the needle is completely engulfed within the nipple. Depth and insertion rate of the needle and nipple dimpling are not monitored and may vary due to nipple shape and size [72, 73]. An infusion rates of 40  $\mu\text{L}/\text{min}$  and 100  $\mu\text{L}/\text{min}$  in mice and rats respectively has been consistently used [14, 41, 72, 73] but other rates for minimizing tissue damage have not explored. Therefore, these technical aspects of ablation by intraductal infusions should be further studied and consistently applied by all operators.

**Targeting all glands for breast cancer prevention:** In this dissertation, I utilized two breast cancer models to study breast cancer prevention: a genetically engineered C(3)1-TAg mouse model and a chemically induced MNU rat model. While these rodent models are effective for studying breast cancer, identification of tumor location in mammary glands prior to actual tumor formation is challenging and limits the stability of these models for prevention studies [74]. To mitigate this challenge, intraductal ablation is attempted in every gland in all animals, however, most animals were injected in up to 6 glands primarily within the thoracic and abdominal areas due to ease of cannulation (Chapter 4, [41, 72, 73]). Gao et al have begun to investigate an approach to induce targeted tumor formation. The authors demonstrated predictable tumor formation of intraductal MNU infusions in designated mammary gland compared to that of intraperitoneal injections. ID MNU tumors had higher tumor incidence, but disease progression was unaffected. Intraductal infusions of chemotherapeutics after ID infusions of MNU-induced mammary glands with established tumors maintained efficacy, leading to tumor regression [74]. Therefore, this approach is feasible for selective tumor formation and also demonstrated the feasibility of multiple intraductal treatments in a single gland. However, it is important to note that while multiple infusions are possible, this is also dependent on the solution being infused. Gao et al intraductally infused MNU and after tumor formation, intraductally infused albumin bound paclitaxel which inhibits cancer cell growth through inhibition of cell cycle arrest [75]. Due to the immediate ablation effects of ID 70% ethanol infusion on epithelial cells, secondary intraductal ablation infusions to ensure complete eradication of epithelial cells may not be feasible, however, I have shown that a single ID infusion of 70%

ethanol is capable to ablating nearly all epithelial cells, rendering further round of infusions unnecessary.

**Wound healing and Age:** To study breast cancer prevention, intraductal ablation is performed in MNU induced rodents at age 9 weeks of age; after sexual maturation and ductal trees are fully formed but prior to tumor formation (Chapter 4, [41]). The human equivalent age match is approximately 18 years old, which is under the desired target age range of 25-30 years old for human prevention approaches [15]. Age is a known factor for breast cancer risk with tissue composition changing over time. In the breast, age related lobular involution causes decreases in connective tissue, reduced myoepithelial cells, and increased luminal epithelial cells in response to aging [76-80]. No impact was seen on epithelial cell changes within the estrous cycle and therefore it is hypothesized that changes to epithelial cell due to aging would not impact the ablative intraductal infusions. However, T cells have been shown to decrease in density with age and was more pronounced in high-risk women compared to average risk women. The other prominent immune cell in the breast, macrophages, had steady density among all women regardless of risk level or age [81]. During wound healing, initial macrophage response helps to remove debris while T cells aid in wound healing progression and tissue repair [82-84]. Decreased T cell concentrations are associated with impair wound healing [85]. As wound healing and immune response to cell ablation with 70% ethanol is not fully understood, it is feasible that declining lymphocytes numbers in response to increasing age may prolong wound healing responses after intraductal ablation affecting recovery times and quality of life.

Gradual mammary gland degeneration has been observed in mice to the extent that by 18 months of age, there is very little ductal structure remaining and is consistent with the human breast [86]. However, dissimilar to humans, a recent study in mice observed an increased in T cell population in the aged cohort [87]. Therefore, it is important to explore the possibility that age may impact the efficacy of 70% ethanol ablation effectiveness by intraductal infusions in aged matched rodent models while considering potential species variations.

**Intraductal Infusions and Male Breast Cancer:** Male breast cancer accounts for approximately 1% of all breast cancer cases [88, 89]. The male breast is underdeveloped compared to the female breast due to androgen hormones inhibiting glandular proliferation by estrogen and progesterone [90]. Therefore, the male breast consists of limited rudimentary mammary epithelia without lobule formation and is largely composed of fatty stroma [91, 82]. Despite this, majority of male breast cancer arises from epithelial cells with 90% of cases being diagnosed as invasive ductal carcinoma. Similarly to females, age, family history, genetic mutations such as BRCA2 and other factors may put a male individual at higher risk of breast cancer [93, 94]. However, due to low prevalence of this disease in men, no current preventive measures are established for male breast cancer. Additionally, male rodents undergo atrophy or complete loss of epithelial cells within the mammary gland upon sexual maturation making it unrealistic to study or establish a feasible male breast cancer model [95, 96]. The low prevalence of male breast cancer coupled with a lack of established ductal trees in rodents renders this preventive method of intraductal ablation with 70% ethanol impractical for these individuals.

## **Conclusions.**

Breast cancer is the highest diagnosed cancers among women in the United States [88]. Despite the yearly rises in new cases, prevention options to negate these numbers remain unchanged and underused in consequence of painful physical recoveries, crippling psychological harm, undesirable cancers risks and systemic side effects. Therefore, there is an immediate need for new prevention strategies aimed at reducing breast cancer incidence with lowered negative adverse events in women. Intraductal infusions directly targeting precancerous epithelial cells of the ductal tree may pave the way for numerous future prevention applications. Furthermore, refining 70% ethanol with tantalum oxide and ethyl cellulose with imaging capabilities speaks to the feasibility of this solution as an ablative agent. Together the data in this dissertation suggests that intraductal delivery of 70% ethanol is an effective, local ablation procedure capable of high-risk reduction with minimal physical damage that is already equipped for translation into first in human clinical trials.

## REFERENCES

1. Kuang M, Lu MD, Xie XY, Xu HX, Xu ZF, Liu GJ, Yin XY, Huang JF, Lencioni R: Ethanol ablation of hepatocellular carcinoma Up to 5.0 cm by using a multipronged injection needle with high-dose strategy. *Radiology* 2009, 253(2):552-561.
2. Ebara M, Okabe S, Kita K, Sugiura N, Fukuda H, Yoshikawa M, Kondo F, Saisho H: Percutaneous ethanol injection for small hepatocellular carcinoma: therapeutic efficacy based on 20-year observation. *J Hepatol* 2005, 43(3):458-464.
3. Gournay J, Tchuenbou J, Richou C, Masliah C, Lerat F, Dupas B, Martin T, Nouel JF, Schnee M, Montigny P et al: Percutaneous ethanol injection vs. resection in patients with small single hepatocellular carcinoma: a retrospective case-control study with cost analysis. *Aliment Pharmacol Ther* 2002, 16(8):1529-1538.
4. Huang GT, Lee PH, Tsang YM, Lai MY, Yang PM, Hu RH, Chen PJ, Kao JH, Sheu JC, Lee CZ et al: Percutaneous ethanol injection versus surgical resection for the treatment of small hepatocellular carcinoma: a prospective study. *Ann Surg* 2005, 242(1):36-42.
5. Green JE, Shibata MA, Yoshidome K, Liu ML, Jorczyk C, Anver MR, Wigginton J, Wiltrout R, Shibata E, Kaczmarczyk S et al: The C3(1)/SV40 T-antigen transgenic mouse model of mammary cancer: ductal epithelial cell targeting with multistage progression to carcinoma. *Oncogene* 2000, 19(8):1020-1027.
6. Regua AT, Arrigo A, Doheny D, Wong GL, Lo HW: Transgenic mouse models of breast cancer. *Cancer Lett* 2021, 516:73-83.
7. Welsh J: *Animal Models for Studying Prevention and Treatment of Breast Cancer*, 1 edn. Academic Press; 2013.
8. Alvarado A, Lopes AC, Faustino-Rocha AI, Cabrita AMS, Ferreira R, Oliveira PA, Colaço B: Prognostic factors in MNU and DMBA-induced mammary tumors in female rats. *Pathol Res Pract* 2017, 213(5):441-446.
9. Sannier K, Domp Martin A, Theron J, Labbe D, Barrellier MT, Leroyer R, Toure P, Leroy D: A new sclerosing agent in the treatment of venous malformations. Study on 23 cases. *Interv Neuroradiol* 2004, 10(2):113-127.
10. Domp Martin A, Blaizot X, Theron J, Hammer F, Chene Y, Labbe D, Barrellier MT, Gaillard C, Leroyer R, Chedru V et al: Radio-opaque ethylcellulose-ethanol is a safe and efficient sclerosing agent for venous malformations. *Eur Radiol* 2011, 21(12):2647-2656.
11. Morhard R, Mueller JL, Tang Q, Nief C, Chelales E, Lam CT, Alvarez DA, Rubinstein M, Katz DF, Ramanujam N: Understanding Factors Governing Distribution Volume of Ethyl Cellulose-Ethanol to Optimize Ablative Therapy in the Liver. *IEEE Trans Biomed Eng* 2020, 67(8):2337-2348.
12. Morhard R, Nief C, Barrero Castedo C, Hu F, Madonna M, Mueller JL, Dewhirst MW, Katz DF, Ramanujam N: Development of enhanced ethanol ablation as an alternative to surgery in treatment of superficial solid tumors. *Sci Rep* 2017, 7(1):8750.

13. Chakravarty S, Hix JML, Wiewiora KA, Volk MC, Kenyon E, Shuboni-Mulligan DD, Blanco-Fernandez B, Kiupel M, Thomas J, Sempere LF et al: Tantalum oxide nanoparticles as versatile contrast agents for X-ray computed tomography. *Nanoscale* 2020, 12(14):7720-7734.
14. Zaluzec EK, Kenyon E, Volk M, Hayat H, Powell K, Loomis A, Chakravarty S, Hix JML, Schipper J, Chang C et al: Tantalum oxide nanoparticles as versatile and high-resolution X-ray contrast agent for intraductal image-guided ablative procedure in rodent models of breast cancer. *npj Imaging* 2024, 2(1):3.
15. Tilanus-Linthorst MM, Lingsma HF, Evans DG, Thompson D, Kaas R, Manders P, van Asperen CJ, Adank M, Hoening MJ, Kwan Lim GE et al: Optimal age to start preventive measures in women with BRCA1/2 mutations or high familial breast cancer risk. *Int J Cancer* 2013, 133(1):156-163.
16. Greendale GA, Hogan P, Kritz-Silverstein D, Langer R, Johnson SR, Bush T: Age at Menopause in Women Participating in the Postmenopausal Estrogen/Progestins Interventions (PEPI) Trial: An Example of Bias Introduced by Selection Criteria. *Menopause* 1995, 2(1):27-34.
17. McKinlay SM, Brambilla DJ, Posner JG: The normal menopause transition. *Am J Hum Biol* 1992, 4(1):37-46.
18. Luoto R, Kaprio J, Uutela A: Age at natural menopause and sociodemographic status in Finland. *Am J Epidemiol* 1994, 139(1):64-76.
19. Stanford JL, Hartge P, Brinton LA, Hoover RN, Brookmeyer R: Factors influencing the age at natural menopause. *J Chronic Dis* 1987, 40(11):995-1002.
20. Shehata M, Waterhouse PD, Casey AE, Fang H, Hazelwood L, Khokha R: Proliferative heterogeneity of murine epithelial cells in the adult mammary gland. *Commun Biol* 2018, 1:111.
21. Joshi PA, Jackson HW, Beristain AG, Di Grappa MA, Mote PA, Clarke CL, Stingl J, Waterhouse PD, Khokha R: Progesterone induces adult mammary stem cell expansion. *Nature* 2010, 465(7299):803-807.
22. Asselin-Labat ML, Vaillant F, Sheridan JM, Pal B, Wu D, Simpson ER, Yasuda H, Smyth GK, Martin TJ, Lindeman GJ et al: Control of mammary stem cell function by steroid hormone signalling. *Nature* 2010, 465(7299):798-802.
23. Navarrete MA, Maier CM, Falzoni R, Quadros LG, Lima GR, Baracat EC, Nazário AC: Assessment of the proliferative, apoptotic and cellular renovation indices of the human mammary epithelium during the follicular and luteal phases of the menstrual cycle. *Breast Cancer Res* 2005, 7(3):R306-313.
24. Fu NY, Nolan E, Lindeman GJ, Visvader JE: Stem Cells and the Differentiation Hierarchy in Mammary Gland Development. *Physiol Rev* 2020, 100(2):489-523.
25. Oakes SR, Hilton HN, Ormandy CJ: The alveolar switch: coordinating the proliferative cues and cell fate decisions that drive the formation of lobuloalveoli from ductal epithelium. *Breast Cancer Res* 2006, 8(2):207.

26. Arendt LM, Kuperwasser C: Form and function: how estrogen and progesterone regulate the mammary epithelial hierarchy. *J Mammary Gland Biol Neoplasia* 2015, 20(1-2):9-25.
27. Deome KB, Faulkin LJ, Jr., Bern HA, Blair PB: Development of mammary tumors from hyperplastic alveolar nodules transplanted into gland-free mammary fat pads of female C3H mice. *Cancer Res* 1959, 19(5):515-520.
28. Shackleton M, Vaillant F, Simpson KJ, Stingl J, Smyth GK, Asselin-Labat ML, Wu L, Lindeman GJ, Visvader JE: Generation of a functional mammary gland from a single stem cell. *Nature* 2006, 439(7072):84-88.
29. Hoshino K, Gardner WU: Transplantability and life span of mammary gland during serial transplantation in mice. *Nature* 1967, 213(5072):193-194.
30. Degnim AC, Brahmabhatt RD, Radisky DC, Hoskin TL, Stallings-Mann M, Laudenschlager M, Mansfield A, Frost MH, Murphy L, Knutson K et al: Immune cell quantitation in normal breast tissue lobules with and without lobulitis. *Breast Cancer Res Treat* 2014, 144(3):539-549.
31. Ferguson DJ: Intraepithelial lymphocytes and macrophages in the normal breast. *Virchows Arch A Pathol Anat Histopathol* 1985, 407(4):369-378.
32. Hadadi E, Deschoemaeker S, Vicente Venegas G, Laoui D: Heterogeneity and function of macrophages in the breast during homeostasis and cancer. *Int Rev Cell Mol Biol* 2022, 367:149-182.
33. Wang Y, Chaffee TS, LaRue RS, Huggins DN, Witschen PM, Ibrahim AM, Nelson AC, Machado HL, Schwertfeger KL: Tissue-resident macrophages promote extracellular matrix homeostasis in the mammary gland stroma of nulliparous mice. *Elife* 2020, 9.
34. Reed JR, Schwertfeger KL: Immune cell location and function during post-natal mammary gland development. *J Mammary Gland Biol Neoplasia* 2010, 15(3):329-339.
35. Zumwalde NA, Haag JD, Sharma D, Mirrielees JA, Wilke LG, Gould MN, Gumperz JE: Analysis of Immune Cells from Human Mammary Ductal Epithelial Organoids Reveals Vdelta2+ T Cells That Efficiently Target Breast Carcinoma Cells in the Presence of Bisphosphonate. *Cancer Prev Res (Phila)* 2016, 9(4):305-316.
36. Chen CL, Liao MN, Chen SC, Chan PL, Chen SC: Body image and its predictors in breast cancer patients receiving surgery. *Cancer Nurs* 2012, 35(5):E10-16.
37. Brandberg Y, Sandelin K, Erikson S, Jurell G, Liljegren A, Lindblom A, Linden A, von Wachenfeldt A, Wickman M, Arver B: Psychological reactions, quality of life, and body image after bilateral prophylactic mastectomy in women at high risk for breast cancer: a prospective 1-year follow-up study. *J Clin Oncol* 2008, 26(24):3943-3949.
38. Metcalfe KA, Semple J, Quan ML, Vadaparampil ST, Holloway C, Brown M, Bower B, Sun P, Narod SA: Changes in psychosocial functioning 1 year after mastectomy alone, delayed breast reconstruction, or immediate breast reconstruction. *Ann Surg Oncol* 2012, 19(1):233-241.
39. Howard-McNatt MM: Patients opting for breast reconstruction following mastectomy: an analysis of uptake rates and benefit. *Breast Cancer (Dove Med Press)* 2013, 5:9-15.

40. Song Y, Zeng J, Tian X, Zheng H, Wu X: A review of different breast reconstruction methods. *Am J Transl Res* 2023, 15(6):3846-3855.
41. Kenyon E, Westerhuis JJ, Volk M, Hix J, Chakravarty S, Claucherty E, Zaluzec E, Ramsey L, Madaj Z, Hostetter G et al: Ductal tree ablation by local delivery of ethanol prevents tumor formation in an aggressive mouse model of breast cancer. *Breast Cancer Res* 2019, 21(1):129.
42. Scoccianti C, Lauby-Secretan B, Bello PY, Chajes V, Romieu I: Female breast cancer and alcohol consumption: a review of the literature. *Am J Prev Med* 2014, 46(3 Suppl 1):S16-25.
43. Seitz HK, Stickel F: Acetaldehyde as an underestimated risk factor for cancer development: role of genetics in ethanol metabolism. *Genes Nutr* 2010, 5(2):121-128.
44. Zakhari S: Overview: how is alcohol metabolized by the body? *Alcohol Res Health* 2006, 29(4):245-254.
45. Liu Y, Nguyen N, Colditz GA: Links between alcohol consumption and breast cancer: a look at the evidence. *Womens Health (Lond)* 2015, 11(1):65-77.
46. Wang Y, Xu M, Ke ZJ, Luo J: Cellular and molecular mechanisms underlying alcohol-induced aggressiveness of breast cancer. *Pharmacol Res* 2017, 115:299-308.
47. Gelfand R, Vernet D, Bruhn K, Vadgama J, Gonzalez-Cadauid NF: Long-term exposure of MCF-12A normal human breast epithelial cells to ethanol induces epithelial mesenchymal transition and oncogenic features. *Int J Oncol* 2016, 48(6):2399-2414.
48. Garaycochea JI, Crossan GP, Langevin F, Mulderrig L, Louzada S, Yang F, Guilbaud G, Park N, Roerink S, Nik-Zainal S et al: Alcohol and endogenous aldehydes damage chromosomes and mutate stem cells. *Nature* 2018, 553(7687):171-177.
49. Patel S, Sparman NZR, Arneson D, Alvarsson A, Santos LC, Duesman SJ, Centonze A, Hathaway E, Ahn IS, Diamante G et al: Mammary duct luminal epithelium controls adipocyte thermogenic programme. *Nature* 2023, 620(7972):192-199.
50. Yokoyama A, Muramatsu T, Ohmori T, Yokoyama T, Okuyama K, Takahashi H, Hasegawa Y, Higuchi S, Maruyama K, Shirakura K et al: Alcohol-related cancers and aldehyde dehydrogenase-2 in Japanese alcoholics. *Carcinogenesis* 1998, 19(8):1383-1387.
51. Chang JS, Hsiao JR, Chen CH: ALDH2 polymorphism and alcohol-related cancers in Asians: a public health perspective. *J Biomed Sci* 2017, 24(1):19.
52. Lanz J, Biniiaz-Harris N, Kuvaldina M, Jain S, Lewis K, Fallon BA: Disulfiram: Mechanisms, Applications, and Challenges. *Antibiotics (Basel)* 2023, 12(3).
53. King BL, Love SM: The intraductal approach to the breast: raison d'etre. *Breast Cancer Res* 2006, 8(2):206.
54. Love SM, Barsky SH: Anatomy of the nipple and breast ducts revisited. *Cancer* 2004, 101(9):1947-1957.

55. Hughes K: Comparative mammary gland postnatal development and tumourigenesis in the sheep, cow, cat and rabbit: Exploring the menagerie. *Semin Cell Dev Biol* 2021, 114:186-195.
56. Sorenmo KU, Rasotto R, Zappulli V, Goldschmidt MH: Development, anatomy, histology, lymphatic drainage, clinical features, and cell differentiation markers of canine mammary gland neoplasms. *Vet Pathol* 2011, 48(1):85-97.
57. Clark A, Bird NK, Brock A: Intraductal Delivery to the Rabbit Mammary Gland. *J Vis Exp* 2017(121).
58. Bourne RA, Bryant JA, Falconer IR: Stimulation of DNA synthesis by prolactin in rabbit mammary tissue. *J Cell Sci* 1974, 14(1):105-111.
59. Falconer IR: The distribution of <sup>131</sup>I- or <sup>125</sup>I-labelled prolactin in rabbit mammary tissue after intravenous or intraductal injection. *J Endocrinol* 1972, 53(3):58-59.
60. Fiddler TJ, Birkinshaw M, Falconer IR: Effects of intraductal prolactin on some aspects of the ultrastructure and biochemistry of mammary tissue in the pseudopregnant rabbit. *J Endocrinol* 1971, 49(3):459-469.
61. Fiddler TJ, Falconer IR: The effect of intraductal prolactin on protein and nucleic acid biosynthesis in the rabbit mammary gland. *Biochem J* 1969, 115(5):58P-59P.
62. Chadwick A: Detection and Assay of Prolactin by the Local Lactogenic Response in the Rabbit. *J Endocrinol* 1963, 27:253-263.
63. Baum B, Hewicker-Trautwein M: Classification and Epidemiology of Mammary Tumours in Pet Rabbits (*Oryctolagus cuniculus*). *J Comp Pathol* 2015, 152(4):291-298.
64. Schoniger S, Degner S, Jasani B, Schoon HA: A Review on Mammary Tumors in Rabbits: Translation of Pathology into Medical Care. *Animals (Basel)* 2019, 9(10).
65. Alikhassi A, Curpen B: Breast ductography: to do or not to do? A pictorial essay. *Insights Imaging* 2023, 14(1):201.
66. Stearns V, Mori T, Jacobs LK, Khouri NF, Gabrielson E, Yoshida T, Kominsky SL, Huso DL, Jeter S, Powers P et al: Preclinical and clinical evaluation of intraductally administered agents in early breast cancer. *Sci Transl Med* 2011, 3(106):106ra108.
67. Love SM, Zhang W, Gordon EJ, Rao J, Yang H, Li J, Zhang B, Wang X, Chen G, Zhang B: A feasibility study of the intraductal administration of chemotherapy. *Cancer Prev Res (Phila)* 2013, 6(1):51-58.
68. Classification of Products as Drugs and Devices and Additional Product Classification Issues [<https://www.fda.gov/regulatory-information/search-fda-guidance-documents/classification-products-drugs-and-devices-and-additional-product-classification-issues#keyprovisions>]
69. Burton KR, O'Dwyer H, Scudamore C: Percutaneous ethanol ablation of hepatocellular carcinoma: periprocedural onset alcohol toxicity and pancreatitis following conventional percutaneous ethanol ablation treatment. *Can J Gastroenterol* 2009, 23(8):554-556.

70. Mathew F, Goyal A: Ethanol. In: StatPearls. edn. Treasure Island (FL); 2024.
71. Mueller JL, Morhard R, DeSoto M, Chelales E, Yang J, Nief C, Crouch B, Everitt J, Previs R, Katz D et al: Optimizing ethyl cellulose-ethanol delivery towards enabling ablation of cervical dysplasia. *Sci Rep* 2021, 11(1):16869.
72. Kenyon E, Zaluzec E, Powell K, Volk M, Chakravarty S, Hix J, Kiupel M, Shapiro EM, Sempere LF: X-Ray Visualization of Intraductal Ethanol-Based Ablative Treatment for Prevention of Breast Cancer in Rat Models. *J Vis Exp* 2022(190).
73. Kenyon E, Zaluzec EK, Powell K, Volk M, Chakravarty S, Hix J, Arora R, Westerhuis JJ, Kiupel M, Shapiro EM et al: Intraductal Delivery and X-ray Visualization of Ethanol-Based Ablative Solution for Prevention and Local Treatment of Breast Cancer in Mouse Models. *J Vis Exp* 2022(182).
74. Gao D, Liu J, Yuan J, Wu J, Kuang X, Kong D, Zheng W, Wang G, Sukumar S, Tu Y et al: Intraductal administration of N-methyl-N-nitrosourea as a novel rodent mammary tumor model. *Ann Transl Med* 2021, 9(7):576.
75. Miele E, Spinelli GP, Miele E, Tomao F, Tomao S: Albumin-bound formulation of paclitaxel (Abraxane ABI-007) in the treatment of breast cancer. *Int J Nanomedicine* 2009, 4:99-105.
76. Hutson SW, Cowen PN, Bird CC: Morphometric studies of age related changes in normal human breast and their significance for evolution of mammary cancer. *J Clin Pathol* 1985, 38(3):281-287.
77. Milanese TR, Hartmann LC, Sellers TA, Frost MH, Vierkant RA, Maloney SD, Pankratz VS, Degnim AC, Vachon CM, Reynolds CA et al: Age-related lobular involution and risk of breast cancer. *J Natl Cancer Inst* 2006, 98(22):1600-1607.
78. Garbe JC, Pepin F, Pelissier FA, Sputova K, Fridriksdottir AJ, Guo DE, Villadsen R, Park M, Petersen OW, Borowsky AD et al: Accumulation of multipotent progenitors with a basal differentiation bias during aging of human mammary epithelia. *Cancer Res* 2012, 72(14):3687-3701.
79. Pelissier Vatter FA, Schapiro D, Chang H, Borowsky AD, Lee JK, Parvin B, Stampfer MR, LaBarge MA, Bodenmiller B, Lorens JB: High-Dimensional Phenotyping Identifies Age-Emergent Cells in Human Mammary Epithelia. *Cell Rep* 2018, 23(4):1205-1219.
80. Pelissier FA, Garbe JC, Ananthanarayanan B, Miyano M, Lin C, Jokela T, Kumar S, Stampfer MR, Lorens JB, LaBarge MA: Age-related dysfunction in mechanotransduction impairs differentiation of human mammary epithelial progenitors. *Cell Rep* 2014, 7(6):1926-1939.
81. Zirbes A, Joseph J, Lopez JC, Sayaman RW, Basam M, Seewaldt VL, LaBarge MA: Changes in Immune Cell Types with Age in Breast are Consistent with a Decline in Immune Surveillance and Increased Immunosuppression. *J Mammary Gland Biol Neoplasia* 2021, 26(3):247-261.
82. Zaiss DM, Minutti CM, Knipper JA: Immune- and non-immune-mediated roles of regulatory T-cells during wound healing. *Immunology* 2019, 157(3):190-197.

83. Li J, Tan J, Martino MM, Lui KO: Regulatory T-Cells: Potential Regulator of Tissue Repair and Regeneration. *Front Immunol* 2018, 9:585.
84. Rodrigues M, Kosaric N, Bonham CA, Gurtner GC: Wound Healing: A Cellular Perspective. *Physiol Rev* 2019, 99(1):665-706.
85. Guo S, Dipietro LA: Factors affecting wound healing. *J Dent Res* 2010, 89(3):219-229.
86. Radisky DC, Hartmann LC: Mammary involution and breast cancer risk: transgenic models and clinical studies. *J Mammary Gland Biol Neoplasia* 2009, 14(2):181-191.
87. Li CM, Shapiro H, Tsiobikas C, Selfors LM, Chen H, Rosenbluth J, Moore K, Gupta KP, Gray GK, Oren Y et al: Aging-Associated Alterations in Mammary Epithelia and Stroma Revealed by Single-Cell RNA Sequencing. *Cell Rep* 2020, 33(13):108566.
88. Siegel RL, Miller KD, Wagle NS, Jemal A: Cancer statistics, 2023. *CA Cancer J Clin* 2023, 73(1):17-48.
89. Deldar R, Sayyed AA, Towfighi P, Aminpour N, Sogunro O, Son JD, Fan KL, Song DH: Postmastectomy Reconstruction in Male Breast Cancer. *Breast J* 2022, 2022:5482261.
90. Lattin GE, Jr., Jesinger RA, Mattu R, Glassman LM: From the radiologic pathology archives: diseases of the male breast: radiologic-pathologic correlation. *Radiographics* 2013, 33(2):461-489.
91. Yang S, Leng Y, Chau CM, Ma KFJ, Fung WY, Chan RLS, Yung WTA, Leong PW, Li OCA, Wong T: The ins and outs of male breast and anterior chest wall lesions from childhood to adulthood. *Clin Radiol* 2022, 77(7):503-513.
92. Fox S, Speirs V, Shaaban AM: Male breast cancer: an update. *Virchows Arch* 2022, 480(1):85-93.
93. Khattab A, Kashyap S, Monga DK: Male Breast Cancer. In: *StatPearls*. edn. Treasure Island (FL); 2023.
94. Gao Y, Goldberg JE, Young TK, Babb JS, Moy L, Heller SL: Breast Cancer Screening in High-Risk Men: A 12-year Longitudinal Observational Study of Male Breast Imaging Utilization and Outcomes. *Radiology* 2019, 293(2):282-291.
95. Lucas JN, Rudmann DG, Credille KM, Irizarry AR, Peter A, Snyder PW: The rat mammary gland: morphologic changes as an indicator of systemic hormonal perturbations induced by xenobiotics. *Toxicol Pathol* 2007, 35(2):199-207.
96. Dunbar ME, Dann PR, Robinson GW, Hennighausen L, Zhang JP, Wysolmerski JJ: Parathyroid hormone-related protein signaling is necessary for sexual dimorphism during embryonic mammary development. *Development* 1999, 126(16):3485-3493.